Universidad Autónoma De Madrid

Facultad de Ciencias

Departamento de Ingeniería Química

STRATEGIES FOR THE REMOVAL OF CHOLINE- AND IMIDAZOLIUM-BASED IONIC LIQUIDS FROM AQUEOUS PHASE

ESTRATEGIAS PARA LA DEGRADACIÓN DE LÍQUIDOS IÓNICOS DE LAS FAMILIAS COLINA E IMIDAZOLIO EN AGUA

MEMORIA

que para optar al grado de

Doctor con mención Internacional

Presenta

Ismael Fernández Mena

Madrid, 2019

Dña. Elena Díaz Nieto, Profesora Contratada Doctor del Departamento de Ingeniería Química de la Universidad Autónoma de Madrid, y D. Ángel Fernández Mohedano, Profesor Titular de Universidad del Departamento de Ingeniería Química de la Universidad Autónoma de Madrid

HACEN CONSTAR: que el presente trabajo, titulado: "Estrategias para la degradación de líquidos iónicos de las familias colina e imidazolio en agua", presentado por D. Ismael Fernández Mena, ha sido realizado bajo su dirección, en los laboratorios del Departamento de Ingeniería Química de la Universidad Autónoma de Madrid y que, a su juicio, reúne los requisitos de originalidad y rigor científico necesarios para ser presentado como Tesis Doctoral.

Y para que conste a efectos oportunos, firmamos el presente informe en Madrid, a veintiuno de marzo de dos mil diecinueve.

Elena Díaz Nieto

Ángel Fernández Mohedano

La realización del presente trabajo ha sido posible gracias al apoyo económico del Ministerio de Economía y Competitividad (CTM2013-43803-P y CTM2016-76564-R), de la Comunidad de Madrid (REMPTAVARES, S2013/MAE-2716) y el convenio UAM-Santander (CEAL-AL/2015-08). El autor ha disfrutado de un contrato predoctoral para la formación de doctores de la convocatoria 2014 (BES-2014-069986) financiado por el Ministerio de Economía y Competitividad y el Fondo Social Europeo.

Index

Index

Resumen

Summary

Resumen

Los líquidos iónicos (LIs) son sales constituidas por un catión orgánico y un anión inorgánico u orgánico con un gran potencial como sustituyentes de los disolventes orgánicos tradicionales. Se consideran "disolventes verdes" debido a su baja presión de vapor y su alta estabilidad térmica y química. Por esta razón, los LIs se han estudiado en procesos de separación, catálisis, reacciones químicas o electroprocesos, entre otros, diseñándose de acuerdo a su uso final. Los LIs se clasifican en función del catión que lo constituye, siendo las principales familias imidazolio, piridinio, piperidinio, pirrolidinio, fosfonio o amonio. Los aniones más empleados son haluros y ácidos orgánicos. Debido a su alta solubilidad en agua, los LIs pueden aparecer en aguas residuales, generadas en su síntesis o como consecuencia de su uso. Este hecho junto a que, en general, se caracterizan por una baja biodegradabilidad y relativa alta toxicidad, puede dar lugar a un problema medioambiental considerable, especialmente en el medio acuático, donde los LIs podrían acumularse.

En este trabajo, LIs de las familias imidazolio y colina se seleccionaron como compuestos de estudio, con el fin de evaluar su comportamiento como contaminantes en fase acuosa. El catión imidazolio tiene una estructura heterocíclica con dos átomos de N no adyacentes, mientras que el catión colina es un amonio cuaternario. De manera general, los LIs imidazolio se consideran compuestos no biodegradables, siendo sólo parcialmente biodegradables aquellos de cadena alquílica superior a 6 átomos de carbono. En ese caso, la cadena alquílica puede degradarse, mientras que el anillo imidazolio permanece inalterable. En relación a la toxicidad, la ecotoxicidad de los LIs imidazolio aumenta con la longitud de la cadena alquílica, siendo ésta muy superior en el

caso de que el constituyente aniónico este formado por hexafluorofosfate o bis(trifluorometilsulfonil)imida (PF_6^- o NTf_2^-). Los LIs basados en colina son considerados "respetuosos con el medio ambiente", debido a la biodegradabilidad asociada al catión colina. Sin embargo, dependiendo del anión con el que se combine, la ecotoxicidad y biodegradabilidad de estos LIs puede variar desde resultar inocuo a ser considerado peligroso para el medio ambiente.

La baja biodegradabilidad exhibida por la mayoría de LIs, ha motivado que se evalúen diferentes procesos de oxidación avanzada (POAs) para su degradación. Así, se han estudiado la viabilidad del reactivo Fenton, procesos fotoquímicos y procesos electroquímicos en la degradación de LIs en fase acuosa, obteniendose diferentes grados de degradación y mineralización.

El objetivo de este trabajo se centra en estudiar la viabilidad de procesos de oxidación biológica y tratamientos de oxidación avanzada para la degradación de LIs de las familias imidazolio y colina en agua, con el fin de establecer estrategias apropiadas para su eliminación de aguas residuales.

En el Capítulo 3, se discute la toxicidad y biodegradabilidad de LIs imidazolio y colina. La primera parte está dedicada a evaluar la ecotoxicidad (en términos de EC_{50} (μM), definida como la concentración de una sustancia que produce el 50 % de inhibición) de 12 LIs imidazolio con diferente cadena alquílica (de 4 a 10 átomos de C) combinados con 3 aniones diferentes (cloruro (Cl^-), tetrafluoroborato (BF_4^-) y bis(trifluorometilsulfonil)imida (NTf_2^-)). En los ensayos se empleó un lodo activo, proveniente de un reactor biológico de membranas de una industria cosmética. Los valores de toxidad se compararon con los obtenidos por medio del test de

ecotoxicidad Microtox® (*Vibrio fischeri*). En ambos ensayos, el aumento de la cadena alquílica originó un aumento en la toxicidad de los LIs, aunque el test Microtox® tendía subestimando el efecto que podrían ocasionar los LIs en el tratamiento biológico de una instalación de depuración de aguas residuales. Los LIs constituidos por aniones fluorados mostraron una reducida EC_{50}, siendo el anión NTf_2^- el que presentó mayor toxicidad. Teniendo en cuenta la clasificación proporcionada por Passino y Smith (1987) sobre los peligros que pueden ocasionar los contaminantes a organismos acuáticos, los cationes imidazolio con 8 y 10 átomos de carbono pudieron clasificarse como altamente tóxicos, resultando inocuos o prácticamente inocuos los LIs imidazolio con 4 átomos de carbono en la cadena alquílica, independientemente de la naturaleza del anión.

La segunda parte del Capítulo 3 recoge los resultados obtenidos en el estudio de ecotoxicidad y biodegradabilidad de LIs constituidos por 1-Butil-3metilimidazolio ($Bmim^+$) y colina ($Choline^+$) mediante ensayos respirométricos. Se seleccionaron tres aniones diferentes: Cl^- como constituyente inerte, acetato (Ac^-) como biodegradable, y NTf_2^- como tóxico y no biodegradable. Se llevaron a cabo ensayos de biodegradabilidad inherente (ensayo Zahn-Wellens) y biodegradabilidad rápida (ensayo respirométrico), prestando especial atención a la posible inhibición que el LI puede originar en el lodo activo. Además, la ecotoxicidad de los 6 LIs se evaluó usando lodo activo sin aclimatar (inhibición respirométrica) y la bacteria marina *Vibrio fischeri* (ensayo Microtox®). $Bmim^+$ y NTf_2^- resultaron ser no biodegradables, mientras que $Choline^+$ y Ac^- se degradaron completamente, resultando que la biodegradación de cada catión/anión no se ve afectada por la naturaleza del contraión con el que se combina. Además, los resultados de la inhibición respirométrica

indicaron que el $Bmim^+$ y el NTf_2^- son los iones más tóxicos. Concentraciones de $CholineNTf_2$ cercanas a la EC_{50} causaron una ligera inhibición del lodo activo.

El Capítulo 4 evalúa la biodegradación de LIs basados en el catión colina en reactores biológicos secuenciales (SBRs). Se seleccionaron los LIs: cloruro de colina (CholineCl), acetato de colina (CholineAc) y bis(trifluorometilsulfonil)imida de colina ($CholineNTf_2$). Después de 30 días de aclimatación, la degradación del catión resultó completa en todos los casos. El lodo granular exhibió buena actividad y alta eliminación de DQO (80–90%) y COT (75–85%) en la degradación de CholineCl y CholineAc, respectivamente, en un intervalo de concentraciones iniciales de 0.25-15 mM. Sin embargo, en el caso de $CholineNTf_2$ el aumento de concentración originó un efecto inhibitorio en el lodo, acumulándose el anión NTf_2^- en el reactor. El análisis de los efluentes de reacción reveló la presencia de los principales intermedios en la degradación de colina: etanol y metil-, dimetil- y trimetilamina. Mediante pirosecuenciación se caracterizaron las comunidades microbianas del lodo inicial y final, encontrando en las muestras finales los grupos Alfa-, Beta- y Gammaproteobactria principlamente.

En el Capítulo 5 se estudia la oxidación húmeda catalítica con peróxido de hidrógeno (CWPO por sus siglas en inglés) de varios LIs de la familia imidazolio. La sección 5.1 se centra en la degradación de cloruro de 1-Butil-3-metilimidazolio (BmimCl), acetato de 1-Butil-3-metilimidazolio (BmimAc), bis(trifluorometilsulfonil)imida de 1-Butil-3-metilimidazolio ($BmimNTf_2$), cloruro de 1-Hexil-3-metilimidazolio (HmimCl) y cloruro de 1-Decil-3-metilimidazolio (DmimCl), usando un catalizador de Fe soportado sobre alúmina (Fe_2O_3/Al_2O_3) preparado por el método de impregnación a humedad incipiente. La variación en

la dosis de H_2O_2, de 0,5 a 1,5 veces la cantidad estequiométrica, proporcionó resultados similares en términos de mg de COT eliminado por mg H_2O_2 consumido, consiguiendo en todos los casos eliminación completa del catión $Bmim^+$. Un incremento de la temperatura de reacción hasta 90 ºC originó un aumento en la mineralización alcanzada (> 40 %), que no se vió influido por el tipo de constituyente aniónico (Cl^-, Ac^- y NTf_2^-). Se propuso una ruta de degradación que incluía compuestos hidroxilados, compuestos parcialmente oxidados y ácidos de cadena corta como intermedios de reacción. La reacción CWPO a 80 ºC aumentó la biodegradabilidad de los efluentes obtenidos, alcanzando la secuencia CWPO–biodegradabilidad conversiones del 55-60 % de COT. El catalizador Fe_2O_3/Al_2O_3 exhibió una gran estabilidad, siendo la lixiviación de Fe despreciable.

La segunda parte del Capítulo 5 estudia la estabilidad de 3 catalizadores de Fe soportados sobre diferentes materiales carbonosos en la CWPO de BmimAc. Un catalizador se preparó por activación química de lodo activo deshidratado con tricloruro de hierro ($FeCl_3$) en un ratio másico de 3 ($FeCl_3$:lodo activo) (Fe/AS), otro por carbonización hidrotermal de lodo activo con $FeCl_3$ usando el mismo ratio (Fe/HTCS), y un tercero por impregnación a humedad incipiente ($FeCl_3$, 5 % en Fe) de una carbón activo comercial (Fe/AC). En los ensayos de reacción (80 h, 80 ºC, 0.133 kg_{Fe} h mol_{BmimAc}^{-1}) el catalizador Fe/HTCS mostró una estabilidad relativamente buena y despreciable lixiviación de Fe, mientras que el catalizador Fe/AC perdió su actividad debido a una alta lixiviación de Fe (90 %). El mejor resultado se consiguió con el catalizador Fe/AS, que logró una completa eliminación del $Bmim^+$ y conversiones de COT en torno al 30 %. Se propuso una ruta de degradación que incluía el ataque de radicales hidroxilo al catión imidazolio produciendo compuestos hidroxilados, que eran

progresivamente degradados a ácidos de cadena corta, nitrato, NO_x, H_2O y CO_2.

El Capítulo 6 incluye la degradación de LIs imidazolio mediante procesos de electrooxidación usando ánodos de diamante dopado con boro (BDD). La sección 6.1 estudia la electrolisis de BmimCl, HmimCl and DmimCl. Aunque la elevada conductividad de los LIs en disolución acuosa permite aplicar la electrólisis sin la adición de un electrolito, se evaluó además el efecto de adicionar anion sulfato al medio de reacción. La eficiencia de la electrolisis mejoró con la adición de electrolito en el caso de la oxidación de BmimCl y HmimCl, lográndose la eliminación completa del catión y conversiones de COT del 70–94 % (30 mA cm^2, $[IL]_0$ = 1mM, $[H_2SO_4]_0$ = 3000 mg L^{-1},25 ºC). El $Dmim^+$ se eliminó rápidamente debido a la formación de un polímero, que no se observó en la electroxidación con sulfato como electrolito. Se identificaron compuestos hidroxilados en el medio de reacción, la formación de iones nitrato, nitrito y amonio, así como clorato y perclorato por oxidación de cloruro.

La sección 6.2 se centra en la degradación de BmimCl y BmimAc por electrólisis, sonoelectrólisis (ultrasonidos de alta frecuencia, US) y fotoelectrólisis (radiación de luz UV) con ánodos de BDD. En todos los casos, se alcanzó la eliminación completa de $Bmim^+$, observándose que la eliminación del catión fue más lenta que la oxidación de los aniones. La electrólisis y fotoelectrólisis del BmimAc resultó menos efectiva que la sonoelectrólisis (57, 55 y 80 % de conversión de COT; 30 mA cm^2, $[IL]_0$ = 1mM, UV (254 nm) = 930 µW $cm^{-}2$, US = 10 MHz, 25 ºC), mientras que en el caso del BmimCl no se apreciaron cambios significativos entre las técnicas estudiadas, resultando la fotoelectrólisis el proceso más eficiente (93 % de eliminación de COT). En la reacción

se observó la oxidación del cloruro y la formación de nitrato, nitrito, amonio, compuestos heterocíclicos y ácidos orgánicos.

Por último, la sección 6.3 recoge el estudio de la degradación de $BmimNTf_2$ con ánodos de BDD en procesos de electrólisis, electrólisis con promotores de peroxosulfato, fotoelectrólisis y sonoelectrólisis. En todos los casos se consiguió una eliminación completa de $Bmim^+$, alcanzando en el caso de la sonoelectrólisis una velocidad de reacción más elevada. Sin embargo, la mayor mineralización se consiguó en el proceso de electrólisis con adición de sulfato, indicando el papel relevante de los radicales persulfato y sulfato en la degradación de compuestos alifáticos formados en la degradación de $Bmim^+$. La concentración del anión NTf_2^- permaneció inalterable, siendo los radicales formados ineficientes en la ruptura de los enlaces C–F, C–S y S–N.

Summary

Ionic liquids (ILs) are salts based on an organic cation and inorganic or organic anion with a great potential as substitutes for traditional solvents. They are considered "green solvents" because of their low vapor pressure and high thermal and chemical stability. For this reason, the ILs have been studied, among others, in separation processes, catalysis, chemical reactions or electroprocesses, being designed according to their final use. The ILs are classified depending on the cation employed, being imidazolium, pyridinium, piperidinium, pyrrolidinium, phosphonium and ammonium the main families studied. Among the anions, the halides and organic acids are the most employed compounds. Due to their high solubility in water, the ionic liquids can appear in wastewater generated during their synthesis or application. This fact together with that, in general, ionic liquids are characterized by their low biodegradability and relative high toxicity, can cause an important problem in the environment, specifically in the aquatic medium, where these pollutants are accumulated.

In this work, the imidazolium and choline ionic liquid families are selected as target compound, to study their behavior as pollutants in aqueous medium, because of their different structure. Imidazolium-based ILs present a heterocycle structure with 2 non-adjacent N atoms, while the choline is a quaternary ammonium cation. The imidazolium ILs have been categorized as non-biodegradable compounds, being only partially biodegraded when the alkyl side chain has more than 6 C atoms. In these cases, the alkyl chain is transformed remaining the imidazolium core inalterable. The ecotoxicity of the imidazolium ILs increases using cations with higher alkyl side chain or fluorinated anions, such as PF_6^- or NTf_2^-. The choline-based ILs belong to a new

generation of "environmental friendly" ILs. This fact is related to the biodegradable behavior that the choline cation presents. However, depending on the anion combined with this cation, the ecotoxicity and the biodegradability can vary from being innocuous to dangerous for the environment.

Because of the low biodegradability exhibited by most of the ILs, different advanced oxidation processes (AOPs) have been studied for their degradation. Among the AOPs, Fenton, photodegradation and electrochemical processes have been efficiently applied for ILs abatement in aqueous phase, obtaining high degradation and mineralization rates.

The aim of this work is to study the degradation feasibility of imidazolium and choline ILs in aqueous phase by biological and advanced oxidation treatments in order to stablish a treatment strategy for removal those compounds from wastewater.

In Chapter 3, the ecotoxicity and biodegradability of imidazolium and choline ILs are discussed. The first part is devoted to evaluate the ecotoxicity (in terms of EC_{50} (μM), defined as the effective concentration of a sample that causes 50 % inhibition) of 12 imidazolium ILs with different alkyl side chains (from 4 to 10 C atoms) combined with 3 different anions (chloride (Cl^-), tetrafluoroborate (BF_4^-) and bis(trifluoromethanesulfonyl)imide) (NTf_2^-)). The ecotoxicity results were obtained using an activated sludge, collected from a membrane bioreactor of a cosmetic industry. These results were compared with the obtained by the Microtox test® (*Vibrio fischeri*). In both ecotoxicity assays, the increase in the alkyl side chain length increased the ecotoxicity of the ILs, although the latter tends to overestimate the effect of the ILs on biological wastewater treatment

facilities. In all studied cases, ILs constituted by fluorinated anions were characterized by low EC_{50} values, being the NTf_2^- the most toxic anion. Taking into account the hazard ranking for aquatic organisms provided by Passino and Smith (1987), the imidazolium cations with 8 and 10 carbon atoms were classified as highly toxic, being classified as harmless or practically harmless the imidazolium ILs with 4 carbon atoms in the alkyl side chain, regardless of the anion nature.

The second part of Chapter 3 includes the ecotoxicity and biodegradability studies of 1-Butyl-3-methylimidazolium ($Bmim^+$) and choline-based ILs by respitrometric assays. Three different anions were selected: chloride (Cl^-) as inert compound, acetate (Ac^-) as biodegradable compound and bis(trifluoromethanesulfonyl)imide (NTf_2^-) as toxic and non-biodegradable compound. Inherent (Zahn-Wellens test) and fast (respirometric test) biodegradability assays were used, paying attention to the possible inhibition that the IL can produce in the activated sludge. Moreover, the ecotoxicity of the six ILs wereevaluated by using unacclimated sludge (respiration inhibition) and *Vibrio fischeri* (Microtox® test). $Bmim^+$ and NTf_2^- proved to be non-biodegradable, whereas $Choline^+$ and Ac^- were completely degraded, finding that the biodegradation of each cation/anion is nearly unaffected by counter-ion nature. Regarding the results of the respiration inhibition, it was stablished that the $Bmim^+$ and the NTf_2^- were the most toxic ions. Moreover, concentrations close to the EC_{50} value of the $CholineNTf_2$ caused a slight inhibition of the activated sludge.

The Chapter 4 evaluates the biodegradation of the choline-based ILs in sequencing batch reactors (SBRs). Choline chloride (CholineCl), choline acetate (CholineAc) and choline

bis(trifluoromethanesulfonyl)imide (CholineNTf$_2$) were selected as target choline-based ILs . After 30 days of acclimation period, the granular activated sludge exhibited good activity, and high COD (80–90%) and TOC removal (75–85%) with initial concentrations of CholineCl and CholineAc over the range 0.25–15 mM. However, increased concentrations of CholineNTf$_2$ (from 0.25 to 15 mM) had an inhibitory effect in the sludge. In all the cases, the choline cation degradation was complete. An analysis of the reaction effluent revealed the presence of the main intermediates of choline degradation: ethanol, and methyl-, dimethyl- and trimethylamine. The initial and final microbial communities of the sludge were characterized by pyrosequencing analysis, and the latter was found to consist mainly of Alfa-, Beta- and Gamma-proteobacteria.

Chapter 5 studies the Catalytic Wet Peroxide Oxidation (CWPO) of several imidazolium-based ILs. The section 5.1 is focused on the degradation of 1-Butyl-3-methylimidazolium chloride (BmimCl), 1-Butyl-3-methylimidazolium acetate (BmimAc), 1-Butyl-3-methylimidazoliumbis(trifluoromethanesulfonyl)imide (BmimNTf$_2$), 1-Hexyl-3-methylimidazolium chloride (HmimCl) and 1-Decyl-3-methylimidazolium chloride (DmimCl) by using a Fe catalyst supported on alumina (Fe_2O_3/Al_2O_3) that was prepared by incipient wetness impregnation. Variable H_2O_2 doses from 0.5 to 1.5 times the stoichiometric value provided similar results in terms mg TOC removed per mg H_2O_2, all allowing complete $Bmim^+$ removal. Raising the reaction temperature to 90 ºC increased the mineralization rate up to 40 % TOC conversion. Differences in TOC conversion among counteranions (chloride, acetate and NTf_2^-) were negligible. A plausible reaction pathway involving hydroxylated compounds, partially oxidized compounds and short-chain organic acids as reaction

byproducts is proposed. CWPO at 80 ºC markedly increased biodegradability of the IL solutions and CWPO-biodegradability process led to TOC conversions of 55-60 %. The Fe_2O_3/Al_2O_3 catalyst exhibited high long-term stability; thus, it retained most of its properties and underwent negligible Fe leaching.

The second part of Chapter 5 studies the stability of 3 different carbon-supported iron catalysts in the CWPO of BmimAc, one obtained by chemical activation of sewage sludge with iron chloride ($FeCl_3$) in a mass ratio of 3 ($FeCl_3$:sewage sludge) (Fe/AS), other by hydrothermal carbonization of sewage sludge with $FeCl_3$ at the same ratio (Fe/HTCS) and a third one obtained by wetness impregnation of a commercial activated carbon Fe/AC. The catalysts obtained from the sewage sludge showed a negligible Fe leaching and a fairly good stability (80 ºC, 0.133 kg_{Fe} h mol_{BmimAc}^{-1}), whereas the Fe/AC lost its activity due to a high Fe leaching (90 %) at the same conditions. The best results were obtained with the Fe/AS catalyst, achieving a complete $Bmim^+$ removal and 30 % TOC conversion. A possible reaction pathway included the hydroxyl attack of the imidazolium cation producing hydroxylated compounds, that were progressively degraded to short-chain organic acids, nitrate, NO_x, H_2O and CO_2.

The Chapter 6 reflects the degradation of imidazolium-based ILs by electrooxidation processes using Boron doped diamond (BDD) anodes. The section 6.1 studies the electrolysis of BmimCl, HmimCl and DmimCl. Despite of the fact that the high conductivity of ILs aqueous solutions allows them to be treated by electrolysis without the addition of an electrolyte, the effect of the presence of sulfate anions in the reaction medium was also evaluated. An improvement of the efficient of electrolysis associate to the addition of the electrolyte was observed

in the case of BmimCl and HmimCl leading to a complete cation degradation and TOC removal in the range 70–94 % (30 mA cm^2, $[IL]_0$ = 1mM, $[H_2SO_4]_0$ = 3000 mg L^{-1}, 25 ºC). $Dmim^+$ was removed quickly due to the rapid formation of a polymer, which was not observed when sulfate anions were added to the reaction medium. Hydroxylated intermediates were identified in the reaction medium, while, the chloride anion was transformed into perchlorate and nitrite, nitrate and ammonium were also formed.

The section 6.2 is focused on the degradation of BmimCl and BmimAc by electrolysis, sonoelectrolysis (high-frequency ultrasound, US) and photoelectrolysis (UV light irradiation) with BDD anodes. Although $Bmim^+$ was depleted in all cases, the removal of the heterocyclic ring was much less efficient than oxidation of the counter-anions. The electrolysis and photoelectrolysis of BmimAc were less efficient than sonoelectrolysis (57, 55 and 80 % of TOC removal; 30 mA cm^2, $[IL]_0$ = 1mM, UV (254 nm) = 930 μW $cm^{-}2$, US = 10 MHz, 25 ºC), whereas for BmimCl no significant changes were detected among the techniques, being the photoelectrolysis the most efficient process (93 % of TOC removal). Oxidation of chloride was produced whereas nitrite, nitrate ammonium, different heterocyclic compounds and organic acids were formed in the electrolysis of both ILs.

Finally, section 6.3 includes the study of $BmimNTf_2$ degradation with BDD anodes in bare electrolysis, electrolysis enhanced with peroxosulfate promoters, irradiated with UV light and with US. In all cases, the $Bmim^+$ removal was complete, achieving the highest reaction rate by means the sonoelectrolysis. However, the most efficient process in terms of mineralization was the electrolysis with the addition of sulfates, pointing out the significant role of persulfate and sulfate radicals in the degradation of aliphatic compounds formed in the

$Bmim^+$ degradation. The NTf_2^- concentration remained unalterable, being the radicals formed inefficient for breaking the C–F, C–S or S–N bounds.

1

Introduction

Introduction

Ionic liquids (ILs) are compounds formed by an organic cation and organic or inorganic anion, that can be selected based on the application that they are going to perform. ILs are considered as "green solvents" due to their main characteristics: low vapor pressure, high thermal stability and low melting point. These properties make them perfect substitutes for volatile conventional solvents (Markiewicz et al., 2013; Neumann and Pawlik, 2014; Stolte et al., 2012). In recent decades, many authors have focused their research on the application of these compounds as substitutes of traditional solvent, in catalyst or in chemical or electroprocesses, among other uses (Armand et al., 2009; Frade and Afonso, 2010; Goodenough and Park, 2013; Han et al., 2011; Palomar et al., 2011; Santiago et al., 2016; Sheldon, 2005; Ventura et al., 2012; Welton, 2004). Nowadays, a great variety of ILs are synthetized for commercial use (> 500ILs) (Diaz et al., 2016), even, ILs can be designed on demand for the process in which they will be involved. The ILs are classified in function of the cation family they belong. The main cations employ are imidazolium, pyridinium, pyperidinium, pyrrolidinium and quaternary ammonium and phosphonium. In terms of anions, halides, organic acids, and inorganic compound containing fluoride, sulfate or cyanamide groups, among others, are the most synthetize. The structure of cations and anions of the ILs evaluated along the present study can be appreciated in the Table 1.1.

Table 1.1. Main cations and anions of ILs and their structure.

Cations	Anions
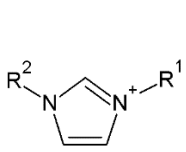 Imidazolium 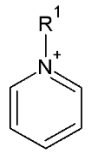 Pyridinium 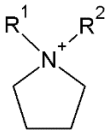 Piperidinium 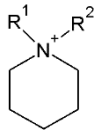 Pyrrolidinium 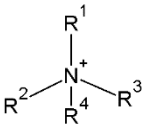 Ammonium 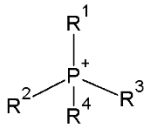 Phosphonium	 Halides 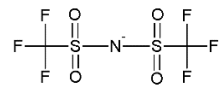 Bis(trifluoromethanesulfonyl)imide 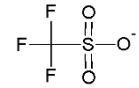 Triflate 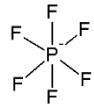 Hexafluorophosphate 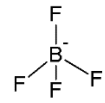 Tetrafluoroborate 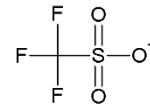 Trifluoromethanesulfonate 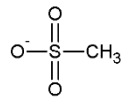 Methanesulfonate 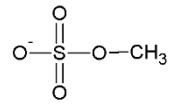 Methylsulfate 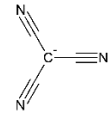 Tricyanomethanide  Acetate 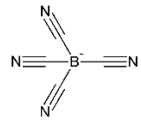 Tetracyanoborate 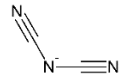 Dicyanamide 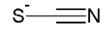 Tiocyanate 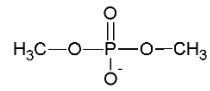 Dimethylphosphate 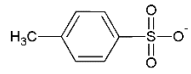 p-Toluenesulfonate  Trifluoroacetate 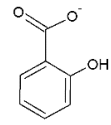 Salicylate 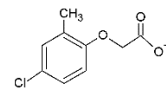 (4-Chloro-2-methylphenoxy) acetatetosylate 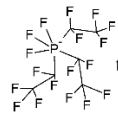 tris(pentafluoroethyl) trifluorophosphate

The IL can be transferred to superficial and groundwater due to their relative high solubility in water. ILs can appear in water streams as consequence of their use in several applications or in their synthesis process what can produce wastewater containing low concentrations of these pollutants (Diaz et al., 2016; Vekariya, 2017). Depending on the cation-anion combination, the ILs can present high ecotoxicity and/orlow biodegradability in water. It is widely settled that the

imidazolium, pyridinium and thiazolium cation are low biodegradable or recalcitrant to biological treatment and present relative high toxicity (Abrusci et al., 2011; Amde et al., 2015; Cho et al., 2008; Costa et al., 2015a, 2015b; Docherty et al., 2015; Hernández-Fernández et al., 2015; Khan et al., 2016; Romero et al., 2008; Stolte et al., 2008; Thuy Pham et al., 2010; Ventura et al., 2014). On the contrary, amine derived cations and organic acid derived anions can be considered less biodegradables and lower toxics than fluorinated anions (Abrusci et al., 2011; Biczak et al., 2014; Costa et al., 2015a; Hernández-Fernández et al., 2015; Phuong et al., 2010; Romero et al., 2008). Due to traditional biological treatment are, in general, not effective in the degradation of most of the ILs, certain researches have been focused on the Advanced Oxidation Process for the IL wastewater treatment.

1.1. Advanced Oxidation Processes

Advanced Oxidation Process (AOPs) have been used in the wastewater treatments obtaining excellent results in the removal of different pollutants from water. The AOPs are based on the generation of hydroxyl radicals in order to degrade the organic matter using soft temperatures and pressures. The hydroxyl radicals are high reactive and non-selective oxidants that must be generated in the reaction medium continuously. Traditionally, the AOPs can be classified in chemical, electrochemical and photochemical processes depending on the hydroxyl radical generation.

Chemical processes

Fenton is based on the generation of hydroxyl radicals from the hydrogen peroxide decomposition in the presence of Fe^{2+} at acid pH giving rise the formation of Fe^{3+} (Reaction 1) (Neyens and Baeyens, 2003). Then, Fe^{3+} reacts with hydrogen peroxide giving rise

hydroperoxyl radicals regenerating the catalyst into Fe^{2+} (Reaction 2). Additionally, there are more reaction involves in the Fenton process, that can favor or reduce the availability of oxidant species (Babuponnusami and Muthukumar, 2014).

$$Fe^{2+} + H_2O_2 \rightarrow Fe^{3+} + HO^{\cdot} + HO^{-} \quad (1)$$

$$Fe^{3+} + H_2O_2 \rightarrow Fe^{2+} + HOO^{\cdot} + H^{+} \quad (2)$$

Fenton is a low cost and effective process for wastewater treatment. The organic matter is transformed into intermediates species and finally degraded to CO_2, H_2O and inorganic salts (if there is a heteroatom in the pollutant) (Mirzaei et al., 2017). The main highlights associated to Fenton are the cost of the Fe catalyst and the safe use of reactants, being the main drawbacks the cost of the hydrogen peroxide and the generation of Fe sludge (Salari et al., 2018; Ye et al., 2018). Fenton oxidation has been applied for the treatment of chemical, textile, food and pharmaceutical industry effluents (Ahmadi et al., 2005; Barbusiński and Filipek, 2001; Bautista et al., 2008).

The Catalytic Wet Peroxide Oxidation (CWPO) emerges as a heterogeneous system based on the Fenton process. The iron can be immobilized in different supports with the objective of eliminating the Fe sludge formation (Karthikeyan et al., 2013). Moreover, the Fe can be dispersed in small particle sizes, favoring the surface area in contact with the oxidant. Different supports have been studied, such as zeolites (Centi et al., 2000; Prihod'ko et al., 2011; Valkaj et al., 2011; Yan et al., 2015), pillared clays (Barrault et al., 2000; Carriazo et al., 2003; Khankhasaeva et al., 2017), silica (Crowther and Larachi, 2003; Satishkumar et al., 2013; Xiang et al., 2009), alumina (Bautista et al., 2011; Munoz et al., 2013) or carbon materials (Mena et al., 2016; Messele et al., 2014, 2012; Rey et al., 2011). The main drawback of this

process is the Fe leaching, leading to catalytic deactivation (Bautista et al., 2011; Mena et al., 2016).

Photochemical process

Photochemical processes rely on the generation of hydroxyl radicals by means of combining radiation, oxidants and/or catalysts. Different sources of radiation have been developed such as ultraviolet (UV), generated from artificial high or low-pressure lamps; or solar radiation, either natural or simulated. Processes involving radiation can be classified according to the oxidant species and catalyst used. Regarding the oxidant combined with radiation, the processes can be classified in UV combined with hydrogen peroxide (UV/H_2O_2), UV using persulfate (UV/PS), UV with peroxymonosulfate (UV/PMS), UV-aided chlorination (UV/chlorine), or photolytic ozonation (UV/O_3), among others. In the case of photocatalysis treatment, the titanium dioxide is the catalyst more researched (UV/TiO_2) (Vilhunen and Sillanpää, 2010; Wols and Hofman-Caris, 2012). Similar processes can apply modifying the radiation source towards more environmentally friendly options such as solar or visible radiation (Giannis et al., 2018; Kotzamanidi et al., 2018; Yuan et al., 2018).

In the UV/H_2O_2 process, radiation of enough energy is able to break the peroxy bond of hydrogen peroxide, triggering the formation of $HO^{\cdot}$ (Miklos et al., 2018). Some compounds, depending on the radiation applied, can undergo transformation by the irradiating source by itself. In the UV/PS process, the peroxy bond is also broken leading to the formation of two sulfate radicals (Reaction 3); therefore, hydroxyl radical can be generated in water from the reaction of water molecules and the generated sulfate radicals (Reaction 4 and 5) (Xie et al., 2015).

$$S_2O_8^{2-} + h\nu \rightarrow 2\ SO_4^{\cdot -} \quad (3)$$

$$SO_4^{\cdot -} + H2O \rightarrow SO_4^{2-} + HO^{\cdot} + H^+ \quad (4)$$

$$SO_4^{\cdot -} + HO^- \rightarrow SO_4^{2-} + HO^{\cdot} \quad (5)$$

The photocatalytic process starts with the activation of a semiconductor, TiO_2 generally, in which an electron is excited and moved to the conduction band, leaving in the valence band a deficit area of charge (named as hollow). The photogenerated e^- and h^+ launch a series of reactions that in water solution in presence of dissolved oxygen are describes as follows (Reactions 6 – 9) (An et al., 2018).

$$TiO_2 + h\nu \rightarrow e^- + h^+ \quad (6)$$

$$h^+ + H_2O \rightarrow HO^{\cdot} + H^+ \quad (7)$$

$$e^- + O_2 \rightarrow {\cdot}O_2^- \quad (8)$$

$$2\ {\cdot}O_2^- + 2\ H_2O \rightarrow 2\ HO^{\cdot} + 2\ HO^- + O_2 \quad (9)$$

With the objective of increasing the efficiency of the process and reducing the light energy requirements, the addition of different metal particles in the TiO_2 surface, such as Pt, Au or Pd has been studied in the photocatalytic treatment of wastewater (Sakthivel et al., 2004; Sood et al., 2015; Suri et al., 1993).

The main advantages of the photodegradation treatments lie on the operating conditions (mild temperature and pressure) (Hennig and Billing, 1993) being the main drawback of the process the cost associated to the radiation source, which can be solved by using solar radiation (Rey et al., 2014). The photodegradation processes have been effectively applied in petroleum refinery wastewater, pharmaceutical and personal care products effluents or food wastewater, among others (Kim et al., 2009; Krzemińska et al., 2015; Stepnowski et al., 2002).

Electrochemical process

In the last decades, the electrolytic technologies are considered as promising alternatives for the wastewater treatment. The simple operation and the high degradation degree of many harmful pollutants make the electrochemical techniques adequate to the wastewater treatment. Additionally, these processes do not involve excessive use of reagents, considering them as "green technologies" (Särkkä et al., 2015). However, the main drawbacks associated to the electrochemical process are related to the relative high cost compared with other AOPs and the formation of toxic intermediates (Cañizares et al., 2009; Wang et al., 2018).The hydroxyl radicals are generated in situ on the anode surface and can directly oxidize the pollutants (Reaction 10) (Candia-Onfray et al., 2018; Souza et al., 2017). In addition, indirect process can occur in the system, like the formation of hydrogen peroxide or ozone (Reactions 11 - 13).

$$H_2O \rightarrow HO\cdot + H^+ + e^- \quad (10)$$

$$2\ HO\cdot \rightarrow H_2O_2 \quad (11)$$

$$H_2O_2 \rightarrow O_2 + 2\ H^+ + 2e^- \quad (12)$$

$$O_2 + \cdot O \rightarrow O_3 \quad (13)$$

Moreover, the addition of different electrolytes in the reaction medium like the chloride or the sulfate anions can produce indirect species involved in the electroxidation process (Reactions 14 - 18) (Ganzenko et al., 2014; Sirés et al., 2014):

$$2\ Cl^- \rightarrow Cl_2 + 2e^- \quad (14)$$

$$Cl_2 + H_2O \rightarrow HOCl + H^+ + Cl^- \quad (15)$$

$$HOCl \rightarrow H^+ + OCl^- \quad (16)$$

$$2\ SO_4^{2-} \rightarrow S_2O_8^{2-} + 2\ e^- \quad (17)$$

$$2\ SO_4^{2-} + HO^{\cdot} \rightarrow S_2O_8^{2-} + HO^- + e^- \quad (18)$$

Different anodes materials have been studied in the wastewater treatment, such Pt, IrO_2, graphite, PbO_2, SnO_2, TiO_2 or boron doped diamond (BDD) (Anglada et al., 2009), being determinant in the efficiency and the selectivity of the electroxidation (Brillas and Martínez-Huitle, 2015). The electrolytic treatments have been also applied in refinery, pharmaceutical and food wastewater obtaining high degradation rates (Al-Malack and Siddiqui, 2013; Can, 2014; Linares-Hernández et al., 2010; Pérez et al., 2017).

1.2. AOPs for ILs wastewater

Fenton and Catalytic Wet Peroxide Oxidation of ILs

Table 1.2 collects the main results obtained in the IL degradation by means of Fenton and CWPO. The variables studied in these processes are the IL composition (cations and anions), the concentration of H_2O_2 employed, the amount and type of catalyst, the pH value and the temperature used.

Table 1.2. Summary of researches on IL degradation based on Fenton and CWPO.

IL	Conditions	Process Catalyst	IL´s cation removal (%/reaction time)	Mineralization (%)	Main results	Reference
1-Butyl-3-methylimidazolium chloride	$[IL]_0$ = 1 mM, $[H_2O_2]_0$ = 100 mM, V = 0.3 L, T = 25 ºC, pH: 3	Fenton $Fe(ClO_4)_3$ 0.5-1.5 mM	80-100/150 min	-	The increase Fe^{3+} concentration from 0.5 to 1.5mM induced the increased rate of degradation of the IL.	(Siedlecka et al., 2008)
	$[IL]_0$ = 1 mM, $[H_2O_2]_0$ = 10 - 400 mM, V = 0.3 L, T = 25 ºC, pH: 3	Fenton $Fe(ClO_4)_3$ 1 mM	22-100/90 min	-	Higher H_2O_2 dose lead to the oxidation not only by reaction with $HO^{\cdot}$ radicals, but with other radical species generated in vigorous Fenton	
	$[IL]_0$ = 1 mM, $[H_2O_2]_0$ = 400 mM, V = 0.3 L, T = 25 ºC, pH: 3-4	Fenton $Fe(ClO_4)_3$ 1 mM	70-100/150 min	-	High IL degradation rate at pH 3.5, against pH 3 and 4.	
1-Butyl-3-methylimidazolium chloride 1-Butyl-3-methylimidazolium trifluoromethanesulfonate 1-Butyl-3-methylimidazolium tricyanomethanide	$[IL]_0$ = 1 mM, $[H_2O_2]_0$ = 100 mM, V = 0.3 L, T = 25 ºC, pH: 3	Fenton $Fe(ClO_4)_3$ 1 mM	100/45-150 min	-	The rate of 1-Butyl-3-methyl-imidazolium degradation in Fenton-like systems is influenced by the anions as follows: $Cl^- > C(CN)_3^- > CF_3SO_3^-$	(Siedlecka et al., 2009)

Table 1.2. Continued

IL	Conditions	Process Catalyst	IL´s cation removal (%/reaction time)	Mineralization (%)	Main results	Reference
1-Ethyl-3-methylimidazolium chloride 1-Butyl-3-methylimidazolium chloride 1-Methyl-3-octylimidazolium chloride 1-Dodecyl-3-methylimidazolium chloride 1-Methyl-3-tetradecylimidazolium chloride 1-Hexadecyl-3-methylimidazolium chloride 1-Butyl-3-methylimidazolium methanesulfonate 1-Butyl-3-methylimidazolium methylsulfate 1-Butyl-3-methylimidazolium acetate	$[IL]_0$ = 1000 mg L^{-1}, $[H_2O_2]_0$ = stoichiometric dose, V = 0.05 L, T = 70 ºC, pH: 3, 240 min	Fenton $Fe(NO_3)_3$ 50 mg L^{-1}	85-100/240 min	10-65 (TOC)	The rate of mineralization increased with the length of the alkyl chain. The nature of the anion also affected the mineralization showing a particularly remarkable effect in the case of acetate, where a very low reduction of TOC (10 %) was reached.	(Dominguez et al., 2014)
1-Ethyl-3-methylimidazolium chloride	$[IL]_0$ = 1000 mg L^{-1}, $[H_2O_2]_0$ = stoichiometric dose, V = 0.5 L, T = 50-90 ºC, pH: 3, 240 min	Fenton $Fe(NO_3)_3$ 50 mg L^{-1}	100/0.25-5 min	48-54 (TOC)	Increasing the temperature improved the IL degradation.	(Munoz et al., 2015a)
	$[IL]_0$ = 1000 mg L^{-1}, $[H_2O_2]_0$ = stoichiometric dose, V = 0.5 L, T = 70 ºC, pH: 3, 240 min	Fenton $Fe(NO_3)_3$ 10-125 mg L^{-1}	-	18-56 (TOC)	The use of very low iron concentrations leads to increase reaction times to achieve acceptable efficiencies.	

Table 1.2. Continued

IL	Conditions	Process Catalyst	IL´s cation removal (%/reaction time)	Mineralization (%)	Main results	Reference
1-Butyl-4-methypyridinium chloride Tetrabutylammonium chloride Tetrabutylphosphonium chloride	$[IL]_0$ = 1000 mg L^{-1}, $[H_2O_2]_0$ = stoichiometric dose, V = 0.5 L, T = 70 ºC, pH: 3, 240 min	Fenton $Fe(NO_3)_3$ 50 mg L^{-1}	100/<10 min	28-45 (TOC)	Different mineralization percentages were achieved for the different families, being the phosphonium core the most difficult to degrade.	
1-Ethyl-3-methylimidazolium chloride 1-Butyl-4-methylpyridinium chloride 1-Ethyl-3-methylimidazolium tetracyanoborate 1-Ethyl-3-methylimidazolium dicyanamide 1-Ethyl-3-methylimidazolium tricyanomethanide 1-Ethyl-3-methylimidazolium thiocyanate 1-Ethyl-3-methylimidazolium dimethylphosphate 1-Ethyl-3-methylimidazolium p-toluenesulfonate Tetrabutylammonium chloride Tetrabutylphosphonium chloride Choline chloride	$[IL]_0$ = 1000 mg L^{-1}, $[H_2O_2]_0$ = stoichiometric dose, V = 0.05 L, T = 70 ºC, pH: 3, 240 min	Fenton $Fe(NO_3)_3$ 50 mg L^{-1}	-	44-80 (TOC)	Aromatic ILs are more readily oxidized than the aliphatic ones, due to the presence of unsaturated bonds.	(Munoz et al., 2015b)
1-Ethyl-3-methylimidazolium hexafluorophosphate	$[IL]_0$ = 2mM, $[H_2O_2]_0$ = 20 mM, T = 25 ºC, pH: 3-11, 120 min	Fenton $FeSO_4$ 1 mM	35-55/120 min	-	As the solution pH increased from 3.0 to 11.0, the degradation efficiency decreased gradually.	(Cheng et al., 2016)

Table 1.2. Continued

IL	Conditions	Process Catalyst	IL´s cation removal (%/reaction time)	Mineralization (%)	Main results	Reference
	$[IL]_0$ = 2mM, $[H_2O_2]_0$ = 20 mM, T = 40 ºC, pH: 3, 120 min	Fenton $FeSO_4$ 0.5-5 mM	31-89/120 min	-	Increasing Fe concentration accelerates the decomposition of H_2O_2 and induces higher availability of $HO^{\cdot}$	
	$[IL]_0$ = 2mM, $[H_2O_2]_0$ = 5-50 mM, T = 40 ºC, pH: 3, 120 min	Fenton $FeSO_4$ 1 mM	34-73/120 min	-	An increase in the H_2O_2 concentration produces an increase in the IL degradation.	
	$[IL]_0$ = 0.5-10 mM $[H_2O_2]_0$ = 20 mM, T = 40 ºC, pH: 3 120 min	Fenton $FeSO_4$ 5 mM	28-97/120 min	49-52 (TOC)	As the IL concentration increased, the amount of the hydroxyl radical was insufficient for oxidizing the substrates.	
	$[IL]_0$ = 2 mM, $[H_2O_2]_0$ = 20 mM, T = 25-70 ºC, pH: 3 120 min	Fenton $FeSO_4$ 2 mM	28-96/120 min	-	High temperature can increase the efficiency of hydrogen peroxide consumption and reduce the reaction time.	
1-Ethyl-3-methylimidazolium hexafluorophosphate 1-Ethyl-3-methylimidazolium acetate 1-Ethyl-3-methylimidazolium trifuoroacetate 1-Ethyl-3-methylimidazolium methanesulfonate 1-Ethyl-3-methylimidazolium trifuoromethanesulfonate	$[IL]_0$ = 1 mM, $[H_2O_2]_0$ = 20 mM, T = 40 ºC, pH: 3 60 min	Fenton $FeSO_4$ 5 mM	82-92/60 min	-	The counter-anion nature does not have great influence in the degradation efficiency.	

Table 1.2. Continued

IL	Conditions	Process Catalyst	IL´s cation removal (%/reaction time)	Mineralization (%)	Main results	Reference
1-Butyl-3-methylimidazolium chloride	$[IL]_0$ = 100-2000 mg L^{-1}, $[H_2O_2]_0$ = stoichiometric dose, V = 0.05 L, T = 70 ºC, pH: 3	Fenton $Fe(NO_3)_3$ 50 mg L^{-1}	100/4 min	-	The IL conversion is independent of the initial concentration tested indicating that IL oxidation by the Fenton process follows a first order reaction with respect to the initial pollutant concentration	(Domínguez et al., 2017)
	$[IL]_0$ = 1000 mg L^{-1}, $[H_2O_2]_0$ = 50-200 % stoich. dose, V = 0.05 L, T = 70 ºC, pH: 3	Fenton $Fe(NO_3)_3$ 50 mg L^{-1}	91-100/1-4 min	-	The IL oxidation rate gradually increased with the H_2O_2 concentration due to the higher amount of oxidant species ($HO^{\cdot}$ and $HOO^{\cdot}$) in the reaction medium.	
	$[IL]_0$ = 1000 mg L^{-1}, $[H_2O_2]_0$ = stoichiometric dose, V = 0.05 L, T = 70 ºC, pH: 3	Fenton $Fe(NO_3)_3$ 10-50 mg L^{-1}	75-100/4 min	-	IL degradation rate increased with iron load, as a result of the higher amount of actives sites available for the decomposition of hydrogen peroxide.	
	$[IL]_0$ = 1000 mg L^{-1}, $[H_2O_2]_0$ = stoichiometric dose, V = 0.05 L, T = 50-90 ºC, pH: 3	Fenton $Fe(NO_3)_3$ 50 mg L^{-1}	86-100/1.5-5 min	-	The IL degradation rate increased with the temperature.	

Table 1.2. Continued

IL	Conditions	Process Catalyst	IL´s cation removal (%/reaction time)	Mineralization (%)	Main results	Reference
1-Hexyl-3-methylimidazolium chloride	$[IL]_0$ = 1000 mg L^{-1}, $[H_2O_2]_0$ = 20-100% stoich. dose, V = 1 L, T = 70 ºC, pH: 3	Fenton $Fe(NO_3)_3$ Fe^{3+}/H_2O_2: 1/10 (M/M)	58-100/240 min	6-53 (TOC)	The use of high H_2O_2 dose produced the complete conversion of both ILs, although the imidazolium IL showed greater resistance to be removed than the pyridinium.	(Gomez-Herrero et al., 2018)
1-Butyl-4-methylpyridinium chloride	$[IL]_0$ = 1000 mg L^{-1}, $[H_2O_2]_0$ = 20-100% stoich. dose, V = 1 L, T = 70 ºC, pH: 3	Fenton $Fe(NO_3)_3$ Fe^{3+}/H_2O_2: 1/10 (M/M)	93-100/240 min	2-41 (TOC)		
1-Ethyl-3-methylimidazolium chloride	$[IL]_0$ = 1000 mg L^{-1}, $[H_2O_2]_0$ = 20-100% stoich. dose, V = 1 L, T = 70 ºC, pH: 3	Fenton $Fe(NO_3)_3$ Fe^{3+}/H_2O_2: 1/10 (M/M)	92-100/240 min	15-50 (TOC) 23-62 (COD) 7-41 (TN)	The increase of oxidant produced a higher mineralization of the IL.	(Gomez-Herrero et al., 2019)

Table 1.2. Continued

IL	Conditions	Process Catalyst	IL´s cation removal (%/reaction time)	Mineralization (%)		Main results	Reference
1-Ethyl-3-methylimidazolium chloride 1-Butyl-3-methylimidazolium chloride 1-Octyl-3-methylimidazolium chloride 1-Hexadecyl-3-methylimidazolium chloride	$[IL]_0$ = 1000 mg L^{-1}, $[H_2O_2]_0$ = stoichiometric dose, V = 0.07 L, T = 90 ºC, pH: 3 240 min	CWPO Fe_3O_4/γ-Al_2O_3 2 g L^{-1}	100/30-60 min	33-44 (TOC)	A decay on the mineralization with increasing alkyl chain length was observed using both catalysts. Fe_3O_4/γ-Al_2O_3 is the most stable catalyst, with a leached iron concentration of 0.25mg L^{-1} at 4 h.	(Munoz et al., 2016)
		CWPO Graphite 2 g L^{-1}	100/30 min	36-53 (TOC)		

The first study based on the degradation of ILs by Fenton corresponds to Siedlecka et al. (2008). They investigated the degradation of the 1-Butyl-3-methylimidazolium chloride modifying the Fe concentration, the hydrogen peroxide concentration and the pH value, obtaining the best results with higher Fe and H_2O_2 concentrations (1.5 mM and 400 mM, respectively) and a pH value of 3.5. Chen et al. (2016) obtained similar results in the 1-Ethyl-3-methylimidazolium hexafluorophosphate degradation by Fenton. Moreover, they modified the substrate concentration, being the degradation less efficient when the initial IL concentration increased; and the reaction temperature, being the process more effective when the temperature increased from 20 to 80 ºC. The relevance of the IL's nature (composition) in order to be transformed by Fenton was studied, firstly in terms of cation family, and then, analyzing the influence of the alkyl side chain on the degradation process. Munoz et al. (2015 a, b) studied the degradation of 4 IL families: the imidazolium, the pyridinium, the phosphonium and the ammonium. They appreciated that the aromatics cations are more readily oxidizables than aliphatic ones, due to the presence in their structure of the double bounds. At the same conditions, the choline and phosphonium IL families presented the lowest mineralization in Fenton reaction. Dominguez et al. (2014) studied the structure of the imidazolium ILs in the Fenton reaction, obtaining that the mineralization rate increased when the alkyl side chain increased. Regarding the anion, the following rules of thumbs have been obtained from different studies: i) the influence of the anion was lower than the nature of the cation in the ILs degradation, ii) aromatic anions could be degraded by Fenton obtaining high mineralization degree and iii) if a IL consisted of an organic anion refractory to Fenton process, such as

acetate, TOC conversion is reduced (Cheng et al., 2016; Dominguez et al., 2014; Munoz et al., 2015b; Siedlecka et al., 2009).

The IL CWPO has been studied in minor extent than Fenton process. Munoz et al. (2016) evaluated the influence of the alkyl side chain of the imidazolium ILs using graphene and an iron oxide supported on alumina catalyst. CWPO reaction rates were slower than the homogeneous ones and it was appreciated a decay on the mineralization with increasing alkyl chain length, an opposite trend respect to the observed in the Fenton reaction. Higher CWPO reaction rates were obtained using graphene as catalyst compared to Fe_2O_3/γ-Al_2O_3, whereas the latter showed higher stability due to the negligible Fe leaching.

Photolysis and photocatalysis of ILs

The Table 1.3 collects the main results obtained in ILs degradation in aqueous phase by means of phototreatments, in terms of IL concentration and composition (cations and anions), the sources of radiation, the oxidant species used, the concentration and type of catalyst, the pH value or the reaction matrix.

Table 1.3. Summary of researches on IL degradation based on phototreatments.

IL	Operating conditions	Process/Catalyst concentration	IL cation removal (%/time)	Degradation (%)	Main results	Reference
1-Butyl-3-methylimidazolium chloride 1-Hexyl-3-methylimidazolium chloride 1-Methyl-3-octylimidazolium chloride 1-Ethyl-3-ethylimidazolium tetrafluoroborate 1-Methylimidazolium	$[IL]_0$ = 1 mM, V = 0.1 L, T = 16 ºC, Xe Lamp 1000W	UV	8-58/360min	-	An increase in the alkyl chain (from 4 to 8 carbons) produces a reduction in the IL degradation. The 1-Butyl-3-methylimidazolium was the most easily degradable IL.	(Stepnowski and Zaleska, 2005)
		UV/H_2O_2 0.05 %	40-85/360 min	-	The lower extent of the reaction happened with the 1-ethyl-3-ethylimidazolium, and when the alkyl chain increases, the degradation rate decayed.	
		UV/TiO_2 P25 500 mg L^{-1}	16-100/180-360 min	-	Degradation of ionic liquids in the UV/TiO_2 system is much slower than UV-H_2O_2, except for the 1-Butyl-3-methylimidazolium chloride.	

Table 1.3. Continued

IL	Operating conditions	Process/Catalyst concentration	IL cation removal (%/time)	Degradation (%)	Main results	Reference
1-Ethyl-3-methylimidazolium chloride 1-Butyl-3-methylimidazolium chloride 1-Hexyl-3-methylimidazolium chloride 1-Methyl-3-octylimidazolium chloride	$[IL]_0$ = 1 mM, V = 0.25 L, T = 16 ºC, UV Lamp 3x20W λ = 254-366 nm	UV/H_2O_2 0.2 %	-	-	This study is focused on thededuction of the IL pathway, being the continuation of the Stepnowski et al. (2005) study.	(Czerwicka et al., 2009)
1-Ethyl-3-methylimidazolium bromide 1-Ethyl-3-methylimidazolium hexafluorophosphate 1-Butyl-3-methylimidazolium tetrafluoroborate	$[IL]_0$ = 20 mg L^{-1}, V = 0.01 L, T = room temperature, 300W Xe Lamp λ = 220-400 nm	UV/TiO_2 10 g L^{-1}	100/24 h	-	Using the Pt/TiO_2, a complete removal was achieved in 24 h except for the 1-Ethyl-3-methylimidazolium bromide.	(Itakura et al., 2009)
		$UV/Pt/TiO_2$ 10 g L^{-1}	88-100/24 h	-		
1-Butyl-3-methylimidazolium salicylate	$[IL]_0$ = 0.38 mM, V = 0.03 L, T = 25 ºC, pH = 2.8, a) UVA High-pressure mercury lamp 125 W λ > 290 nm b) Simulated sunlight (SS) four 35 W halogen lamp λ > 300 nm	UVA/H_2O_2 45 mM+0.7 μL h^{-1} UVA/TiO_2 P25 (1.67 g L^{-1}) $UVA/H_2O_2/Fe/TiO_2$ 45 mM+70 μL h^{-1} + Fe/TiO_2 (1.67 g L^{-1})	40-100/180 min	-	The anion was completely degraded in all cases except for UVA photolysis. In terms of cation, the most efficient degradation process was H_2O_2 coupled with Fe/TiO_2 catalysts.	(Banić et al., 2016)

Table 1.3. Continued

IL	Operating conditions	Process/Catalyst concentration	IL cation removal (%/time)	Degradation (%)	Main results	Reference
		SS/H_2O_2 45 mM+0.7 µL h^{-1} SS/TiO_2 P25 (1.67 g L^{-1}) $SS/H_2O_2/Fe/TiO_2$ 45 mM+70 µL h^{-1} + Fe/TiO_2 (1.67 g L^{-1})	10-30/180 min	-	Ionic liquid photodegradation efficiency was significantly lower using SS radiation than UVA radiation.	
		$SS/H_2O_2/Fe/TiO_2$ 45 mM+70 µL h^{-1} + Fe/TiO_2 (1.67 g L^{-1}) Tap, condensate, pond, river and rain water	50-60/180 min	-	The ionic liquid degradation was increased due to the powerful sensitization effect for the presence of DOC together with SS radiation.	
Imidazole 1-Methylimidazole 1-Ethyl-3-methyl-imidazolium chloride 1-Butyl-3-methyl-imidazolium chloride	[IL] = 150 mg L^{-1}, V = 0.48 L, T = 25 ºC, pH = 5.5-8.5, UVC Lamp 17W λ = 254 nm	UVC/H_2O_2 36 mM	100/21-82 min	22-42 (TOC) 38-56 (COD)	Ecotoxicity analysis indicate that the effluents were more toxic than the initial solution ones.	(Spasiano et al., 2016)

Table 1.3. Continued

IL	Operating conditions	Process/Catalyst concentration	IL cation removal (%/time)	Degradation (%)	Main results	Reference
1-Butyl-3-methyl-imidazolium chloride	[IL] = 1-5 mM, pH = 3-12, Simulated sunlight (SS) 500 W halogen lamp λ = mainly 400-600 nm	SS/Fe/TiO_2/AC (0-0.5 wt % Fe, 0.5-8 g L^{-1})	13-36/120 min	-	Selection of the optimum reaction conditions: 0.2 wt. % Fe and pH 10.	(Zawawi et al., 2017)
1-Hexyl-3-methylimidazolium chloride	[IL] = 10 µM, pH = 7, Simulated sunlight (SS) Xe Lamp 765 W m^{-2} λ > 290 nm	SS in ultrapure water, wastewater effluent and river water	13-80/60 min	-	The contribution of indirect photochemical transformation ranged between 81% and 94% of total degradation.	(Pati and Arnold, 2017)
1-Ethyl-3-methyl-imidazolium chloride 1-Butyl-3-methyl-imidazolium chloride 1-Methyl-3-octylimidazolium chloride 1-Decyl-3-methyl-imidazolium chloride		SS/H_2O_2 1 mM + 10 µM benzoic acid	33-67/50 min	-	An increase in the alkyl chain produces an increase in the IL degradation.	
1-Butylpyridinium chloride 1-Butyl-1-methylpyrrolidinium chloride 1-Butyl-1-methylpiperidinium bromide		SS/H_2O_2 1 mM + 10 µM benzoic acid	19-25/50 min	-	Degradation of pyridinium, pyrrolidinium and piperidinium were smaller than imidazolium	

Table 1.3. Continued

IL	Operating conditions	Process/Catalyst concentration	IL cation removal (%/time)	Degradation (%)	Main results	Reference
1-Ethyl-3-methyl-imidazolium chloride 1-Butyl-3-methyl-imidazolium chloride 1-Hexyl-3-methylimidazolium chloride 1-Methyl-3-octylimidazolium chloride 1-Decyl-1-methylpyrrolidinium chloride 1-Butylpyridinium chloride 1-Butyl-1-methylpyrrolidinium bromide 1-Butyl-1-methylpiperidinium bromide	[IL] = 10-20 μM, pH = 7, Mercury Lamp 450 W λ > 280 nm	UV/H_2O_2 1 mM	10-50/20 min	-	The presence of an additional N atom caused an increase oxidability of that imidazolium rings.	(Pati and Arnold, 2018)
		UV/persulfate 1 mM $K_2S_2O_8$	45-90/20 min	-		
		UV/chlorine 150 μM NaClO	25-90/20 min	-		
1-Ethyl-3-methylimidazolium chloride 1-Butyl-3-methylimidazolium chloride 1-Decyl-3-methylimidazolium chloride, 1-Butyl-3-methylimidazolium tetrafluoroborate 1-Butyl-3-methylimidazolium tris(pentafluoroethyl)trifluorophosphate, 1-Allyl-3-methylimidazolium chloride 1-(2-Hydroxyethyl)-3-methylimidazolium chloride 1-Butyl-4-methylpyridinium chloride	[IL] = 20 mg L^{-1}, T = 35 °C, Simulated sunlight (SS) Xe Lamp 450 W m^{-2} λ = 320-800 nm	SS	10-65/600 min	4-38/600 min	The IL can be degraded completely by means of photocatalyst using SS in 600 min with a relative low TiO_2 concentration. The pyridinium IL was more susceptible to the treatment. The presence of an OH group in the alkyl chain reduced the degradation.	(Bedia et al., 2019)
		SS/TiO_2 75 mg L^{-1}	100/600 min	30-80/600 min		

Table 1.3. Continued

IL	Operating conditions	Process/Catalyst concentration	IL cation removal (%/time)	Degradation (%)	Main results	Reference
1-Butyl-3-methylimidazolium chloride 1-Butyl-3-methylimidazolium hexafluorophosphate 1-Butyl-3-methylimidazolium bis(trifluoromethylsulfonyl)imide 1-Butyl-2,3-dimethylimidazolium chloride 1-Butyl-2,3-dimethylimidazolium bis(trifluoromethylsulfonyl)imide	[IL] = 20 mg L^{-1}, T=30 ºC, UV Lamp 125 W 61.8 W m^{-2} Mercury Lamp 125 W 202 W m^{-2} λ > 380 nm	UV Visible radiation	33-50/120 min	-	Photocatalyst doped with Mg obtained by the impregnation of a petrochemical residue on fumed silica exhibited high stability and caused a reduction of toxicity of the effluents.	(Leonardo da Silva et al., 2019)
		UV/P25 Visible radiation/P25	40-50/120 min	-		
		UV/Mg/SiO_2TiO_2 Visible radiation /Mg/SiO_2TiO_2	65/120 min	-		

The direct photolysis of ILs using UV light has been studied by Stepnowski and Zalenska (2005). The degradation of the 1-Butyl-3-methylimidazolium cation was higher than the obtained for longer alkyl chains. The direct photolysis was also studied by Banic et al. (2016) and Leonardo da Silva et al. (2019) obtaining as best result a 50 % in the degradation of 1-Butyl-3-methylimidazolium chloride in 120 min.

The effect of the H_2O_2 on the direct photodegradation has been widely studied by several authors. Stepnowski et al. (2005) and Czerwicka et al. (2009) evidenced the improvement of the UV/H_2O_2 process in the oxidation of ILs, obtaining lower degradation as the alkyl side chain increased. The addition of H_2O_2 in the UVA photolysis of 1-Butyl-3-methylimidazolium salicylate led to an improvement of 44 % if compared to the 5 % observed during UVA-photolysis in 180 min (Banić et al., 2016). Regarding the mineralization extent in the UV/H_2O_2 system, Spassiano et al. (2016) achieved TOC reductions of 37 and 22 % for 1-Ethyl-3-methylimidazolium chloride and 1-Butyl-3-methylimidazolium chloride in 54 and 42 min, respectively. Moreover, the effluents obtained after treatment by the UV/H_2O_2 system are generally more toxic than the initial ones, due to the intermediates produced are more hazardous as consequence of an incomplete oxidation. Pati and Arnold (2018) compared the degradation of imidazolium-, pyridinium-, pyrrolidinium- and piperidinium-based ILs, obtaining better results in the degradation of the imidazolium one than in the others. Moreover, they combined the UV photolysis with persulfate and chlorine resulting in an improvement on the degradation of the process respect with the H_2O_2 process.

The phototocatalytic process for ILs oxidation with oxygen using UV radiation and TiO_2 as photocatalyst was first studied by Stepnowski et al. (2005), and followed by Itakura et al., (2008) Banic et al. (2016) and

Leonardo da Silva et al. (2019). From the results achieved, photocatalysis seems to be less efficient than the UV/H_2O_2 process. However, after addition of H_2O_2 to the photocatalytic process, the results were improved. Moreover, the modification of the TiO_2 catalyst doping with Fe or Pt caused a slightly reduction in the photocatalysis treatment with UV, whereas the doping with Mg improved considerably the cation degradation.

The treatment of ILs in wastewater accomplished with simulated sunlight (SS) has been studied by many authors. Bedia et al. (2019) studied the photo-stability of the ILs under solar radiation. It was concluded that ILs are stable after being irradiated with SS for a long time, except for 1-Butyl-3-methylimidazolium tris(pentafluoroethyl)trifluorophosphate, due to its strong hydrophobic character. When adding TiO_2 to the system, a complete degradation of the non-photolyzed IL cations was achieved. Moreover, the mineralization extent varied depending on the target IL between 30-80 % in 600 min. In general, the application of SS seems to be less effective than UV. For example, Banic et al. (2016) studied the processes SS/H_2O_2 and SS/photocatalysis in the degradation of 1-Butyl-3-methylimidazolium cation, observing less efficiency when irradiating with SS if compared to UVA (44 versus 100% degradation for SS/H_2O_2 and UVA/H_2O_2, respectively; and 10 versus 30% for photocatalysis with SS versus UVA). However, the use of tap, condensate, pond, river and rain water with SS produced an increase of the cation removal, achieving values of 50-60 % in 180 min. Pati and Arnold (2017) also reported the same behavior with the 1-Hexyl-3-methylimidazolium cation, obtaining 13 % of cation conversion in ultrapure water at 60 min and 50-80 % in wastewater and river water. Moreover, the enlarged in the alkyl side chain from 2 to 10 carbon atoms produced an increment

from 33 to 67 % of cation degradation, under the system SS/H_2O_2. Furthermore, the degradation of cations such as 1-Butylpyridinium, 1-Butyl-1-methylpyrrolidinium or 1-Butyl-1-methylpiperidinium is lower than imidazolium one. Zawawi et al. (2017) studied the influence of the Fe presence in the titanium dioxide supported onto oxidized activated carbon (TiO_2/AC) catalyst for the SS/phtotocatalytic process. The better result was obtained when Fe concentration in the photocatalyst correspond to 0.2 wt % and the pH of the process was 10.

Electrotreatment of ILs

Table 1.4 collects the anodic electrolysis, and its improvement with UV light and high frequency ultrasounds in the ILs degradation. The reaction evolution is evaluated in terms of time or applied charge (Q, A h L^{-1}). The main variables studied in these processes are the IL composition (cations and anions), the electrode material, the temperature or the type and concentration of electrolyte used.

Table 1.4. Summary of researches on IL degradation based on anodic oxidation.

IL	Conditions	Anodic material	IL cation removal (%/time)	Degradation (%)	Main results	Reference
1-Butyl-3-methylimidazolium chloride 1-Methyl-3-octylimidazolium chloride 1-(3-Hydroxypropyl)-3-methylimidazolium chloride 1-(2-Ethoxyethyl)-3-methylimidazolium bromide 1-Benzyl-3-methylimidazolium chloride 1-Methylimidazolium	[IL] = 0.21 mM, 22 mA/cm^2, V = 0.73 L, T = 28 ºC, [Na_2SO_4] = 87 mM	PbO_2 145 cm^2	100/<45-240 min	69-97 (COD)	The imidazolium core was less likely to be attacked when the substituted side chain increased.	(Siedlecka et al., 2012)
1-Butyl-3-methylimidazolium chloride 1-Butyl-3-methylimidazolium bromide 1-Butyl-3-methylimidazolium triflate 1-Butyl-3-methylimidazolium tetrafluoroborate 1-Butyl-3-methylimidazolium hexafluorophosphate 1-Butyl-3-methylimidazolium p-toluenesulfonate	[IL] = 0.24 mM, 16 mA/cm^2, V = 0.385 L, T = 25 ºC, [Na_2SO_4] = 0.87 mM	BDD 10 cm^2	80-100/180 min	-	The influence of the anion in the reaction rates was the following: Cl^- > Br^- > BF_4^- > PF_6^- > triflate > p-toluenesulfonate. Moreover, the p-toluenesulphonate anion competed with the imidazolium cation for $HO^·$ radicals	(Fabiańska et al., 2012)
1-Methylimidazolium	[IL] = 0.24 mM, 16 mA/cm^2, V = 0.385 L, T = 25 ºC, [Na_2SO_4] = 17 mM [$NaClO_4$] = 87 mM	BDD 10 cm^2	Only Na_2SO_4: 42/180 min Na_2SO_4+ $NaClO_4$ 48/180 min	-	The presence of $NaClO_4$ favored the $HO^·$ radical generation at the BDD anode.	

Table 1.4. Continued

IL	Conditions	Anodic material	IL cation removal (%/time)	Degradation (%)	Main results	Reference
1-Butyl-3-methylimidazolium tetrafluoroborate	[IL] = 0.48 mM, 16 mA/cm^2, V = 0.385 L, T = 25 ºC, [Na_2SO_4] = 87 mM [Cl^-] = 17 mM [Br^-] = 17 mM	BDD 10 cm^2	Only Na_2SO_4: 93/180 min Na_2SO_4 + Cl^- 100/180 min Na_2SO_4 + Br^- 100/180 min	-	The active halogen species oxidized organic compounds but they were unable to mineralize them. ILs could be mineralized with halogen radicals (·Cl, ·Br) and dihalogen radicals ($Cl_2^{\cdot-}$, $Br_2^{\cdot-}$)	
1-Butyl-3-methylimidazolium chloride	[IL] = 0.21 mM, 8-24 mA/cm^2, [Na_2SO_4] = 87 mM	IrPt, 145 cm^2	30-98/7-25 AhL^{-1}	0-40 (COD)	High electrical charge was consumed for total IL degradation. Additionally, it was obtained lower oxidation rate.	(Siedlecka et al., 2013)
	[IL] = 0.21 mM, 8-16 mA/cm^2, [Na_2SO_4] = 87 mM	IrO_2 145 cm^2	45-70/5-8 AhL^{-1}	15-20 (COD)	The anion was oxidized to chlorine species and cation was decomposed. The anode was deactivated by deposition of organic matter on the surface.	
	[IL] = 0.21 mM, 8-16 mA/cm^2, [Na_2SO_4] = 87 mM	PbO_2 145 cm^2	75-95/4-8.5 AhL^{-1}	45-60 (COD)	In contrast to "non-active" electrodes, oxidation with PbO_2 electrodes did not remove aromaticity in IL.	

Table 1.4. Continued

IL	Conditions	Anodic material	IL cation removal (%/time)	Degradation (%)	Main results	Reference
	[IL] = 0.21 mM, 8-24 mA/cm^2, [Na_2SO_4] = 87 mM	Si/BDD 10 cm^2	90-100/3-7 AhL^{-1}	80 (COD)	The Si/BDD anodes presented high activity. The HO$^{\cdot}$ radical concentration is closely correlated with COD removal, generating the main oxidants on the anode surface.	
1-Butyl-3-methylimidazolium chloride 1-Hexyl-3-methylimidazolium chloride 1-Methyl-3-(2-phenylethyl)imidazolium chloride 1-Butyl-4-methylpyridinium chloride 1-Butyl-4-(dimethylamino)pyridinium chloride	[IL] = 0.21 mM, 16 mA/cm^2, V = 0.10 L, T = 25-60 ºC, pH = 3.5-9.0, [Na_2SO_4] = 3.5 g L^{-1}	BDD 10 cm^2	100/180 min	-	There was no temperature influence while alkaline conditions caused a decrease in the removal rate. The pyridinium degradation rates were higher than imidazolium ones.	(Pieczyńska et al., 2015)

Siedlecka et al. (2012) can be considered as the first study focused on the ILs degradation based on anodic oxidation. The electroxidation of several imidazolium ILs were carried out using a PbO_2 anode (145 cm^2) and Na_2SO_4 as electrolyte (87 mM). The ILs studied were completely removed obtaining 69-97 % of degradation in terms of COD. When the alkyl side chain increased from 4 to 8 C atoms, the degradation was less effective, and the incorporation of an ether group in the alkyl side chain produced a greater resistance to oxidation. In another study, Siedlecka et al. (2013) investigated the use of different anode materials varying the current density and using Na_2SO_4 as electrolyte (87 mM). The IrPt and IrO_2 anodes were not effective and were deactivated in the 1-Butyl-3-methylimidazolium chloride degradation. The PbO_2 anode was able to transform the IL, but the aromaticity in the IL was not completely removed. The best result were achieved using the BDD anode (χ_{COD}: 80 %) of all anodes studied in this work. The influence of the cation family was evaluated by Pieczyńska et al. (2015). The imidazolium cation was more stable than the pyridinium one, and generally, similar degradation rates were obtained for the ILs of the same family. Additionally, they evaluated the effect of pH and the reaction temperature on the process. A pH value of 6 was selected as optimum while no influence of temperature (25-60 ºC) was detected.

The influence of the anion was studied by Fabianska et al. (2012), using 6 different ILs with 1-Butyl-3-methylimidazolium as cation in the presence of Na_2SO_4 as electrolyte. The use of chloride anion favored the degradation of the cation for the possible formation of chlorine, hypochlorous and hypochlorite species, actives in the degradation of organic matter. On the other hand, the p-toluenesulphonate anion had a negative influence on the cation degradation due to the competition with the cation to be oxidized, being faster the degradation of the anion

than the cation. ILs constituted by fluorinated and bromide anions did not cause any effect on the cation degradation, because of they are not involved in the reaction.

Combined treatments

The combination of different AOPs has been studied in order to overcome the drawbacks of the single treatments. Among them, the anodic oxidation combined with cathodic hydrogen peroxide process merges the degradation of the electrolysis treatment with the generation of hydrogen peroxide from the oxygen reduction using carbonaceous cathodes (Yahya et al., 2014). This process can be enhanced with the addition of Fe^{2+} salts to produce the Fenton reaction (Cruz-González et al., 2012). This process is known as electroFenton process. The application of UV light in the electroFenton gives rise to photoelectroFenton, producing the decarboxylation of Fe(III) complexed generated in the degradation of heteroaromatic compounds (Martínez-Pachón et al., 2018). Moreover, heterogeneous electroFenton process has been also studied to overcome the main drawbacks associated to homogenous process (the removal of Fe in the final effluent and its recovery) (Ganiyu et al., 2018).

Table 5 collects the main results obtained in the ILs degradation by means of the combination of different AOPs. The variables studied in these processes are the IL composition (cations and anions), intensity, the amount and type of catalyst, pH and/or IL concentration.

Table 1.5. Summary of researches on IL degradation based on combined treatments.

IL	Conditions	Process/anodic electrode	IL cation removal (%/time)	Degradation (%)	Main results	Reference
1-Butyl-4-methylpyridinium chloride 1-Ethyl-3-methylimidazolium chloride	[IL] = 0.83-1.39 mM, T = 35 ºC, V = 0.1 L, pH = 3, air = 0.3 L min^{-1}, [Na_2SO_4] = 50 mM, j= 16.7-100 mA cm^{-2}, t = 360min	Electrolysis BDD/air-diffusion 3 cm^2	-	70-95 (DOC)	High mineralization rates were achieved at the higher electric density. The order in the efficiency process was: electrolysis<electro-Fenton<photoelectro-Fenton.	(Garcia-Segura et al., 2016)
		Electro-Fenton 0.50 mM Fe^{2+} BDD/air-diffusion 3 cm^2	-	62-90 (DOC)		
		Photoelectro-Fenton 0.50 mM Fe^{2+} 6 W UVA λmax = 360 nm. BDD/air-diffusion 3 cm^2	-	68-97 (DOC)		
1-Butyl-3-methylimidazolium triflate	[IL] = 500 mg L^{-1}, V = 0.2 L, pH = 3, air = 0.75 L min^{-1}, [Na_2SO_4/NaCl/$NaNO_3$] = 0.0125-0.075 M, I = 0.3 A	Electro-Fenton. $Fe_2(SO_4)_3$ 0.25 mM Carbon felt and BDD 72 cm^2	100/120 min	69-99 (TOC)	The electrolyte influenced influenced the reactrion rate as follows: NaCl < Na_2SO_4 < $NaNO_3$	(Bocos et al., 2017)
Didecyldimethylammonium (4-chloro-2-methylphenoxy)acetate	[IL] = 50 mg L^{-1}, V = 0.1 L, [Na_2SO_4] = 100 mM, I = 0.01 A, t= 360 min	Electrolysis. Carbon felt and Pt	100/360 min	25 (TOC)	Cation and anion were attacked by hydroxyl radicals, being more effective the electro-Fenton treatment than the conventional electrolysis.	(Pęziak-Kowalska et al., 2017)
	[IL] = 50 mg L^{-1}, V = 0.1 L, pH = 3, [Na_2SO_4] = 100 mM, I = 0.01 A, t = 360 min	Electro-Fenton. Carbon felt and Pt $FeSO_4 \cdot 7H_2O$	100/360 min	80 (TOC)		

Table 1.5. Continued

IL	Conditions	Process/catalyst	IL cation removal (%/time)	Degradation (%)	Main results	Reference
1-Ethyl-3-methylimidazolium dicyanamide 1-Butyl-3-methylimidazolium dicyanamide 1-Hexyl-3-methylimidazolium dicyanamide 1-Ethyl-3-methylimidazolium acetate 1-Ethyl-3-methylimidazolium methylsulfate	[IL] = 500 mg L^{-1}, V = 0.2 L, pH = 3, air = 0.75 L min^{-1}, [Na_2SO_4] = 50 mM, I = 0.1-0.3 A, t= 500 min	Heterogeneous electro-Fenton. Iron alginate beads 3.2-5.33 g L^{-1} Carbon felt and BDD 72 cm^2	80-100/120 min	40-100 (TOC)	An increasing of the alkyl side chain of the cation and the use of acetate as anion produced a reduction in the mineralization degree.	(Bocos et al., 2016)
1-Butylpyridinium chloride	[IL] = 500 mg L^{-1}, V = 0.15 L, pH = 2-7, air = 1 L min^{-1}, [Na_2SO_4] = 10 mM, I = 0.3 A, t = 480 min	Heterogeneous electro-Fenton. Goethite polyvinyl alcohol-alginate beads 0.5-4 g L^{-1} Carbon felt and BDD 7.7 cm^2	85-100/120 min	38-94 (TOC)	The evaluation of operating conditions allowed selecting a pH value of 3 and a catalyst concentration of 2 g L^{-1} as optimum.	(Meijide et al., 2017)
1,3-Bis(2,4,6-trimethylphenyl)imidazolinium chloride	[IL] = 67-270 mg L^{-1}, V = 0.15 L, pH = 3, air = 0.5 L min^{-1}, [Na_2SO_4] = 10 mM, I = 0.05-0.25 A	Heterogeneous electro-Fenton. Iron alginate gel spheres 1-5 g L^{-1} Carbon felt and BDD 12.5 cm^2	-	36-77 (TOC)	The optimum conditions obtained for the degradation of this IL are the following: I: 175 mA, catalyst: 5g, $[IL]_0$ = 50 mgC L^{-1}.	(Poza-Nogueiras et al., 2018a)
1,3-dicyclohexylbenzimidazolium chloride	[IL] = 70-280 mg L^{-1}, V = 0.15 L, pH = 3, air = 0.5 L min^{-1}, [Na_2SO_4] = 10 mM, I = 0.05-0.30 A	Heterogeneous electro-Fenton. Iron alginate gel spheres 1-5 g L^{-1} Carbon felt and BDD 12.5 cm^2	-	3-90 (TOC)	The heterogeneous electro-Fenton process was more effective with low catalyst concentration (1 g L^{-1}) and high high current (250 mA).	(Poza-Nogueiras et al., 2018b)

García-Segura et al. (2016) focused their research on the evaluation of the anodic oxidation, the electro-Fenton and the phtoelectro-Fenton of the 1-Butyl-4-methylpyridinium chloride and the 1-Ethyl-3-methylimidazolium chloride using a BDD anode and an air diffusion cathode. In the case of the pyridinium based IL the three processes obtained similar results in terms of DOC conversion, whereas in the imidazolium based IL the anodic oxidation produced a lower DOC decrease than the electro-Fenton and the photoelectro-Fenton. However, in both cases, the degradation in terms of efficiency of mineralization per current unit followed the trend: electrolysis<electro-Fenton<photoelectro-Fenton. Peziak-Kowalska et al. (2017) also evidenced an improvenment in the mineralization (from 25 to 80 %) using the electro-Fenton against the anodic oxidation in the Didecyldimethylammonium (4-chloro-2-methylphenoxy)acetate removal using a carbon felt cathode and a Pt counter electrode. Bocos et al. (2017) studied the influence of the use of different electrolytes in the electro-Fenton process of 1-Butyl-3-methylimidazolium triflate with a BDD anode and a carbon felt cathode, being the most efficient the nitrate salt followed by sulfate salt. The sodium chloride was the least effective, even than the system without electrolyte, due to the scavenging effect showed by chloride anion in its transformation into chlorate and perchlorate by hydroxyl radicals. Moreover, the use of a high electrolyte concentration (0.0750 mM of $NaNO_3$) produced an increase in the mineralization degree, achieving in the best case a 99 % of TOC reduction. The heterogeneous electro-Fenton process (HEF) was investigated by different authors with high mineralization yields using iron alginate beads/gel spheres and goethite polyvinyl alcohol-alginate beads as heterogeneous catalyst using carbon felt as cathode and BDD as anode. Bocos et al. (2016) evidenced lower degradation yields in the HEF when the alkyl side chain increased or when acetate

was used as anion; and Poza-Nogueiras et al. 2018b evidenced an improvement in the system using low catalyst concentration (1 g L^{-1} against 5 g L^{-1}) because high catalyst concentrations favored the secondary reaction between Fe^{2+} and hydroxyl radicals on the catalyst surface.

1.3. Breakdown product and reaction pathways in AOPs for ILs

The reaction pathway of the ILs in the different AOPs is a concern area for the researchers, because it is necessary in order to understand the degradation processes. The AOPs are non-selective processes, and, for this reason, a high amount of intermediates can formed in the ILs degradation.

Figure 1.1 depicts the reaction pathway proposed for the imidazolium ILs in AOPs from contribution of several studies (Banić et al., 2016; Bocos et al., 2017, 2016; Fabiańska et al., 2012; Garcia-Segura et al., 2016; Gomez-Herrero et al., 2019, 2018; Munoz et al., 2015a; Pati and Arnold, 2018; Pieczyńska et al., 2015; Siedlecka et al., 2013, 2012). The analysis of the intermediates evolution in the oxidation of imidazolium ILs led to deduce the following steps: i) the hydroxylation of the initial imidazolium IL in the alkyl side chain or in the imidazolium core, ii) the side chain cleavage remaining inalterable the imidazolium core, iii) the ring opening giving rise lineal organic molecules and iv) the formation of short-chain organic acids, CO_2, H_2O, NO_2^-, NO_3^-, NO, NO_2 and NH_4^+. As can be seen, some intermediates have been detected in different AOPs, so the $HO^{\cdot}$ radicals could attack the ILs in the same positions independently of the process used for their generation.

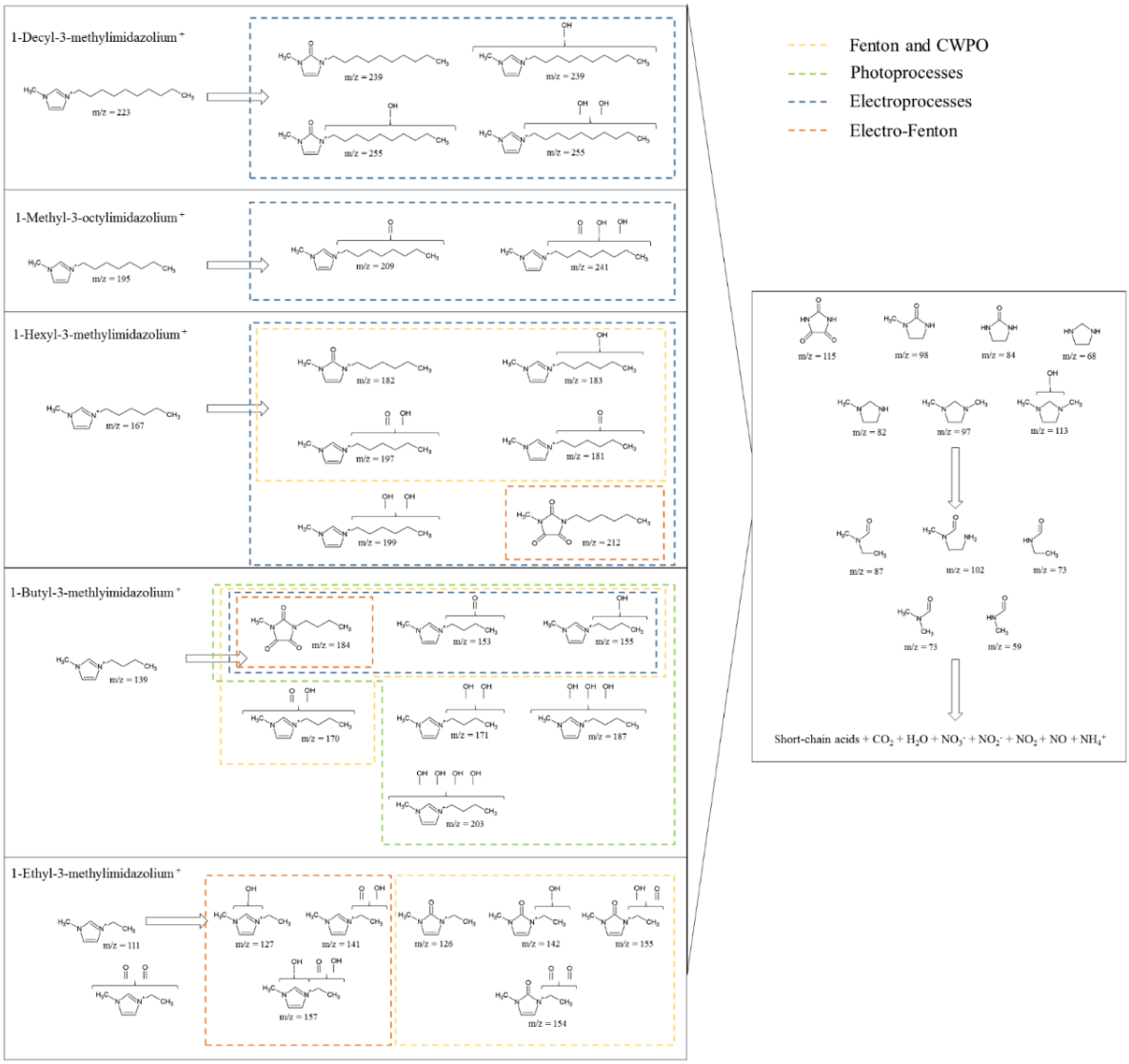

Figure 1.1. Imidazolium ionic liquids pathway degradation by means of AOPs (yellow squares for Fenton and CWPO, green squares for photoprocesses, blue squares for electroprocesses and orange squares for Electro-Fenton). Collected from Banić et al., 2016; Bocos et al., 2017, 2016; Fabiańska et al., 2012; Garcia-Segura et al., 2016; Gomez-Herrero et al., 2019, 2018; Munoz et al., 2015a; Pati and Arnold, 2018; Pieczyńska et al., 2015; Siedlecka et al., 2013, 2012.

Moreover, the degradation treatments including sodium chloride or chlorine in the reaction medium (such as the 1-Butyl-3-methyl-imidazolium chloride degradation by means of UV/chlorine or anodic oxidation of studied by Pati and Arnold (2018) and Pieczyńska et al. (2015), respectively), gives rise to some intermediates that incorporate the Cl atoms in the IL structure. Moreover, the imidazolium ILs can be attacked in the alkyl-side chain, producing the transformation from the (n+1)-alkyl-3-methylimidazolium intermediates to the n-alkyl-3-methylimidazolium ones.

In the case of the degradation of pyridinium ILs by AOPs, the reaction pathway has being mainly studied using the 1-Butyl-4-methylpyridinium chloride as target pollutant (Garcia-Segura et al., 2016; Gomez-Herrero et al., 2018; Munoz et al., 2015a; Pieczyńska et al., 2015). Figure 1.2 shows a compilation of the pathways proposed by several authors. As occurs for the imidazolium ILs, some intermediates appeared in different AOPs, evidencing the similar degradation routes.

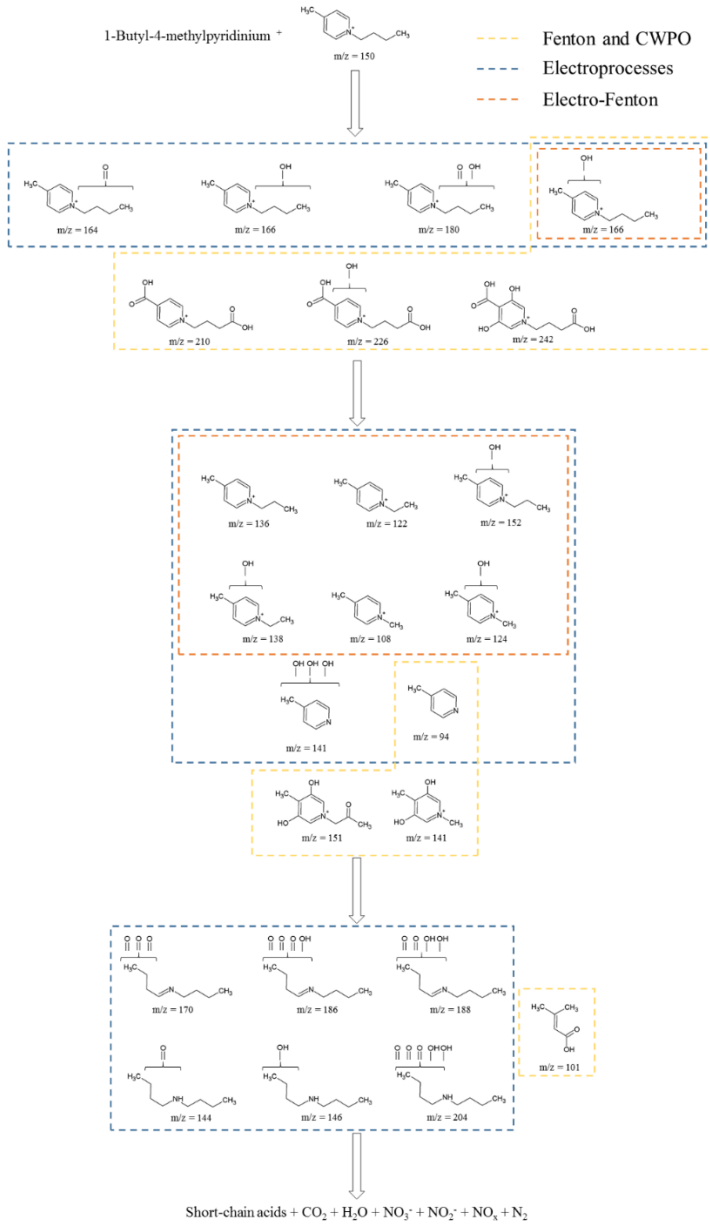

Figure 1.2. Pyridinium ionic liquids pathway degradation by means of AOPs (yellow squares for Fenton and CWPO, blue squares for electroprocesses and orange squares for Electro-Fenton). Collected from Garcia-Segura et al., 2016; Gomez-Herrero et al., 2018; Munoz et al., 2015a; Pieczyńska et al., 2015.

Furthermore, Munoz et al. (2015a) studied the reaction pathway of the ammonium- and phosphonium-based ILs, stablishing the degradation steps in first, a hydroxylation of the cation, and later the breakdown of the compounds generated to different intermediates and, finally, CO_2 and H_2O.

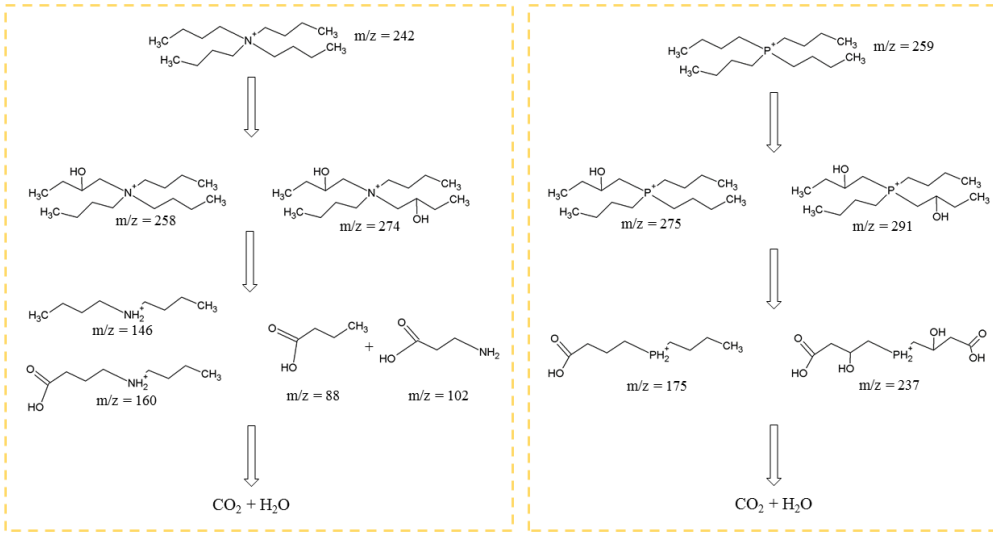

Figure 1.3. Ammonium and phosphonium ionic liquids pathway degradation by means of AOPs (yellow squares for Fenton and CWPO). Collected from Munoz et al., 2015a.

1.4. Objectives

The aim of the PhD Thesis is focused on the treatment of imidazolium- and choline-based ionic liquid from aqueous phase by means of biological and advanced oxidation processes in order to stablish a treatment strategy for the removal of those compounds from wastewater. The overall objective develops through the following specific objectives:

- To study of the toxicity and biodegradability of several imidazolium- and choline-based ILs in order to determine their behavior in a sewage treatment plant. The analysis includes, on the one hand, the evaluation of ILs toxicity by means of Microtox® test with *Vibrio fischeri* and respiration inhibition test with activated sludge, determining the EC_{50}, and, on the other hand, the evaluation of the IL biodegradability towards inherent (Zahn-Wellens) and fast biodegradability tests.
- To study of the biological degradation of choline-based ILs in sequencing batch reactors using an acclimated granular sludge to assess the influence of the anion used (chloride, acetate and bis(trifluoromethylsulfonyl)imide), analyzing the kinetic of $Choline^+$ removal, the intermediates and the specialization of the biomass.
- To study the catalytic wet peroxide oxidation (CWPO) of imidazolium-based ILs in aqueous solution analyzing the operation conditions (temperature and H_2O_2 dose), the possible reaction intermediates formed as well as the enhancement of the biodegradability. Furthermore, catalyst activity and stability in long-term continuous experiments were assessed for different iron catalyst supported on alumina and carbon materials, some of them obtained from sewage sludge.

- To study of the degradation of imidazolium-based ILs in aqueous phase by means of electrolysis processes with boron-doped diamond anodes in absence of electrolyte due to their high conductivity. Moreover, the intensification of this process with UV light, high-frequency ultrasounds and the addition of sulfate anions have been also evaluated.

1.5. References

- Abrusci, C., Palomar, J., Pablos, J.L., Rodriguez, F., Catalina, F., 2011. Efficient biodegradation of common ionic liquids by *Sphingomonas paucimobilis bacterium*. Green Chem. 13, 709–717.
- Ahmadi, M., Vahabzadeh, F., Bonakdarpour, B., Mofarrah, E., Mehranian, M., 2005. Application of the central composite design and response surface methodology to the advanced treatment of olive oil processing wastewater using Fenton's peroxidation. J. Hazard. Mater. 123, 187–195
- Al-Malack, M.H., Siddiqui, M., 2013. Treatment of synthetic petroleum refinery wastewater in a continuous electro-oxidation process. Desalin. Water Treat. 51, 6580–6591.
- Amde, M., Liu, J., Pang, L., 2015. Environmental application, fate, effects and concerns of ionic liquids : A review. Environ. Sci. Technol. 49, 12611–12627.
- An, S.N., Choi, N.C., Choi, J.W., Lee, S., 2018. Photodegradation of bisphenol A with ZnO and TiO_2: Influence of metal ions and Fenton process. Water. Air. Soil Pollut. 229. 43.
- Anglada, A., Urtiaga, A., Ortiz, I., 2009. Contributions of electrochemical oxidation to waste-water treatment: Fundamentals and review of applications. J. Chem. Technol. Biotechnol. 84, 1747–1755.
- Armand, M., Endres, F., MacFarlane, D.R., Ohno, H., Scrosati, B., 2009. Ionic-liquid materials for the electrochemical challenges of the future. Nat. Mater. 8, 621–629.
- Babuponnusami, A., Muthukumar, K., 2014. A review on Fenton and improvements to the Fenton process for wastewater treatment. J. Environ. Chem. Eng. 2, 557–572.
- Banić, N., Abramović, B., Šibul, F., Orčić, D., Watson, M., Vraneš, M., Gadžurić, S., 2016. Advanced oxidation processes for the removal of [bmim][Sal] third generation ionic liquids: Effect of water matrices and intermediates identification. RSC Adv. 6, 52826–52837.
- Barbusiński, K., Filipek, K., 2001. Use of Fenton's Reagent for Removal of Pesticides from Industrial Wastewater. Polish J. Environ. Stud. 10, 207–212.
- Barrault, J., Tatibouët, J.-M., Papayannakos, N., 2000. Catalytic wet peroxide oxidation of phenol over pillared clays containing iron or copper species. Comptes Rendus l'Académie des Sci. - Ser. IIC - Chem. 3, 777–783.

- Bautista, P., Mohedano, A.F., Casas, J.A., Zazo, J.A., Rodriguez, J.J., 2011. Highly stable Fe/γ-Al_2O_3 catalyst for catalytic wet peroxide oxidation. J. Chem. Technol. Biotechnol. 86, 497–504.
- Bautista, P., Mohedano, A.F., Casas, J.A., Zazo, J.A., Rodriguez, J.J., 2008. An overview of the application of Fenton oxidation to industrial wastewaters treatment. J. Chem. Technol. Biotechnol. 83, 1323–1338.
- Bedia, J., Rodriguez, J.J., Moreno, D., Palomar, J., Belver, C., 2019. Photostability and photocatalytic degradation of ionic liquids in water under solar light. RSC Adv. 9, 2026–2033.
- Biczak, R., Pawlowska, B., Balczewski, P., Rychter, P., 2014. The role of the anion in the toxicity of imidazolium ionic liquids. J. Hazard. Mater. 274, 181–190.
- Bocos, E., González-Romero, E., Pazos, M., Sanromán, M.A., 2017. Application of electro-Fenton treatment for the elimination of 1-Butyl-3-methylimidazolium triflate from polluted water. Chem. Eng. J. 318, 19–28.
- Bocos, E., Pazos, M., Sanromán, M.Á., 2016. Electro-Fenton treatment of imidazolium-based ionic liquids: Kinetics and degradation pathways. RSC Adv. 6, 1958–1965.
- Brillas, E., Martínez-Huitle, C.A., 2015. Decontamination of wastewaters containing synthetic organic dyes by electrochemical methods. An updated review. Appl. Catal. B Environ. 166-167, 603–643.
- Can, O.T., 2014. COD removal from fruit-juice production wastewater by electrooxidation electrocoagulation and electro-Fenton processes. Desalin. Water Treat. 52, 65–73.
- Candia-Onfray, C., Espinoza, N., Sabino da Silva, E.B., Toledo-Neira, C., Espinoza, L.C., Santander, R., García, V., Salazar, R., 2018. Treatment of winery wastewater by anodic oxidation using BDD electrode. Chemosphere 206, 709–717.
- Cañizares, P., Paz, R., Sáez, C., Rodrigo, M.A., 2009. Costs of the electrochemical oxidation of wastewaters: A comparison with ozonation and Fenton oxidation processes. J. Environ. Manage. 90, 410–420.
- Carriazo, J.G., Guelou, E., Barrault, J., Tatiboue, J.M., 2003. Catalytic wet peroxide oxidation of phenol over Al–Cu or Al–Fe modified clays. Appl. Clay Sci. 22, 303–308.
- Centi, G., Perathoner, S., Torre, T., Verduna, M.G., 2000. Catalytic wet oxidation with H2O2 of carboxylic acids on homogeneous and heterogeneous Fenton-type catalysts. Catal. Today 55, 61–69.
- Cheng, H., Chen, G., Qiu, Y., Li, B., Stenstrom, M.K., 2016. Factors that influence the degradation of 1-ethyl-3- methylimidazolium hexafluorophosphate by Fenton oxidation. R. Soc. Chem. 6, 59889–59895.

- Cho, C.-W., Jeon, Y.-C., Pham, T.P.T., Vijayaraghavan, K., Yun, Y.-S., 2008. The ecotoxicity of ionic liquids and traditional organic solvents on microalga Selenastrum capricornutum. Ecotoxicol. Environ. Saf. 71, 166–171.
- Costa, S.P.F., Pinto, P.C.A.G., Lapa, R.A.S., Saraiva, M.L.M.F.S., 2015a. Toxicity assessment of ionic liquids with Vibrio fischeri: An alternative fully automated methodology. J. Hazard. Mater. 284, 136–142.
- Costa, S.P.F., Pinto, P.C.A.G., Saraiva, M.L.M.F.S., Rocha, F.R.P., Santos, J.R.P., Monteiro, R.T.R., 2015b. The aquatic impact of ionic liquids on freshwater organisms. Chemosphere 139, 288–294.
- Crowther, N., Larachi, F., 2003. Iron-containing silicalites for phenol catalytic wet peroxidation. Appl. Catal. B Environ. 46, 293–305.
- Cruz-González, K., Torres-Lopez, O., García-León, A.M., Brillas, E., Hernández-Ramírez, A., Peralta-Hernández, J.M., 2012. Optimization of electro-Fenton/BDD process for decolorization of a model azo dye wastewater by means of response surface methodology. Desalination 286, 63–68.
- Czerwicka, M., Stolte, S., Müller, A., Siedlecka, E.M., Gołębiowski, M., Kumirska, J., Stepnowski, P., 2009. Identification of ionic liquid breakdown products in an advanced oxidation system. J. Hazard. Mater. 171, 478–483.
- Diaz, E., Monsalvo, V., Palomar, J., Mohedano, A.F., 2016. Ionic Liquids: Bacterial Degradation in Wastewater Treatment Plants, in: Encyclopedia of Inorganic and Bioinorganic Chemistry. John Wiley & Sons, Ltd.
- Docherty, K.M., Aiello, S.W., Buehler, B.K., Jones, S.E., Szymczyna, B.R., Walker, K.A., 2015. Ionic liquid biodegradability depends on specific wastewater microbial consortia. Chemosphere 136, 160–166.
- Domínguez, C.M., Munoz, M., Quintanilla, A., de Pedro, Z.M., Casas, J.A., 2017. Kinetics of imidazolium-based ionic liquids degradation in aqueous solution by Fenton oxidation. Environ. Sci. Pollut. Res.
- Dominguez, C.M., Munoz, M., Quintanilla, A., de Pedro, Z.M., Ventura, S.P.M., Coutinho, J.A.P., Casas, J.A., Rodriguez, J.J., 2014. Degradation of imidazolium-based ionic liquids in aqueous solution by Fenton oxidation. J. Chem. Technol. Biotechnol. 89, 1197–1202.
- Fabiańska, A., Ossowski, T., Stepnowski, P., Stolte, S., Thöming, J., Siedlecka, E.M., 2012. Electrochemical oxidation of imidazolium-based ionic liquids: The influence of anions. Chem. Eng. J. 198-199, 338–345.
- Frade, R.F.M., Afonso, C.A.M., 2010. Impact of ionic liquids in environment and humans: An overview. Hum. Exp. Toxicol. 29, 1038–1054.
- Ganiyu, S.O., Zhou, M., Martínez-Huitle, C.A., 2018. Heterogeneous electro-Fenton and photoelectro-Fenton processes: A critical review of

fundamental principles and application for water/wastewater treatment. Appl. Catal. B Environ. 235, 103–129.

- Ganzenko, O., Huguenot, D., van Hullebusch, E.D., Esposito, G., Oturan, M. a., 2014. Electrochemical advanced oxidation and biological processes for wastewater treatment: A review of the combined approaches. Environ. Sci. Pollut. Res. 21, 8493–8524.
- Garcia-Segura, S., Lima, Á.S., Cavalcanti, E.B., Brillas, E., 2016. Anodic oxidation, electro-Fenton and photoelectro-Fenton degradations of pyridinium- and imidazolium-based ionic liquids in waters using a BDD/air-diffusion cell. Electrochim. Acta 198, 268–279.
- Giannis, A., Lim, T.-T., Veksha, A., Oh, W.-D., Lok, L.-W., 2018. Enhanced photocatalytic degradation of bisphenol A with Ag-decorated S-doped g-C_3N_4 under solar irradiation: Performance and mechanistic studies. Chem. Eng. J. 333, 739–749.
- Gomez-Herrero, E., Tobajas, M., Polo, A., Rodriguez, J.J., Mohedano, A.F., 2019. Removal of imidazolium-based ionic liquid by coupling Fenton and biological oxidation. J. Hazard. Mater. 365, 289–296.
- Gomez-Herrero, E., Tobajas, M., Polo, A., Rodriguez, J.J., Mohedano, A.F., 2018. Removal of imidazolium- and pyridinium-based ionic liquids by Fenton oxidation. Environ. Sci. Pollut. Res. 25, 34930–34937.
- Goodenough, J.B., Park, K.S., 2013. The Li-ion rechargeable battery: A perspective. J. Am. Chem. Soc. 135, 1167–1176.
- Han, J., Wang, Y., Yu, C., Li, C., Yan, Y., Liu, Y., Wang, L., 2011. Separation, concentration and determination of chloramphenicol in environment and food using an ionic liquid/salt aqueous two-phase flotation system coupled with high-performance liquid chromatography. Anal. Chim. Acta 685, 138–145.
- Hennig, H., Billing, R., 1993. Advantages and disadvantages of photocatalysis induced by light-sensitive coordination compounds. Coord. Chem. Rev. 125, 89–100.
- Hernández-Fernández, F.J., Bayo, J., Pérez de los Ríos, A., Vicente, M.A., Bernal, F.J., Quesada-Medina, J., 2015. Discovering less toxic ionic liquids by using the Microtox® toxicity test. Ecotoxicol. Environ. Saf. 116, 29–33.
- Inchaurrondo, N., Cechini, J., Font, J., Haure, P., 2012. Strategies for enhanced CWPO of phenol solutions. Appl. Catal. B Environ. 111-112, 641–648.
- Itakura, T., Hirata, K., Aoki, M., Sasai, R., Yoshida, H., Itoh, H., 2009. Decomposition and removal of ionic liquid in aqueous solution by hydrothermal and photocatalytic treatment. Environ. Chem. Lett. 7, 343–345.
- Karthikeyan, S., Boopathy, R., Gupta, V.K., Sekaran, G., 2013. Preparation, characterizations and its application of heterogeneous Fenton

catalyst for the treatment of synthetic phenol solution. J. Mol. Liq. 177, 402–408.

- Khan, M.I., Zaini, D., Shariff, A.M., 2016. Framework for ecotoxicological risk assessment of ionic liquids. Procedia Eng. 148, 1141–1148.
- Khankhasaeva, S.T., Dashinamzhilova, E.T., Dambueva, D. V., 2017. Oxidative degradation of sulfanilamide catalyzed by Fe/Cu/Al-pillared clays. Appl. Clay Sci. 146, 92–99.
- Kim, I., Yamashita, N., Tanaka, H., 2009. Photodegradation of pharmaceuticals and personal care products during UV and UV/H_2O_2 treatments. Chemosphere 77, 518–525.
- Kotzamanidi, S., Frontistis, Z., Binas, V., Kiriakidis, G., Mantzavinos, D., 2018. Solar photocatalytic degradation of propyl paraben in Al-doped TiO_2 suspensions. Catal. Today 313, 148–154.
- Krzemińska, D., Neczaj, E., Borowski, G., 2015. Advanced oxidation processes for food industrial wastewater decontamination. J. Ecol. Eng. 16, 61–71.
- Leonardo da Silva, W., Caroline Leal, B., Luiza Ziulkoski, A., W. N. M. van Leeuwen, P., Henrique Zimnoch dos Santos, J., Stephan Schrekker, H., 2019. Petrochemical residue-derived silica-supported titania-magnesium catalysts for the photocatalytic degradation of imidazolium ionic liquids in Water. Sep. Purif. Technol. 218, 191–199.
- Linares-Hernández, I., Barrera-Díaz, C., Bilyeu, B., Juárez-GarcíaRojas, P., Campos-Medina, E., 2010. A combined electrocoagulation-electrooxidation treatment for industrial wastewater. J. Hazard. Mater. 175, 688–694.
- Markiewicz, M., Piszora, M., Caicedo, N., Jungnickel, C., Stolte, S., 2013. Toxicity of ionic liquid cations and anions towards activated sewage sludge organisms from different sources - Consequences for biodegradation testing and wastewater treatment plant operation. Water Res. 47, 2921–2928.
- Martínez-Pachón, D., Ibáñez, M., Hernández, F., Torres-Palma, R.A., Moncayo-Lasso, A., 2018. Photo-electro-Fenton process applied to the degradation of valsartan: Effect of parameters, identification of degradation routes and mineralization in combination with a biological system. J. Environ. Chem. Eng. 6, 7302–7311.
- Meijide, J., Pazos, M., Sanromán, M.Á., 2017. Heterogeneous electro-Fenton catalyst for 1-butylpyridinium chloride degradation. Environ. Sci. Pollut. Res. 26, 3145–3156.
- Mena, I.F., Diaz, E., Rodriguez, J.J., Mohedano, A.F., 2016. CWPO of bisphenol A with iron catalysts supported on microporous carbons from grape seeds activation. Chem. Eng. J. 318, 153–160.

- Messele, S.A., Soares, O.S.G.P., Órfão, J.J.M., Stüber, F., Bengoa, C., Fortuny, A., Fabregat, A., Font, J., 2014. Zero-valent iron supported on nitrogen-containing activated carbon for catalytic wet peroxide oxidation of phenol. Appl. Catal. B Environ. 154-155, 329–338.
- Messele, S.A., Stüber, F., Bengoa, C., Fortuny, A., Fabregat, A., Font, J., 2012. Phenol degradation by heterogeneous Fenton-like reaction using Fe supported over activated carbon. Procedia Eng. 42, 1373–1377.
- Miklos, D.B., Hartl, R., Michel, P., Linden, K.G., Drewes, J.E., Hübner, U., 2018. UV/H_2O_2 process stability and pilot-scale validation for trace organic chemical removal from wastewater treatment plant effluents. Water Res. 136, 169–179.
- Mirzaei, A., Chen, Z., Haghighat, F., Yerushalmi, L., 2017. Removal of pharmaceuticals from water by homo/heterogonous Fenton-type processes – A review. Chemosphere 174, 665–688.
- Munoz, M., de Pedro, Z.M., Menendez, N., Casas, J.A., Rodriguez, J.J., 2013. A ferromagnetic γ-alumina-supported iron catalyst for CWPO. Application to chlorophenols. Appl. Catal. B Environ. 136-137, 218–224.
- Munoz, M., Dominguez, C.M., De Pedro, Z.M., Quintanilla, A., Casas, J.A., Rodriguez, J.J., 2015a. Ionic liquids breakdown by Fenton oxidation. Catal. Today 240, 16–21.
- Munoz, M., Domínguez, C.M., De Pedro, Z.M., Quintanilla, A., Casas, J.A., Ventura, S.P.M., Coutinho, J.A.P., 2015b. Role of the chemical structure of ionic liquids in their ecotoxicity and reactivity towards Fenton oxidation. Sep. Purif. Technol. 150, 252–256.
- Munoz, M., Domínguez, C.M., de Pedro, Z.M., Quintanilla, A., Casas, J.A., Rodriguez, J.J., 2016. Degradation of imidazolium-based ionic liquids by catalytic wet peroxide oxidation with carbon and magnetic iron catalysts. J. Chem. Technol. Biotechnol. 91, 2882–2887.
- Neumann, J., Pawlik, M., 2014. Biodegradation potential of cyano-based ionic liquid anions in a culture of *Cupriavidus spp*. and their in vitro enzymatic hydrolysis by nitrile hydratase. Environ. Sci. Pollut. Res. 21, 9495–9505.
- Neyens, E., Baeyens, J., 2003. A review of classic Fenton's peroxidation as an advanced oxidation technique. J. Hazard. Mater. 98, 33–50.
- Palomar, J., Gonzalez-Miquel, M., Bedia, J., Rodriguez, F., Rodriguez, J.J., 2011. Task-specific ionic liquids for efficient ammonia absorption. Sep. Purif. Technol. 82, 43–52.
- Pati, S.G., Arnold, W.A., 2018. Reaction rates and product formation during advanced oxidation of ionic liquid cations by UV/peroxide, UV/persulfate, and UV/chlorine. Environ. Sci. Water Res. Technol. 4, 1310–1320.

- Pati, S.G., Arnold, W.A., 2017. Photochemical transformation of four ionic liquid cation structures in aqueous solution. Environ. Sci. Technol. 51, 11780–11787.
- Pérez, J.F., Llanos, J., Sáez, C., López, C., Cañizares, P., Rodrigo, M.A., 2017. Treatment of real effluents from the pharmaceutical industry: A comparison between Fenton oxidation and conductive-diamond electro-oxidation. J. Environ. Manage. 195, 216–223.
- Pęziak-Kowalska, D., Fourcade, F., Niemczak, M., Amrane, A., Chrzanowski, Ł., Lota, G., 2017. Removal of herbicidal ionic liquids by electrochemical advanced oxidation processes combined with biological treatment. Environ. Technol. 38, 1093–1099.
- Phuong, T., Pham, T., Cho, C., Yun, Y., 2010. Environmental fate and toxicity of ionic liquids : A review. Water Res. 44, 352–372.
- Pieczyńska, A., Ofiarska, A., Borzyszkowska, A.F., Białk-Bielińska, A., Stepnowski, P., Stolte, S., Siedlecka, E.M., 2015. A comparative study of electrochemical degradation of imidazolium and pyridinium ionic liquids: A reaction pathway and ecotoxicity evaluation. Sep. Purif. Technol. 156, 522–534.
- Poza-Nogueiras, V., Arellano, M., Rosales, E., Pazos, M., González-Romero, E., Sanromán, M.A., 2018a. Heterogeneous electro-Fenton as plausible technology for the degradation of imidazolinium-based ionic liquids. Chemosphere 199, 68–75.
- Poza-Nogueiras, V., Arellano, M., Rosales, E., Pazos, M., Sanromán, M.A., González-Romero, E., 2018b. Electroanalytical techniques applied to monitoring the electro-Fenton degradation of aromatic imidazolium-based ionic liquids. J. Appl. Electrochem. 48, 1331–1341.
- Prihod'ko, R., Stolyarova, I., Gündüz, G., Taran, O., Yashnik, S., Parmon, V., Goncharuk, V., 2011. Fe-exchanged zeolites as materials for catalytic wet peroxide oxidation. Degradation of Rodamine G dye. Appl. Catal. B Environ. 104, 201–210.
- Rey, A., García-Muñoz, P., Hernández-Alonso, M.D., Mena, E., García-Rodríguez, S., Beltrán, F.J., 2014. WO_3-TiO_2 based catalysts for the simulated solar radiation assisted photocatalytic ozonation of emerging contaminants in a municipal wastewater treatment plant effluent. Appl. Catal. B Environ. 154-155, 274–284.
- Rey, A., Zazo, J.A., Casas, J.A., Bahamonde, A., Rodriguez, J.J., 2011. Influence of the structural and surface characteristics of activated carbon on the catalytic decomposition of hydrogen peroxide. Appl. Catal. A Gen. 402, 146–155.
- Romero, A., Santos, A., Tojo, J., Rodriguez, A., 2008. Toxicity and biodegradability of imidazolium ionic liquids. J. Hazard. Mater. 151, 268–273.

- Sakthivel, S., Shankar, M. V., Palanichamy, M., Arabindoo, B., Bahnemann, D.W., Murugesan, V., 2004. Enhancement of photocatalytic activity by metal deposition: Characterisation and photonic efficiency of Pt, Au and Pd deposited on TiO_2 catalyst. Water Res. 38, 3001–3008.
- Salari, M., Rakhshandehroo, G.R., Nikoo, M.R., 2018. Degradation of ciprofloxacin antibiotic by homogeneous Fenton oxidation: Hybrid AHP-PROMETHEE method, optimization, biodegradability improvement and identification of oxidized by-products. Chemosphere 206, 157–167.
- Santiago, A., Castillo, R., Guihéneuf, S., Le, R., 2016. Synthesis and toxicity evaluation of hydrophobic ionic liquids for volatile organic compounds biodegradation in a two-phase partitioning bioreactor. J. Hazard. Mater. 307, 221–230.
- Särkkä, H., Bhatnagar, A., Sillanpää, M., 2015. Recent developments of electro-oxidation in water treatment - A review. J. Electroanal. Chem. 754, 46–56.
- Satishkumar, G., Landau, M. V., Buzaglo, T., Frimet, L., Ferentz, M., Vidruk, R., Wagner, F., Gal, Y., Herskowitz, M., 2013. Fe/SiO_2 heterogeneous Fenton catalyst for continuous catalytic wet peroxide oxidation prepared in situ by grafting of iron released from $LaFeO_3$. Appl. Catal. B Environ. 138-139, 276–284.
- Sheldon, R.A., 2005. Green solvents for sustainable organic synthesis: State of the art. Green Chem. 7, 267–278.
- Siedlecka, E.M., Fabiańska, A., Stolte, S., Nienstedt, A., Ossowski, T., Stepnowski, P., Thöming, J., 2013. Electrocatalytic oxidation of 1-butyl-3-methylimidazolium chloride: Effect of the electrode material. Int. J. Electrochem. Sci. 8, 5560–5574.
- Siedlecka, E.M., Gołebiowski, M., Kaczyński, Z., Czupryniak, J., Ossowski, T., Stepnowski, P., 2009. Degradation of ionic liquids by Fenton reaction; the effect of anions as counter and background ions. Appl. Catal. B Environ. 91, 573–579.
- Siedlecka, E.M., Mrozik, W., Kaczyński, Z., Stepnowski, P., 2008. Degradation of 1-butyl-3-methylimidazolium chloride ionic liquid in a Fenton-like system. J. Hazard. Mater. 154, 893–900.
- Siedlecka, E.M., Stolte, S., Golebiowski, M., Nienstedt, A., Stepnowski, P., Thöming, J., 2012. Advanced oxidation process for the removal of ionic liquids from water: The influence of functionalized side chains on the electrochemical degradability of imidazolium cations. Sep. Purif. Technol. 101, 26–33.
- Sirés, I., Brillas, E., Oturan, M.A., Rodrigo, M.A., Panizza, M., 2014. Electrochemical advanced oxidation processes: Today and tomorrow. A review. Environ. Sci. Pollut. Res. 21, 8336–8367.

- Sood, S., Umar, A., Mehta, S.K., Kansal, S.K., 2015. Highly effective Fe-doped TiO_2 nanoparticles photocatalysts for visible-light driven photocatalytic degradation of toxic organic compounds. J. Colloid Interface Sci. 450, 213–223.
- Souza, F., Quijorna, S., Lanza, M.R.V., Sáez, C., Cañizares, P., Rodrigo, M.A., Candia-Onfray, C., Espinoza, N., Sabino da Silva, E.B., Toledo-Neira, C., Espinoza, L.C., Santander, R., García, V., Salazar, R., 2017. Applicability of electrochemical oxidation using diamond anodes to the treatment of a sulfonylurea herbicide. Catal. Today 206, 709–717.
- Spasiano, D., Siciliano, A., Race, M., Marotta, R., Guida, M., Andreozzi, R., Pirozzi, F., 2016. Biodegradation, ecotoxicity and UV_{254}/H_2O_2 treatment of imidazole, 1-methyl-imidazole and N,N'-alkyl-imidazolium chlorides in water. Water Res. 106, 450–460.
- Stepnowski, P., Siedlecka, E.M., Behrend, P., Jastorff, B., 2002. Enhanced photo-degradation of contaminants in petroleum refinery wastewater. Water Res. 36, 2167–2172.
- Stepnowski, P., Zaleska, A., 2005. Comparison of different advanced oxidation processes for the degradation of room temperature ionic liquids. J. Photochem. Photobiol. A Chem. 170, 45–50.
- Stolte, S., Abdulkarim, S., Arning, J., Blomeyer-Nienstedt, A.K., Bottin-Weber, U., Matzke, M., Ranke, J., Jastorff, B., Thoming, J., 2008. Primary biodegradation of ionic liquid cations, identification of degradation products of 1-methyl-3-octylimidazolium chloride and electrochemical wastewater treatment of poorly biodegradable compounds. Green Chem. 10, 214–224.
- Stolte, S., Steudte, S., Areitioaurtena, O., Pagano, F., Thöming, J., Stepnowski, P., Igartua, A., 2012. Ionic liquids as lubricants or lubrication additives: An ecotoxicity and biodegradability assessment. Chemosphere 89, 1135–1141.
- Suri, R.P.S., Liu, J., Hand, D.W., Crittenden, J.C., David, L., Mullins, M.E., David, W., Crittenden, J.C., Perram, L., Mullins, E., 1993. Heterogeneous photocatalytic oxidation of hazardous organic contaminants in water. Water Environ. Reasearch 65, 665–673.
- Thuy Pham, T.P., Cho, C.W., Yun, Y.S., 2010. Environmental fate and toxicity of ionic liquids: A review. Water Res. 44, 352–372.
- Valkaj, K.M., Wittine, O., Margeta, K., Granato, T., Katović, A., Zrnčević, S., 2011. Phenol oxidation with hydrogen peroxide using Cu/ZSM5 and Cu/Y5 catalysts. Polish J. Chem. Technol. 13, 28–36.
- Vekariya, R.L., 2017. A review of ionic liquids: Applications towards catalytic organic transformations. J. Mol. Liq. 227, 44–60.
- Ventura, S.P.M., e Silva, F.A., Gonçalves, A.M.M., Pereira, J.L., Gonçalves, F., Coutinho, J.A.P., 2014. Ecotoxicity analysis of cholinium-

based ionic liquids to *Vibrio fischeri* marine bacteria. Ecotoxicol. Environ. Saf. 102, 48–54.

- Ventura, S.P.M., Marques, C.S., Rosatella, A.A., Afonso, C.A.M., Gonçalves, F., Coutinho, J.A.P., 2012. Toxicity assessment of various ionic liquid families towards *Vibrio fischeri* marine bacteria. Ecotoxicol. Environ. Saf. 76, 162–168.
- Vilhunen, S., Sillanpää, M., 2010. Recent developments in photochemical and chemical AOPs in water treatment: A mini-review. Rev. Environ. Sci. Biotechnol. 9, 323–330.
- Wang, Y., Yu, G., Deng, S., Huang, J., Wang, B., 2018. The electro-peroxone process for the abatement of emerging contaminants: Mechanisms, recent advances, and prospects. Chemosphere 208, 640–654.
- Welton, T., 2004. Ionic liquids in catalysis. Coord. Chem. Rev. 248, 2459–2477.
- Wols, B.A., Hofman-Caris, C.H.M., 2012. Review of photochemical reaction constants of organic micropollutants required for UV advanced oxidation processes in water. Water Res. 46, 2815–2827.
- Xiang, L., Royer, S., Zhang, H., Tatibout, J.M., Barrault, J., Valange, S., 2009. Properties of iron-based mesoporous silica for the CWPO of phenol: A comparison between impregnation and co-condensation routes. J. Hazard. Mater. 172, 1175–1184.
- Xie, P., Ma, J., Liu, W., Zou, J., Yue, S., Li, X., Wiesner, M.R., Fang, J., 2015. Removal of 2-MIB and geosmin using UV/persulfate: Contributions of hydroxyl and sulfate radicals. Water Res. 69, 223–233.
- Yahya, M.S., Oturan, N., El Kacemi, K., El Karbane, M., Aravindakumar, C.T., Oturan, M.A., 2014. Oxidative degradation study on antimicrobial agent ciprofloxacin by electro-fenton process: Kinetics and oxidation products. Chemosphere 117, 447–454.
- Yan, Y., Jiang, S., Zhang, H., Zhang, X., 2015. Preparation of novel Fe-ZSM-5 zeolite membrane catalysts for catalytic wet peroxide oxidation of phenol in a membrane reactor. Chem. Eng. J. 259, 243–251.
- Ye, Y., Yang, H., Wang, X., Feng, W., 2018. Photocatalytic, Fenton and photo-Fenton degradation of RhB over Z-scheme g-C_3N_4/$LaFeO_3$ heterojunction photocatalysts. Mater. Sci. Semicond. Process. 82, 14–24.
- Yuan, X., Chen, X., Wang, H., Wang, H., Leng, L., Wu, Z., Liang, J., Jiang, L., Zeng, G., 2018. Metal-free efficient photocatalyst for stable visible-light photocatalytic degradation of refractory pollutant. Appl. Catal. B Environ. 221, 715–725.
- Zawawi, A., Ramli, R., Yub Harun, N., 2017. Photodegradation of 1-Butyl-3-methylimidazolium Chloride [Bmim]Cl via Synergistic Effect of Adsorption–Photodegradation of Fe-TiO_2/AC. Technologies 5, 82.

2

Materials and methods

Materials and methods

2.1 Ionic liquids

Table 2.1 collects the different ILs used in this study, with their abbreviation and purity.

Table 2.1. Information on ionic liquids used in this work.

Ionic liquid	Supplier	Purity % (w/w)	Abbreviation
1-Butyl-3-methylimidazolium chloride	Sigma-Aldrich	>98%	BmimCl
1-Hexyl-3-methylimidazolium chloride	Sigma-Aldrich	>97%	HmimCl
1-Methyl-3-octylimidazolium chloride	Solchemar	>98%	OmimCl
1-Decyl-3-methylimidazolium chloride	Sigma-Aldrich	>96%	DmimCl
1-Butyl-3-methylimidazolium tetrafluoroborate	Iolitec	>99%	$BmimBF_4$
1-Hexyl-3-methylimidazolium tetrafluoroborate	Iolitec	>99%	$HmimBF_4$
1-Methyl-3-octylimidazolium tetrafluoroborate	Solchemar	>98%	$OmimBF_4$
1-Decyl-3-methylimidazolium tetrafluoroborate	Iolitec	>98%	$DmimBF_4$
1-Butyl-3-methylimidazolium bis(trifluoromethylsulfonyl) imide	Iolitec	99%	$BmimNTf_2$
1-Hexyl-3-methylimidazolium bis(trifluoromethylsulfonyl) imide	Iolitec	99%	$HmimNTf_2$
1-Methyl-3-octylimidazolium bis(trifluoromethylsulfonyl) imide	Iolitec	99%	$OmimNTf_2$
1-Decyl-3-methylimidazolium bis(trifluoromethylsulfonyl) imide	Iolitec	>98%	$DmimNTf_2$
1-Butyl-3-methylimidazolium acetate	Sigma-Aldrich	>95%	BmimAc
(2-Hydroxyethyl)trimethylammonium chloride	Sigma-Aldrich	>98%	CholineCl
(2-Hydroxyethyl)trimethylammonium acetate	Sigma-Aldrich	>95%	CholineAc
(2-Hydroxyethyl)trimethylammonium bis(trifluoromethylsulfonyl)imide	Iolitec	99%	$CholineNTf_2$

2.2 Inoculum source

Activated sludge was collected from the membrane bioreactor (MBR) of a cosmetic factory in Madrid (Spain). The same sludge was used for the respiration inhibition test (OECD 209, ISO 8192), the biodegradability assays (inherent biodegradability and fast biodegradability tests), the biodegradation assays in biological reactors and as carbonaceous source to obtain activated carbons used as catalytic supports. The sludge was maintained with an organic load rate (sodium acetate and glucose) of 0.4 mg COD mg VSS^{-1} day^{-1} in a sequencing batch reactor (SBR) operated at room temperature. Ammonium sulfate and phosphoric acid were used as nitrogen and phosphorous source, respectively. A COD:N:P of 100:5:1 (w/w) was fixed and mineral salts ($FeCl_3$, $CaCl_2$, KCl and $MgCl_2$) were added as micronutrients supply in a COD:micronutrients (Fe, Ca, K and Mg) ratio of 100:0.05 (w/w).

2.3 Ecotoxicity tests

Respirometric inhibition assays

Respiration inhibition tests for activated sludge consisted of short-term respirometric measurements carried out in a Liquid-Static-Static (LSS) respirometer, using unacclimated sludge (350 mgVSS L^{-1}) in the presence of an easily biodegradable substrate (sodium acetate) alone or together with different concentrations of the ILs (5-500 mg L^{-1} depending on the IL solubility) in triplicate. Aeration and oxygen probes were controlled by an electronic interface. The respirometer operated with two independent reactors simultaneously to check the reproducibility of the assay. They were placed in a thermostatic bath and continuously stirred by magnetic bars. Fresh activated sludge was used in each test to avoid partial acclimation of the microorganisms to the target chemicals, which could lead to possible underestimation of

the toxic effects. The biomass activity was measured in terms of specific exogenous oxygen uptake rate (SOUR). The inhibition (Eq. (1)) is defined as function of the parameter γ (Eq. (2)) and the ratio the specific exogenous oxygen uptake rate for the reference substance (sodium acetate) in presence of a given concentration of the ILs ($SOUR_T$) and SOUR the obtained value for the reference substance ($SOUR_R$). Both measures were corrected by the value for the endogenous SOUR.

$$\text{Inhibition } (\%) = (\gamma) \cdot \frac{SOUR_T}{SOUR_R} \quad (1)$$

$$\gamma = \frac{SOUR_R - SOUR_T}{SOUR_R} \quad (2)$$

Inhibition was estimated in terms of EC_{50} defined as the effective concentration of a sample that causes 50% reduction of SOUR (γ=1).

Microtox test

Ecotoxicity measurements were performed according to standard Microtox test procedure (ISO 11348, 2007), based on the decreasing of light emission by the marine bacteria *Vibrio fischeri* (*Photobacterium phosphoreum*) after 15 min in presence of IL at pH within 6-8 and 15 °C, using a Microtox M500 Analyzer (Azur Environmental).

Lyophilized bacteria are reconstituted by suspension in 1 mL of aqueous NaCl solution (0.7 % w/w). A decrease in luminescence implies a reduction in cellular respiration. The luminescence was determined using a luxometer, a device that quantifies the intensity of light emitted by fluorescence. Metabolic inhibition leads to a reduction in the emission of light proportional to the toxicity of the compound tested until the death of the bacteria is reached. The luminosity reduction data are processed to obtain a standardized value of ecotoxicity.

The IC_{50} (defined as the dilution that must be applied to a sample to achieve an inhibitory effect of 50%) is calculated using a factor γ for each of the emission data obtained according to the equation 1.

$$\gamma = (I_0 - I_t) - 1 \quad (1)$$

where I_0 correspond to the light emission of a sample that has not been put in contact with the pollutant and I_t to the light emission value obtained at 15 min from the contact of the contaminant sample with the bacteria.

The graphical representation of equation 2 was adjusted by linear regression, obtaining the intercept and the slope of the equation.

$$\log\gamma = n + m \cdot \log(\text{pollutant concentration}) \quad (2)$$

An inhibitory effect of 50% is reaches for a value of $\gamma = 1$. Substituting the value of γ in equation 2 gives the concentration whose value corresponds to the IC_{50} value.

The results were expressed in terms of EC_{50}, defined as the effective concentration of IL that causes a 50 % inhibitory effect. The EC_{50} value are obtained according to the equation 3.

$$EC_{50} = C_i \cdot (IC_{50}/100) \quad (3)$$

Daphnia magna test

Daphtoxkit F (MicroBioTest Inc., Gent, Belgium) was used for 48 h to conduct an acute immobilization test with *Daphnia magna* according to ISO 6341. Different solution concentrations were adjusted to the particular IL. All runs were done in duplicate, using four replicates of each concentration in 10 mL of mineral medium (controls) or solution of test substances in mineral medium. Each replicate involved using five pre-fed Daphnia neonates that were less than 90 h old and obtained at

20 °C under continuous lighting. Sample toxicity was assessed from the number of immobilized or dead organisms after 24 and 48 h as a fraction of unaffected organisms compared to the controls.

2.4 Biodegradability tests

Inherent biodegradability test

The Zahn-Wellens test (OECD 302 B 1992) was carried out in amber glass reactors (2.5 L) with 10 mg L^{-1} of IL in aqueous solution in triplicate. The IL carbon content to inoculum (dry-weight) ratio was 1:4 and mineral medium (phosphate buffer with $CaCl_2$ (27.5 mg L^{-1}), $MgSO_4 \cdot 7H_2O$ (22.5 mg L^{-1}) and $FeCl_3 \cdot 6H_2O$ (0.25 mg L^{-1})) was also added. The mixture was agitated and aerated at room temperature for 28 days. Samples were taken periodically to quantify the TOC and IL concentration. Ethylene glycol was used as reference compound to ensure the activity of the microorganisms and three replicates of each assay were carried out to guarantee the reproducibility.

Fast biodegradability test

Fast biodegradability tests were carried out in close reactors with a mixture of unacclimated activated sludge (350 mg L^{-1}) with a known concentration of pollutant (10-50 mg L^{-1} of IL) and mineral medium (APHA 1992) by triplicate. Before the assay, in order to eliminate any residual organic matter, the activated sludge was maintained in starvation and continuous aeration overnight. The reactors were continuously fed with air to avoid oxygen limitation. The evolution of IL concentration, TOC and specific oxygen uptake rate (SOUR) profile was registered. SOUR profile was obtained interrupting the air supply and measuring the oxygen consumption in a range of 0.3 mg L^{-1}. Test were carried out for 100 h at 25 °C.

2.5 Catalysts preparation

The iron supported alumina catalyst (Fe_2O_3/Al_2O_3) was prepared by incipient wetness impregnation of Al_2O_3 supplied by Merck (Germany), using an aqueous solution of $Fe(NO_3)_3 \cdot 9H_2O$ to obtain a nominal 4 % (w/w) concentration. Once impregnated, the solid was dried at 60 ºC for 12 h and calcined for 4 h at 300 ºC by heating at 3 ºC min^{-1}.

The iron catalyst supported on a commercial active carbon supplied by Merck (Fe/AC, BET surface area ≈ 950 m^2 g^{-1}, bulk density ≈ 0.5 g cm^{-3}) was prepared by incipient wetness impregnation using an aqueous solution of $Fe(NO_3)_3 \cdot 9H_2O$ to obtain a nominal 4 % (w/w) concentration. The solid was dried at 60 ºC overnight and calcined for 3 h at 200 ºC, which was reached at 10 ºC min^{-1}.

Two-iron catalysts were prepared using aerobic granular sludge. The first one, named Fe/AS, was synthesized mixing $FeCl_3 \cdot 6H_2O$ with dried sludge (dried at 105 ºC overnight and sieved to particle sizes of 0.10-0.25 nm) in a mass ratio of 3 (mg $FeCl_3$/mg biosolid) and dried at 60 ºC for 20 h. The chemical activation of the resulting material consisted in a heating at 750 ºC for 2 h, under an N_2 atmosphere (30 mL N min^{-1}), in a Nabertherm Series R tubular furnace (ramping up 10 ºC min^{-1}). Once activated, the catalyst was washed with an HCl solution (3 M) at 80 ºC for 1 h and with water until neutral pH in order to remove excess activating reagent. The catalyst was used after being dried at 60 ºC.

The second sludge-based catalyst (Fe/HTCS) were obtained by hydrothermal carbonization (HTC) of a mixture of $FeCl_3 \cdot 6H_2O$ and wet granular sludge in a mass ratio of 3 (mg $FeCl_3$/ mg dried sludge; sludge moisture content, 85 %) in a 250 mL stainless steel batch reactor with an inner Teflon lining. The HTC process was performed at 208 °C for 1

h, with heating at 10 ºC min^{-1}. Then, the material was washed with a 3 M HCl solution at 80 ºC to remove excess Fe.

Table 2.2 collects the catalyst used in this work.

Table 2.2. Catalysts description and abbreviation

Catalyst	Description
Fe_2O_3/Al_2O_3	Fe catalyst supported on commercial γ-alumina
Fe/AC	Fe catalyst supported on commercial active carbon
Fe/AS	Fe catalyst obtained by chemical activation with $FeCl_3$ of granular sludge
Fe/HTCS	Fe catalyst obtained by hydrothermal carbonization of granular sludge and $FeCl_3$

2.6 Experimental set-up

Sequencing batch reactors (SBR)

The biological oxidation of the ILs has been carried out in three thermostated SBRs of 2.5 L equipped with dissolved oxygen and pH probes. Peristaltic pumps were used for charge the feeding and effluent discharge, as well as the addition of sodium hydroxide to ensure an adequate pH. Air was supplied by a flow compressor through a ceramic diffuser, using a flow rate of 5 LN min^{-1} to ensure an adequate dissolved oxygen concentration. All degradation experiments were carried out at room temperature and 300 rpm, using a hydraulic retention time of 6 days and a biomass concentration of 3000 mg L^{-1}, as volatile suspend solids, with a cell retention time of 25 days. Tests were conducted stepwise in 8-h sequences including anoxic filling (0.5 h), aerated reaction (7.0 h), settling (0.25 h) and drawing (0.25 h).

A mixture of each IL at an increasing concentration (0.25, 0.5, 1, 2, 5, 10 and 15 mmol L^{-1}) and glucose (22.7 mmol L^{-1}) for biomass support were added as feed solution in each reactor. The COD/nitrogen

(N)/phosphorus (P)/micronutrient ratio was 100:5:1:0.05 (w/w), adding ammonium sulfate and phosphoric acid as N and P source, respectively, and mineral salts as micronutrients supply ($FeCl_3$, $CaCl_2$, KCl and $MgSO_4$).

The dairy evolution of TOC, COD, choline, glucose and biomass concentration have been evaluated withdrawing liquid samples (20 mL) from the reactor, previously filtered through a sringe filter of PTFE (0.22 μm pore size). Additionally, at different stages of the sequence, samples were collected and analyzed to monitor the biodegradation process.

CWPO experiments

CWPO runs were conducted in duplicate at atmospheric pressure in a 400 mL glass batch reactor equipped with a magnetic stirrer (500 rpm) and temperature control. The starting concentration of IL was 1 mM, the catalyst concentration 1000 mg L^{-1} (40 mg Fe L^{-1}), and the initial pH 3. The variables studied were $[H_2O_2]_0$ (0.5–1.5 times the stoichiometric doses, which was the theoretical amount of H_2O_2 needed for complete mineralization to CO_2, H_2O and N_2 of the starting compound) and reaction temperature (70–90 °C). Blank runs in the absence of catalyst were also carried out at all temperatures and negligible conversions of all ILs (< 3%) were obtained in them. The process was monitored by periodically analyzing samples from the batchwise runs. A Fenton run was also performed in parallel for comparison with CWPO by using the same Fe concentration (40 mg L^{-1}, provided by $FeCl_3 \cdot 6H_2O$ salt), 1 mM BmimCl, the stoichiometric amount of H_2O_2, pH 3 and 80 °C. Long-term runs (80 h on stream) were performed by duplicate in a continuous stirred batch reactor (CSTR) fitted with a Gilson FC 203B autosampler to collect reaction aliquots at

atmospheric pressure. The IL and H_2O_2 were fed to the reactor at a 1 mL min^{-1} flow rate in order to deliver an IL concentration of 1 mM and the stoichiometric H_2O_2 dose for a space–time of 0.133 kg_{Fe} h mol_{IL}^{-1}.

Electrochemical experiments

Bare electrolysis experiments were performed in a single-compartment electrochemical flow cell. Boron-doped diamond (BDD) (Neocoat, disc Φ 100 mm) with a geometric area of 78 cm^2 (WaterDiam, Switzerland) was used as the anode and cathode. However, a cathode material consisted of a stainless steel grid, and one of the cell covers of quartz, were used to allow irradiation with UV light inside the electrochemical cell. The inter-electrode gap between both electrodes was 9 mm. A low-pressure Hg vapor UV lampVL-215MC (Vilber Lourmat), λ= 254 nm, intensity of 930 μW cm^{-2} and energy 4.89 eV irradiated the quartz cover directly at 4 W. High-frequency ultrasound (Epoch 650 ultrasound horn, Olympus) was used to introduce waves into the system at 10 MHz with a power of 200 W. In the electrolysis promoted by sulfate anions, a concentration of 3000 mg L^{-1} of H_2SO_4 were added in the reaction medium. A Delta Electronika ES030-10 power supply (0–30 V, 0–10 A) provided the electric current. Wastewater was stored in a glass tank (0.6 dm^3). The BDD anode presents a boron concentration of 500 mg dm^{-3}, a thickness of 2.72 μm and a sp3/sp2 ratio of 220, and it is supported on p-Si. Experiments were performed under galvanostatic conditions (30 mA cm^{-2}) and a discontinuous mode. The process was monitored by periodically analyzing TOC, IL concentration, pH, conductivity and ionic species of samples from the batchwise runs. The results were evaluated in terms of charge, calculated as the current applied during a specific time per volume (Ah dm^{-3}).

2.7 Analytical methods

Characterization of the catalysts

Table 2.3 collects a summary of the different techniques employed for the characterization of the catalysts and the information that each one provided.

Table 2.3. Characterization techniques.

Technique	Information	Equipment	Laboratory
N_2 adsorption-desorption isotherms	BET Area, pore volumen (meso- and mircoporosity)	Micromeritics Tristar 3020	Chemical Engineering (UAM)
Total reflection X-Ray Fluorescence (TXRF)	Fe content supported on the catalyst	TXRF Extra-II Rich & Seifert spectrometer - Si–Li detector	SIdI (UAM)
X-ray photoelectron spectroscopy - Energy dispersive X-ray spectroscopy analysis (XPS-EDAX)	Concentration and iron species on the catalyst surface	Physical Electronics 5700C Multitechnique instrument from Physical Electronics - MgKa radiation	SAIUEx (UEX)
Scanning Electron Microscopy - Energy Dispersive X-ray spectroscopy (SEM-EDX)	Morphology and surface composition of the catalyst	Hitachi S-3000N apparatus	SIdI (UAM)
X-ray Diffraction (XRD)	Crystalline phases in the catalyst	Siemens model D-5000 diffractometer	SIdI (UAM)
Elemental analysis	Composition of the catalyst in terms of C, N, S and H	LECO CHNS-932 analyzer	Chemical Engineering (UAM)
Ash content	Amount of ash in the catalyst	-	Chemical Engineering (UAM)

The pore structure of the catalysts was established from N_2 adsorption–desorption isotherms at −196 ºC obtained with a MicromeriticsTristar 3020 automated volumetric gas adsorption instrument. Prior to the adsorption measurements, a sample of 0.15 g of each catalyst was degassed to vacuum in a glass container at 150 ºC for 7 h by using a Micromeritics VacPrep 061 degassing apparatus. The micropore volume was calculated using the "t" method from the desorption data,

whereas the narrow mesopore (2-8 nm) was determine from the nitrogen adsorbed between relative pressures of 0.385 and 0.787.

The iron content of the catalyst was determined by total reflection X-ray fluorescence (TXRF) spectroscopy, using a TXRF Extra-II Rich & Seifert spectrometer equipped with a Si–Li detector. In this analysis, the sample is irradiated in total relexion conditions, emitting secondary photons characteristics of each atoms present in it.

The identification and composition of the Fe species on the catalyst surface were determined by X-ray photoelectron spectroscopy (XPS) on a Physical Electronics 5700C Multitechnique instrument from Physical Electronics using MgKa radiation (1253.6 eV) in combination with energy dispersive X-ray spectroscopy analysis (EDAX). The Fe catalysts evidenced a main band centered at 711.4 eV, accompanied by a secondary one at 725.1 eV, and a satellite peak around 719.0 eV associated to the presence of Fe^{3+} species in the catalyst surface

The morphology and surface composition of the catalyst were analyzed by Scanning Electron Microscopy–Energy Dispersive X- ray spectroscopy (SEM-EDX) with a Hitachi S-3000N apparatus. The equipment allowed to determine the morphology of the active layer in the matrix of alumina, by contrast difference between it and the metal layer.

The crystalline phases in the catalysts were analyzed by X-ray diffraction (XRD) using a Siemens model D-5000 diffractometer with Cu Kα radiation. X-ray was directed at the sample and the diffracted rays are collected determining the crystalline phase presented in the sample.

C, H, N and S were quantified with a LECO CHNS-932 elemental analyzer. The analysis is based on the complete oxidation of the sample in an instant combustion transforming the sample in CO_2, H_2O, SO_2 and N_2. The first three are analyzed in individual and selective infrared cells. The N_2 was measured by thermoconductivity after the elimination of the other compounds generated.

Total suspended (TSS) and volatile suspended solids (VSS)

The concentration of the total suspended solids (TSS) and volatile suspended solids (VSS) were obtained following the 2540 D and E procedures (APHA, 1992). A determined volume was filtered using a glass fiber filter (previously washed and weighed). The filter with the solid was dried at 105 ºC for 1 h and weighed. The difference between both weight values was the TSS contained in the sample. For the VSS quantification, the filter was heated at 550 ºC for 30 min. The difference between the weight after 105 ºC and the obtained after 550 ºC provide the VSS concentration in the sample.

Biomass characterization

An Upright Microscope Eclipse Ci-S/Ci-L image analyzer from Nikon equipped with a DS-Fi2 digital camera and a DS-U3 control unit, both from Nikon, were used to obtain micrographs of the granular morphology of the sludge. Microbial populations in the SBR were characterized by next-generation sequencing. Total genomic DNA in the aerobic granular biomass was determined, and paired-end sequencing of extracted DNA accomplished, by using an Illumina MiSeq platform from Research and Testing Laboratory Genomics (Lubbock, Texas, USA). The bacterial 16S rRNA variable regions V1–V3 were targeted by using the 28F-519R primer pair.

Total Organic Carbon (TOC)

Total Organic Carbon (TOC) was measured with a Shimadzu TOC-VCSH TOC analyzer and a Multi N/C 3100 Analytik Jena analyzer. These equipments allow the determination of the total carbon (TC) and the inorganic carbon (IC) content on a liquid sample, obtaining by difference the TOC value. TC was analyzed by oxidation of the sample with air at 680 ºC using a Pd/alumina catalyst. The CO_2 generated was quantified by an infrared detector, generating a peak whose area was proportional to the TC concentration. The IC quantification was carried out acidifying a new sample aliquot with hydrochloric acid, degrading the carbonates and/or bicarbonates compound into CO_2. The CO_2 measurement was processed similar than in the TC measure.

Chemical Oxygen Demand (COD)

The determination of the COD was carried out following the 5220D (APHA 1992) protocol. This method consist on the digestion of a known volume of water with potassium dichromate ($K_2Cr_2O_7$) in acid medium (H_2SO_4). In the analysis, 1.5 mL of $K_2Cr_2O_7$ solution (15 g L^{-1}), 3.5 mL of sulfuric acid solution (5.5 g of Ag_2SO_4 for each kg of H_2SO_4) and 2.5 mL of the sample were mixed. The resulting solution was digested at 150 ºC for 2 h in an ET108 Lovibond equipment. The absorbance of the solution was measured at 610 nm by an Agilent Cary 60 UV-Vis spectrophotometer, being proportional to the COD concentration.

Ion chromatography (IC)

Choline concentration was measured by using a Metrohm 790 Personal IC ion chromatograph with a Metrosep C4-250/4.0 column (stationary phase) and a mixture of 0.7 mM of 2,6-pyridinedicarboxylic acid and

1.7 mM of HNO_3 at a flow-rate of 0.9 mL min^{-1} (mobile phase). The injected sample volume was 20 µL. Chloride and acetate ions were determined on a DIONEX ICS-900 ion chromatograph with chemical suppression, using a Dionex IonPac AS22 4 × 250 mm column as stationary phase and a 1.4 mM $NaHCO_3$/4.5 mM Na_2CO_3 solution at 1 mL min^{-1} as mobile phase, being the injected sample volume 25 µL.

The DIONEX ICS-900 ion chromatography was also used for analyze, with the abovementioned conditions, the short chain organic acids (acetic, formic and oxalic acids) produced in the CWPO and electrolysis treatments.

The electrolysis intermediates have been measured using a Metrosep A Supp 7 column for the chloride, chlorate, perchlorate, nitrite and nitrate concentration and a Metrosep A Supp 4 column for the ammonium concentration. The mobile phase consisted of 85:15 v/v 3.6 mM Na_2CO_3/acetone solution for the determination of anions (flow rate: 0.80 cm^3 min^{-1}) and 1.7 mM HNO_3 and 1.7 mM 2,6-pyridinedicarboxylic acid solution for the determination of cations (flowrate: 0.90 cm^3 min^{-1}). The temperature of the oven was 45 and 30 °C for the determination of anions and cations, respectively. The volume injection was 20 µL.

High performance liquid chromatography (HPLC)

The quantification of the imidazolium cations has been carried out by means of high performance liquid chromatography (HPLC) using two different equipments: a Varian Prostar 325 high performance liquid chromatograph equipped with an UV–Vis detector and an Agilent 1100 series chromatograph equipped with a UV detector. The cations were determined at 218 nm and using a Synergy 4 mm Phenomenex Polar-RP 80 A column 15 cm long × 4.6 mm i.d. as stationary phase at 35 ºC.

The mobile phase (0.75 mL min^{-1}) was a mixture of phosphate buffer and acetonitrile at different concentrations from 5 to 40 % v/v depending on the particular imidazolium cation. The injection volume was 20 µL.

High performance liquid chromatography – mass spectrometry (HPLC-MS)

The concentration of NTf_2 ion was determined by liquid chromatography–mass spectrometry on an Agilent LC/MS SQ instrument, using an ACE Excel 3 C18-Amide 150 × 4.6 mm column at 40 °C as stationary phase and a 10:90 v/v mixture of formic acid and acetonitrile at 0.2 mL min^{-1} as mobile phase (injected sample volume, 1 µL; dilution, 1:100). This instrument was also used for the tentative identification of reaction byproducts. The mobile phase was a 99.9:0.1 v/v mixture of water and formic acid, and its flow rate 0.5 mL min^{-1}. Mass spectra were acquired over the *m/z* range 40–400.

H_2O_2 and Fe leached concentration

The H_2O_2 concentration was evaluated using a colorimetric method based on the yellow peroxocomplex formed between the titanium oxysulfate ($TiOSO_4$) and the H_2O_2. To determine the H_2O_2 concentration in a sample (0 - 1000 mg L^{-1}), 0.5 mL of the sample were mixed with 0.5 mL of $TiOSO_4$ and 4.5 mL of milli-Q water. The absorbance of the complex was measured in an Agilent Cary 60 UV-Vis spectrophotometer at 410 nm and related to the H_2O_2 concentration.

Fe leached concentration (0 – 10 mg L^{-1}) was measured by a colorimetric method based on the red Fe^{2+} complex formed with 1,10-fenantroline (0.25% in a 0.1 M HCl solution). The Fe^{3+} was reduced in presence of hydroxylamine (10 % w/w). The sample (4 mL) was mixed

with 0.5 mL of hydroxylamine solution, and after 15 min, 0.5 mL of fenantroline solution. The absorbance of the complex was measured in

3

Assessment of the ecotoxicity and biodegradability of imidazolium and choline-based ionic liquids

3.1

Assessment the ecotoxicity and inhibition of imidazolium ionic liquids by respiration inhibition assays

Diaz, E., Monsalvo, V.M., Lopez, J., Mena, I.F., Palomar, J., Rodriguez, J.J., Mohedano, A.F. 2018. Assessment the ecotoxicity and inhibition of imidazolium ionic liquids by respiration inhibition assays. Ecotoxicol. Environ. Saf. 162, 29–34

Assessment the ecotoxicity and inhibition of imidazolium ionic liquids by respiration inhibition assays

Abstract

The ecotoxicity and inhibition of 12 imidazolium ionic liquids (ILs) with alkyl chain from C4 to C10 and chloride (Cl^-), tetrafluoroborate ($BF4^-$) and bis(trifluoromethanesulfonyl)imide (NTf_2^-) anions have been studied by means of respiration inhibition assays using activated sludge collected from a wastewater treatment plant. This test represents an alternative easy, economic and quick way to evaluate the true impact of ILs on activated sludgebased wastewater treatment. For comparison purposes, the EC_{50} values were also determined by the Microtox test (*Vibrio fischeri*). It was observed that this widely used microbial test overestimates the effect of the ILs on biological wastewater treatment facilities, especially in the case of ILs with lower ecotoxicity. The results of the biological tests showed that the alkyl chain length plays a crucial role in the ecotoxicity of ILs. A significant increase of the toxicity with the length of the n-alkyl chain was found. Regarding to the impact of the anion, the ecotoxicity measured by respiration inhibition assays follows the order NTf_2^-> Cl^-> BF_4^-, being the anion effect higher as decreasing the length of cation alkyl chain. According to the hazard substances ranking for aquatic organisms (Passino and Smith, 1987), imidazolium ILs with C4 alkyl chain can be classified as "practically

harmless" compounds whereas those with alkyl chains C8 or C10 correspond to "highly toxic" species.

3.1 Assessment the ecotoxicity and inhibition of imidazolium ionic liquids by respiration inhibition assays

3.1.1. Introduction

In the past 20 years, ionic liquids (ILs) have attracted increasing attention as a new generation of green solvents with potential uses in various industrial fields (Petkovic et al., 2011). ILs are based on combined organic cations and organic or inorganic anions with a melting point below 100 °C. They are characterized by low vapor pressure and high thermal and chemical stabilities. Due to the large number of feasible combinations, it is possible to synthesize ILs with selected properties for numerous applications (Plechkova and Seddon, 2008). The increasing interest for these novel and versatile compounds is mainly focused on the following potential industrial applications: separation processes, catalysis, electrochemistry and materials science. However, the impact that ILs, especially those with high water solubility, can cause on aquatic organisms has been scarcely studied so far (Pham et al., 2010; Docherty et al., 2015).

ILs can be discharged into the aquatic environment due to accidental spills, containers washing operations, leaching from waste disposal sites, as well as waste streams inefficiently treated in current wastewater treatment plants (Tsarpali and Dailianis, 2015). Conventional biological processes are widely used as a cost-effective strategy for wastewater treatment. However, the potential application of such processes to a given effluent must consider some critical issues, as ecotoxicity and biodegradability. Preliminary results have revealed that there is insufficient evidence to confirm the degradation of imidazolium, thiazolium and pyridium ILs, whereas those derived from aliphatic amines and organic acids could be considered as potentially biodegradable (Peric et al., 2013; Neumann et al., 2014; Jordan and Gathergood, 2015; Diaz et al., 2016). In addition, the IL structure plays

a key role on the inhibitory effect over the activated sludge performance. As example, alkyl methyl imidazolium ILs have been claimed as non-biodegradable compounds and they do not provoke any toxic effect on activated sludge (Gathergood et al., 2006; Romero et al., 2008; Quijano et al., 2011; Diaz et al., 2016; Rodriguez Castillo et al., 2016). The degradation of easily biodegradable substrates, like sodium n-dodecyl sulfate or glucose in presence of ILs, after long acclimation periods has been reported (Quijano et al., 2011; Rodriguez Castillo et al., 2016). However, the addition of ILs as Aliquat, 1-methyl-3–2-methoxyethyl-imidazolium or 1-methyl-3-butenyl-imidazolium provoked complete inhibition of the microbial community present in activated sludge (Quijano et al., 2011; Rodriguez Castillo et al., 2016).

Different standard toxicity tests have been proposed in the literature and regulations. Several organisms have been used as bioindicators, including invertebrate (*Daphnia magna*, ISO 6341) (Samorì et al., 2010; Pham et al., 2010; Stolte et al., 2012), algae (*Selenastrum capricornutum*, ISO 8692) (Cho et al., 2008; Peric et al., 2013; Costa et al., 2015), plant (*Lemna minor*, ISO/CD 20079) (Jastorff et al., 2005; Matzke et al., 2007; Stolte et al., 2007) or mammalian cells (*Rat leukemia cells,* IPC-81) (Ranke et al., 2007; Stolte et al., 2013), as a reproducible IL toxicity screening tool. These micro/organisms are exposed to different concentrations of ILs under controlled conditions and the evolution of a characteristic response of each organism is monitored. Among them, luminescent microbial test with the microorganism *Vibrio fischeri* (ISO 11348) is one of the most used for acute toxicity measurements because it is quick, simple, cost-effective and sensitive to evaluate IL ecotoxicity (Ranke et al., 2004; Johnson, 2005; Romero et al., 2008; Viboud et al., 2012; Ventura et al., 2014; Costa et al., 2015; Hernández-Fernández et

al., 2015). However, the main drawback of the aforementioned methods is that the response of the microorganism used does not represent the behavior of the microbial community present in activated sludge from biological wastewater treatment systems. Consequently, the ecotoxicity data from those tests could over/underestimate the effect of ILs on wastewater treatment facilities. Meanwhile, the toxicity of ILs can be studied by a respiration inhibition test (OECD 209, ISO 8192) where the impact of ILs on activated sludge is inferred from specific dissolved oxygen uptake rate measurements, intimately related to the microbial activity. After data collection, the EC_{50} value (defined as the effective concentration of a sample that causes 50% inhibition) can be determined. Markiewicz et al. (2013) reported a pioneer work investigating the influence of ILs on activated sewage sludge communities. A respiration inhibition test was applied using activated sludge from different domestic and industrial sources. Results obtained generally match the IL ecotoxicity trends found for other organism and test systems. It was suggested that EC_{50} values obtained from *Vibrio fischeri* can be reliably used to assess the IL inhibition potential.

The alkyl methyl imidazolium ILs are non-volatile, non-flammable and present high thermal stability, being excellent wide-range solvents (Gordon, 2001; van Rantwijk et al., 2003). Thus, that family has a high potential of entering the water bodies through to industrial discharges. In the current work, the ecotoxicity of 12 imidazolium ILs in aqueous phase has been assessed by obtaining the EC_{50} values upon respiration inhibition assays with an activated sludge from a domestic sewage treatment plant. The effect of the IL structure in the ecotoxicity has been systematically analyzed by studying common cation/anion series, including imidazolium ring with different alkyl chain length (C4-C10) and three remarkably different anions (Cl^-, BF_4^-, NTf_2^-). For the sake of

comparison, EC_{50} values were also obtained by the Microtox standard procedure. Structure-activity relationships were stablished to analyze simultaneously the cation and anion influence. Results obtained from two different tests were compare in order to check if the tests provide analogous information, which could be used to define a treatment strategy to deal with these compounds.

3.1.2. Materials and methods

Ionic liquids

Imidazolium ILs with different chain lengths (4, 6, 8 and 10 carbons) and anions (chloride (Cl^-), tetrafluoroborate (BF_4^-) and bis(trifluoromethilsulfonyl)imide (NTf_2^-)) were selected for this study (Table 3.1.1).

3.1 Assessment the ecotoxicity and inhibition of imidazolium ionic liquids by respiration inhibition assays

Table 3.1.1. Information on ionic liquids used in this work.

Ionic liquid	Supplier	Purity % (w/w)	K_{ow}
1-Butyl-3-methylimidazolium chloride	Sigma-Aldrich	>98%	0.001 a
1-Hexyl-3-methylimidazolium chloride	Sigma-Aldrich	>97%	0.013 a
1-Methyl-3-octylimidazolium chloride	Solchemar	>98%	0.123 a
1-Decyl-3-methylimidazolium chloride	Sigma-Aldrich	>96%	0.520 b
1-Butyl-3-methylimidazolium tetrafluoroborate	Iolitec	>99%	0.036 c
1-Hexyl-3-methylimidazolium tetrafluoroborate	Iolitec	>99%	0.195 c
1-Methyl-3-octylimidazolium tetrafluoroborate	Solchemar	>98%	0.209 d
1-Decyl-3-methylimidazolium tetrafluoroborate	Iolitec	>98%	-
1-Butyl-3-methylimidazolium bis(trifluoromethylsulfonyl) imide	Iolitec	99%	0.110 e
1-Hexyl-3-methylimidazolium bis(trifluoromethylsulfonyl) imide	Iolitec	99%	1.42 e
1-Methyl-3-octylimidazolium bis(trifluoromethylsulfonyl) imide	Iolitec	99%	6.30 e
1-Decyl-3-methylimidazolium bis(trifluoromethylsulfonyl) imide	Iolitec	>98%	-

a Palomar et al. (2009).
b Domanska et al. (2008).
c Stepnowski and Storoniak (2005).
d Montalbán et al. (2015).
e Ropel et al. (2005).

ILs are used without previous purification and named according to the number of carbons of the alkyl chain substituent as the butyl group "B", hexyl group "H", octyl group "O" and decyl group "D", and the termination Cl, BF_4 or NTf_2 corresponds to the anion. The suffix "mim" corresponds with the imidazolium group (Table 3.1.2).

Table 3.1.2. Cations and anions used in this study.

Anion	Alkyl chain length
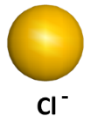 Cl^-	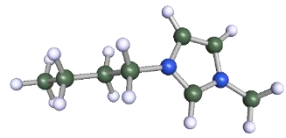 **$Bmim^+$**
 BF_4^-	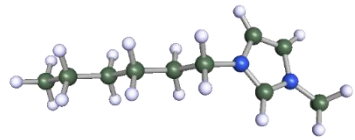 **$Hmim^+$**
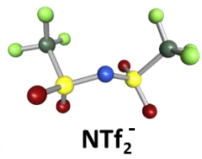 NTf_2^-	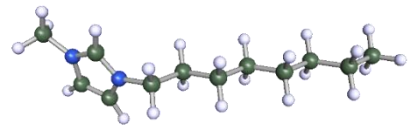 **$Omim^+$**
	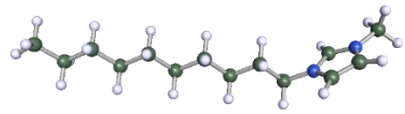 **$Dmim^+$**

Inoculum and culture medium

Activated sludge for the respiration inhibition test (OECD 209, ISO 8192) was collected from a domestic sewage treatment plant (Madrid, Spain), and did not undergo to any acclimation process to the ILs studied. Waste sewage sludge was maintained in a sequencing batch reactor (SBR) at 25 °C and supplied with sodium acetate and glucose as carbon sources (50:50 w/w on chemical oxygen demand (COD) basis)

at an organic load rate of 0.4 mg COD mg VSS^{-1} day^{-1}, referring VSS to volatile suspended solids. The medium was supplemented with ammonium sulfate, phosphoric acid and mineral salts as nitrogen, phosphorous and micronutrients sources ($FeCl_3$, $CaCl_2$, KCl and $MgCl_2$), respectively. A COD:N:P ratio of 100:5:1 (w/w) was fixed and mineral salts were also added as micronutrients supply in a COD: micronutrients (Fe, Ca, K and Mg) ratio of 1:0.05. Biomass concentration in the reactor was maintained at around 3500 mg VSS L^{-1}.

Inhibition assays

Respiration inhibition tests with activated sludge were carried out according to the method proposed by Polo et al. (2011). The procedure consists on short-term respirometric measurements using unacclimated sludge (350 mg VSS L^{-1}) where an easily biodegradable substrate (sodium acetate) is fed alone or together with different concentrations of ILs. Assays were carried out in a Liquid-Static-Static (LSS) respirometer (Chica et al., 2007), monitoring the dissolved oxygen concentration decay. Aeration and oxygen probes were controlled by an electronic interface. The respirometer operated with two independent reactors simultaneously to check the reproducibility. The reactors have very small headspace so that oxygen transfer from the gas to the liquid can be neglected. They were placed in a thermostatic bath and continuously stirred by magnetic bars. Nitrification was inhibited by using N-allyltiourea. Fresh activated sludge was used in each test to avoid partial acclimation of the microorganisms to the target chemicals, which could lead to possible underestimation of the toxic effects. The biomass activity was measured in terms of specific exogenous oxygen uptake rate (SOUR). The inhibition (Eq. (1)) is defined as function of

the parameter γ (Eq. (2)) and the ratio the specific exogenous oxygen uptake rate for the reference substance (sodium acetate) in presence of a given concentration of the ILs ($SOUR_T$) and SOUR the obtained value for the reference substance ($SOUR_R$). Both measures are corrected by the value for the endogenous SOUR.

$$\text{Inhibition } (\%) = (\gamma) \cdot \frac{SOUR_T}{SOUR_R} \quad (1)$$

$$\gamma = \frac{SOUR_R - SOUR_T}{SOUR_R} \quad (2)$$

Inhibition caused by the ILs was assessed in terms of EC_{50}, defined as the effective concentration causing 50% reduction of SOUR (γ=1). It is calculated using i) a logistic model that establish a relationship between the inhibition percentage and the logarithm compound concentration (Eq. (3)) and ii) a linear fit between the logarithm of parameter γ and the logarithm of IL concentration (Eq. (4)):

$$\text{Inhibition } (\%) = \frac{100}{1 + 10^{-k(\log C - \log EC_{50})}} \quad (3)$$

$$\log\gamma = a + b \cdot \log C\,;\ EC_{50} = 10^{-a/b} \quad (4)$$

Ecotoxicity test

Ecotoxicity measurements were also carried out following the standard Microtox ® test procedure (ISO, 11348-3, 1998). This test is based on the decrease of light emission by the marine bacteria *Vibrio fischeri* (*Photobacterium phosphoreum*). A Microtox M500 Analyzer (Azur Environmental) was used to measure the inhibition of the light emitted by the bacteria after 15 min contact time with the sample. Previously, the pH was adjusted into the range 6-8. The results were expressed as EC_{50} defined as the effective concentration causing 50% reduction of

light emission, calculated using the abovementioned linear model (Eq. (4)).

3.1.3. Results and discussion

Table 3.1.3 shows the EC_{50} values obtained from the Microtox test for the ILs tested and, for the sake of comparison, also includes values from the literature. As can be seen, there is a good agreement between the values of the current work and those previously reported by other authors. Moreover, the low standard deviation values confirm the reproducibility of the test. It can be clearly observed a general trend towards ecotoxicity increase (lower EC_{50}) with the length of the linear alkyl chain of the ILs. That effect becomes more pronounced for ILs with longer chains, so that the ILs with octyl and decyl groups have frankly high ecotoxicities compared to those of same species recognized as highly toxic, like hydroquinone (Zazo et al., 2007), benzoquinone (Zazo et al., 2007) or chlorophenols (Calvo et al., 2004). Even the less ecotoxic IL (the butyl ones) yielded EC_{50} values significantly lower (higher ecotoxicity) than those reported for conventional solvents like methanol (EC_{50}, μM: 10^7), acetone (EC_{50}, μM: $3.1 \cdot 10^5$) and acetonitrile (EC_{50}, μM: $6.3 \cdot 10^5$) (Kaiser and Palabrica, 1991).

Table 3.1.3. EC_{50} values (mean ± standard deviation; n = 2) for imidazolium ILs from Microtox and inhibition respiration tests (r^2: determination coefficient).

ILs	Microtox Test				Respiration Inhibition Test			
	This study		Other studies		Logistic fit		Linear fit	
	EC_{50} (µM)	r^2	EC_{50} (µM)	References	EC_{50} (µM)	r^2	EC_{50} (µM)	r^2
BmimCl	3162±1.91	0.994	891-5128	Docherty and Kulpa, 2005; Garcia et al., 2005; Couling et al., 2006; Stolte et al., 2007; Romero et al., 2008; Peric et al., 2013; Montalbán et al., 2016	2089±1259	0.757	2398±174	0.992
HmimCl	182±1.29	0.998	87.1-813	Ranke et al., 2004; Garcia et al 2005; Luis et al., 2007 Romero et al., 2008; Montalbán et al., 2016	339±229	0.963	331±51.3	0.993
OmimCl	4.79±1.45	0.979	4.26-15.5	Garcia et al 2005; Luis et al., 2007; Stolte et al 2007 Romero et al., 2008; Montalbán et al., 2016	23.4±8.32	0.932	23.4±7.08	0.989
DmimCl	0.69±1.02	0.999	0.59-3.16	Stolte et al 2007	3.47±1.10	0.992	3.31±1.10	0.996
$BmimBF_4$	3236±2.75	0.983	1259-3548	Ranke et al., 2004; Garcia et al 2005; Samori et al., 2007; Samori et al., 2010; Montalbán et al., 2016	15849±200	0.838	14125±178	0.998
$HmimBF_4$	331±2.19	0.985	1513	Ranke et al., 2004	1202±70.8	0.925	1174±67.6	0.949
$OmimBF_4$	10.0 ±1.23	0.994	8.13-25.7	Ranke et al., 2004; Matzke et al., 2007; Montalbán et al., 2016	45.7±6.61	0.907	49.1±5.12	0.939
$DmimBF_4$	1.41±1.01	0.994	0.66	Ranke et al., 2004	6.31±1.07	0.992	6.31±1.07	0.991
$BmimNTf_2$	871±2.04	0.987	295-4677	Garcia et al., 2005; Couling et al., 2006; Matzke et al., 2007; Montalbán et al., 2016	347±43.7	0.917	346±37.1	0.996
$HmimNTf_2$	81.3±1.23	0.997	66.1	Montalbán et al., 2016	91.2±37.2	0.983	91.2±12.9	0.990
$OmimNTf_2$	15.8±1.66	0.986	9.77	Montalbán et al., 2016	ND	ND	11.7±1.44	0.971
$DmimNTf_2$	2.95±1.12	0.978			1.95±1.05	0.991	1.95±1.05	0.992

In the respirometric tests with activated sludge, the EC_{50} values were obtained by two fitting methods: logistic and linear (Polo et al.,2011). The former requires inhibition extension up to almost 100% to be reached in order to obtain good fitting parameters. This fact limits its applicability since some ILs have water solubility below the concentration required to provoke high inhibition. However, as can be seen in Table 3.1.3, in most of the studied cases, the EC_{50} values obtained from both fitting methods were similar. Previous studies about

the inhibition of ILs on activated sludge respiration have revealed differences in the EC_{50} values depending on the source of inoculum. This fact seems to be related to the adaptability of a taxonomically complex community, as activated sludge, to degrade xenobiotic compounds (Gutiérrez et al., 2002). That was the case for imidazolium ILs with four sewage sludge sources (EC_{50} values (μM): HmimCl: 708-15136; OmimCl: 141-1820; DmimCl: 12.6-105) (Markiewicz et al., 2013).

Figure 3.1.1 depicts the EC_{50} values (expressed as log) for both the inhibition bioassay with activated sludge and the Microtox test using *Vibrio fischeri*. It can be observed a similar general trend towards ecotoxicity increase with the length of the linear alkyl chain, depending on the IL anion. However, the EC_{50} values in Table 3.1.3 reveal that the respiration test provides a significant wider range of EC_{50} values depending on IL structure than Microtox test; in addition, it is generally observed higher toxicity effects measured by Microtox Test. In fact, the EC_{50} values from *Vibrio fischeri* can be used to evaluate the sludge inhibition potential of ILs, at least for the less toxic ones.

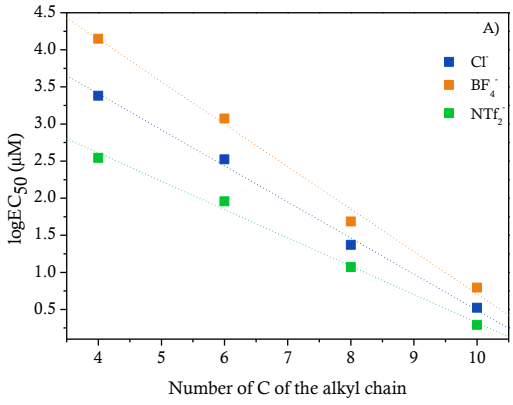

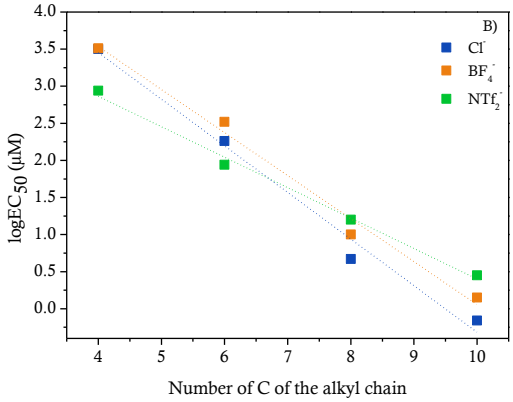

Figure 3.1.1. Relationship between $logEC_{50}$ and the length of alkyl chain for A) inhibition respiration (linear fit) assay and B) Microtox test.

The wide range of toxicity values for the ILs tested (Table 3.1.3) is related to the diversity of their cationic and anionic groups. Figure 3.1.1 also illustrates the cation and anion effects on the $logEC_{50}$ values of the ILs studied in this work. A clear linear relationship between $logEC_{50}$ and the alkyl chain length can be observed. Table 3.1.4 summarizes the linear regression equations and the corresponding values of the determination coefficient. Goodness of fit yielded somewhat better for the respiration inhibition assays than for the Microtox test, although it was fairly good in all cases. Both tests show an ecotoxicity increase with the length of the linear chain, which has been related to the loss of polarity or the accentuation of their lipophilic character at increasing chain length (Ranke et al., 2007; Costello et al., 2009; Cvjetko Bubalo et al., 2013; Diaz et al., 2016;). Consequently, EC_{50} ecotoxicity values of Table 3.1.3 can be related to the octanol-water partition coefficient (K_{OW} in Table 3.1.1) that increased with the length of the imidazolium cation alkyl chain and the hydrophobicity of the anion (Deng et al., 2011; Montalbán et al., 2015, 2018). This has been associated with a

higher capacity to accumulate the ILs in the biological membranes that are essentially nonpolar interfaces (Garcia et al., 2005). Stolte et al. (2007) observed a strong interaction of hydrophobic IL cations, using a variety of microorganisms, with two different types of common biological lipidic bilayers.

Table 3.1.4. Fitting equations of $logEC_{50}$ (μM) vs the length of alkyl chain (number of carbons, C).

Anions	**Respiration Inhibition Assay***		**Microtox Test**	
	Linear fit	**r^2**	**Linear fit**	**r^2**
Cl^-	$logEC_{50}$= 5.35-0.49·C	0.998	$logEC_{50}$= 5.97-0.63·C	0.981
BF_4^-	$logEC_{50}$=6.43-0.57·C	0.997	$logEC_{50}$=5.86-0.58·C	0.983
NTf_2^-	$logEC_{50}$=4.14-0.38·C	0.997	$logEC_{50}$=4.51-0.41·C	0.991

* EC_{50} values obtained from linear fit in Table 3.1.2

Regarding the anion, it has been commonly considered of minor effect (and nearly constant) on the toxicity in the literature so far (Ranke et al., 2004; Couling et al., 2006; Luis et al., 2007; Romero et al., 2008; Pretti et al., 2009). However, the results of respirometric tests show a clear effect of the nature of the IL anion on the inhibition of activated sludge (Fig. 1A), particularly in the case of ILs with imidazolium cation and short alkyl chain. The values of the intercept of the aforementioned linear relationship (Table 3.1.4) reveal some significant differences between the IL families with different anions, increasing the IL ecotoxicity in the order NTf_2^-> Cl^-> BF_4^-. The higher toxicity values obtained for the ILs with NTf_2^- has been also related to its K_{OW} value, more than one order of magnitude higher than ILs containing other anions such as BF_4^- or Cl^- (Ropel et al., 2005; Kamath et al., 2012; Montalbán et al., 2015). The different slope and intercept values of Table 3.1.4 imply mixed cation-anion inhibitory effects on the activated sludge performance rather than an additive effect of the intrinsic

toxicities of the cations and anions. The anion toxic effects are clearly stronger in the ILs containing shorter cation alkyl chain, whereas increasing the chain length mitigates the toxic effect of the anion (as example, the EC_{50} ratios for $BmimBF_4$/$BmimNTf_2$ and $DmimBF_4$ /$DmimNTf_2$ are, respectively, 41 and 3, see Table 3.1.3). These different anion effects were already observed in previous works but in a lesser extent (Torrecilla et al., 2010).

Looking at the hazard ranking for aquatic organisms (Passino and Smith, 1987), the ILs tested can be classified from harmless to highly toxic according to their EC_{50} values expressed in mg L^{-1}. As can be seen in Table 3.1.5, several differences have been observed in the classification of some ILs depending on the test used to evaluate the ecotoxicity. *Vibrio fischeri* shows a higher sensitivity to ILs than activated sludge, but regardless the test used, $Bmim^+$ IL can be classified as "practically harmless" compounds whereas $Omin^+$ and $Dmim^+$ IL are "highly toxic" ones.

Table 3.1.5. Ecotoxicity of the tested ILs according to Passino and Smith classification (Passino and Smith, 1987).

Ionic liquid	Harmless EC_{50} > 1000 mg·L^{-1}		Practically Harmless EC_{50}: 100 - 1000 mg·L^{-1}		Moderately Toxic EC_{50}: 10 - 100 mg·L^{-1}		Highly Toxic EC_{50} < 10 mg·L^{-1}	
	Activated sludge	*Vibrio fischeri*	Activated sludge	*Vibrio fischeri*	Activated sludge	*Vibrio fischeri*	Activated sludge	*Vibrio fischeri*
$BmimNTf_2$			✓	✓				
$BmimBF_4$	✓			✓				
BmimCl			✓	✓				
$HmimNTf_2$					✓	✓		
$HmimBF_4$			✓			✓		
HmimCl					✓	✓		
$OmimNTf_2$							✓	✓
$OmimBF_4$					✓			✓
OmimCl							✓	✓
$DmimNTf_2$							✓	✓
$DmimBF_4$							✓	✓
DmimCl							✓	✓

3.1.4. Conclusions

The Microtox test, using the microorganism *Vibrio fischeri*, and respiration inhibition assays with activated sludge collected from a wastewater treatment plant have been used to analyze the toxicity and the inhibition effect of different ILs. Both tests have showed similar ecotoxicity trends, although EC_{50} values tend to be lower in the case of Microtox Test.

A well-fitting linear correlation between the toxicity ($logEC_{50}$) and the length of the alkyl chain substituent (C4-C10) of imidazolium ILs has been found in most of the cases. The toxicity increases significantly with the chain length, which can be related to the loss of IL polarity or their lipophilic character. The NTf_2^- anion was more toxic than BF_4^- or Cl^-, but its relative impact on toxicity is reduced for ILs with long alkyl side chain (> 6 C atoms). Attending to the obtained results, imidazolium ILs with C4 alkyl chain can be classified as "practically harmless" compounds whereas those with alkyl chains C8 or C10 correspond to "highly toxic" species.

Taking into account the high water solubility of these ILs, their high ecotoxicity inhibition potential and poor biodegradability of most of them, they would be recalcitrant in conventional activated sludge wastewater treatment. Moreover, some of the ILs can cause severe undesirable effects on the microbial consortium, which can destabilize the biological system. Thus, it is necessary to develop cost-effective solutions to avoid or mitigate their negative impact in aquatic environments.

3.1.5. References

- Calvo, L., Mohedano, A.F., Casas, J.A., Gilarranz, M.A., Rodriguez, J.J., 2004. Treatment of chlorophenols-bearing wastewaters through hydrodechlorination using Pd/activated carbon catalysts. Carbon 42, 1377–1381.
- Chica, A.F., Martin, A., Vazquez, F.J., Carmona, F.J., Mohedo, J.J., 2007. Respirometer to analyze measure dissolved oxygen and oxygen demand of microbes in leachate from municipal waste. ES 2283171.
- Cho, C.W., Jeon, Y.C., Pham, T.P.T., Vijayaraghavan, K., Yun, Y.S., 2008. The ecotoxicity of ionic liquids and traditional organic solvents on microalga *Selenastrum capricornutum*. Ecotoxicol. Environ. Saf. 71, 166–171.
- Costa, S.P.F., Pinto, P.C.A.G., Saraiva, M.L.M.F.S., Rocha, F.R.P., Santos, J.R.P., Monteiro, R.T.R., 2015. The aquatic impact of ionic liquids on freshwater organisms. Chemosphere 139, 288–294.
- Costello, D.M., Brown, L.M., Lamberti, G.A., 2009. Acute toxic effects of ionic liquids on zebra mussel (*Dreissena polymorpha*) survival and feeding. Green Chem. 11, 548–553.
- Couling, D.J., Bernot, R.J., Docherty, K.M., Dixon, J.K., Maginn, E.J., 2006. Assessing the factors responsible for ionic liquid toxicity to aquatic organisms via quantitative structure-property relationship modeling. Green Chem. 8, 82–90.
- Cvjetko Bubalo, M., Radošević, K., Redovniković, I., Halambek, J., Gaurina Srček, V., 2013. A brief overview of the potential environmental hazards of ionic liquids. Ecotoxicol. Environ. Saf. 99, 1–12.
- Deng, Y., Besse-Hoggan, P., Sancelme, M., Delort, A.-M., Husson, P., Costa Gomes, M.F., 2011. Influence of oxygen functionalities on the environmental impact of imidazolium based ionic liquids. J. Hazard. Mater. 198, 165–174.
- Diaz, E., Monsalvo, V., Palomar, J., Mohedano, A.F., 2016. In: Atwood, David A. (Ed.), Ionic Liquids: Bacterial Degradation in Wastewater Treatment Plants, in Encyclopedia of Inorganic and Bioinorganic Chemistry. John Wiley & Sons, Ltd, Chichester, UK.
- Docherty, K.M., Kulpa, J.C.F., 2005. Toxicity and antimicrobial activity of imidazolium and pyridinium ionic liquids. Green Chem. 7, 185–189.
- Docherty, K.M., Aiello, S.W., Buehler, B.K., Jones, S.E., Szymczyna, B.R., Walker, K.A., 2015. Ionic liquid biodegradability depends on specific wastewater microbial consortia. Chemosphere 136, 160–166.

- Domanska, U., Rekawek, A., Marciniak, A., 2008. Solubility of 1-Alkyl-3-ethylimidazolium-Based Ionic liquids in water and 1-Octanol. J. Chem. Eng. Data 53, 1126‑1132.
- Garcia, M.T., Gathergood, N., Scammells, P.J., 2005. Biodegradable ionic liquids Part II. Effect of the anion and toxicology. Green Chem. 7, 9‑14.
- Gathergood, N., Scammells, P.J., Garcia, M.T., 2006. Biodegradable ionic liquids Part III. The first readily biodegradable ionic liquids. Green Chem. 8, 156‑160.
- Gordon, C.M., 2001. New developments in catalysis using ionic liquids. Appl. Catal. A: Gen. 222, 101‑117.
- Gutiérrez, M., Etxebarria, J., De las Fuentes, L., 2002. Evaluation of wastewater toxicity: comparative study between Microtox and activated sludge oxygen uptake inhibition. Water Res. 36, 919‑924.
- Hernández-Fernández, F.J., Bayo, J., Pérez de los Ríos, A., Vicente, M.A., Bernal, F.J., Quesada-Medina, J., 2015. Discovering less toxic ionic liquids by using the Microtox toxicity test. Ecotoxicol. Environ. Saf. 116, 29‑33.
- ISO 11348-3, 1998. water quality ‑ determination of the inhibitory effect of water samples on the light emission of *Vibrio fischeri* (Luminescent bacteria test) ‑ Part 3: method using freeze-dried bacteria, 1998.
- Jastorff, B., Molter, K., Behrend, P., Bottin-Weber, U., Filser, J., Heimers, A., Ondruschka, B., Ranke, J., Schaefer, M., Schroder, H., Stark, A., Stepnowski, P., Stock, F., Stormann, R., Stolte, S., Welz-Biermann, U., Ziegert, S., Thoming, J., 2005. Progress in evaluation of risk potential of ionic liquids–basis for an eco-design of sustainable products. Green Chem. 7, 362‑372.
- Johnson, B.T., 2005. In: Blaise, C., Férard, J.F. (Eds.), Small-Scale Freshwater Toxicity Investigations-Microtoxs Acute Toxicity Test, 1. Springer, Netherlands, 69‑105.
- Jordan, A., Gathergood, N., 2015. Biodegradation of ionic liquids ‑ a critical review. Chem. Soc. Rev. 44, 8200‑8237.
- Kaiser, K.L.E., Palabrica, V.S., 1991. *Photobacterium phosphoreum* toxicity data index. Water Pollut. Res. J. Can. 26, 361‑431.
- Kamath, G., Bhatnagar, N., Baker, G.A., Baker, S.N., Potoff, J.J., 2012. Computational prediction of ionic liquid 1-octanol/water partition coefficients. Phys. Chem. Chem. Phys. 14, 4339‑4342.
- Luis, P., Ortiz, I., Aldaco, R., Irabien, A., 2007. A novel group contribution method in the development of a QSAR for predicting the toxicity (*Vibrio fischeri* EC_{50}) of ionic liquids. Ecotoxicol. Environ. Saf. 67, 423‑429.

- Markiewicz, M., Piszora, M., Caicedo, N., Jungnickel, C., Stolte, S., 2013. Toxicity of ionic liquid cations and anions towards activated sewage sludge organisms from different sources - Consequences for biodegradation testing and wastewater treatment plant operation. Water Res. 47, 2921-2928.
- Matzke, M., Stolte, S., Thiele, K., Juffernholz, T., Arning, J., Ranke, J., Welz-Biermann, U., Jastorff, B., 2007. The influence of anion species on the toxicity of 1-alkyl-3-methylimidazolium ionic liquids observed in an (eco) toxicological test battery. Green Chem. 9, 1198-1207.
- Mester, P., Wagner, M., Rossmanith, P., 2015. Antimicrobial effects of short chained imidazolium-based ionic liquids–Influence of anion chaotropicity. Ecotoxicol. Environ. Saf. 111, 96-101.
- Montalbán, M.G., Collado-González, M., Trigo, R., Díaz Baños, F.G., Víllora, G., 2015. Experimental measurements of octanol-water partition coefficients of ionic liquids. J. Adv. Chem. Eng. 5, 133.
- Montalbán, M.G., Hidalgo, J.M., Collado-González, M., Díaz Baños, F.G., Víllora, G., 2016. Assesing chemical toxicity of ionic liquids on *Vibrio fischeri*: correlation with structure and composition. Chemosphere 155, 405-414.
- Montalbán, Víllora, G., Licence, P., 2018. Ecotoxicity assessment of dicationic versus monocationic ionic liquids as a more environmentally friendly alternative. Ecotoxicol. Environ. Saf. 150, 129-135.
- Neumann, J., Pawlik, M., Bryniok, D., Thöming, J., Stolte, S., 2014. Biodegradation potential of cyano-based ionic liquid anions in a culture of *Cupriavidus spp*. and their in vitro enzymatic hydrolysis by nitrile hydratase. Environ. Sci. Pollut. Res. 21, 9495-9505.
- Palomar, J., Lemus, J., Gilarranz, M.A., Rodriguez, J.J., 2009. Adsorption of ionic liquids from aqueous effluents by activated carbon. Carbon 47, 1846-1856.
- Passino, D.R.M., Smith, S.B., 1987. Acute bioassays and hazard evaluation of representative contaminants detected in Great lakes fish. Environ. Chem. 6, 901-907.
- Peric, B., Sierra, J., Martí, E., Cruanas, R., Garau, M.A., Arning, J., Bottin-Weber, U., Stolte, S., 2013. Ecotoxicity and biodegradability of selected protic and aprotic ionic liquids. J. Hazard. Mater. 261, 99-105.
- Petkovic, M., Seddon, K.R., Rebelo, L.P.N., Pereira, C.S., 2011. Ionic liquids: a pathway to environmental acceptability. Chem. Soc. Rev. 40, 1383-1403.
- Plechkova, N.V., Seddon, K.R., 2008. Applications of ionic liquids in the chemical industry. Chem. Soc. Rev. 37, 123-150.

- Pham, T.P.T., Cho, C.W., Yun, Y.S., 2010. Environmental fate and toxicity of ionic liquids: a review. Water Res. 44, 352-372.
- Polo, A.M., Tobajas, M., Sanchis, S., Mohedano, A.F., Rodriguez, J.J., 2011. Comparison of experimental methods for determination of toxicity and biodegradability of xenobiotic compounds. Biodegradation 22, 751-761.
- Pretti, C., Chiappe, C., Baldetti, I., Brunini, S., Monni, G., Intorre, L., 2009. Acute toxicity of ionic liquids for three freshwater organisms: *Pseudokirchneriella subcapitata, Daphnia magna* and *Danio rerio*. Ecotoxicol. Environ. Saf. 72, 1170-1176.
- Quijano, G., Couvert, A., Amrane, A., Darracq, G., Couriol, C., Le Cloirec, P., Paquin, L., Carrié, D., 2011. Toxicity and biodegradability of ionic liquids: new perspectives towards whole-cell biotechnological applications. Chem. Eng. J. 174, 27-32.
- Ranke, J., Mölter, K., Stock, F., Bottin-Weber, U., Poczobutt, J., Hoffmann, J., Ondruschka, B., Filser, J., Jastorff, B., 2004. Biological effects of imidazolium ionic liquids with varying chain lengths in acute *Vibrio fischeri* and *WST-1* cell viability assays. Ecotoxicol. Environ. Saf. 58, 396-404.
- Ranke, J., Muller, A., Bottin-Weber, U., Stock, F., Stolte, S., Arning, J., Stormann, R., Jastorff, B., 2007. Lipophilicity parameters for ionic liquid cations and their correlation to in vitro cytotoxicity. Ecotoxicol. Environ. Saf. 67, 430-438.
- Rodriguez Castillo, A.S., Guihéneuf, S., Le Guéveld, R., Biard, P.-F., Paquin, L., Amrane, A., Couvert, A., 2016. Synthesis and toxicity evaluation of hydrophobic ionic liquids for volatile organic compounds biodegradation in a two-phase partitioning bioreactor. J. Hazard. Mater. 307, 221-230.
- Romero, A., Santos, A., Tojo, J., Rodríguez, A., 2008. Toxicity and biodegradability of imidazolium ionic liquids. J. Hazard. Mater. 151, 268-273.
- Ropel, L., Belvèze, L.S., Aki, S.N.V.K., Stadtherr, M.A., Brennecke, J.F., 2005. Octanol-water partition coefficients of imidazolium-based ionic liquids. Green Chem. 7, 83-90.
- Samorì, C., Pasteris, A., Galletti, P., Tagliavini, E., 2007. Acute toxicity of oxygenated and nonoxygenated imidazolium - based ionic liquids to *Daphnia magna* and *Vibrio fischeri*. Environ. Toxicol. Chem. 26, 2379-2382.
- Samorì, C., Malferrari, D., Valbonesi, P., Montecavalli, A., Moretti, F., Galletti, P., Sartor, G., Tagliavini, E., Fabbri, E., Pasteris, A., 2010.

Introduction of oxygenated side chain into imidazolium ionic liquids: evaluation of the effects at different biological organization levels. Ecotoxicol. Environ. Saf. 73, 1456-1464.

- Stepnowski, P., Storoniak, P., 2005. Lipophilicity and metabolic route prediction of imidazolium ionic liquids. Environ. Sci. Pollut. Res. 12, 199-204.
- Stolte, S., Arning, J., Bottin-Weber, U., Matze, M., Stock, F., Thiele, K., Uerdingen, M., Welz-Biermann, U., Jastorff, B., Ranke, J., 2006. Anion effects on the cytoxicity of ionic liquids. Green Chem. 8, 621-629.
- Stolte, S., Matzke, M., Arning, J., Boschen, A., Pitner, W.R., Welz-Biermann, U., Jastorff, B., Ranke, J., 2007. Effects of different head groups and functionalised side chains on the aquatic toxicity of ionic liquids. Green Chem. 9, 1170-1179.
- Stolte, S., Steudte, S., Areitioaurtena, O., Pagano, F., Thöming, J., Stepnowski, P., Igartua, A., 2012. Ionic liquids as lubricants or lubrication additives: an ecotoxicity and biodegradability assessment. Chemosphere 89, 1135-1141.
- Stolte, S., Schulz, T., Cho, C.W., Arning, J., Strassner, T., 2013. Synthesis, toxicity, and biodegradation of tuneable aryl alkyl ionic liquids (TAAILs). Sustain. Chem. Eng. 1, 410-418 (ACS).
- Torrecilla, J.S., Palomar, J., Lemus, J., Rodriguez, F., 2010. A quantum-chemical-based guide to analyze/quantify the cytotoxicity of ionic liquids. Green Chem. 12, 123-134.
- Tsarpali, V., Dailianis, S., 2015. Toxicity of two imidazolium ionic liquids, [bmim][BF4] and [omim][BF4], to standard aquatic test organisms: role of acetone in the induced toxicity. Ecotoxicol. Environ. Saf. 117, 62-71.
- van Rantwijk, F., Madeira Lau, R., Sheldon, R.A., 2003. Biocatalytic transformations in ionic liquids. Trends Biotechnol. 21, 131-138.
- Ventura, S.P.M., Silva, F.A., Gonçalves, A.M.M., Pereira, J.L., Gonçalves, F., Coutinho, J.A.P., 2014. Ecotoxicity analysis of cholinium-based ionic liquids to *Vibrio fischeri* marine bacteria. Ecotoxicol. Environ. Saf. 102, 48-54.
- Viboud, S., Papaiconomou, N., Cortesi, A., Chatel, G., Draye, M., Fontvieille, D., 2012. Correlating the structure and composition of ionic liquids with their toxicity on *Vibrio fischeri*: a systematic study. J. Hazard. Mater. 215- 216, 40-48.
- Zazo, J.A., Casas, J.A., Molina, C.B., Quintanilla, A., Rodriguez, J.J., 2007. Evolution of ecotoxicity upon Fenton's oxidation of phenol in water. Environ. Sci. Technol. 41, 7164-7170.

3.2

Respirometric test analysis of the cation and anion effect on biodegradability and toxicity of ionic liquids

Mena, I.F., Diaz, E., I.F., Palomar, J., Rodriguez, J.J., Mohedano, A.F. Respirometric test analysis of the cation and anion effect on biodegradability and toxicity of ionic liquids. Submitted for publication

Respirometric test analysis of the cation and anion effect on biodegradability and toxicity of ionic liquids

Abstract

Respirometric assays are shown as an effective technique to separately analyze the cation and anion effect on inhibition of ionic liquids (ILs) using activated sludge collected from a wastewater treatment plant. Current study includes a sample of six commercial ILs, formed by combination of 1-Butyl-3-methylimidazolium ($Bmim^+$) and N,N,N-trimethylethanolammonium ($Choline^+$) cations and chloride (Cl^-), acetate (Ac^-) and bis(trifluoromethanesulfonyl)imide (NTf_2^-) anions; all representative counter-ions with markedly different toxicity and biodegradability. Inherent (Zahn-Wellens test, OECD 302B) and fast (respirometric test) biodegradability tests are used to evaluate both the microorganism inhibition and the IL biodegradability, including the measurement of the anion and the cation composition. In addition, respiration inhibition assays are used to analyze the ecotoxicological response (EC_{50}) of the studied ILs in unacclimated sludge. For comparison purposes, IL toxicity is also evaluated by Microtox Test (*Vibrio fischeri*). $Bmim^+$ and NTf_2^- can be considered as non-biodegradable constituents of ILs, whereas aerobic microorganisms easily degraded $Choline^+$ and Ac^-, finding that the biodegradation of each cation/anion is nearly unaffected by counter-ion nature.

Moreover, CholineNTf_2 concentrations higher than 50 mg L^{-1} caused a partial inhibition on microbial activity, in good concordance with low EC_{50} (54 mg L^{-1}) of this compound measured by respiration inhibition test, what alerts about the negative environmental impact of NTf_2^- containing ILs on the performance of wastewater treatment plants.

3.2 Respirometric test analysis of the cation and anion effect on biodegradability and toxicity of ionic liquids

3.2.1. Introduction

Ionic liquids are salts with a melting point lower than 100 ºC at 1 atm formed through the combination of an organic cation and organic or inorganic anion with interesting properties such as low vapor pressure, physical and chemical stability, and high polarity. They have been designed to be robust at several reaction conditions and, consequently, to became essential chemicals as reaction solvents, battery electrolytes, lubricants, surfactants, catalysts, dielectric fluids as transformers and capacitors (Olivier-Bourbigou et al., 2010; Plechkova and Seddon, 2008). However, several studies have questioned the impact of these compounds on the environment suggesting that not all of them can be considered as green chemicals (Jordan and Gathergood, 2015; Richardson and Ternes, 2014). Recent works have made evident how the release of ILs to the aquatic environment could cause an environmental concern, due to some of them are considered as toxic and non-biodegradable (Amde et al., 2015; Chatel et al., 2017; Diaz et al., 2016; Frade and Afonso, 2010; Thuy Pham et al., 2010). In this context, these aspects must be included in the studies focused on the whole life cycle of ILs in order to establish a real eco-design strategy of the IL.

Some biodegradability assays can be useful to determine ILs biodegradability in the environment, and consequently, minimize negative impacts due to its persistence and/or accumulation (Polo et al., 2011; Sanchis et al., 2014). Ecotoxicological determinations, which are dependent on the studied model and environment conditions, can be used at a first assessment of the potential effect of ILs on a specific group of aquatic organisms (Costa et al., 2015b; Khan et al., 2016). In both cases, it is essential to select those assays whose results provide

realistic effects of the exposure risk to ILs, and let (a) know more about the impact of these compounds on sewage wastewater treatment, and (b) select an efficient degradation process of ILs to remove them from water (Diaz et al., 2016; Peric et al., 2013; Richardson and Kimura, 2016).

The choice of an adequate test must consider the end-point discharge of wastewater and, consequently, try to predict the behavior of ILs in a sewage treatment plant. Different biodegradation methods have been adopted by OECD and ISO (Diaz et al., 2016; Jordan and Gathergood, 2015; Pagga, 1997) to provide biodegradation data as the OECD 301B (CO_2 evolution) (Stolte et al., 2012), the OECD 301D (Closed bottle test) (Stolte et al., 2008), the OECD 301F (O_2 consumption) (Neumann et al., 2014b) and the OECD 310 (Ready biodegradability – Headspace test) (Atefi et al., 2009; Ford et al., 2010; Pretti et al., 2011). Specifically, Zahn-Wellens test (OECD 302B) evaluates the inherent biodegradability of a pollutant in water solution by means of an activated sludge along 28 days and can provide an idea of the abovementioned behavior, but it presents as a disadvantage that it is quite time-consuming. In this sense, a simple and fast respirometric test, based on the typical operation conditions of an activated sludge process, which provides data from the activity of the microorganisms and toxicant removal, has been proposed to obtain biodegradability data in a relatively short-time (100 h) (Polo et al., 2011).

Previous results from the studies focused on the biodegradability of ILs have established some rules of thumb. According to structural design, both the head group and the substituted side chain have influence on the IL degradability. The following sequence of biodegradability could be established regarding head group as long as the same side chain is

substituted: pyrrolidinium ≈ pyridinium > piperidinium ≈ morpholinium >> imidazolium (Neumann et al., 2014a). In general, regardless IL family, the biodegradability increases as the length of alkyl chain of cation or by the introduction of functional groups such as hydroxyl, carboxylic, alcohol or ether in this chain (Egorova and Ananikov, 2014; Jordan and Gathergood, 2015). On the other hand, the use of natural building blocks as choline or nicotinic acid as cations has a positive influence on the biodegradability of the ILs. In relation to the anion, organic anions (carboxylic acids, amino acids, carbohydrates, sulphates) can be considered as biodegradable. In the case of inorganic anion, their biodegradation cannot take into account, but while halide anions (chloride or bromide) do not interfere on the potential biodegradability of the IL, the degradation of ILs with perfluorinated anions (PF_6^-, BF_4^-) can lead to more toxic compounds (Freire et al., 2010; Gathergood et al., 2006; Jordan and Gathergood, 2015).

With regard to the ecotoxicty, standardized tests can provide different answers depending on the micro/organism employed in the analysis (Rizzo, 2011), and again, underestimate or overestimate the behavior of the aquatic system in the presence of a certain pollutant. The standardized toxicity tests traditionally used are the ISO 11348 with *Vibrio fischeri* (Costa et al., 2015a; Diaz et al., 2018; Garcia et al., 2005; Montalbán et al., 2018; Oulego et al., 2018; Ventura et al., 2014; Viboud et al., 2012), the ISO 8692 with *Selenastrum capricornutum* (Cho et al., 2008; Stolte et al., 2012), the USEPA-ISO 6341 with *Daphnia magna* (Costa et al., 2015b; Samori et al., 2010; Stolte et al., 2012; Vieira et al., 2019) or the OECD 201 (Freshwater Alga and Cyanobacteria, Growth Inhibition Test) with *Scenedesmus rubescens* (Tsarpali and Dailianis,

2015), among others. Despite of Microtox® test is not a standard toxicity test defined in the European Union legislation, it is widely accepted to establish a first-approach of a toxicity of a xenobitic compound due to be fast, simple and cost-efficient (Sintra et al., 2017). However, the bacteria *Vibrio fischeri* is not representative of the microorganisms that constitute a sewage sludge. In this sense and following the idea to obtain useful ecotoxicity data to establish a reliable assessment of potential toxicity of a xenobiotic in a wastewater treatment plant, a respiration inhibition using an activated sludge (OECD 209 - Activated Sludge, Respiration Inhibition Test) is recommendable (Polo et al., 2011; Rizzo, 2011). In this sense, although it is known that toxicity of ILs depends on the nature of a biological system,there are some principal factors that seem to modulate the ILs toxicity: i) length of an alkyl chain in the cation; ii) degree and nature of functionalization in the side chain of the cation; iii) nature of the anion; iv) nature of the cation; and v) mutual influence of anion and cation (Egorova and Ananikov, 2014). In general, an increase of the alkyl chain length causes a drastic increase of the toxicity, which seems to be related to the higher lipophilicity, and the introduction of oxygenated groups provokes a decrease on the IL toxicity (Costello et al., 2009; Cvjetko Bubalo et al., 2014; Diaz et al., 2016; Ranke et al., 2007; Stolte et al., 2007). Despite of the idea that the anion nature contributes less than the cation to the overall IL toxicity, the toxicity of anions as NTf_2^- and $C_8SO_4^-$ must not be underestimated, being this contribution more evident in the case of IL with short cation alkyl chain (Diaz et al., 2018; Petkovic et al., 2011).

In this work, we study the toxicity and biodegradability of several imidazolium- and choline-based ILs in order to analyze their behavior in a sewage treatment plant. For it, inherent (Zahn-Wellens) and fast

biodegradability tests have been applied. Respiration inhibition test, using an activated sludge, has been employed to evaluate ILs toxicity. With respect to ILs, imidazolium family present a huge potential for industrial applications (Chatel et al., 2017). They have been used as surfactants (Bhadani et al., 2016; Nandwani et al., 2017), in CO_2 absorption (Karadas et al., 2013) and as solvents and homogeneous catalyst in organic reaction. $Bmim^+$ is used as representative specie of the widely used imidazolium cation family. On the other hand, choline-based ILs refers to a quaternary ammonium salts with a counter anion with application in organic synthesis and polymerization reactions (Liu et al., 2015; Plechkova and Seddon, 2008; Zhang et al., 2012), NH_3 and CO_2 absorption (Palomar et al., 2011; Pandey et al., 2013), biomass conversion to specialties (An et al., 2015; Zhang et al., 2012) and dye degradation (Sekar et al., 2012). In the last years, the latter have shown a huge potential to replace traditional organic solvents and imidazolium ILs, which apparently have shown a higher adverse environmental impact than choline-based ILs (Gadilohar and Shankarling, 2017; Petkovic et al., 2011). The selected chloride (Cl^-) and acetate (Ac^-) are representative hydrophilic inorganic and organic anions, respectively, generally related to low toxic ILs; whereas bis(trifluoromethanesulfonyl)imide (NTf_2^-) is an hydrophobic anion, that increases the IL toxicity.

3.2.2. Materials and methods

Ionic liquids

Table 3.2.1 collects the ionic liquids from imidazolium (1-Butyl-3-methylimidazolium, $Bmim^+$) and choline (N,N,N-trimethylethanolammonium, $Choline^+$) families with chloride (Cl^-),

acetate (Ac^-) and bis(trifluoromethanesulfonyl)imide (NTf_2^-) as anions, used in this study, together with their nomenclature.

Table 3.2.1. Chemical structure and nomenclature of imidazolium- and choline-based ILs.

Anion	Cation
 Cl^-	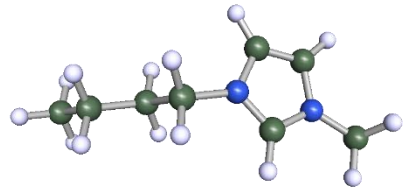 $Bmim^+$
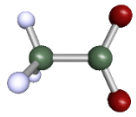 Ac^-	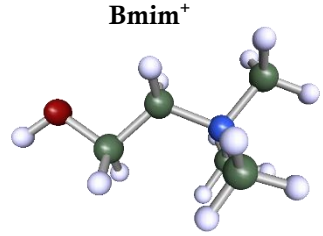 $Choline^+$
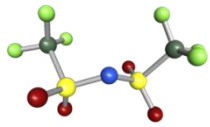 NTf_2^-	

Inoculum and culture medium

Unacclimated activated sludge, obtained from a domestic sewage treatment plant, has been used as inoculum in the biodegradability assays (inherent biodegradability and fast biodegradability tests) and in the respiration inhibition tests (OECD 209, ISO 8192). The sludge was maintained with an organic load rate (sodium acetate and glucose) of 0.4 mg COD mg VSS^{-1} day^{-1} as carbon source in a sequencing batch reactor (SBR) operated at room temperature. Ammonium sulphate and

phosphoric acid were used as nitrogen and phosphorous sources, respectively. A COD:N:P of 100:5:1 (w/w) was fixed and mineral salts ($FeCl_3$, $CaCl_2$, KCl and $MgCl_2$) were also added as micronutrients supply in a COD:micronutrients (Fe, Ca, K and Mg) ratio of 100:0.05 (w/w).

Inherent biodegradability test

The Zahn-Wellens test (OECD 302 B 1992) was carried in amber glass reactors (2.5 L) with 10 mg L^{-1} of IL in aqueous solution by triplicate. The IL carbon content to inoculum (dry-weight) ratio was 1:4 and mineral medium (phosphate buffer with $CaCl_2$ (27.5 mg L^{-1}), $MgSO_4 \cdot 7H_2O$ (22.5 mg L^{-1}) and $FeCl_3 \cdot 6H_2O$ (0.25 mg L^{-1})) was also added. The mixture was agitated and aerated at room temperature for 28 days. Samples were taken periodically to quantify the TOC and IL concentration.

Fast biodegradability test

Fast biodegradability tests were carried out in close reactors with a mixture of unacclimated activated sludge (350 mg L^{-1}), IL (10 and 50 mg L^{-1}) and mineral medium as previously described (Polo et al., 2011) by triplicate. The evolution of IL concentration, TOC and specific oxygen uptake rate (SOUR) profile was registered.

Respirometric inhibition assays

Respiration inhibition tests for activated sludge were carried out according to the method proposed by Polo et al. (2011). The procedure consisted in short-term respirometric measurements carried out in a Liquid-Static-Static (LSS) respirometer (Chica et al., 2007), using unacclimated sludge (350 mgVSS L^{-1}) in the presence of an easily

biodegradable substrate (sodium acetate) alone or together with different concentrations of the ILs. The biomass activity was measured in terms of SOUR. Inhibition was also estimated in terms of EC_{50} defined as the effective concentration of a sample that causes 50% reduction of SOUR.

Ecotoxicity test

Ecotoxicity measurements were performed according to standard Microtox test procedure (ISO 11348, 2007), based on the decreasing of light emission by the marine bacteria *Vibrio fischeri* (*Photobacterium phosphoreum*) after 15 min in presence of IL at pH within 6-8, using a Microtox M500 Analyzer (Azur Environmental). The results were expressed in terms of EC_{50}, defined as the effective concentration of IL that causes a 50 % inhibitory effect.

Analytical methods

$Bmim^+$ was analyzed by means of HPLC (Varian Pro-Start 240) with a visible UV detector (Prostar 325 UV-Vis) at 218 nm. A Synergy 4 mm Polar-RP 80 A (Phenomenex) column (15 cm length, 4.6 mm diameter) was used as stationary phase and a mixture of acetonitrile and water (5:95, v/v) at 0.75 mL min^{-1} as mobile phase.

$Choline^+$ identification was carried out by means of ionic chromatography (Metrohm 790 Persona IC) fitted with a Metrosep C4-250/4.0 column as stationary phase. The mobile phase (0.9 mL min^{-1}) was a mixture of 0.7 mM of 2,6-pyridinedicarboxylic acid and 1.7 mM of HNO_3. Ion chromatography with chemical suppression (DIONEX ICS-900) was employed to detect the anionic species (chloride and acetate) using a Dionex IonPac AS22 4 x 250 mm column at 1 mL min^{-1} of 1.4 mM $NaHCO_3$/4.5 mM Na_2CO_3 as mobile phase. The NTf_2^-

anion was identified by liquid chromatography coupled with mass spectrometry (LC/MS SQ Agilent) fitted with an ACE Excel 3 C18-Amide, 250 x 2.1 mm column at 40 ºC as stationary phase. A formic acid (0.1 % v/v) and acetonitrile (10:90 % v/v) at 0.2 mL min^{-1} was used as mobile phase. Total organic carbon (TOC) was measured using a TOC apparatus from Shimadzu (Shimadzu TOC-VCSH). Before analysis, samples were filtered through 0.45 µm syringe filters (OlimPeak PTFE, 25 mm, Teknokroma).

3.2.3. Results and discussion

Figures 3.2.1 and 3.2.2 show the biodegradability of Bmim- and choline-based ILs determined by Zahn-Wellens test. A control test using ethylene glycol was carried out in order to ensure the activity of the sludge (data not shown). In preliminary tests, neither ILs volatilization nor adsorption occurred during the testing period. In the case of Bmim-based ILs, no biodegradation was observed for BmimCl and $BmimNTf_2$ and only a partial biodegradation happened for BmimAc IL, which was attributed to the complete mineralization of acetate anion. Along the experimental time, biomass did not adapted to degrade $Bmim^+$, NTf_2^- or head group. On the other hand, organic acid anions, as acetate, appear to be the best selection for promoting biodegradability of ILs (Jordan and Gathergood, 2015; Quijano et al., 2011). However, in the cases of choline-based ILs the cation showed complete biodegradation in less than 6 days, being acetate anion (CholineAc) totally degraded in few hours [33]. As can be seen in Figures 3.2.1 and 3.2.2, the separately observed biodegradability of each cation or anion does not seem be strongly affected by the nature of the counter-ion. It suggests that the IL biodegradation occurs through dissociated ionic species in water, rather than ion-pair or associated

species. TOC significantly decreased during the first hours, and after that time, its decrease happened at a lower rate. TOC conversion achieved 85 and 87 % for CholineCl and CholineAc, respectively, and consequently, both compounds can be considered biodegradable. The biodegradability of CholineCl has been previously observed according to the ready biodegradability test 301D OECD, reaching more than 90 % removal within 14 days (Radošević et al., 2015), and also for CholineNTf$_2$, with a TOC removal (~70 %) corresponding to the cation mineralization.

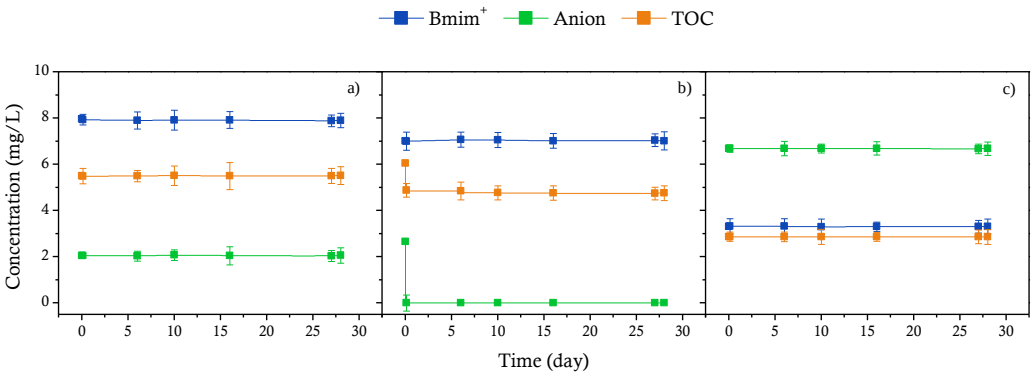

Figure 3.2.1. Time course of (a) BmimCl, (b) BmimAc, (c) BmimNTf$_2$ and TOC removal along Zahn-Wellens test.

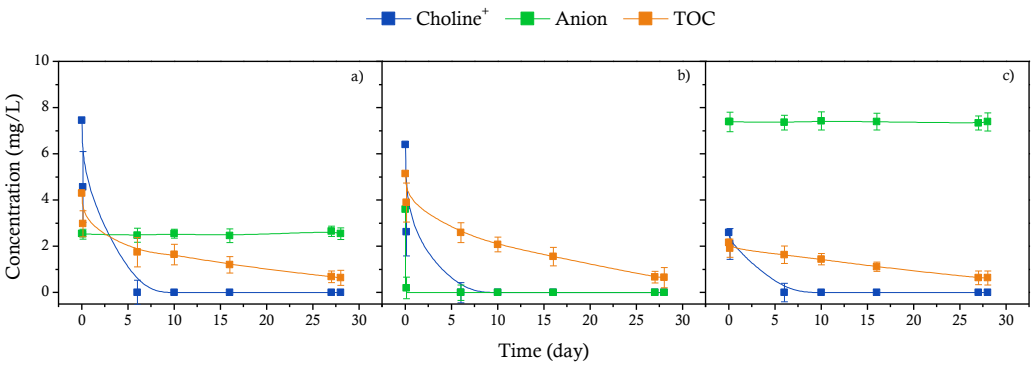

Figure 3.2.2. Time course of CholineCl (a), CholineAc (b), and CholineNTf$_2$ (c) and TOC removal along Zahn-Wellens test.

ILs biodegradability was further measured by the fast biodegradability respirometric test (Polo et al., 2011). Figure 3.2.3 shows the time course of SOUR and the concentration of each cation and anion for Bmim-based ILs using an initial concentration of 10 and 50 mg L^{-1}. Time-evolution ILs concentration is maintained practically unalterable for BmimCl and BmimNTf$_2$, regardless of the IL initial concentration. The respirometric profiles did not suffer any significant changes for the lowest IL concentration (10 mg L^{-1}), whereas an initial decay of endogenous respiration was observed for the highest one (50 mg L^{-1}), which could be attributed to the partial inhibition of the microbial activity, followed by a slight increase of the sludge respiration after an adaptation time. The unacclimated sludge was able to degrade acetate concentrations of 3 and 15 mg L^{-1} in the first 8 h of each experiment for BmimAc IL. SOUR values were proportional to the initial acetate concentration, and after the complete decay of this substrate, the microbial activity remained unalterable. The results of the fast biodegradability test are comparable to the obtained by the Zahn-Wellens test, although the former also indicates that a concentration of

$BmimNTf_2$ superior to 50 mg L^{-1} can cause detrimental effects on the biomass, which seems to be related to the highest toxicity attributed to NTf_2^- (Diaz et al., 2018; Santos et al., 2014).

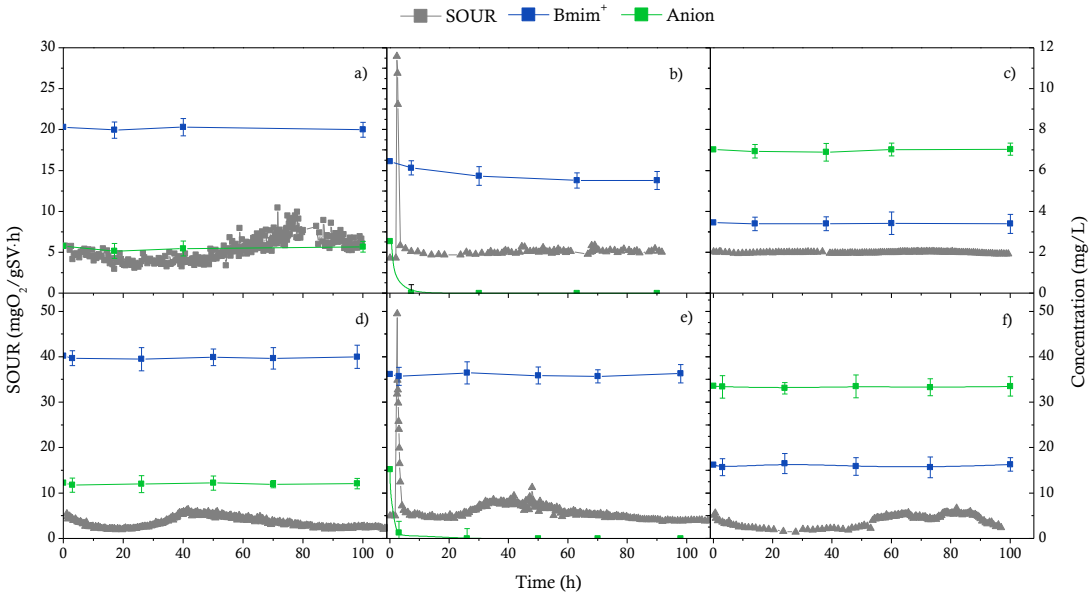

Figure 3.2.3. Time course of IL concentration and SOUR profiles along the respirometric assays for an initial concentration of 10 mg L^{-1} (BmimCl (a), BmimAc (b), and $BmimNTf_2$ (c)) and 50 mg L^{-1} (BmimCl (d), BmimAc (e), and $BmimNTf_2$ (f)).

The respirometric profiles obtained using 10 mg L^{-1} choline ILs (Figure 3.2.4) showed an increase of sludge respiration, after an acclimation time (15 and 25 h), which is associated with the degradation $Choline^+$. In the case of CholineCl, the presence of Cl^- did not interfere to $Choline^+$ degradation, whereas in presence of organic anions as Ac^- and NTf_2^-, the cation transformation happened at a lower rate. It could be related, on the one hand, to the fast assimilation of acetate as carbon source for the microorganisms, which took place in the first 8 h of the

experiment, and on the other hand, to the presence of a non-biodegradable compound in the reaction medium as NTf_2^-. An increase of the choline-based ILs concentration (50 mg L^{-1}) did not cause any important effect on the microbial activity in the case of degradation of CholineCl and CholineAc ILs. In both cases, the respirometric profiles were similar to the obtained with a lower concentration, except that the maximum value of the SOUR was higher for the highest IL concentration. It may be related to the hydrophilic nature of Cl^- and Ac^- anions, which promotes their solvation by water molecular and dominant presences of dissociated ionic species in the solution (Li et al., 2007; Palomar et al., 2007; Stassen et al., 2015). In the case of $CholineNTf_2$, a fall of the endogenous respiration took placed along the first hours of the assay and neither degradation of $Choline^+$ nor NTf_2^- were observed. This suggests that $CholineNTf_2$, at the highest concentration used (50 mg L^{-1}), caused a negative effect on the endogenous biomass respiration, probably due to the hydrophobic nature of this anion, which promotes the presence of aggregated cation-anion species when increasing IL concentration (Li et al., 2007; Stassen et al., 2015). Ion-pair structures are less polar and more lipophilic than dissociated ions (González et al., 2018), increasing the toxic effects of the IL compound and preventing its biodegradation (Torrecilla et al., 2010).

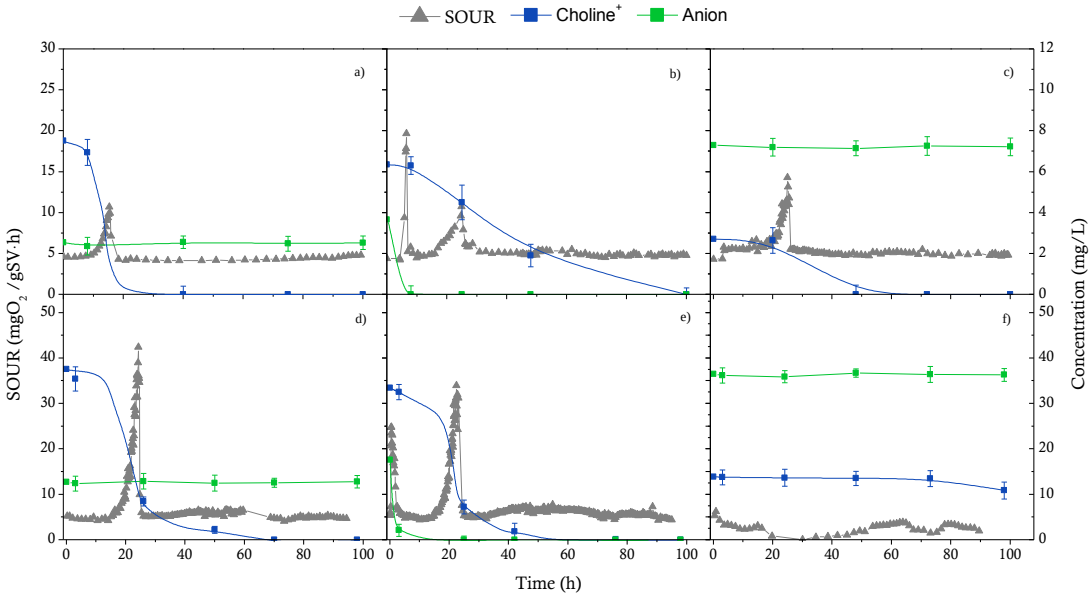

Figure 3.2.4. Time course of IL concentration and SOUR profiles along the respirometric assays for an initial concentration of 10 mg L^{-1} (CholineCl (a), CholineAc (b), and CholineNTf_2 (c)) and 50 mg L^{-1} (CholineCl (d), CholineAc (e), and CholineNTf_2 (f)).

In order to gain information on the toxicity of Bmim- and choline-based ILs, a series of respirometric tests were carried out for each IL over a wide range of concentrations (10 – 500 mg L^{-1}), with the aim of establishing the inhibition of the activated sludge in terms of logEC_{50} values. In spite of the fact that the required time to carry out the experiments is less than 30 min, it was not possible to obtain values of EC_{50} for compounds constituted by an easily biodegrable substrate as acetate, since in these cases, an increase in the BmimAc or CholineAc concentration did not cause a proportional decrease on the respiration rate of the microorganisms. This was also observed in the case of the experiments performed adding different concentrations of CholineCl,

because of the high biodegradability of $Choline^+$, and Cl^- did not show an intrinsic toxicity effect. However, the high toxicity associated with the anion NTf_2^- allowed establishing a $logEC_{50}$ value for $CholineNTf_2$ (1.731± 0.214, equivalent to 54 mg L^{-1}). This value explains the behavior exhibited by the microorganisms of the activated sludge in the biodegradability assay (Figure 3.2.4f), which were exposed to an inhibitory concentration of $CholineNTf_2$. Moreover, $logEC_{50}$ values from BmimCl (3.432 ± 0.518, equivalent to 2704 mg L^{-1}) and $BmimNTf_2$ (2.416 ± 0.530, equivalent to 261 mg L^{-1}) could be also determined due to both ILs present null biodegradability. For comparison purposes, the $logEC_{50}$ were also determined by Microtox® test, being the obtained values in reasonable agreement with those reported in the literature using the same test (Table 3.2.2) (Couling et al., 2006; Diaz et al., 2018; Docherty and Kulpa, Jr., 2005; Garcia et al., 2005; Montalbán et al., 2016; Peric et al., 2013; Romero et al., 2008; Stolte et al., 2007; Ventura et al., 2014). EC_{50} values of ILs constituted by Cl^- and Ac^- anions were superior to 500 mg L^{-1}, being slightly lower the values associated to Bmim ILs than to choline ILs. This fact agrees with the ILs with aromatic rings present more toxicity than whose with non-aromatic groups (Costa et al., 2015b). On the other hand, the presence of the anion NTf_2^- in the IL structure caused a considerable increase of its ecotoxicity. In general, the influence of the anion on the toxicity of IL has been considered of minor importance, but the results of this test makes evident that some anions, specifically those that contain fluorine atoms in their structure, can affect drastically to the IL toxicity (Costa et al., 2015b; Diaz et al., 2018; Montalbán et al., 2016). The comparison of the results obtained for both tests lets conclude that the Microtox test can be used to establish a toxicity trend about the behavior of ILs on the activated sludge of a wastewater treatment plant.

However, it is important to take into account that this test may not anticipate the toxicity of an IL on the activated sludge of wastewater plants.

Table 3.2.2. EC_{50} values for imidazolium- and choline-based ILs from Microtox Test reported in the literature and obtained in this work.

Imidazolium-based ILs	$logEC_{50}$ (mg L^{-1})	References	Choline-based ILs	$logEC_{50}$ (mg L^{-1})	References
BmimCl	2.95 ± 0.122 2.582 ± 0.129 2.952 ± 0.140 2.715 ± 0.045 2.640 2.632 ± 0.150 2.458 ± 0.289 2.722 ± 0.130 2.742 ± 0.001	Docherty & Kulpa, 2005 Garcia et al., 2005 Couling et al., 2006 Stolte et al., 2007 Matzke et al., 2007 Romero et al., 2008 Peric et al., 2013 Montalbán et al., 2016 Diaz et al., 2018	CholineCl	>4.13 1.877 ± 0.170 3.646 ± 0.082	Couling et al., 2006 Ventura et al., 2014 This work
BmimAc	3.465 ± 0.263	This work	CholineAc	2.135 ± 0.093 3.665 ± 0.249	Ventura et al., 2014 This work
$BmimNTf_2$	3.012 ± 0.080 2.099 2.152 ± 0.301 2.182 ± 0.250 2.562 ± 0.002	Couling et al., 2006 Matzke et al., 2007 Ventura et al., 2011 Montalbán et al., 2016 Diaz et al., 2018	$CholineNTf_2$	3.732 ± 0.030 3.069 ± 0.223	Couling et al., 2006 This work

3.2.4. Conclusions

The detailed analysis of the evolution of the ILs concentration along biodegradability studies revealed that $BmimNTf_2$ could not be degraded by an activated sludge, even at low concentrations (10 mg L^{-1}), whereas CholineAc concentrations up to 50 mg L^{-1} can be completely removed. Moreover, the microorganisms can assimilate $Choline^+$ and acetate as constituents of other ILs, depending on the structure and the concentration of the counter-ion. A partial inhibition of the microbial

activity was observed in the fast biodegradability test performed with 50 mg L^{-1} of CholineNTf_2.

EC_{50} values from Microtox Test for BmimCl and CholineCl lead the conclusion that toxic effects of these ILs are directly related to both ILs constituents. $Choline^+$ was slightly less toxic than $Bmim^+$ and that the presence of NTf_2^- increased considerably the toxicity of ILs. According to the results from inhibition tests, ILs formed by a natural building block as $Choline^+$ can lead to nontoxic ILs for activated sludge microbiota, as well as occurred to BmimAc and CholineAc. However, the presence of an anion with intrinsic toxicity as NTf_2^- must not be underestimated, being this negative contribution more evident in $Choline^+$ ILs than in $Bmim^+$ ones. Consequently, the negative environmental impact of NTf_2-containing ILs should take into account for their use in chemical processes, which can generate aqueous wastes.

5.1.5. References

- Amde, M., Liu, J., Pang, L., 2015. Environmental application, fate, effects and concerns of ionic liquids : A review. Environ. Sci. Technol. 49, 12611–12627.
- An, Y.X., Zong, M.H., Wu, H., Li, N., 2015. Pretreatment of lignocellulosic biomass with renewable cholinium ionic liquids: Biomass fractionation, enzymatic digestion and ionic liquid reuse. Bioresour. Technol. 192, 165–171.
- Atefi, F., Garcia, M.T., Singer, R.D., Scammells, P.J., 2009. Phosphonium ionic liquids: design, synthesis and evaluation of biodegradability. Green Chem. 11, 1595–1604.
- Bhadani, A., Misono, T., Singh, S., Sakai, K., Sakai, H., Abe, M., 2016. Structural diversity, physicochemical properties and application of imidazolium surfactants: Recent advances. Adv. Colloid Interface Sci. 231, 36–58.
- Chatel, G., Naffrechoux, E., Draye, M., 2017. Avoid the PCB mistakes: A more sustainable future for ionic liquids. J. Hazard. Mater. 324, 773–780.
- Chica, A.F., Martin, A., Vazquez, F.J., Carmona, F.J., Mohedo, J.J., 2007. Respirometer to analyze measure dissolved oxygen and oxygen demand of microbes in leachate from municipal waste. ES 2283171.
- Cho, C.-W., Jeon, Y.-C., Pham, T.P.T., Vijayaraghavan, K., Yun, Y.-S., 2008. The ecotoxicity of ionic liquids and traditional organic solvents on microalga *Selenastrum capricornutum*. Ecotoxicol. Environ. Saf. 71, 166–171.
- Costa, S.P.F., Pinto, P.C.A.G., Lapa, R.A.S., Saraiva, M.L.M.F.S., 2015a. Toxicity assessment of ionic liquids with *Vibrio fischeri*: An alternative fully automated methodology. J. Hazard. Mater. 284, 136–142.
- Costa, S.P.F., Pinto, P.C.A.G., Saraiva, M.L.M.F.S., Rocha, F.R.P., Santos, J.R.P., Monteiro, R.T.R., 2015b. The aquatic impact of ionic liquids on freshwater organisms. Chemosphere 139, 288–294.
- Costello, D.M., Brown, L.M., Lamberti, G.A., 2009. Acute toxic effects of ionic liquids on zebra mussel (*Dreissena polymorpha*) survival and feeding. Green Chem. 11, 548–553.
- Couling, D.J., Bernot, R.J., Docherty, K.M., Dixon, J.K., Maginn, E.J., 2006. Assessing the factors responsible for ionic liquid toxicity to aquatic organisms via quantitative structure–property relationship modeling. Green Chem. 8, 82–90.
- Cvjetko Bubalo, M., Radošević, K., Radojčić Redovniković, I., Halambek, J., Gaurina Srček, V., 2014. A brief overview of the potential environmental hazards of ionic liquids. Ecotoxicol. Environ. Saf. 99, 1–12.
- Diaz, E., Monsalvo, V., Palomar, J., Mohedano, A.F., 2016. Ionic Liquids:

Bacterial Degradation in Wastewater Treatment Plants, in: Encyclopedia of Inorganic and Bioinorganic Chemistry. John Wiley & Sons, Ltd.

- Diaz, E., Monsalvo, V.M., Lopez, J., Mena, I.F., Palomar, J., Rodriguez, J.J., Mohedano, A.F., 2018. Assessment the ecotoxicity and inhibition of imidazolium ionic liquids by respiration inhibition assays. Ecotoxicol. Environ. Saf. 162, 29–34.
- Docherty, K.M., Kulpa, Jr., C.F., 2005. Toxicity and antimicrobial activity of imidazolium and pyridinium ionic liquids. Green Chem. 7, 185.
- Egorova, K.S., Ananikov, V.P., 2014. Toxicity of ionic liquids: Eco(cyto)activity as complicated, but unavoidable parameter for task-specific optimization. ChemSusChem 7, 336–360.
- Ford, L., Harjani, J.R., Atefi, F., Garcia, M.T., Singer, R.D., Scammells, P.J., 2010. Further studies on the biodegradation of ionic liquids. Green Chem. 12, 1783–1789.
- Frade, R.F.M., Afonso, C.A.M., 2010. Impact of ionic liquids in environment and humans: An overview. Hum. Exp. Toxicol. 29, 1038–1054.
- Freire, M.G., Neves, C.M.S.S., Marrucho, I.M., Coutinho, J.A.P., Fernandes, A.M., 2010. Hydrolysis of tetrafluoroborate and hexafluorophosphate counter ions in imidazolium-based ionic liquids. J. Phys. Chem. A 114, 3744–3749.
- Gadilohar, B.L., Shankarling, G.S., 2017. Choline based ionic liquids and their applications in organic transformation. J. Mol. Liq. 227, 234–261.
- Garcia, M.T., Gathergood, N., Scammells, P.J., 2005. Biodegradable ionic liquids - Part II. Effect of the anion and toxicology. Green Chem. 7, 9–14.
- Gathergood, N., Scammells, P.J., Garcia, M.T., 2006. Biodegradable ionic liquids - Part III. The first readily biodegradable ionic liquids. Green Chem. 8, 156–160.
- González, E.J., Palomar, J., Navarro, P., Larriba, M., García, J., Rodríguez, F., 2018. On the volatility of aromatic hydrocarbons in ionic liquids: Vapor-liquid equilibrium measurements and theoretical analysis. J. Mol. Liq. 250, 9–18.
- ISO 8192:2007 Water quality - Test for inhibition of oxygen consumption by activated sludge for carbonaceous and ammonium oxidation
- ISO 8692:2012 Water quality - Fresh water algal growth inhibition test with unicellular green algae
- ISO 11348:2007 Water quality - Determination of the inhibitory effect of water samples on the light emission of *Vibrio fischeri* (Luminescent bacteria test)
- Jordan, A., Gathergood, N., 2015. Biodegradation of ionic liquids - a critical review. Chem. Soc. Rev. 44, 8200–8237.

- Karadas, F., Köz, B., Jacquemin, J., Deniz, E., Rooney, D., Thompson, J., Yavuz, C.T., Khraisheh, M., Aparicio, S., Atihan, M., 2013. High pressure CO_2 absorption studies on imidazolium-based ionic liquids: Experimental and simulation approaches. Fluid Phase Equilib. 351, 74–86.
- Khan, M.I., Zaini, D., Shariff, A.M., Moniruzzaman, M., 2016. Framework for ecotoxicological risk assessment of ionic liquids. Procedia Eng. 148, 1141 – 1148.
- Li, W., Zhang, Z., Han, B., Hu, S., Xie, Y., Yang, G., 2007. Effect of Water and Organic Solvents on the Ionic Dissociation of Ionic Liquids. J. Phys. Chem. B. 111, 6452-6456.
- Liu, H., Zhang, X., Chen, C., Du, S., Dong, Y., 2015. Effects of imidazolium chloride ionic liquids and their toxicity to *Scenedesmus obliquus*. Ecotoxicol. Environ. Saf. 122, 83–90.
- Montalbán, M.G., Hidalgo, J.M., Collado-González, M., Díaz Baños, F.G., Víllora, G., 2016. Assessing chemical toxicity of ionic liquids on *Vibrio fischeri*: Correlation with structure and composition. Chemosphere 155, 405–414.
- Montalbán, M.G., Víllora, G., Licence P., 2018. Ecotoxicity assessment of dicationic versus monocationic ionic liquids as a more environmentally friendly alternative. Ecotoxicol. Environ. Saf. 150, 129–135.
- Nandwani, S.K., Malek, N.I., Lad, V.N., Chakraborty, M., Gupta, S., 2017. Study on interfacial properties of Imidazolium ionic liquids as surfactant and their application in enhanced oil recovery. Colloids Surfaces A Physicochem. Eng. Asp. 516, 383–393.
- Neumann, J., Pawlik, M., Bryniok, D., Thöming, J., Stolte, S., 2014a. Biodegradation potential of cyano-based ionic liquid anions in a culture of *Cupriavidus spp.* and their in vitro enzymatic hydrolysis by nitrile hydratase. Environ. Sci. Pollut. Res. 21, 9495–9505.
- Neumann, J., Steudte, S., Cho, C.-W., Thöming, J., Stolte, S., 2014b. Biodegradability of 27 pyrrolidinium, morpholinium, piperidinium, imidazolium and pyridinium ionic liquid cations under aerobic conditions. Green Chem. 16, 2174–2184.
- Organisation for Economic Co-operation and Development (OECD), OECD guideline for testing of chemicals 201 Freshwater Alga and Cyanobacteria, Growth Inhibition Test
- Organisation for Economic Co-operation and Development (OECD), OECD guideline for testing of chemicals 209: Activated Sludge, Respiration Inhibition Test (Carbon and Ammonium Oxidation)
- Organisation for Economic Co-operation and Development (OECD), OECD guideline for testing of chemicals 301B – Biodegradation test – CO_2 evolution.

- Organisation for Economic Co-operation and Development (OECD), OECD guideline for testing of chemicals 301D – Biodegradation closed bottle test.
- Organisation for Economic Co-operation and Development (OECD), OECD guideline for testing of chemicals 301F – Biodegradation test – O_2 consumption.
- Organisation for Economic Co-operation and Development (OECD), OECD guideline for testing of chemicals 310 – Ready biodegradability – CO2 in sealed vessels (Headspace Test).
- Organisation for Economic Co-operation and Development (OECD), OECD guideline for testing of chemicals 302B: Inherent Biodegradability: Zahn-Wellens/ EVPA Test
- Olivier-Bourbigou, H., Magna, L., Morvan, D., 2010. Ionic liquids and catalysis: Recent progress from knowledge to applications. Appl. Catal. A Gen. 373, 1–56.
- Oulego P., Blanco D., Ramos D., Viesca J.L., Díaz M., Hernández Battez A., 2018. Environmental properties of phosphonium, imidazolium and ammonium cation-based ionic liquids as potential lubricant additives. J. Mol. Liq. 272, 937–947.
- Pagga, U., 1997. Testing biodegradability whit standardized methods. Chemosphere 35, 2953–2972.
- Palomar, J., Ferro, V.R., Gilarranz, M.A., Rodriguez, J.J., 2007. Computational approach to nuclear magnetic resonance in 1-Alkyl-3-methylimidazolium ionic liquids. J. Phys. Chem. B. 111, 168–180.
- Palomar, J., Gonzalez-Miquel, M., Bedia, J., Rodriguez, F., Rodriguez, J.J., 2011. Task-specific ionic liquids for efficient ammonia absorption. Sep. Purif. Technol. 82, 43–52.
- Pandey, S., Baker, G.A., Sze, L., Pandey, S., Kamath, G., Zhao, H., Baker, S.N., 2013. Ionic liquids containing fluorinated β-diketonate anions: synthesis, characterization and potential applications. New J. Chem. 37, 909–919.
- Peric, B., Sierra, J., Martí, E., Cruañas, R., Garau, M.A., Arning, J., Bottin-Weber, U., Stolte, S., 2013. (Eco)toxicity and biodegradability of selected protic and aprotic ionic liquids. J. Hazard. Mater. 261, 99–105.
- Petkovic, M., Seddon, K.R., Rebelo, L.P.N., Pereira, C.S., 2011. Ionic liquids: a pathway to environmental acceptability. Chem. Soc. Rev. 40, 1383–1403.
- Plechkova, N. V, Seddon, K.R., 2008. Applications of ionic liquids in the chemical industry. Chem. Soc. Rev. 37, 123–150.
- Polo, A.M., Tobajas, M., Sanchis, S., Mohedano, A.F., Rodriguez, J.J., 2011. Comparison of experimental methods for determination of toxicity

and biodegradability of xenobiotic compounds. Biodegradation 22, 751–761.

- Pretti, C., Renzi, M., Ettore Focardi, S., Giovani, A., Monni, G., Melai, B., Rajamani, S., Chiappe, C., 2011. Acute toxicity and biodegradability of N-alkyl-N-methylmorpholinium and N-alkyl-DABCO based ionic liquids. Ecotoxicol. Environ. Saf. 74, 748–753.
- Quijano, G., Couvert, A., Amrane, A., Darracq, G., Couriol, C., Le Cloirec, P., Paquin, L., Carrié, D., 2011. Toxicity and biodegradability of ionic liquids: New perspectives towards whole-cell biotechnological applications. Chem. Eng. J. 174, 27–32.
- Radošević, K., Cvjetko Bubalo, M., Gaurina Srček, V., Grgas, D., Landeka Dragičević, T., Redovniković, R.I., 2015. Evaluation of toxicity and biodegradability of choline chloride based deep eutectic solvents. Ecotoxicol. Environ. Saf. 112, 46–53.
- Ranke, J., Müller, A., Bottin-Weber, U., Stock, F., Stolte, S., Arning, J., Störmann, R., Jastorff, B., 2007. Lipophilicity parameters for ionic liquid cations and their correlation to in vitro cytotoxicity. Ecotoxicol. Environ. Saf. 67, 430–438.
- Richardson, S.D., Kimura, S.Y., 2016. Water analysis: Emerging contaminants and current issues. Anal. Chem. 88, 546–582.
- Richardson, S.D., Ternes, T.A., 2014. Water analysis: Emerging contaminants and current issues. Anal. Chem. 86, 2813–2848.
- Rizzo, L., 2011. Bioassays as a tool for evaluating advanced oxidation processes in water and wastewater treatment. Water Res. 45, 4311–4340.
- Romero, A., Santos, A., Tojo, J., Rodriguez, A., 2008. Toxicity and biodegradability of imidazolium ionic liquids. J. Hazard. Mater. 151, 268–273.
- Samori, C., Malferrari, D., Valbonesi, P., Montecavalli, A., Moretti, F., Galletti, P., Sartor, G., Tagliavini, E., Fabbri, E., Pasteris, A., 2010. Introduction of oxygenated side chain into imidazolium ionic liquids: Evaluation of the effects at different biological organization levels. Ecotoxicol. Environ. Saf. 73, 1456–1464.
- Sanchis, S., Polo, A.M., Tobajas, M., Rodriguez, J.J., Mohedano, A.F., 2014. Strategies to evaluate biodegradability: application to chlorinated herbicides. Environ. Sci. Pollut. Res. 21, 9445–9452.
- Santos, A.G., Ribeiro, B.D., Alviano, D.S., Coelho, M.A.Z., 2014. Toxicity of ionic liquids toward microorganisms interesting to the food industry. RSC Adv. 4, 37157–37163.
- Sekar, S., Surianarayanan, M., Ranganathan, V., Macfarlane, D.R., Mandal, A.B., 2012. Choline-based ionic liquids-enhanced biodegradation of azo dyes. Environ. Sci. Technol. 46, 4902–4908.

- Sintra, T.E., Nasirpour, M., Siopa, F., Rosatella, A.A., Gonçalves, F., Coutinho, J.A.P., Afonso, C.A.M., Ventura, S.P.M., 2017. Ecotoxicological evaluation of magnetic ionic liquids. Ecotoxicol. Environ. Saf. 143, 315–321.
- Stassen, H.K., Ludwig, R., Wulf, R., Dupont, J., 2015. Imidazolium salt ion Pairs in solution. Chem. Eur. J. 21, 8324–8335.
- Stolte, S., Abdulkarim, S., Arning, J., Blomeyer-Nienstedt, A.K., Bottin-Weber, U., Matzke, M., Ranke, J., Jastorff, B., Thoming, J., 2008. Primary biodegradation of ionic liquid cations, identification of degradation products of 1-methyl-3-octylimidazolium chloride and electrochemical wastewater treatment of poorly biodegradable compounds. Green Chem. 10, 214–224.
- Stolte, S., Arning, J., Bottin-Weber, U., Müller, A., Pitner, W.-R., Welz-Biermann, U., Jastorff, B., Ranke, J., 2007. Effects of different head groups and functionalised side chains on the cytotoxicity of ionic liquids. Green Chem. 9, 1170–1179.
- Stolte, S., Steudte, S., Areitioaurtena, O., Pagano, F., Thöming, J., Stepnowski, P., Igartua, A., 2012. Ionic liquids as lubricants or lubrication additives: An ecotoxicity and biodegradability assessment. Chemosphere 89, 1135–1141.
- Thuy Pham, T.P., Cho, C.W., Yun, Y.S., 2010. Environmental fate and toxicity of ionic liquids: A review. Water Res. 44, 352–372.
- Torrecilla, J.S., Palomar, J., Lemus, J., Rodríguez, F., 2010. A quantum-chemical-based guide to analyze/quantify the cytotoxicity of ionic liquids. Green Chem. 12, 123–134.
- Tsarpali, V., Dailianis, S., 2015. Toxicity of two imidazolium ionic liquids, [bmim][BF4] and [omim][BF4], to standard aquatic test organisms: Role of acetone in the induced toxicity. Ecotoxicol. Environ. Saf. 117, 62–71.
- USEPA-ISO 6341: 2012 Water quality — Determination of the inhibition of the mobility of *Daphnia magna Straus* (Cladocera, Crustacea) — Acute toxicity test
- Ventura, S.P.M., e Silva, F.A., Gonçalves, A.M.M., Pereira, J.L., Gonçalves, F., Coutinho, J.A.P., 2014. Ecotoxicity analysis of cholinium-based ionic liquids to *Vibrio fischeri* marine bacteria. Ecotoxicol. Environ. Saf. 102, 48–54.
- Viboud, S., Papaiconomou, N., Cortesi, A., Chatel, G., Draye, M., Fontvieille, D., 2012. Correlating the structure and composition of ionic liquids with their toxicity on *Vibrio fischeri*: A systematic study. J. Hazard. Mater. 215-216, 40–48.
- Vieira, N.S.M., Stolte, S., Araújo, J.M.M., Rebelo, L.P.N., Pereiro, A.B., Markiewicz, M., 2019 (In press). Acute Aquatic Toxicity and

Biodegradability of Fluorinated Ionic Liquids. ACS Sustainable Chem. Eng.

- Zhang, Q., De Oliveira Vigier, K., Royer, S., Jérôme, F., 2012. Deep eutectic solvents: syntheses, properties and applications. Chem. Soc. Rev. 41, 7108–7146.

4

Biological oxidation of choline-based ionic liquids in sequencing batch reactors

Mena, I.F., Diaz, E., Rodriguez, J.J., Mohedano, A.F. 2019. Biological oxidation of choline-based ionic liquids in sequencing batch reactors. J. Chem. Technol. Biotechnol. (In press)

Biological oxidation of choline-based ionic liquids in sequencing batch reactors

Abstract

Ionic liquids (ILs) are salts consisting of an organic cation and an organic or inorganic anion that are potential use for organic synthesis, biomass conversion, gas absorption, polymerization, metal extraction and lubrication. We examined the biodegradability of choline chloride (CholineCl), choline acetate (CholineAc) and choline bis(trifluoromethylsulfonyl)imide (Cholin$eNTf_2$) in a sequencing batch reactor (SBR) to assess the influence of the IL anion

Following acclimation, activated sludge exhibited good activity, and high COD (80–90 %) and TOC removal (75–85 %) with initial concentrations of CholineCl and CholineAc over the range 0.25–15 mM. On the other hand, increased concentrations of Cholin$eNTf_2$ in the reactor feed had an inhibitory effect on the sludge. An analysis of the reaction effluent revealed the presence of the main intermediates of choline degradation, namely: ethanol, and methyl-, dimethyl- and trimethylamine. The initial and final microbial communities of the sludge were characterized by pyrosequencing analysis, and the latter was found to consist mainly of Alfa-, Beta- and Gamma-proteobacteria.

Choline-based ionic liquids can be efficiently removed in SBRs. Complete choline degradation (0.25–15 mM) was accomplished at a

variable depletion rate depending on the particular IL anion (chloride, acetate or NTf_2.

4 Biological oxidation of choline-based ionic liquids in sequencing batch reactors

4.1. Introduction

Ionic Liquids (ILs) are organic salts consisting of an organic cation and an organic or inorganic anion. They typically have a boiling point below 100 ºC and a low vapor pressure, and possess chemical and thermal stability (Markiewicz et al., 2013; Stolte et al., 2012). In recent decades, ILs have gain importance as an alternative of traditional organic solvents(Abrusci et al., 2011; Docherty et al., 2007; Phuong et al., 2010; Spasiano et al., 2016). Their structure can be easily adapted to their intended use (Plechkova and Seddon, 2008).

Ionic liquids are usually classified according to their cation, the most important IL families being those of imidazolium, pyridinium, pyrrolidinium, morpholinium, phosphonium and ammonium ions (Jordan and Gathergood, 2015). Because of their relatively high solubility in water, ILs can easily reach aquifers and raise serious environmental problems (Alvarez-Guerra and Irabien, 2011; Bruzzone et al., 2011; Quijano et al., 2011). This has led a number of authors to study the biodegradability and ecotoxicity of ILs in water (Alvarez-Guerra and Irabien, 2011; Biczak et al., 2014; Cvjetko Bubalo et al., 2014; Peric et al., 2013; Steudte et al., 2014; Stolte et al., 2007). The standard biodegradability tests for this purpose, which are endorsed by the Organization for Economic Co-operation and Development (OECD), involve determining overall parameters such as total organic carbon (TOC), chemical oxygen demand (COD) or biological oxygen demand (BOD). Tests OECD 301B (Biodegradation test – CO_2 evolution)(Gosu et al., 2018) and OECD 310 (Ready biodegradability – CO_2 in sealed vessels (Headspace Test))(Zhong et al., 2012) determined in terms of TOC; on the other hand, OECD 301D (Biodegradation closed bottle test)(Xiang et al., 2009) measured as

COD and OECD 301F (Biodegradation test – O_2 consumption)(Inchaurrondo et al., 2012) as BOD. The results of these tests have been found to differ among IL families. Table 4.1 shows the percent biodegradation of various ILs on activated sludge.

Table 4.1. Previous biodegradability and ecotoxicity studies on activated sludge.

IL family	Biodegradabilty (%)*	References	EC_{50} (µM)	References
Imidazolium	**Modified OECD 301 D (biodegradability according to cation)**: 1-Ethyl-3-methylimidazolium chloride: 0 1-Butyl-3-methylimidazolium chloride: 0 1-Hexyl-3-methylimidazolium chloride: 11 3-Methy-1-octylimidazolium chloride: 100	Stolte et al. (2008)	1-Butyl-3-methylimidazolium chloride: 2089 1-Hexyl-3-methylimidazolium chloride: 339 3-Methy1-octyllimidazolium chloride: 23.4 1-Butyl-3-methylimidazolium bis(trifluoromethanesulfonyl)imide: 347	Diaz et al. (2018)
	OECD 301 F (biodegradability in terms of BOD): 3-Methy-1-propylimidazolium hexafluorophosphate: 0	Neumann et al. (2014)	1-Hexyl-3-methylimidazolium chloride: 1047 3-Methy1-octylimidazolium chloride: 182 1-Ethyl-3-methylimidazolium bis(trifluoromethanesulfonyl)imide: 3630	Markievwicz et al. (2013)
Pyridinium	**OECD 310 (biodegradability in terms of TOC)**: 1-(2-Hydroxyethyl)pyridinium bromide: 65 1-(2-Hydroxyethyl)pyridinium bis(trifluoromethanesulfonyl)imide: 62	Ford et al. (2010)		
	OECD 301 F (biodegradability in terms of BOD): 1-Ethylpyridinium chloride: 0 1-Propylpyridinium bromide: 0 1-Butylpyridinium bromide: 0 1-(2-Hydroxyethyl)pyridinium iodide: 65 1-(3-Hydroxypropyl)pyridinium chloride: 51	Neumann et al. (2014)	1-Butylpyridinium chloride: 7943	Markievwicz et al. (2013)

* As percent biodegradability.

Table 4.1. Continued

IL family	Biodegradabilty (%)*	References	EC_{50} (μM)	References
Pyrrolidinium	**OECD 301 B (biodegradability in terms of TOC)**: 1-Butyl-1-methylpyrrolidinium methylsulfate: < 10	Stolte et al. (2012)		
	OECD 301 F (biodegradability in terms of BOD): 1-Butyl-1-methylpyrrolidinium methylsulfate: < 5		1-Butyl-1-methylpyrrolidinium chloride: > 20000	Markievwicz et al. (2013)
	OECD 301 F (biodegradability in terms of BOD): 1-Ethyl-1-methylpyrrolidinium ethylsulfate: 0 1-Butyl-1-methylpyrrolidinium bromide: 0 1-Methyl-1-octylpyrrolidinium chloride: 100	Neumann et al. (2014)		
Morpholinium	**OECD 310 (biodegradability in terms of TOC)**: 1-Ethyl-1-methylmorpholinium bromide: 30 1-Butyl-1-methylmorpholinium bromide: 12 1-Hexyl-1-methylmorpholinium bromide: < 5 1-Methyl-1-octylmorpholinium bromide: < 5 1-Decyl-1-methylmorpholinium bromide: < 5	Pretti et al. (2011)	–	
	OECD 301 F (biodegradability in terms of BOD): 1-Butyl-1-methylmorpholinium bromide: 0 1-(2-Hydroxyethyl)-1-methylmorpholinium iodide: 17 1-(3-Hydroxypropyl)-1-methylmorpholinium chloride: 12 1-Cyanomethyl-1-methylmorpholinium chloride: 54	Neumann et al. (2014)		

Table 4.1. Continued

IL family	Biodegradabilty (%)*	References	EC_{50} (µM)	References
Phosphonium	**OECD310 310 (biodegradability in terms of TOC)**: Tricyclohexylphosphonium bromide: <10 % Tricyclohexylphosphonium sulfate: 22 % Tri-n-hexylallylphosphonium bromide: <30 % Tri-n-hexylallylphosphonium bis(trifluoromethanesulfonyl)imide: 0%	Atefi et al. (2009)	–	
Ammonium	**OECD 301 B (biodegradability in terms of TOC)**: Butyltrimethylammonium methylsulfonate: 60 Choline methylsulfonate: 86 Methoxycholine methylsulfonate: 17 Methoxycholine methylsulfate: 0 **OECD 301 F (biodegradability in terms of BOD)**: Butyltrimethylammonium methylsulfonate: 88 Choline methylsulfonate: 89 Methoxycholine methylsulfonate: 28 Methoxycholine methylsulfate: 4	Stolte et al. (2012)	*N*-Ethyl-*N*,*N*-dimethyl-1-butanamonium chloride: > 20000	Markievwicz et al. (2013)

Imidazolium-based ILs are typically poorly biodegradable. Thus, 1-Methyl-1-octylpyrrolidinium chloride undergoes complete degradation of its alkyl chain but no degradation of its imidazolium core (Docherty et al., 2007; Jordan and Gathergood, 2015; Stolte et al., 2008). In pyridinium-based ILs, only hydroxylated species are degraded by more than 50% in the OECD 301 test (Ford et al., 2010; Neumann et al., 2014). Ionic liquids from the pyrrolidinium and phosphonium families are usually non-biodegradable, and morpholinium-based ILs can only be degraded by 55 % or less (Atefi et al., 2009; Neumann et al., 2016; Pretti et al., 2011). Butyltrimethylammonium- and choline-based compounds, which contain methylsulfonate anion, are the only ready biodegraded member of the ammonium IL family (Stolte et al., 2012).

The toxicity of ILs to a variety of microorganisms has been assessed in terms of EC_{50}, which is the effective concentration reducing a microbial population by 50%. The toxicity of an IL depends on both cation and anion. In general, fluorinated anions are more toxic to activated sludge and *Vibrio fischeri* than are chloride and bromide (Costa et al., 2015a; Diaz et al., 2018; Markiewicz et al., 2013); also, ILs containing non-aromatic cyclic cations such as those of the pyrrolidinium and morpholinium families are less toxic (Stolte et al., 2007; Viboud et al., 2012) than conventional solvents such as chloroform or toluene (Hernández-Fernández et al., 2015). By virtue of their surfactant-like structure(Costa et al., 2015b), phosphonium-based ILs are more toxic to *Selenastrum capricornutum* microalgae and *Daphnia magna*, among other microorganisms, than are ILs containing aromatic rings (Cho et al., 2008). Markiewicz et al. (2013) found quaternary ammonium ILs to be less toxic on two different industrial activated sludges than ILs with other cations such as imidazolium or pyridinium (Markiewicz et al., 2013). Table 4.1 shows the ecotoxicity as EC_{50} of various IL families

on activated sludge as measured in terms of the reduction of the specific exogenous oxygen uptake rate (SOUR) for a reference substance.

Choline cation, *N*,*N*,*N*-trimethylethanolammonium, is an essential nutrient posted as vitamin B to humans (Linder, 2014; Morandeira et al., 2017). Betaine is a metabolite of choline presents at high levels in the liver and the kidney (Glier et al., 2014), and acetylcholine is involved in memory functions and muscle control (Gadilohar and Shankarling, 2017). In recent years, choline-based ILs have been widely studied on account of their potential uses for organic synthesis (Patil and Pratap, 2016), biomass conversion (Zhang et al., 2012), gas absorption (Palomar et al., 2011), polymerization (Sundar et al., 2011), metal extraction (Abbott et al., 2005) and lubrication (Mu et al., 2016). Although these ILs are non-toxic and biodegradable thanks to the nature of their cation, effluents from their treatment may pose environmental problems. Formerly, ILs were typically eliminated through Advanced Oxidation Processes (AOPs). Thus, ILs can be efficiently removed from water by Fenton oxidation (Cheng et al., 2016; Dominguez et al., 2014; Gomez-Herrero et al., 2018; Siedlecka et al., 2008), catalytic wet peroxide oxidation (Mena et al., 2018b, 2018c; Munoz et al., 2016), electroxidation (Fabiańska et al., 2012; Garcia-Segura et al., 2016; Mena et al., 2018a, 2017; Pieczyńska et al., 2015) or photodegradation (Czerwicka et al., 2009; Pati and Arnold, 2017; Spasiano et al., 2016; Stepnowski and Zaleska, 2005). Specifically, Munoz et al, 2015b studied the Fenton oxidation of the IL CholineCl at an initial concentration of 1000 mg L^{-1} with a stoichiometric dose of H_2O_2 and 50 mg Fe^{3+} L^{-1} at pH 3 at 70 ºC and obtained a very low mineralization rate in terms of total organic carbon removal (36.1 %) relative to ILs from other families such as EmimCl (65.3 %) and

BmpyCl (43.7 %) under identical conditions (Munoz et al., 2015). Moreover, the toxicity of the Fenton effluent was slightly higher than that of the initial CholineCl solution.

Biological treatments using activated sludge in sequencing batch reactors (SBRs) are widely used to detoxify industrial wastewater on the grounds of their feeding flexibility, versatility and cost-effectiveness relative to other biological technologies. SBR afford using microorganisms tolerant of toxic compounds and environments (oxic, anoxic), which facilitates nutrient removal (Liu et al., 2018; Monsalvo et al., 2009; Yusoff et al., 2016). Also, they promote adaptation of microbial populations to specific pollutants. Sequencing batch reactors have proved effective for degrading pollutants such as phenols and chlorophenols (Monsalvo et al., 2009), herbicides (Sanchis et al., 2014), coke wastewater (Marañón et al., 2008) and pharmaceutical wastewater (Abu Hasan et al., 2016).

In this work, we examined the aerobic biodegradation of choline-based ILs in sequencing batch reactors to assess the influence of various anions (viz., chloride as an inert anion, acetate as a easily biodegraded ion and bis(trifluoromethylsulfonyl)imide as a refractory, toxic ion) on treatment performance. We also studied the kinetics of choline removal, the intermediates formed and specialization of the biomass.

4.2. Materials and methods

Chemicals

Choline chloride (CholineCl, > 98 %) and choline acetate (CholineAc, > 95 %) were supplied by Sigma–Aldrich, and choline bis(trifluoromethylsulfonyl)imide (Cholin$eNTf_2$, 99%) by Iolitec. Table

4.2 shows the molecular formula and structure of the IL used in this study.

Table 4.2. Ionic Liquids used in this study.

Ionic liquid	Molecular formula	Abbreviation	Anion	Cation
(2-Hydroxyethyl)trimethylammonium chloride	$C_5H_{14}ClNO$	CholineCl	 **Cl^-**	
(2-Hydroxyethyl)trimethylammonium acetate	$C_7H_{17}NO_3$	CholineAc	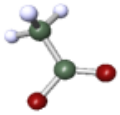 **Ac^-**	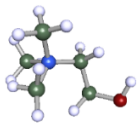 **$Choline^+$**
(2-Hydroxyethyl)trimethylammonium bis(trifluoromethylsulfonyl)imide	$C_7H_{14}F_6N_2O_5S_2$	CholineNTf_2	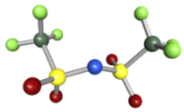 **NTf_2^-**	

Inoculum source

Activated sludge was collected from the membrane bioreactor (MBR) of a cosmetic factory in Madrid (Spain). The sludge was allowed to acclimate for 30 days in a SBR that was fed with a 0.1 mM concentration of each IL and a concentration of 22.7 mM of glucose, as carbon substrate, to obtain an organic load rate of 0.2 mg COD mg^{-1} VSS d^{-1} at room temperature. Using an easily biodegradable substrate was previously found to increase the biodegradability of recalcitrant

pollutants (Monsalvo et al., 2009; Tarighian et al., 2003; Tobajas et al., 2012).

Sequencing batch reactors

The equipment used included three thermostated SBRs with a working volume of 2.5 L equipped with dissolved oxygen and pH probes, mechanical stirring, and peristaltic pumps for feed and effluent discharge, and also for adding sodium hydroxide (NaOH) solution for pH control. Air was supplied by a flow compressor through a ceramic diffuser, using a flow rate of 5 L min^{-1} to ensure an adequate dissolved oxygen concentration. Tests were conducted stepwise in 8 h sequences including anoxic filling (0.5 h), aerated reaction (7.0 h), settling (0.25 h) and drawing (0.25 h). All were carried out at room temperature, using a hydraulic retention time of 6 days. Biomass concentration, as volatile suspended solids (VSS), was kept at around 3000 mg L^{-1} by using a cell retention time of 25 days.

The feed solution consisted of a mixture of each IL at an increasing concentration (0.25, 0.5, 1, 2, 5, 10 and 15 mM) and glucose (22.7 mM) for biomass support. The COD/N/P/micronutrient proportion was 100:5:1:0.05 (w/w) (Sanchis et al., 2014). Ammonium sulfate and phosphoric acid were used as nitrogen and phosphorous source, respectively, and mineral salts ($FeCl_3$, $CaCl_2$, KCl and $MgSO_4$) were added in a COD:micronutrient (Fe, Ca, K and Mg) proportion of 1:0.05 (w/w) as micronutrient supply.

Liquid samples were withdrawn from the reactor at the end of each cycle, passed through a filter of 0.22 μm pore size and analyzed for TOC, COD, choline, glucose and VSS. Additional samples were

periodically withdrawn at different stages of the treatment cycle to monitor the biodegradation process.

Analytical methods

Choline concentration was measured by using a Metrohm 790 Personal IC ion chromatograph with a Metrosep C4-250/4.0 column (stationary phase) and a mixture of 0.7 mM of 2,6-pyridinedicarboxylic acid and 1.7 mM of HNO_3 at a flow-rate of 0.9 mL min^{-1} (mobile phase). The injected sample volume was 20 µL. TOC was determined on a Shimadzu TOC-VCSH analyzer. COD and total biomass concentration, as VSS, were determined by following the APHA procedures 5220 D and 2540 E, respectively. Chloride and acetate ions were determined on a DIONEX ICS-900 ion chromatograph with chemical suppression, using a Dionex IonPac AS22 4 × 250 mm column as stationary phase and a 1.4 mM $NaHCO_3$/4.5 mM Na_2CO_3 solution at 1 mL min^{-1} as mobile phase. The injected sample volume was 25 µL. The concentration of NTf_2^- ion was determined by liquid chromatography–mass spectrometry on an Agilent LC/MS SQ instrument, using an ACE Excel 3 C18-Amide 150 × 4.6 mm column at 40 ºC as stationary phase and a 10:90 v/v mixture of formic acid and acetonitrile at 0.2 mL min^{-1} as mobile phase (injected sample volume, 1 µL; dilution, 1:100).

An Upright Microscope Eclipse Ci-S/Ci-L image analyzer from Nikon equipped with a DS-Fi2 digital camera and a DS-U3 control unit, both also from Nikon, were used to obtain micrographs of the granular morphology of the sludge. Microbial populations in the SBR were characterized by next-generation sequencing. Total genomic DNA in the aerobic granular biomass was determined, and paired-end sequencing of extracted DNA accomplished, by using an Illumina

MiSeq platform from Research and Testing Laboratory Genomics (Lubbock, Texas, USA). The bacterial 16S rRNA variable regions V1–V3 were targeted by using the 28F-519R primer pair.

4.3. Results and discussion

Figure 4.1 illustrates the changes in sludge morphology over the acclimation period. As can be seen, the sludge exhibited a flocculent appearance, and a loose, irregular structure. However, after 15 days in contact with a low concentration of Cholin$eNTf_2$ (0.1 mM), the sludge formed grains around 1 mm in size. By the end of the acclimation period, the grains were 3 mm in size, which facilitated biomass settling and retention in the SBR (Nancharaiah and Kiran Kumar Reddy, 2018; Qin and Liu, 2006; Val del Río et al., 2012). According to some authors, granulation protects biomass from toxic compounds when microorganisms are also in the presence of an easily biodegraded substrate (Duque et al., 2011; Tay et al., 2005).

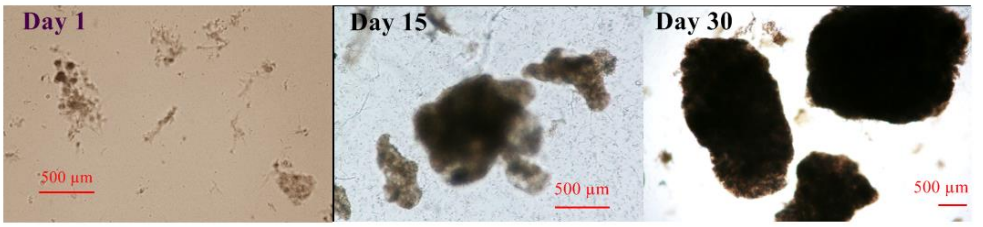

Figure 4.1. Micrographs of the sludge at different times during acclimation stage.

Figure 4.2 shows the time course of TOC, COD and VSS for the choline-based ILs in the long-term degradation tests. As can be seen, CholineCl and CholineAc resulted in no destabilization or inhibition of the sludge —not even when the IL concentration in the feed exceeded the ecotoxicity thresholds determined with *V. fischeri* and activated

sludge. The VSS concentration with CholineCl ranged from 3325 to 4000 mg L^{-1}, which suggests that the sludge adapted to this IL very easily. Increasing the IL concentration in the feed had no effect on degradation activity, the final TOC and COD concentration being 92.3 and 147.4 mg L^{-1}, respectively, and representing around 85 and 90 % of TOC and COD removal, respectively. CholineAc was slightly less markedly degraded (TOC conversion and COD removal amounted to 75 and 80 %, respectively), possibly as a consequence of the increased initial carbon concentration in the feed resulting from carbon accumulating over previous cycles.

The biodegradation of CholineNTf_2 was somewhat special. Thus, the microbial population was gradually reduced from 4000 to 2750 mg L^{-1} in 50 days by effect of the IL concentration being increased from 0.25 to 15 mM. There was thus accumulation of TOC and COD in the medium owing to the inability of the sludge to completely mineralize organic matter. A TOC and COD concentration of 343.6 and 1125.9 mg L^{-1}, respectively, remained in the reactor after 56 days, which suggests that CholineNTf_2 in the feed could have an inhibitory effect on the sludge as a result of the high toxicity of NTf_2^- ion and its null biodegradability (Ventura et al., 2014).

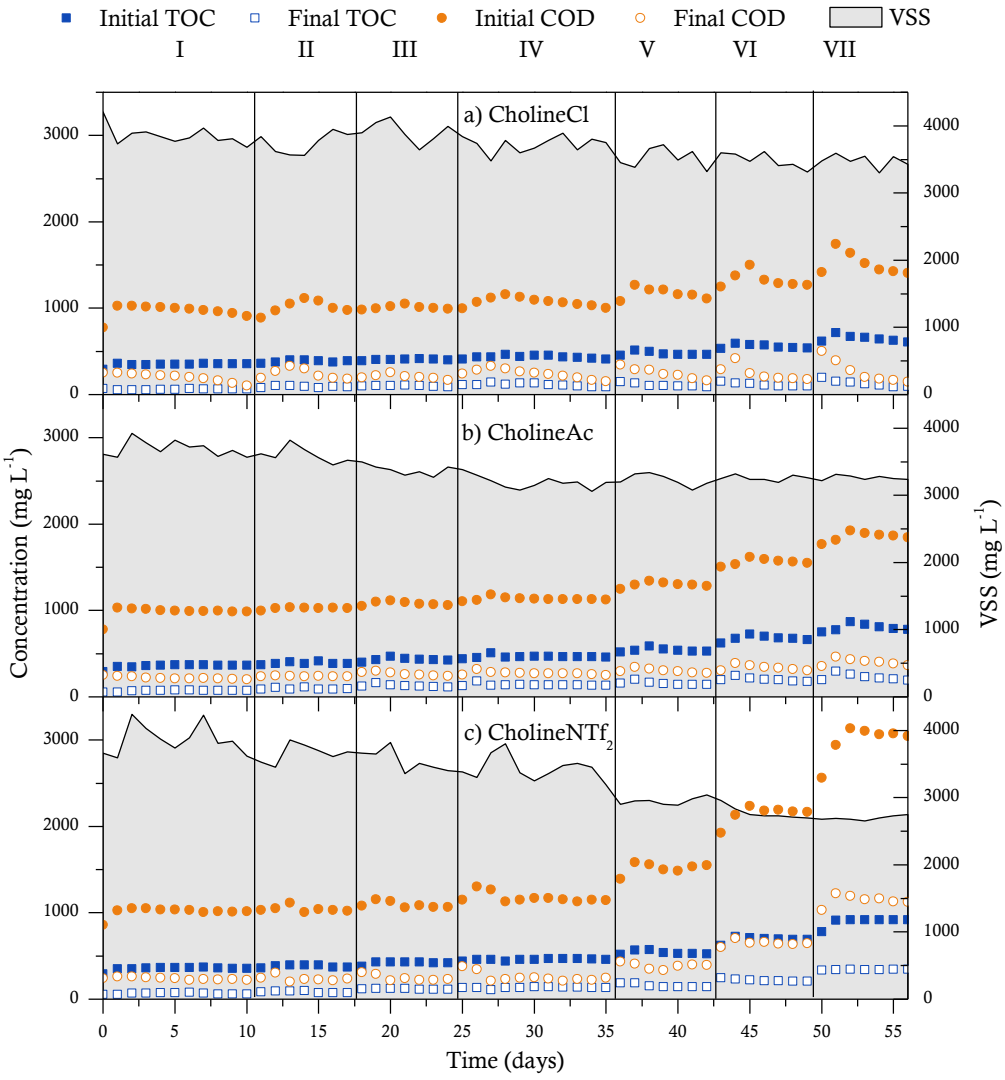

Figure 4.2. TOC and COD concentration after reactor loading (filled symbols) and before unloading (open symbols) in the long-term biodegradation tests with CholineCl (a), CholineAc (b) and CholineNTf$_2$ (c). The grey areas represent the concentrations of VSS in the reactor. IL concentration (mM) in the feed at the different stages: I, 0.25; II, 0.5; III, 1; IV, 2; V, 5; VI, 10; VII, 15.

The time course of choline, COD, TOC and glucose in the aerated reaction step of each cycle was also examined. Figure 4.3 shows TOC and choline conversion in the last cycle at each IL concentration in the feed. As can be seen, TOC profiles were similar irrespective of the CholineCl concentration in the feed, conversion amounting to about 80 %. As previously found with recalcitrant compounds, such as 2,4-dichlorophenol, TOC removal was independent of the pollutant concentration in the feed (Wang et al., 2007). As can be seen from Figure 4.3, the degradation rate in terms of TOC changed with time. Thus, TOC removal over the first 3 h was a result of the decomposition of easily biodegraded compounds; afterwards, however, it was mainly due to degradation of less biodegradable compounds. Although choline was efficiently removed in all cases (Morandeira et al., 2017), the time needed for complete depletion increased with the initial IL concentration. Similar trends were observed in the degradation of choline and TOC in the CholineAc runs. TOC conversion was lower owing to the increased carbon concentration at the beginning of each cycle by effect of the accumulation of unidentified intermediates from the previous cycles. Finally, a slightly reduction in TOC conversion (from 80 to 60 %) was observed with CholineNTf_2 owing to the refractory character of NTf_2^- ion and the above-described biomass loss.

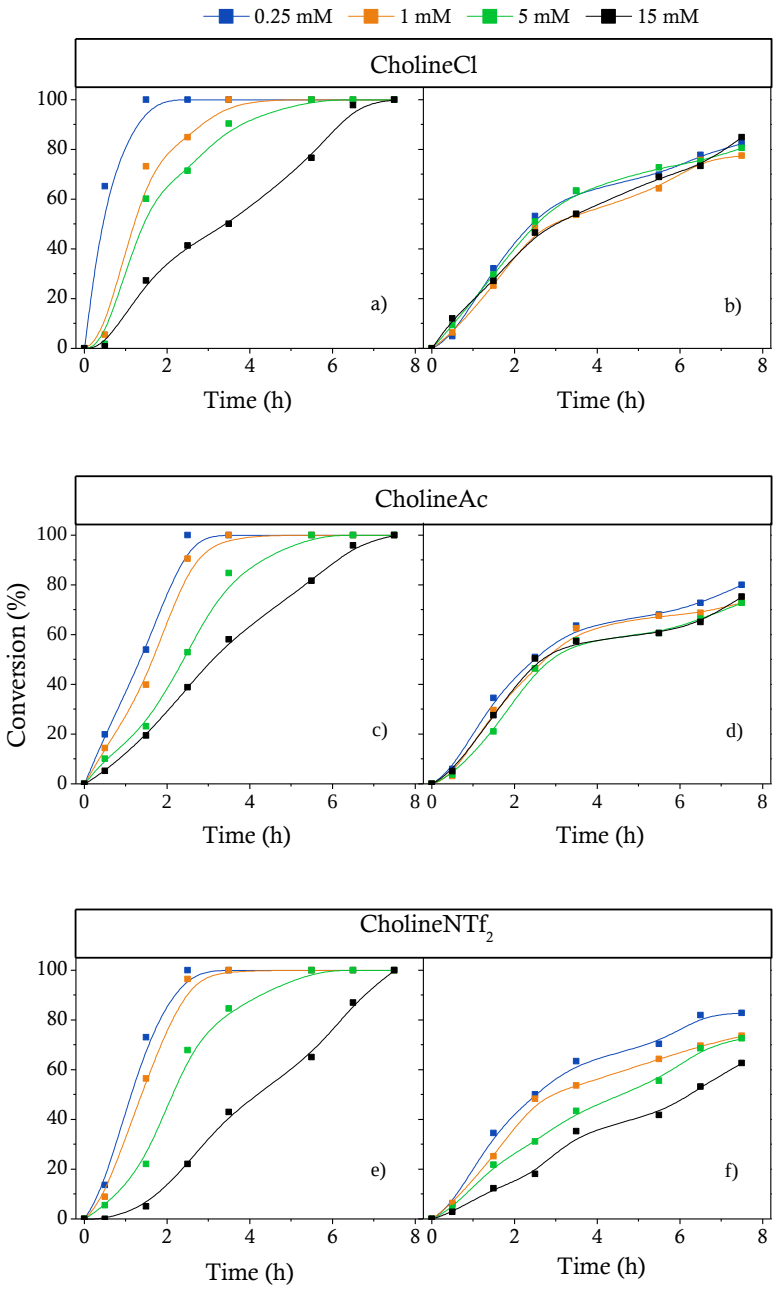

Figure 4.3. Time course of choline (a, c, e) and TOC (b, d, f) conversion in the last cycle at each IL concentration.

TOC biodegradation is illustrated by Figure 4.4, which shows the TOC balance closure in the cycle involving the highest concentration of IL in the feed. With CholineCl, a small amount of unidentified TOC from the previous cycle was measured at the beginning. During the anoxic step (first 0.5 h), TOC was slightly reduced through degradation of the unidentified fraction and also of glucose. In the aerobic step, glucose was completely degraded in less than 2 h —by contrast, choline took 6 h. Also, a residual TOC concentration of 7.6 mM was present at the end of the cycle. With CholineAc, acetate ion was degraded in the anoxic step and the amount of unidentified TOC formed increased as a result. Again, glucose and choline completely disappeared within 2 and 6 h, respectively, in the aerobic step, the unidentified TOC concentration at the end of the cycle being 16 mM. This concentration is higher than that obtained with CholineCl; however, based on the TOC time course, the extent of degradation of this fraction should have increased with time. An identical trend was observed in the glucose and choline profiles for the CholineNTf_2 cycle. Thus, the initial TOC concentration was higher with CholineNTf_2 than it was with CholineCl and CholineAc. TOC associated to NTf_2^- ion remained virtually constant throughout the cycle by effect of carbon accumulation from NTf_2^- anion in the SBR.

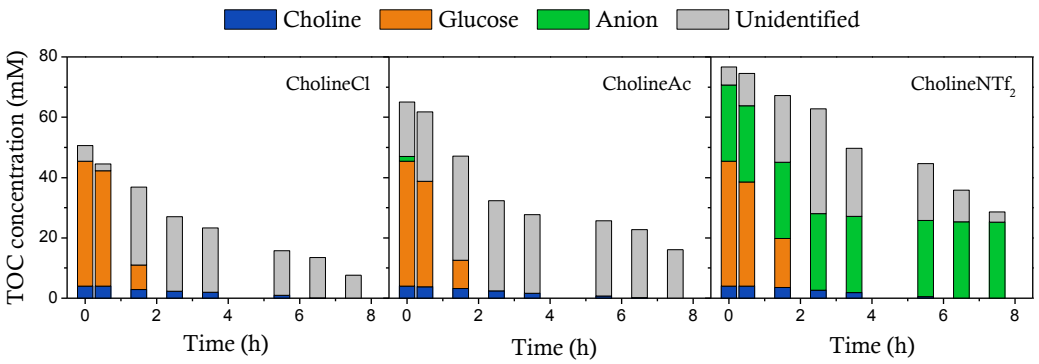

Figure 4.4. Time course of the choline, glucose and anion concentrations, as TOC, in the last cycle at an initial IL concentration of 15 mM.

Effluent composition was characterized from the reaction intermediates identified by HPLC–MS. Based on them, a plausible biodegradation pathway for choline cation is proposed. As can be seen in Figure 4.5, the first step of the degradation process is the formation of various amines (tri-, di- and methylamine) and ethanol, which is consistent with previous reports (Herring et al., 2018; Linder, 2014; Shieh, 1964). Then, the microbial community efficiently degrades these compounds to CO_2, H_2O, nitrite and nitrate as end-products. Intermediates from glucose degradation including xylulose, acetylphosphate and ethanol were also detected in the medium.

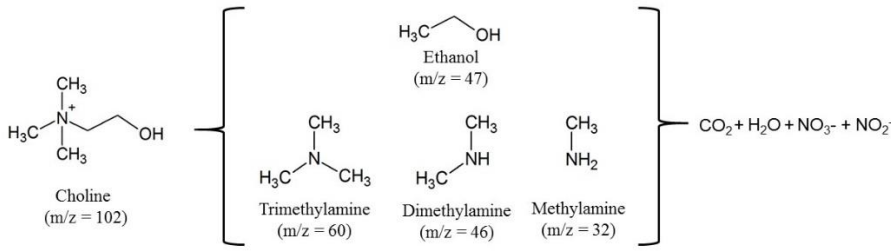

Figure 4.5. Reaction pathway for the biological degradation of choline.

Potential inhibition resulting from increased concentrations of the choline-based ILs was considered. Figure 4.6 shows the variation of the initial reaction rate with the initial concentration of ILs at each stage of the process.

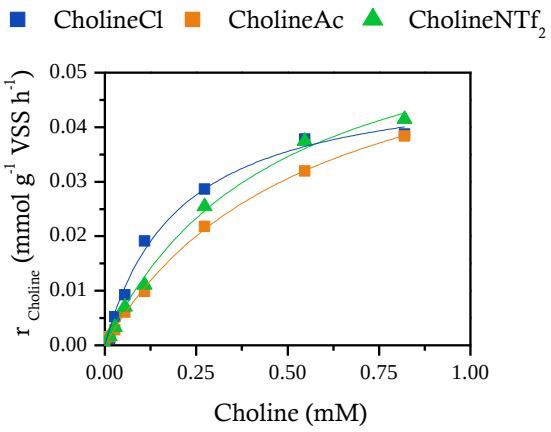

Figure 4.6. Choline removal rate from the Monod equation.

Choline biodegradation was assessed from the kinetic parameters provided by the Monod equation.

Table 4.3. Kinetic parameters obtained from the Monod equation.

IL	r_{max} (mmol·g^{-1} VSS ·h^{-1})	K_m (mM)	R^2
CholineCl	0.049 ± 0.002	0.20 ± 0.03	0.987
CholineAc	0.065 ± 0.002	0.55 ± 0.03	0.999
$CholineNTf_2$	0.067 ± 0.004	0.47 ± 0.06	0.996

As can be seen from Table 4.3, the initial rate of choline degradation per VSS fitted the Monod equation quite well, which is consistent with the absence of substrate inhibition over the studied IL concentration range. The differences among reaction rates were not significant but

decreased in the following sequence: CholineCl > Cholin$eNTf_2$ > CholineAc. The kinetic constants were all about 0.05 mmol g^{-1} VSS h^{-1} and hence considerably lower than those for recalcitrant compounds such as 4-nitrophenol (1–1.38 mmol g^{-1} VSS h^{-1}) (Tomei et al., 2004), diclofenac (1.35 mmol g^{-1} VSS h^{-1}) or 17α-ethinylestradiol (1.16 mmol g^{-1} VSS h^{-1}) (Liwarska-Bizukojc et al., 2018), but higher than that for trichloroethylene ($6.5 \cdot 10^{-3}$ mmol g^{-1} VSS h^{-1}) (Zhang and Tay, 2012). Choline degradation was slightly higher with the ILs containing a biodegradable anion (Ac^-) or a recalcitrant anion (NTf_2^-) as the likely result of increased biomass activity in the presence of a biodegradable counterion and of biomass specialization under adverse conditions, respectively.

Some authors have studied the species involved in the degradation of choline cation. In general, the cation is efficiently removed by proteobacteria such as *Achromobacter cholinophagum* (Betaproteobacteria) (Shieh, 1964), *Agrobacterium, Rhizobium* (Alfaproteobacteria) or *Pseudomonas* (Gammaproteobacteria) (Kortstee, 1970), and also by *Halomonas sp.* (Gammaproteobacteria) (Morandeira et al., 2017). Figure 4.7 shows the results of the pyrosequencing analysis of the initial and final sludge conducted to study specialization in the biomass population. The initial sludge contained a large variety of microorganisms including anaerobic microbes such as the class Anaerolineae, which decomposes carbohydrates by fermentation. The IL treatment under aerobic conditions caused anaerobic biomass, and the classes Flavobacteria and Bacteroidia, to disappear. Also, consistent with previous studies, Alpha-, Beta- and Gammaproteobacteria accounted for more than 90 % of the classes in the final sludge. Betaproteobacteria constituted the main microbial class present at the

end of CholineCl and CholineNTf$_2$ degradation, and Alpha- and Gammaproteobacteria those in CholineAc degradation.

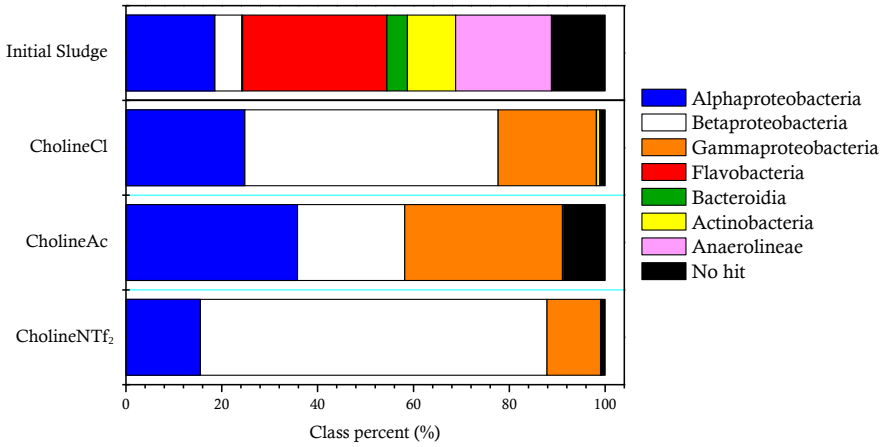

Figure 4.7. Pyrosequencing analysis for CholineCl, CholineAc and CholineNTf$_2$ in the initial and final sludge.

4.4. Conclusions

The ionic liquids CholineCl, CholineAc and CholineNTf$_2$ were all efficiently degraded under aerobic conditions in sequencing batch reactors containing glucose as carbon source. Choline was completely depleted, and COD removal and TOC conversion were both high (80–90 % and 75–85 %, respectively) with CholineCl and CholineAc at concentrations from 0.25 to 15 mM. On the other hand, CholineNTf$_2$ exhibited an inhibitory effect on activated sludge owing to the absence of NTf_2^- degradation and consequent accumulation of the anion in the SBR. A detailed reaction pathway for choline degradation is proposed. Pyrosequencing analysis of the activated sludge allowed the main choline degraders (viz., Alpha-, Beta- and Gammaproteobacteria) to be identified.

4.5. References

- Abbott, A.P., Capper, G., Davies, D.L., Rasheed, R.K., Shikotra, P., 2005. Selective extraction of metals from mixed oxide matrixes using choline-based ionic liquids. Inorg. Chem. 44, 6497–6499.
- Abrusci, C., Palomar, J., Pablos, J.L., Rodriguez, F., Catalina, F., 2011. Efficient biodegradation of common ionic liquids by *Sphingomonas paucimobilis* bacterium. Green Chem. 13, 709–717.
- Abu Hasan, H., Sheikh Abdullah, S.R., Al-Attabi, A.W.N., Nash, D.A.H., Anuar, N., Abd. Rahman, N., Sulistiyaning Titah, H., 2016. Removal of ibuprofen, ketoprofen, COD and nitrogen compounds from pharmaceutical wastewater using aerobic suspension-sequencing batch reactor (ASSBR). Sep. Purif. Technol. 157, 215–221.
- Alvarez-Guerra, M., Irabien, A., 2011. Design of ionic liquids: an ecotoxicity (*Vibrio fischeri*) discrimination approach. Green Chem. 13, 1507.
- Atefi, F., Garcia, M.T., Singer, R.D., Scammells, P.J., 2009. Phosphonium ionic liquids: design, synthesis and evaluation of biodegradability. Green Chem. 11, 1595.
- Biczak, R., Pawlowska, B., Balczewski, P., Rychter, P., 2014. The role of the anion in the toxicity of imidazolium ionic liquids. J. Hazard. Mater. 274, 181–190.
- Bruzzone, S., Chiappe, C., Focardi, S.E., Pretti, C., Renzi, M., 2011. Theoretical descriptor for the correlation of aquatic toxicity of ionic liquids by quantitative structure-toxicity relationships. Chem. Eng. J. 175, 17–23.
- Cheng, H., Chen, G., Qiu, Y., Li, B., Stenstrom, M.K., 2016. Factors that influence the degradation of 1-ethyl-3- methylimidazolium hexafluorophosphate by Fenton oxidation. R. Soc. Chem. 6, 59889–59895.
- Cho, C.-W., Jeon, Y.-C., Pham, T.P.T., Vijayaraghavan, K., Yun, Y.-S., 2008. The ecotoxicity of ionic liquids and traditional organic solvents on microalga *Selenastrum capricornutum*. Ecotoxicol. Environ. Saf. 71, 166–171.
- Costa, S.P.F., Pinto, P.C.A.G., Lapa, R.A.S., Saraiva, M.L.M.F.S., 2015a. Toxicity assessment of ionic liquids with *Vibrio fischeri*: An alternative fully automated methodology. J. Hazard. Mater. 284, 136–142.
- Costa, S.P.F., Pinto, P.C.A.G., Saraiva, M.L.M.F.S., Rocha, F.R.P., Santos, J.R.P., Monteiro, R.T.R., 2015b. The aquatic impact of ionic liquids on freshwater organisms. Chemosphere 139, 288–294.
- Cvjetko Bubalo, M., Radošević, K., Radojčić Redovniković, I., Halambek, J., Gaurina Srček, V., 2014. A brief overview of the potential environmental hazards of ionic liquids. Ecotoxicol. Environ. Saf. 99, 1–12.
- Czerwicka, M., Stolte, S., Müller, A., Siedlecka, E.M., Gołębiowski, M., Kumirska, J., Stepnowski, P., 2009. Identification of ionic liquid breakdown products in an advanced oxidation system. J. Hazard. Mater. 171, 478–483.
- Diaz, E., Monsalvo, V.M., Lopez, J., Mena, I.F., Palomar, J., Rodriguez, J.J., Mohedano, A.F., 2018. Assessment the ecotoxicity and inhibition of imidazolium ionic liquids by respiration inhibition assays. Ecotoxicol. Environ. Saf. 162, 29–34.

- Docherty, K.M., Dixon, J.K., Kulpa, C.F., 2007. Biodegradability of imidazolium and pyridinium ionic liquids by an activated sludge microbial community. Biodegradation 18, 481–493.
- Dominguez, C.M., Munoz, M., Quintanilla, A., de Pedro, Z.M., Ventura, S.P.M., Coutinho, J.A.P., Casas, J.A., Rodriguez, J.J., 2014. Degradation of imidazolium-based ionic liquids in aqueous solution by Fenton oxidation. J. Chem. Technol. Biotechnol. 89, 1197–1202.
- Duque, A.F., Bessa, V.S., Carvalho, M.F., de Kreuk, M.K., van Loosdrecht, M.C.M., Castro, P.M.L., 2011. 2-Fluorophenol degradation by aerobic granular sludge in a sequencing batch reactor. Water Res. 45, 6745–6752.
- Fabiańska, A., Ossowski, T., Stepnowski, P., Stolte, S., Thöming, J., Siedlecka, E.M., 2012. Electrochemical oxidation of imidazolium-based ionic liquids: The influence of anions. Chem. Eng. J. 198-199, 338–345.
- Ford, L., Harjani, J.R., Atefi, F., Garcia, M.T., Singer, R.D., Scammells, P.J., 2010. Further studies on the biodegradation of ionic liquids. Green Chem. 12, 1783–1789.
- Gadilohar, B.L., Shankarling, G.S., 2017. Choline based ionic liquids and their applications in organic transformation. J. Mol. Liq. 227, 234–261.
- Garcia-Segura, S., Lima, Á.S., Cavalcanti, E.B., Brillas, E., 2016. Anodic oxidation, electro-Fenton and photoelectro-Fenton degradations of pyridinium- and imidazolium-based ionic liquids in waters using a BDD/air-diffusion cell. Electrochim. Acta 198, 268–279.
- Glier, M.B., Green, T.J., Devlin, A.M., 2014. Methyl nutrients, DNA methylation, and cardiovascular disease. Mol. Nutr. Food Res. 58, 172–182.
- Gomez-Herrero, E., Tobajas, M., Polo, A., Rodriguez, J.J., Mohedano, A.F., 2018. Removal of imidazolium- and pyridinium-based ionic liquids by Fenton oxidation. Environ. Sci. Pollut. Res. 25, 34930–34937.
- Gosu, V., Sikarwar, P., Subbaramaiah, V., 2018. Mineralization of pyridine by CWPO process using nFe_0/GAC catalyst. J. Environ. Chem. Eng. 6, 1000–1007.
- Hernández-Fernández, F.J., Bayo, J., Pérez de los Ríos, A., Vicente, M.A., Bernal, F.J., Quesada-Medina, J., 2015. Discovering less toxic ionic liquids by using the Microtox® toxicity test. Ecotoxicol. Environ. Saf. 116, 29–33.
- Herring, T.I., Harris, T.N., Chowdhury, C., Mohanty, S.K., Bobik, T.A., 2018. A bacterial microcompartment is used for choline fermentation by *Escherichia coli 536*. J. Bacteriol. 200, 1–13.
- Inchaurrondo, N., Cechini, J., Font, J., Haure, P., 2012. Strategies for enhanced CWPO of phenol solutions. Appl. Catal. B Environ. 111-112, 641–648.
- Jordan, A., Gathergood, N., 2015. Biodegradation of ionic liquids - a critical review. Chem. Soc. Rev. 44, 8200–8237.
- Kortstee, G.J.J., 1970. The aerobic decomposition of choline by microorganisms. Arch. für Mikrobiol. 71, 235–244.
- Linder, T., 2014. CMO1 encodes a putative choline monooxygenase and is

required for the utilization of choline as the sole nitrogen source in the yeast *Scheffersomyces stipitis* (syn. *Pichia stipitis*). Microbiology 160, 929–940.
- Liu, Y., Li, J., Guo, W., Ngo, H.H., Hu, J., Gao, M.T., 2018. Use of magnetic powder to effectively improve the performance of sequencing batch reactors (SBRs) in municipal wastewater treatment. Bioresour. Technol. 248, 135–139.
- Liwarska-Bizukojc, E., Galamon, M., Bernat, P., 2018. Kinetics of biological removal of the selected micropollutants and their effect on activated sludge biomass. Water, Air, Soil Pollut. 229, 356.
- Marañón, E., Vázquez, I., Rodríguez, J., Castrillón, L., Fernández, Y., López, H., 2008. Treatment of coke wastewater in a sequential batch reactor (SBR) at pilot plant scale. Bioresour. Technol. 99, 4192–4198.
- Markiewicz, M., Piszora, M., Caicedo, N., Jungnickel, C., Stolte, S., 2013. Toxicity of ionic liquid cations and anions towards activated sewage sludge organisms from different sources-Consequences for biodegradation testing and wastewater treatment plant operation. Water Res. 47, 2921–2928.
- Mena, I.F., Cotillas, S., Díaz, E., Sáez, C., Mohedano, Á.F., Rodrigo, M.A., 2017. Sono- and photoelectrocatalytic processes for the removal of ionic liquids based on the 1-butyl-3-methylimidazolium cation. J. Hazard. Mater. (In press)
- Mena, I.F., Cotillas, S., Díaz, E., Sáez, C., Rodríguez, J.J., Cañizares, P., Mohedano, Á.F., Rodrigo, M.A., 2018a. Electrolysis with diamond anodes: Eventually, there are refractory species! Chemosphere 195, 771–776.
- Mena, I.F., Diaz, E., Moreno-Andrade, I., Rodriguez, J.J., Mohedano, A.F., 2018b. Stability of carbon-supported iron catalysts for catalytic wet peroxide oxidation of ionic liquids. J. Environ. Chem. Eng. 6, 6444–6450.
- Mena, I.F., Diaz, E., Pérez-Farías, C., Stolte, S., Moreno-Andrade, I., Rodriguez, J.J., Mohedano, A.F., 2018c. Catalytic wet peroxide oxidation of imidazolium-based ionic liquids: Catalyst stability and biodegradability enhancement. Chem. Eng. J. (In press)
- Monsalvo, V.M., Mohedano, A.F., Casas, J.A., Rodríguez, J.J., 2009. Cometabolic biodegradation of 4-chlorophenol by sequencing batch reactors at different temperatures. Bioresour. Technol. 100, 4572–4578.
- Morandeira, L., Álvarez, M.S., Markiewicz, M., Stolte, S., Rodríguez, A., Sanromán, M.Á., Deive, F.J., 2017. Testing true choline ionic liquid biocompatibility from a biotechnological standpoint. ACS Sustain. Chem. Eng. 5, 8302–8309.
- Mu, L., Shi, Y., Ji, T., Chen, L., Yuan, R., Wang, H., Zhu, J., 2016. Ionic grease lubricants: Protic [Triethanolamine][Oleic Acid] and aprotic [Choline][Oleic Acid]. ACS Appl. Mater. Interfaces 8, 4977–4984.
- Munoz, M., Domínguez, C.M., de Pedro, Z.M., Quintanilla, A., Casas, J.A., Rodriguez, J.J., 2016. Degradation of imidazolium-based ionic liquids by catalytic wet peroxide oxidation with carbon and magnetic iron catalysts. J. Chem. Technol. Biotechnol. 91, 2882–2887.
- Munoz, M., Domínguez, C.M., De Pedro, Z.M., Quintanilla, A., Casas, J.A., Ventura, S.P.M., Coutinho, J.A.P., 2015. Role of the chemical

structure of ionic liquids in their ecotoxicity and reactivity towards Fenton oxidation. Sep. Purif. Technol. 150, 252–256.
- Nancharaiah, Y. V., Kiran Kumar Reddy, G., 2018. Aerobic granular sludge technology: Mechanisms of granulation and biotechnological applications. Bioresour. Technol. 247, 1128–1143.
- Neumann, J., Pawlik, M., Bryniok, D., Thöming, J., Stolte, S., 2014. Biodegradation potential of cyano-based ionic liquid anions in a culture of *Cupriavidus spp.* and their in vitro enzymatic hydrolysis by nitrile hydratase. Environ. Sci. Pollut. Res. 21, 9495–9505
- Neumann, J., Steudte, S., Cho, C.-W., Thöming, J., Stolte, S., 2014. Biodegradability of 27 pyrrolidinium, morpholinium, piperidinium, imidazolium and pyridinium ionic liquid cations under aerobic conditions. Green Chem. 16, 2174–2184.
- Palomar, J., Gonzalez-Miquel, M., Bedia, J., Rodriguez, F., Rodriguez, J.J., 2011. Task-specific ionic liquids for efficient ammonia absorption. Sep. Purif. Technol. 82, 43–52.
- Pati, S.G., Arnold, W.A., 2017. Photochemical transformation of four ionic liquid cation structures in aqueous solution. Environ. Sci. Technol. 51, 11780–11787.
- Patil, P., Pratap, A., 2016. Choline chloride catalyzed amidation of fatty acid ester to monoethanolamide : A green approach. J. Oleo Sci. 79, 75–79.
- Peric, B., Sierra, J., Martí, E., Cruañas, R., Garau, M.A., Arning, J., Bottin-Weber, U., Stolte, S., 2013. (Eco)toxicity and biodegradability of selected protic and aprotic ionic liquids. J. Hazard. Mater. 261, 99–105.
- Phuong, T., Pham, T., Cho, C., Yun, Y., 2010. Environmental fate and toxicity of ionic liquids : A review. Water Res. 44, 352–372.
- Pieczyńska, A., Ofiarska, A., Borzyszkowska, A.F., Białk-Bielińska, A., Stepnowski, P., Stolte, S., Siedlecka, E.M., 2015. A comparative study of electrochemical degradation of imidazolium and pyridinium ionic liquids: A reaction pathway and ecotoxicity evaluation. Sep. Purif. Technol. 156, 522–534.
- Plechkova, N. V, Seddon, K.R., 2008. Applications of ionic liquids in the chemical industry. Chem. Soc. Rev. 37, 123–150.
- Pretti, C., Renzi, M., Ettore Focardi, S., Giovani, A., Monni, G., Melai, B., Rajamani, S., Chiappe, C., 2011. Acute toxicity and biodegradability of N-alkyl-N-methylmorpholinium and N-alkyl-DABCO based ionic liquids. Ecotoxicol. Environ. Saf. 74, 748–753.
- Qin, L., Liu, Y., 2006. Aerobic granulation for organic carbon and nitrogen removal in alternating aerobic-anaerobic sequencing batch reactor. Chemosphere 63, 926–933.
- Quijano, G., Couvert, A., Amrane, A., Darracq, G., Couriol, C., Le Cloirec, P., Paquin, L., Carrié, D., 2011. Toxicity and biodegradability of ionic liquids: New perspectives towards whole-cell biotechnological applications. Chem. Eng. J. 174, 27–32.
- Sanchis, S., Polo, A.M., Tobajas, M., Rodriguez, J.J., Mohedano, A.F., 2014. Strategies to evaluate biodegradability: Application to chlorinated herbicides. Environ. Sci. Pollut. Res. 21, 9445–9452.

- Shieh, H.S., 1964. Aerobic degradation of choline. Can. J. Microbiol. 10, 837–842.
- Siedlecka, E.M., Mrozik, W., Kaczyński, Z., Stepnowski, P., 2008. Degradation of 1-butyl-3-methylimidazolium chloride ionic liquid in a Fenton-like system. J. Hazard. Mater. 154, 893–900.
- Spasiano, D., Siciliano, A., Race, M., Marotta, R., Guida, M., Andreozzi, R., Pirozzi, F., 2016. Biodegradation, ecotoxicity and UV_{254}/H_2O_2 treatment of imidazole, 1-methyl-imidazole and N,N'-alkyl-imidazolium chlorides in water. Water Res. 106, 450–460.
- Stepnowski, P., Zaleska, A., 2005. Comparison of different advanced oxidation processes for the degradation of room temperature ionic liquids. J. Photochem. Photobiol. A Chem. 170, 45–50.
- Steudte, S., Bemowsky, S., Mahrova, M., Bottin-Weber, U., Tojo-Suarez, E., Stepnowski, P., Stolte, S., 2014. Toxicity and biodegradability of dicationic ionic liquids. RSC Adv. 4, 5198–5205.
- Stolte, S., Abdulkarim, S., Arning, J., Blomeyer-Nienstedt, A.K., Bottin-Weber, U., Matzke, M., Ranke, J., Jastorff, B., Thoming, J., 2008. Primary biodegradation of ionic liquid cations, identification of degradation products of 1-methyl-3-octylimidazolium chloride and electrochemical wastewater treatment of poorly biodegradable compounds. Green Chem. 10, 214–224.
- Stolte, S., Arning, J., Bottin-Weber, U., Müller, A., Pitner, W.-R., Welz-Biermann, U., Jastorff, B., Ranke, J., 2007. Effects of different head groups and functionalised side chains on the cytotoxicity of ionic liquids. Green Chem. 9, 1170–1179.
- Stolte, S., Steudte, S., Areitioaurtena, O., Pagano, F., Thöming, J., Stepnowski, P., Igartua, A., 2012. Ionic liquids as lubricants or lubrication additives: An ecotoxicity and biodegradability assessment. Chemosphere 89, 1135–1141.
- Sundar, D.S., Vijayaraghavan, R., Subramaniam, J., Surianarayanan, M., Mandal, A.B., 2011. Role of choline formate ionic liquid in the polymerization of vinyl and methacrylic monomers. J. Appl. Polym. Sci. 120, 3733–3739.
- Tarighian, A., Hill, G., Headley, J., Pedras, S., 2003. Enhancement of 4-chlorophenol biodegradation using glucose. Clean Techn Env. Policy 5, 61–65.
- Tay, S.T.L., Moy, B.Y.P., Maszenan, A.M., Tay, J.H., 2005. Comparing activated sludge and aerobic granules as microbial inocula for phenol biodegradation. Appl. Microbiol. Biotechnol. 67, 708–713.
- Tobajas, M., Monsalvo, V.M., Mohedano, A.F., Rodriguez, J.J., 2012. Enhancement of cometabolic biodegradation of 4-chlorophenol induced with phenol and glucose as carbon sources by *Comamonas testosteroni*. J. Environ. Manage. 95, S116–S121.
- Tomei, M.C., Annesini, M.C., Bussoletti, S., 2004. 4-Nitrophenol biodegradation in a sequencing batch reactor: Kinetic study and effect of filling time. Water Res. 38, 375–384.
- Val del Río, A., Figueroa, M., Arrojo, B., Mosquera-Corral, A., Campos,

J.L., García-Torriello, G., Méndez, R., 2012. Aerobic granular SBR systems applied to the treatment of industrial effluents. J. Environ. Manage. 95, S88–S92.

- Ventura, S.P.M., e Silva, F.A., Gonçalves, A.M.M., Pereira, J.L., Gonçalves, F., Coutinho, J.A.P., 2014. Ecotoxicity analysis of cholinium-based ionic liquids to *Vibrio fischeri* marine bacteria. Ecotoxicol. Environ. Saf. 102, 48–54.
- Viboud, S., Papaiconomou, N., Cortesi, A., Chatel, G., Draye, M., Fontvieille, D., 2012. Correlating the structure and composition of ionic liquids with their toxicity on *Vibrio fischeri*: A systematic study. J. Hazard. Mater. 215-216, 40–48.
- Wang, S.G., Liu, X.W., Zhang, H.Y., Gong, W.X., Sun, X.F., Gao, B.Y., 2007. Aerobic granulation for 2,4-dichlorophenol biodegradation in a sequencing batch reactor. Chemosphere 69, 769–775.
- Xiang, L., Royer, S., Zhang, H., Tatibouët, J.M., Barrault, J., Valange, S., 2009. Properties of iron-based mesoporous silica for the CWPO of phenol: A comparison between impregnation and co-condensation routes. J. Hazard. Mater. 172, 1175–1184.
- Yusoff, N.A., Ong, S.A., Ho, L.N., Wong, Y.S., Mohd Saad, F.N., Khalik, W.F., Lee, S.L., 2016. Evaluation of biodegradation process: Comparative study between suspended and hybrid microorganism growth system in sequencing batch reactor (SBR) for removal of phenol. Biochem. Eng. J. 115, 14–22.
- Zhang, Q., Benoit, M., Dea Oliveiraa Vigier, K., Barrault, J., Jérŏme, F., 2012. Green and inexpensive choline-derived solvents for cellulose decrystallization. Chem. - A Eur. J. 18, 1043–1046.
- Zhang, Y., Tay, J.H., 2012. Co-metabolic degradation activities of trichloroethylene by phenol-grown aerobic granules. J. Biotechnol. 162, 274–282.
- Zhong, X., Barbier, J., Duprez, D., Zhang, H., Royer, S., 2012. Modulating the copper oxide morphology and accessibility by using micro-/mesoporous SBA-15 structures as host support: Effect on the activity for the CWPO of phenol reaction. Appl. Catal. B Environ. 121-122, 123–134.

5

Catalytic wet peroxide oxidation for the removal of imidazolium-based ionic liquids in aqueous phase

5.1

Catalytic wet peroxide oxidation of imidazolium-based ionic liquids: Catalyst stability and biodegradability enhancement

Mena, I.F., Diaz, E., Pérez-Farías, C., Stolte, S., Moreno-Andrade, I., Rodriguez, J.J., Mohedano, A.F. 2019. Catalytic wet peroxide oxidation of imidazolium-based ionic liquids: Catalyst stability and biodegradability enhancement. Chem. Eng. J. (In press)

Catalytic wet peroxide oxidation of imidazolium-based ionic liquids: catalyst stability and biodegradability enhancement

Abstract

The catalytic wet peroxide oxidation (CWPO) of the imidazolium-based ionic liquids 1-butyl-3-methylimidazolium chloride (BmimCl), 1-butyl-3-methylimidazolium acetate (BmimAc), 1-butyl-3-methylimidazolium *bis*(trifluoromethanesulfonyl)imide ($BmimNTf_2$), 1-hexyl-3-methylimidazolium chloride (HmimCl) and 1-decyl-3-methylimidazolium chloride (DmimCl) was examined by using a Fe catalyst supported on alumina (Fe_2O_3/Al_2O_3) that was prepared by incipient wetness impregnation. Variable H_2O_2 doses from 0.5 to 1.5 times the stoichiometric value provided similar results in terms mg TOC removed per mg H_2O_2 decomposed at 80 ºC (0.033 mg_{TOC} mg_{H2O2}^{-1}), all allowing complete $Bmim^+$ removal. Raising the reaction temperature to 90 ºC increased the mineralization rate up to 40 % TOC conversion. Differences in TOC conversion among counteranions (chloride, acetate and NTf_2^-) were negligible. A plausible reaction pathway is propose involving hydroxylated compounds and short-chain organic acids as reaction byproducts. CWPO markedly increased the subsequent biodegradability of the IL test solutions and led there to TOC conversions after CWPO-biodegradability assays of 55–60 %. The Fe_2O_3/Al_2O_3 catalyst

exhibited high long-term stability; thus, it retained most of its properties and underwent negligible Fe leaching.

5.1 Catalytic wet peroxide oxidation of imidazolium-based ionic liquids: Catalyst stability and biodegradability enhancement

5.1.1. Introduction

Ionic Liquids (ILs) are salts with melting points below 100 °C formed by an organic cation and an organic or inorganic anion of widely variable nature. ILs can possess a low vapor pressure, good chemical and physical stability, and a high solubility in water, all of which have aroused much attention with a view to their industrial application in green chemistry (Markiewicz et al., 2013; Neumann et al., 2014; Stolte et al., 2012). However, ILs are not necessarily "green" solvents, even though they are less polluting than the typical volatile organic solvents. In fact, the toxic nature and low biodegradability in water of certain ILs may raise environmental concerns arising from their persistence in water (Abrusci et al., 2011; Biczak et al., 2014; Liu et al., 2015; Romero et al., 2008) and polluting potential (Jordan and Gathergood, 2015; Santiago et al., 2016; Ventura et al., 2012).

The imidazolium family of ILs is probably the most extensively studied on account of their wide use as solvents in major chemical (catalysis, biocatalysis, synthesis) and electrochemical processes. As a result, these compounds, which essentially consist of an aromatic heterocycle containing two nitrogen atoms —one in cationic form—, can reach industrial wastewater through production processes and use (Vekariya, 2017). Some studies have examined the ecotoxicity and biodegradability of imidazolium ILs to assess their potential hazards for the aquatic environment [4–6,12–15]. The ecotoxicity of wastewater or inhibitory compounds in aquatic environments is typically assessed with microorganisms such as bacteria or algae, or fish (Hernández-Fernández et al., 2015; Khan et al., 2016; Liu et al., 2015). Overall, the ecotoxicity of imidazolium-based ILs depends on the particular cation and anion. As far as the cation is concerned,

ecotoxicity increases with increasing length of the alkyl chain (Liu et al., 2015; Thuy Pham et al., 2010); for example, EC_{50} values, the concentration of a pollutant that reduces microbial activity by 50 %, against *Vibrio fischeri* have been found to increase from 8.12 mM with a chain of 4 carbon atoms to 12.3 μM with one of 10. Ionic liquids such as BmimCl (Romero et al., 2008) or Bmimethylsulfate (Hernández-Fernández et al., 2015) have EC_{50} values similar to those for conventional organic solvents such as dichloromethane or chloroform (Ventura et al., 2014). However, BmimBr shows much lower effective concentration than conventional solvents (e.g., 700 times more than methanol against *Selenastrum capricornutum* [12]). Also, fluorine-containing anions such as bitriflimide and tetrafluoroborate are more ecotoxic for *Vibrio fischeri* than other anion moieties (Costa et al., 2015a).

Biodegradability in imidazolium ILs is seemingly related to the length of the alkyl side chain. By using a modified OECD Guideline (OECD 1992), Docherty et al. (Docherty et al., 2007) showed that, although HmimBr and OmimBr ILs are classified as non-readily biodegradable, they can be partially mineralized by an activated sludge microbial community incubated for 25 h. Thus, they obtained a TOC conversion of 54 and 41 % for HmimBr and OmimBr, respectively, but found the concentration of BmimBr to remain unchanged; therefore, a longer alkyl side chain resulted in faster degradation rates. On the other hand, Stolte et al. (Stolte et al., 2008) used a modified version of OECD guideline 301 D to measure IL cation concentrations by HPLC–UV. They observed primary biodegradation of activated sludge (5 g L^{-1}) with HmimCl and OmimCl (viz., 11 and 100 % of removal, respectively, after 21 days), but no degradation with BmimCl. The proposed biodegradation pathway for these imidazolium-based ILs

includes transformation of the alkyl chain but no change in the imidazolium ring (Jordan and Gathergood, 2015; Stolte et al., 2008).

Based on the foregoing, it is essential to know whether destructive technologies such as advanced oxidation processes (AOPs), which have so far provided excellent results in removing refractory or nonbiodegradable pollutants from wastewater streams, are also efficient in detoxifying IL-polluted effluents (Neyens and Baeyens, 2003; Pignatello et al., 2006). Scarce research has to date been conducted on the degradation of imidazolium ILs by AOPs. In one study, boron-doped diamond electrodes were used to analyze the electrochemical oxidation of imidazolium ILs for the influence of the anions in Bmim-based ILs; degradation was fastest with BmimCl and slowest in the presence of an aromatic anion ($CH_3C_6H_4SO_3$) (Fabiańska et al., 2012). Siedlecka et al. (2012) studied the influence of the cation on the electrochemical oxidation of BmimCl and OmimCl with a PbO_2 anode and found their degradation rate to be quite similar and slightly higher than that of Omim (Siedlecka et al., 2012). COD removal with BmimCl and OmimCl was 80 and 75 %, respectively, and nitrogen conversion to ammonium and nitrate ions 80 and 60 %, respectively. Pieczynska et al. (Pieczyńska et al., 2015) examined the influence of temperature and pH, and found it to be negligible in BmimCl electrochemical oxidation; also, they proposed a reaction pathway for imidazolium-based ILs involving carboxylic acids of low molecular weight, CO_2, H_2O, NH_4^+ and NO_3^- as end products. Garcia-Segura et al. (Garcia-Segura et al., 2016) studied various electroprocesses for the abatement of 1-Ethyl-3-metylimidazolium chloride (EmimCl) by degradation and found electro-Fenton and photoelectron-Fenton to boost degradation of the cation and mineralization (TOC conversions were close to 80 % in all cases).

5.1 Catalytic wet peroxide oxidation of imidazolium-based ionic liquids: Catalyst stability and biodegradability enhancement

Recent studies of bare-electrolysis, photoelectrolysis, sonoelectrolysis and electrolysis in presence of sulfates anions reveals that the NTf_2^- anion is recalcitrant to electroxidation processes, although are effectives in the degradation of the imidazolium cations, with TOC conversions near 90% in the BmimCl electrolysis with sulfates anions (Mena et al., 2018a, 2018b; Mena et al., 2017). Ultraviolet photolysis, photolysis plus hydrogen peroxide (UV/H_2O_2) and photocatalysis with TiO_2 at room temperature for the removal of BmimCl, HmimCl and OmimCl revealed that the extent of degradation decreased with increasing size of the alkyl side chain and was 60, 85 and 95 %, respectively (Stepnowski and Zaleska, 2005). Czerwicka et al. (Czerwicka et al., 2009) studied the degradation of the imidazolium chloride family of ILs with H_2O_2/UV and found the process to involve a large number of intermediate degradation products. A recent study revealed an increased ecotoxicity of such intermediates to *Daphnia magna* and *Raphidocelis subcapitata* in the UV/H_2O_2 effluent (Spasiano et al., 2016). As can be seen, Siedlecka et al. (2008 and 2009) studied the Fenton reaction of Bmim-based ILs at a 1 mM concentration allowed complete degradation of the cations within 150 min; the outcome was strongly influenced by the IL anion, BmimCl being the least easily degraded IL and $BmimCF_3SO_3$ the most (Siedlecka et al., 2009, 2008). Munoz et al. (2015a,b) studied the influence of the reaction temperature by using a 1 g L^{-1} concentration of EmimCl, 50 mg L^{-1} Fe^{3+} and the stoichiometric amount of H_2O_2; raising the temperature from room level to 50–90 ºC ensured complete degradation within 5 min and mineralization rates of 30–50 % in all cases (Munoz et al., 2015a, 2015b). Catalytic wet peroxide oxidation (CWPO), which involves the formation of HO· radicals by catalytic decomposition of H_2O_2 in an acid medium containing a supported Fe

catalyst (Chen et al., 2017), has been successfully used to degrade imidazolium-based ILs. Thus, Munoz et al. (Munoz et al., 2016) examined the degradation of EmimCl, BmimCl and OmimCl (1 g L^{-1}) with three different catalysts (Fe_3O_4/Al_2O_3, Fe_3O_4/AC Graphite) by using a stoichiometric amount of H_2O_2 at 90 ºC at pH 3. These conditions allowed complete removal of EmimCl within 5 min and provided mineralization rates around 40-50 %. The degradation rate was only slightly influenced by the length of the alkyl chain. Poza-Nogueira et al. (2018) studied the heterogeneous electro-Fenton using iron alginate spheres of 1,3-Bis(2,4,6-trimethylphenyl)imidazolinium chloride achieved a 77% of TOC abatement in 2 h of treatment.

Table 5.1.1 summarizes the main results reported in the literature about the abatement of imidazolium ILs by Fenton and CWPO oxidation.

Table 5.1.1. Summary on the application of Fenton and CWPO oxidation to imidazolium-based ILs.

IL	Process	Operating conditions	IL removal (%/time)	TOC conversion (%/time)	Reference
1-Butyl-3-methylimidazolium chloride	Fenton	[IL] = 1 mM, $[Fe^{2+}]$ = 0.5-1.5 mM, $[H_2O_2]$ = 10-400 mM, T = 25 ºC, pH_0: 3-4	100/150 min	-	(Siedlecka et al., 2008)
1-Butyl-3-methylimidazolium chloride 1-Butyl-3-methylimidazolium trifluoromethanesulfonate 1-Butyl-3-methylimidazolium tricyanmethide	Fenton	[IL] = 1 mM, $[Fe^{2+}]$ = 1 mM, $[H_2O_2]$ = 100 mM, T = 25 ºC, pH_0: 3	100/45-150 min	-	(Siedlecka et al., 2009)
1-Ethyl-3-methylimidazolium chloride 1-Butyl-3-methylimidazolium chloride 1-Methyl-3-octylimidazolium chloride 1-Dodecyl-3-methylimidazolium chloride 1-Methyl-3-tetradecyl imidazolium chloride 1-Hexadecyl-3-methylimidazolium chloride 1-Butyl-3-methylimidazolium methanesulfonate 1-Butyl-3-methylimidazolium methylsulfate 1-Butyl-3-methylimidazolium acetate	Fenton	[IL] = 1000 mg L^{-1}, $[Fe^{3+}]$ = 50 mg L^{-1}, $[H_2O_2]$ = stoichiometric dose, T = 50-90 ºC, pH_0: 3	85-100/10-240 min	10-65/240 min	(Domínguez et al., 2014)

Table 5.1.1. Continued

IL	Process	Operating conditions	IL removal (%/time)	TOC conversion (%/time)	Reference
1-Ethyl-3-methylimidazolium chloride	Fenton	[IL] = 1000 mg L^{-1}, [Fe^{3+}] = 10-125 mg L^{-1}, [H_2O_2] = stoichiometric dose, T = 50-90 ºC, pH_0: 3	100/<10 min	18-56/240 min	(Munoz et al., 2015a)
1-Ethyl-3-methylimidazolium chloride 1-Butyl-4-methylpyridinium chloride 1-Ethyl-3-methylimidazolium tetracyanoborate 1-Ethyl-3-methylimidazolium dicyanamide 1-Ethyl-3-methylimidazolium tricyanomethanide 1-Ethyl-3-methylimidazolium thiocyanate 1-Ethyl-3-methylimidazolium dimethylphosphate 1-Ethyl-3-methylimidazolium tosylate	Fenton	[IL] = 1000 mg L^{-1}, [Fe^{3+}] = 50 mg L^{-1}, [H_2O_2] = stoichiometric dose, T = 70 ºC, pH_0: 3	-	44-80/240 min	(Munoz et al., 2015b)
1-Ethyl-3-methylimidazolium hexafluorophosphate	Fenton	[IL] = 0.5-10 mM, [Fe^{2+}] = 0.5-5 mM, [H_2O_2] = 5-50 mM, T = 25-70 ºC, pH_0: 3-11	28-96/120 min	<52/120 min	(Cheng et al., 2016)

Table 5.1.1. Continued

IL	Process	Operating conditions	IL removal (%/time)	TOC conversion (%/time)	Reference
1-Butyl-3-methylimidazolium chloride	Fenton	[IL] = 100-1000 mg L^{-1}, [Fe^{3+}] = 10-50 mg L^{-1}, [H_2O_2] = 50-200 % stoichiometric doses, T = 50-90 ºC, pH_0: 3	100/1.5-5 min	-	(Domínguez et al., 2017)
1-Hexyl-3-methylimidazolium chloride	Fenton	[IL] = 1000 mg L^{-1}, [Fe^{3+}]/[H_2O_2] = 1/10 (M/M), [H_2O_2] = 20-100 % stoichiometric doses, T = 70 ºC, pH_0: 3	58-100/240 min	6-53/240 min	(Gomez-Herrero et al., 2018)
1-Ethyl-3-methylimidazolium chloride 1-Butyl-3-methylimidazolium chloride 1-Methyl-3-octylimidazolium chloride 1-Hexadecyl-3-methylimidazolium chloride	CWPO	[IL] = 1000 mg L^{-1}, [Fe_3O_4/γ-Al_2O_3] = 2 g L^{-1}, [H_2O_2] = stoichiometric dose, T = 90 ºC, pH_0: 3	100/30-60 min	33-44/240 min	(Munoz et al., 2016)
		[IL] = 1000 mg L^{-1}, [Fe_3O_4/AC] = 2 g L^{1}, [H_2O_2] = stoichiometric dose, T = 90 ºC, pH_0: 3	100/30 min	43/240 min	
		[IL] = 1000 mg L^{-1}, [Graphite] = 2 g L^{-1}, [H_2O_2] = stoichiometric dose, T = 90 ºC, pH_0: 3	100/30 min	36-53/240 min	

Table 5.1.1. Continued

IL	Process	Operating conditions	IL removal (%/time)	TOC conversion (%/time)	Reference
1-Hexyl-3-methylimidazolium dicyanamide 1-Butyl-3-methylimidazolium dicyanamide 1-Ethyl-3-methylimidazolium dicyanamide 1-Ethyl-3-methylimidazolium acetate 1-Ethyl-3-methylimidazolium methylsulfate	Heterogeneous electro-Fenton	[IL] = 0.5 g L^{-1}, current = 100-300 mA, [iron alginate spheres] = 3.2-5.33 g L^{-1}, pH_0: 3	80-100/120 min	40-100/120 min	(Bocos et al., 2016)
1,3-Bis(2,4,6-trimethylphenyl)imidazolinium Chloride	Heterogeneous electro-Fenton	[IL] = 0.2-0.8 mM, current = 50-300 mA, [iron alginate spheres] = 1-5 g L^{-1}, pH_0: 3	-	36-77/120 min	(Poza-Nogueira et al., 2018)

The main aim of this work was to assess the efficiency of CWPO with an Fe_2O_3/Al_2O_3 catalyst to detoxify synthetic wastewater polluted with imidazolium ILs (BmimCl, BmimAc, $BmimNTf_2$, HmimCl and DmimCl) focusing on the influence of the operating conditions (temperature and H_2O_2 dose) and IL structure (nature of the anion and length of the alkyl chain), including a possible reaction pathway for the $Bmim^+$ imidazolium cation. The biodegradability enhancement and the acute toxicity (towards *Daphnia magna*) of the effluents have been also evaluated. Finally, the stability of the catalyst is studied in long-term continuous experiments, including the catalyst characterization before and after the CWPO reactions.

5.1.2. Materials and methods

Ionic liquids

The ILs studied, which included 1-butyl-3-methylimidazolium chloride (BmimCl, > 98 % purity), 1-butyl-3-methylimidazolium acetate (BmimAc, > 95 % purity), 1-butyl-3-methylimidazolium *bis*(trifluoromethanesulfonyl)imide ($BmimNTf_2$, > 99 % purity), 1-hexyl-3-methylimidazolium chloride (HmimCl, > 97 % purity) and 1-decyl-3-methylimidazolium chloride (DmimCl, > 96 % purity), were purchased from either Iolitec or Sigma–Aldrich. Table 5.1.2 shows the structure of the cations and anions selected in this study.

Table 5.1.2. Cations and anions used in this study.

Anion	Cation
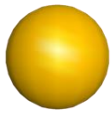 Cl^-	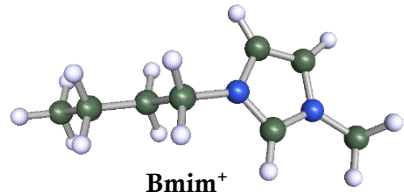 $Bmim^+$
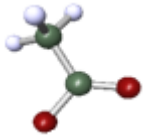 Ac^-	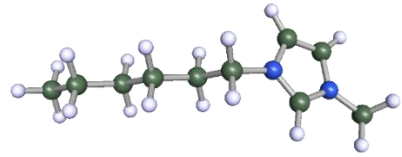 $Hmim^+$
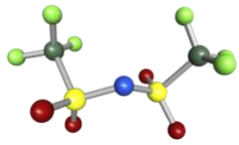 NTf_2^-	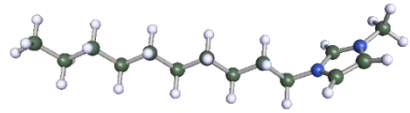 $Dmim^+$

Preparation and characterization of the Fe_2O_3/Al_2O_3 catalyst

The Fe_2O_3/Al_2O_3 catalyst was prepared by incipient wetness impregnation of Al_2O_3 supplied by Merck (Germany), using an aqueous solution of $Fe(NO_3)_3 \cdot 9H_2O$ to obtain a nominal 4 % (w/w) concentration. Once impregnated, the solid was dried at 60 ºC for 12 h and calcined for 4 h at 300 ºC, which was reached at 3 ºC min^{-1} (Bautista et al., 2011).

The catalyst was characterized as follows before and after use in the CWPO reaction. Nitrogen adsorption–desorption isotherms at 77 K

were obtained by using a Micromeritics Tristar 3020 automated volumetric gas adsorption instrument. The samples (0.15 g) were degasified at 150 ºC for 7 h in a Micromeritics VacPrep 061 degassing system under vacuum to determine their BET area and total volume of mesopores. The iron content of the catalyst was determined by total reflection X-ray fluorescence (TXRF) spectroscopy, using a TXRF Extra-II Rich & Seifert spectrometer equipped with a Si–Li detector. C, H, N and S were quantified with a LECO CHNS-932 elemental analyzer. The composition and the Fe species of the catalyst surface was determined by X-ray photoelectron spectroscopy (XPS) on a Physical Electronics 5700C Multitechnique instrument from Physical Electronics using MgKa radiation (1253.6 eV) in combination with energy dispersive X-ray spectroscopy analysis (EDAX). The morphology and surface composition of the catalyst were analyzed by Scanning Electron Microscopy–Energy Dispersive X- ray spectroscopy (SEM-EDX) with a Hitachi S-3000N apparatus. The crystalline phases in the catalysts were analyzed by X-ray diffraction (XRD) using a Siemens model D-5000 diffractometer with Cu Kα radiation.

Table 5.1.3 collects the main characteristics of the fresh Fe_2O_3/Al_2O_3 catalyst. A total Fe content of 3.9 % w/w is uniformly distributed on the catalyst surface as evidence the Fe_{TXRF}/Fe_{XPS} ratio and the SEM analysis (Figure 5.1.1). The XPS spectrum of the Fe 2p region (Figure 5.1.2) presents a main band centered at 711.4 eV, accompanied by a secondary one at 725.1 eV, and a satellite peak around 719.0 eV associated to the presence of Fe^{3+} species in the catalyst surface, as has been previously reported (Bedia et al., 2016; Rey et al., 2016). XRD analysis indicated that the catalyst presents two crystalline phases, γ-Al_2O_3 and hematite, α-Fe_2O_3 (Figure 5.1.3). The N_2 adsorption-

desorption isotherm corresponds with a mainly mesoporous material (Figure 5.1.4).

Table 5.1.3. Representative characterization of the fresh and used Fe_2O_3/Al_2O_3 catalyst in a long-term experiment at 80 h ([BmimAc] = 1 mM, $[H_2O_2]$ = 27 mM, pH_0 = 3, τ = 3.33 $kg_{Fe2O3/Al2O3}$ h mol_{IL}^{-1}).

Fe_2O_3/Al_2O_3 Catalyst	Fresh	Used
Fe_{TXRF} (w/w %)	3.90	3.86
Fe_{XPS} (w/w %)	4.60	4.56
Fe_{TXRF}/Fe_{XPS}	0.85	0.86
BET area (m^{-2} g^{-1})	131	120
$V_{mesopore}$ (cm^3 g^{-1})	0.134	0.110

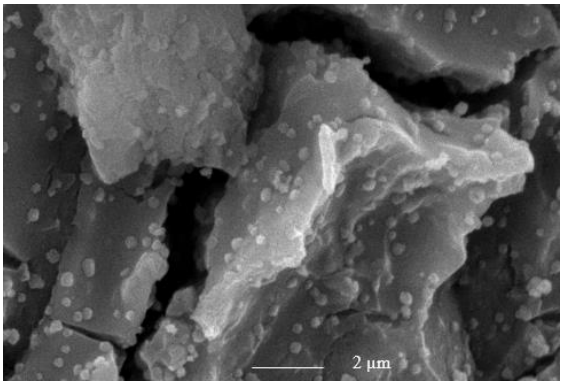

Figure 5.1.1. SEM micrograph of Fe_2O_3/Al_2O_3 catalyst.

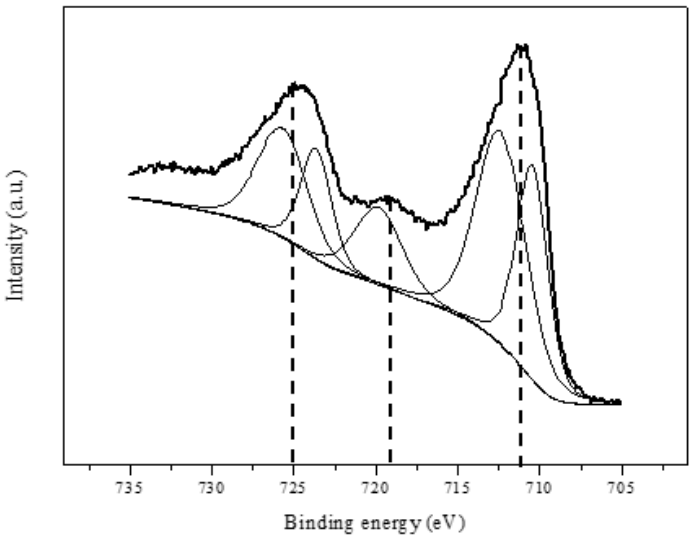

Figure 5.1.2. Fe2p deconvoluted XPS spectrum of Fe_2O_3/Al_2O_3 catalyst.

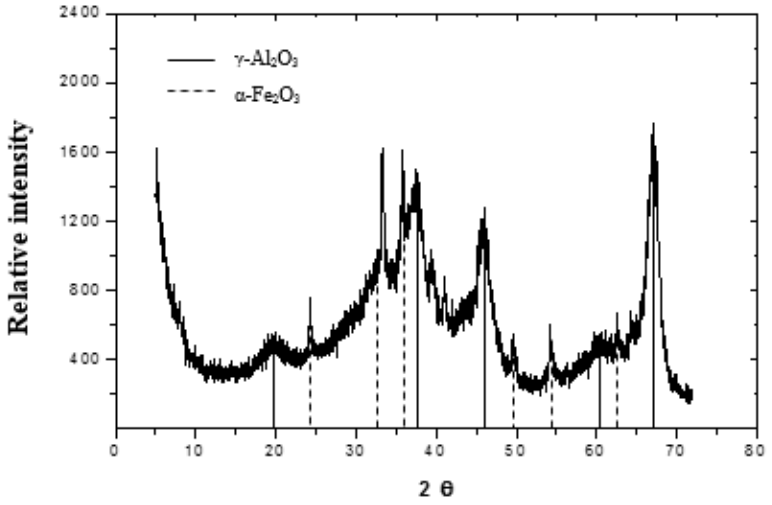

Figure 5.1.3. XRD difractogram of Fe_2O_3/Al_2O_3 catalyst.

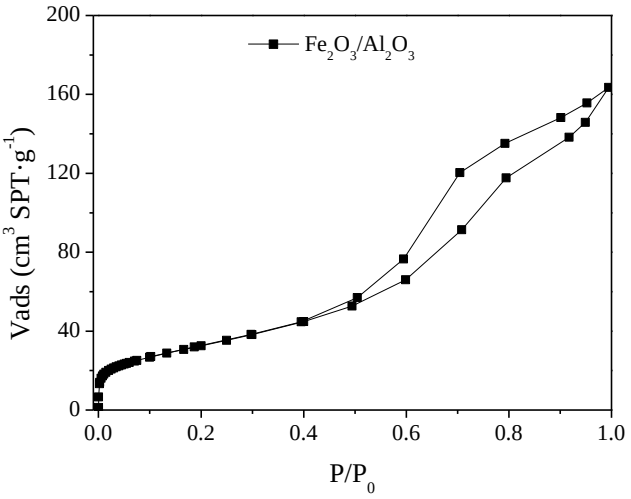

Figure 5.1.4. N_2 adsorption-desorption isotherm of Fe_2O_3/Al_2O_3 catalyst.

CWPO experiments

CWPO runs were conducted in duplicate at atmospheric pressure in a 400 mL glass batch reactor equipped with a magnetic stirrer (500 rpm) and temperature control. The starting concentration of IL was 1 mM, the catalyst concentration 1000 mg L^{-1} (40 mg Fe L^{-1}), and the initial pH 3. The variables studied were $[H_2O_2]_0$ (0.5–1.5 times the stoichiometric doses, which was the theoretical amount of H_2O_2 needed for complete mineralization to CO_2, H_2O and N_2 of the starting compound) and reaction temperature (70–90 ºC). Blank runs in the absence of catalyst were also carried out at all temperatures and negligible conversions of all ILs (< 3%) invariably obtained in them. The process was monitored by periodically analyzing samples from the batchwise runs. A Fenton run was also performed in parallel for

comparison with CWPO by using the same Fe concentration (40 mg L^{-1}, provided by $FeCl_3 \cdot 6H_2O$ salt), 1 mM BmimCl, the stoichiometric amount of H_2O_2, pH 3 and 80 ºC. Long-term runs (80 h on stream) were performed in a continuous stirred batch reactor (CSTR) fitted with a Gilson FC 203B autosampler to collect reaction aliquots. The ionic liquids and H_2O_2 were fed to the reactor at a 1 mL min^{-1} flow rate in order to deliver an IL concentration of 1 mM and the stoichiometric H_2O_2 dose for a space–time of 3.33 $kg_{Fe2O3/Al2O3}$ h mol_{IL}^{-1}. IL concentrations were determined on a Varian Prostar 325 high performance liquid chromatograph equipped with an UV–Vis detector operated at 218 nm and furnished with a Synergy 4 mm Phenomenex Polar-RP 80 A column 15 cm long × 4.6 mm i.d. as stationary phase. The mobile phase, run at 0.75 mL min^{-1}, was a mixture of phosphate buffer and acetonitrile at different concentrations from 5 to 40 % v/v depending on the particular imidazolium cation. Short-chain organic acids (formic, acetic, malonic and oxalic) and anionic species (chloride and nitrate) were determined on a DIONEX ICS-900 ion chromatograph with chemical suppression furnished with a Dionex IonPac AS22 4 × 250 mm column and using 1.4 mM $NaHCO_3$/4.5 mM Na_2CO_3 at 1 mL min^{-1} as mobile phase. TOC was measured with a Shimadzu TOC-VCSH TOC analyzer, and H_2O_2 by colorimetric titration on a Cary 60 UV/Vis spectrophotometer from Agilent that was used at 410 nm to monitor the formation of the Ti(IV)–H_2O_2 complex (Eisenberg, 1943). Iron leached from the catalyst to the liquid phase was measured by colorimetric titration at 510 nm (the *o*-phenanthroline method) (E.B. Sandell, 1959). NTf_2^- anion was identified by liquid chromatography coupled with mass spectrometry (LC/MS SQ Agilent), using an ACE Excel 3 C18-Amide 150 × 4.6 mm column at 40 ºC as stationary phase and a 10:90 v/v mixture of

formic acid and acetonitrile at 0.2 cm^3 min^{-1} as mobile phase. This instrument was also used for the tentative identification of reaction byproducts; by exception, the mobile phase was a 99.9:0.1 v/v mixture of water and formic acid, and its flow rate 0.5 mL min^{-1}. Mass spectra were acquired over the *m/z* range 40–400.

The initial IL solutions and CWPO reaction effluents were assessed for biodegradability in terms of toxicant removal efficiency, which was in turn measured in terms of IL and TOC concentrations, and of microbial activity (Mena et al., 2016; Monsalvo et al., 2015; Polo et al., 2011). For this purpose, a closed reactor was loaded with unacclimated sludge (350 mg L^{-1}) and the target compound. The specific oxygen uptake rate (SOUR) profile was measured interrupting the air supply and registering the dissolved oxygen decay within a range of 0.1 mg L–1 , obtaining the oxygen uptake rate (OUR) as the slope of the oxygen concentration vs time plot, and relating it to the biomass concentration added in the reactor. All runs were carried out at 25 ºC for 100 h.

Daphtoxkit F (MicroBioTest Inc., Gent, Belgium) was used for 48 h to conduct an acute immobilization test with *Daphnia magna* according to ISO 6341. Solution concentrations were adjusted to the particular IL, namely: 5–250 mM for BmimCl, BmimAc and $BmimNTf_2$; 1–50 mM for HmimCl and 0.05–20 mM for DmimCl. All runs were done in duplicate, using four replicates of each concentration in 10 mL of mineral medium (controls) or solution of test substances in mineral medium. Each replicate involved using five pre-fed Daphnia neonates that were less than 90 h old and obtained at 20 °C under continuous lighting. Sample toxicity was assessed from the number of

immobilized or dead organisms after 24 and 48 h as a fraction of unaffected organisms compared to the controls.

5.1.3. Results and discussion

CWPO of Bmim-based ILs

Preliminary runs were used to assess the degradation of the model IL BmimCl under identical conditions in the Fenton and CWPO reaction. As can be seen from Figure 5.1.5, $Bmim^+$ was degraded more rapidly in the homogeneous reaction (complete removal took only 30 min) than by CWPO, which took more than 60 min. The pH value slightly decreased from 3.0 to 2.8, due to the formation of carboxylic acids as final reaction products. The initial reaction rate for $Bmim^+$ disappearance was estimated to be $4.1 \cdot 10^{-1}$ min^{-1} and $5.2 \cdot 10^{-2}$ min^{-1} for Fenton and CWPO, respetively. The difference can be ascribed to the fact that the hydrogen peroxide uptake was initially (first 15 min) three times higher with Fenton but then changed similarly in both reactions and approached 80 % after 240 min. As shown by the increased mineralization achieved relative to CWPO, BmimCl was more efficiently oxidized by the Fenton reagent. Fe leaching during the CWPO reaction was less than 0.04 mg L^{-1} and similar to previous results for alumina-supported Fe catalysts in other CWPO reactions (Bautista et al., 2011, 2010). Therefore, any contribution of the homogeneous reaction to the CWPO process must have been negligible.

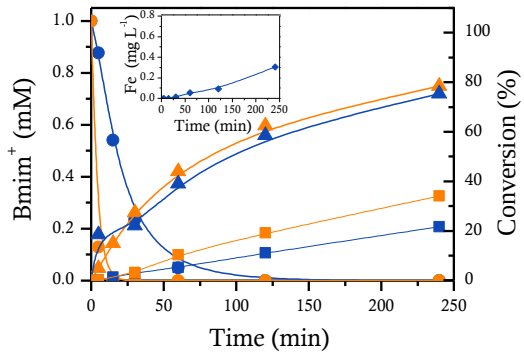

Figure 5.1.5. Time course of $Bmim^+$ concentration (circles), H_2O_2 conversion (triangles) and TOC conversion (square) in the CWPO (blue) and Fenton oxidation (orange) of BmimCl with a stoichiometric dose of H_2O_2 at 80 ºC. $[Fe_2O_3/Al_2O_3]_0$ = 1 g L^{-1}, pH_0 = 3. Insert: Fe leaching in CWPO reaction.

The influence of the H_2O_2 concentration, the highest cost related to the CWPO process, on the CWPO reaction of BmimCl was studied by using variable H_2O_2 doses from 0.5 to 1.5 times the stoichiometric value (12–36 mM) at 80 ºC ($[IL]_0$ = 1 mM, $[Fe_2O_3/Al_2O_3]_0$ = 1g L^{-1}, pH 3, 240 min). Based on the results, the lowest H_2O_2 dose led to the lowest $Bmim^+$ degradation. However, no significant differences in $Bmim^+$ reaction rate were observed with an amount of H_2O_2 equivalent to 1 or 1.5 times the H_2O_2 stoichiometric concentration. H_2O_2 conversion during the CWPO reaction evolved identically with 0.5 and 1.0 times the H_2O_2 stoichiometric doses, but was slightly higher with the highest dose (1.5 times the stoichiometric amount). Despite of TOC conversion at the end of the reaction ranged from 11 and 34 %, which was proportional to the initial H_2O_2 concentration, but a H_2O_2 dose superior to 2 times of stoichiometric did not cause the

same increment (data not shown). The Fe leaching increased when the H_2O_2 dose increased (Figure 5.1.6b), but in all cases these value are below 0.05 mg L^{-1}. The H_2O_2 uptake efficiency as measured through the amount of TOC removed per unit H_2O_2 decomposed was 0.033 $mg_{TOC}\ mg_{H2O2}^{-1}$ in the range of the initial H_2O_2 concentrations studied. This value is 3.4 times lower than that previously obtained in the degradation of phenol with a $\gamma Fe_2O_3/Al_2O_3$ catalyst (Bautista et al., 2011) and bisphenol A with a Fe-carbon support obtained from grape seeds (Mena et al., 2016).

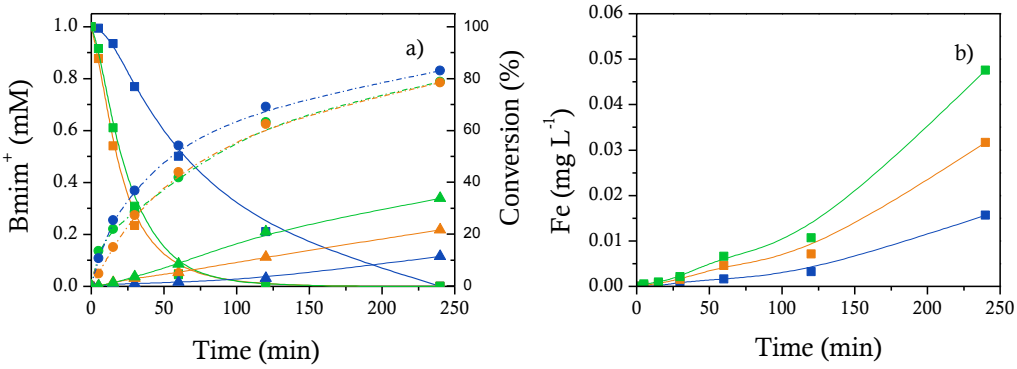

Figure 5.1.6. (a) Time course of $Bmim^+$ concentration (squares), H_2O_2 conversion (circles) and TOC conversion (triangles) and (b) Fe leaching in the CWPO of BmimCl with 0.5 (blue), 1 (orange) and 1.5 (green) times the stoichiometric dose of H_2O_2 at 80 °C. $[Fe_2O_3/Al_2O_3]_0$ = 1 g L^{-1}, pH_0 = 3.

Figure 5.1.7 shows the evolution of short-chain acids (formic, acetic, malonic and oxalic) during the CWPO reaction. The rates of formation and disappearance of formic and malonic acid increased with increasing H_2O_2 dose. On the other hand, the concentrations of

acetic and oxalic acid, which have been deemed refractory to CWPO, increased with increasing dose. Although no nitrite anion was detected in the reaction medium, a concentration of 0.06 mM of nitrate anion was quantified due to the degradation of the imidazolium ring. In order to confirm whether chloride anion took part in the reaction, the CWPO of BmimCl, which was conducted with a IL concentration of 1 mM and the stoichiometric amount of H_2O_2 at 80 ºC at pH 3, was also performed by using 1 mM HNO_3 instead of HCl to adjust the pH of the medium. Chloride anion remained unchanged under the alternative conditions, and, unlike the electrolytic process, no chlorate or perchlorate ion was formed (Neodo et al., 2012).

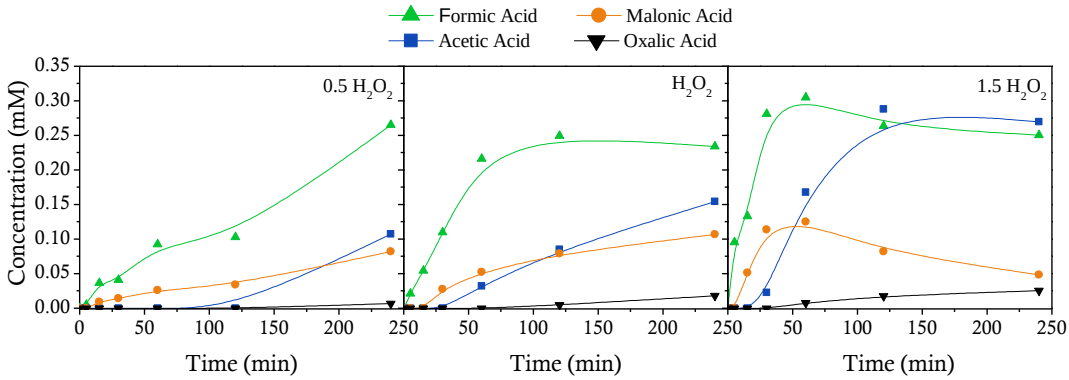

Figure 5.1.7. Time course of short-chain acids identified in the CWPO of BmimCl with different H_2O_2 doses at 80 ºC. $[Fe_2O_3/Al_2O_3]_0$ = 1 g L^{-1}, pH_0 = 3.

Apart from short-chain acids and nitrate anion, heteroaromatic and hydroxylated derivatives of 1-butyl-3-methylimidazolium oxidation were identified by LC–MS at different CWPO reaction times for BmimCl. Figure 5.1.8 depicts a potential reaction pathway for $Bmim^+$ in the CWPO reaction. The initial cation, with m/z = 139, may have

undergone a hydroxyl radical attack on its side-chain or even oxidation of the imidazolium ring, as other authors suggest for imidazolium ILs in Fenton reaction (Gomez-Herrero et al., 2018; Munoz et al., 2015a). The second step involves cleavage of the alkyl chain leading to the formation of different heteroaromatic compounds which are degraded to open-ring intermediates. Subsequent degradation of these compounds gives short-chain acids that are eventually converted into CO_2, H_2O and nitrate. Some of these intermediates were previously identified by other authors in the electrochemical degradation of imidazolium ILs. Siedlecka et al. (2013) and Pieczýnska et al. (2015) observed the m/z = 68, m/z = 82 and m/z = 154 species in the electroxidation of BmimCl (Pieczyńska et al., 2015; Siedlecka et al., 2013) and Mena et al. (2017), besides the abovementioned compounds, detected the m/z = 73 and m/z = 102 ones in the BmimCl and BmimAc electroxidation (Mena et al., 2017). Finally, reaction Gomez-Herrero et al. (2018) observed, as reaction intermediates of HmimCl by Fenton oxidation, the m/z = 73, m/z = 82 and m/z = 154 species (Gomez-Herrero et al., 2018).

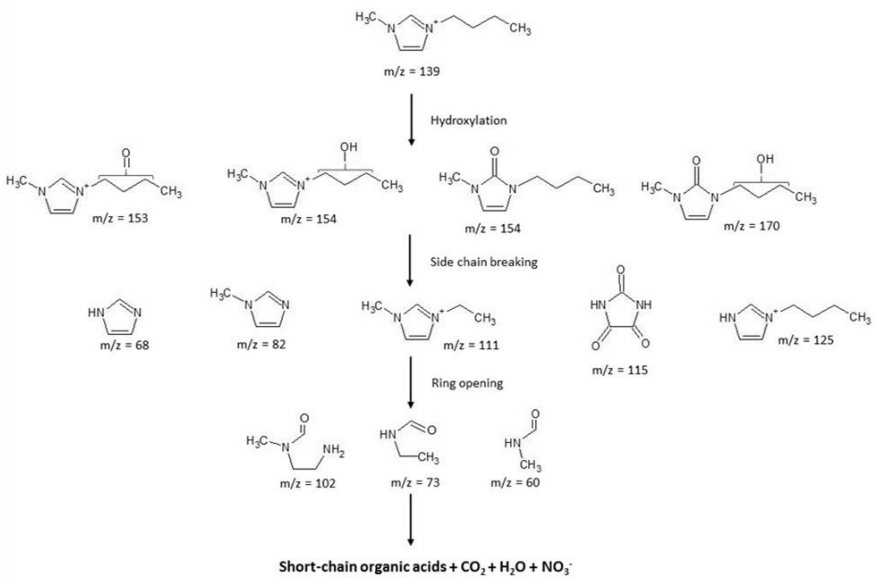

Figure 5.1.8. Reaction pathway for the CWPO of $Bmim^+$ cation with the stoichiometric dose of H_2O_2 at 80 °C. $[Fe_2O_3/Al_2O_3]_0$ = 1 g L^{-1}, pH_0 = 3.

One of the greatest advantages of ionic liquids is that they can be designed for specific purposes by using a suitable cation–anion combination. The composition of an IL can therefore influence its ease of degradation (Fabiańska et al., 2012; Siedlecka et al., 2009). Table 5.1.4 shows the results obtained in the CWPO of BmimCl, BmimAc, and $BmimNTf_2$ at temperatures from 70 to 90 °C. The apparent kinetic constants describing $Bmim^+$ disappearance during the reaction were calculated by assuming a pseudo first-order dependence on the $Bmim^+$ concentration. As expected, the constants increased with increasing reaction temperature; also, there were no significant differences among ILs in this respect. H_2O_2 conversion increased with increasing temperature and amounted to nearly 93 % at 90 °C, again the nature

of the anion seemingly having no influence on the extent of H_2O_2 decomposition in the CWPO process. Nor was the type of anion used influential on TOC conversion, the greatest difference among ILs being less than 5 %. However, raising the temperature increased TOC conversion up to 3 times with all ILs, as previously observed in the Fenton and CWPO reactions of various organic pollutants (Bautista et al., 2011; Inchaurrondo et al., 2012; Mena et al., 2016), and also in the Fenton reaction (Cheng et al., 2016; Munoz et al., 2015a) and electrolysis (Pieczyńska et al., 2015) of diverse ILs. The proposed pathway for BmimCl is applicable to these ILs; therefore, after 240 min, the reaction medium will contain short-chain acids (acetic, oxalic and formic), nitrates and the same intermediates formed in BmimCl degradation. Table 5.1.4 includes an estimate of the carbon balance compliance ($C_{identified}$) at the end of each run as calculated as the ratio of concentrations of short-chain acids (C_{acids}) and anions (C_{anion}) in terms of carbon, and the total organic carbon. The highest reaction temperature favored identification of total organic carbon. TOC was present in large amounts with the ILs containing organic anions (acetate or NTf_2^-), which are typically refractory to CWPO.

Table 5.1.4. Pseudo-first order constants and results after 240 min of CWPO of imidazolium ILs with Fe/γ-Al_2O_3 catalyst.

T (°C)	IL	k_{Bmim} (min^{-1})	χ_{H2O2} (%)	χ_{TOC} (%)	ΣC_{acids} (mg L^{-1})	C_{anion} (mg L^{-1})	$C_{identified}$ (%)
70	BmimCl	$2.5 \cdot 10^{-2}$	73.2	7.3	7.9	–	8.9
	BmimAc	$1.8 \cdot 10^{-2}$	70.9	7.3	12.3	24.3	32.9
	$BmimNTf_2$	$2.0 \cdot 10^{-2}$	73.9	10.6	12.6	24.1	34.2
80	BmimCl	$5.2 \cdot 10^{-2}$	79.4	21.7	10.1	–	13.4
	BmimAc	$6.3 \cdot 10^{-2}$	80.5	24.8	14.2	23.9	42.2
	$BmimNTf_2$	$6.1 \cdot 10^{-2}$	82.0	26.2	14.8	24.2	44.0
90	BmimCl	$7.4 \cdot 10^{-2}$	91.2	42.7	11.8	–	21.5
	BmimAc	$8.0 \cdot 10^{-2}$	92.5	40.7	15.7	23.7	55.4
	$BmimNTf_2$	$7.5 \cdot 10^{-2}$	92.9	40.9	17.8	24.7	59.9

$[IL]_0$ = 1 mM, $[H_2O_2]_0$ = 27 mM, [Fe] = 40 mg L^{-1}, pH_0 = 3

The nature of the anion had virtually no effect on the CWPO reaction. NTf_2^- and Cl^- remained unchanged during the process; by contrast, acetate ion increased slightly in concentration, possibly by effect of its being recalcitrant to CWPO degradation and of its scant formation, together with other short-chain acids, in $Bmim^+$ degradation (Centi et al., 2000).

Influence of the alkyl chain

The length of the alkyl side chain has been related to the degradation rate and toxicity of ILs (Liu et al., 2015; Ranke et al., 2004). This led us to study imidazolium-based ILs with different *n*-alkyl chains (BmimCl, HmimCl and DmimCl) in the CWPO reaction at 70, 80 and 90 °C. For the different temperatures assayed, all cations were completely degraded and no significant differences among the concentrations of $Bmim^+$, $Hmim^+$ and $Dmim^+$ versus reaction time for

each temperature were observed (data not shown). Similar results were reported for Fenton or heterogeneous Fenton reactions, where a slightly increase of reaction rate was only observed for imidazolium ILs with alkyl chain lengths of more than 12 carbons [39,41].

As regards mineralization, TOC conversion ranged from 40 to 50 % and was highest for DmimCl as a result of its increased carbon content. Also related to TOC conversion, the proportion of carbon in the compounds identified at 90 ºC differed slightly: from 21.5 % in BmimCl to 22.5 % in HmimCl to 26 % in DmimCl. The pseudo first-order kinetic constant for cation degradation ranged from $7.3 \cdot 10^{-2}$ to $7.5 \cdot 10^{-2}$ min^{-1} and, consistent with previous results, was not influenced by the length of the alkyl side chain (Domínguez et al., 2014; Munoz et al., 2016). In a previous electrochemical degradation experiment on imidazolium ILs, those with the longer alkyl side chains exhibited faster degradation, their kinetic constants as determined with a boron-doped diamond electrode being $1.97 \cdot 10^{-2}$ min^{-1} for BmimCl and $2.22 \cdot 10^{-2}$ min^{-1} for HmimCl (Pieczyńska et al., 2015). Based on these results, CWPO is more efficient than electrolysis in degrading imidazolium-based ILs.

Biodegradability of the ionic liquids

Wastewater containing ILs is usually poorly biodegradable even though IL cations with a long side chain can be partially degraded (Docherty et al., 2007; Stolte et al., 2008). This led us to conduct CWPO runs of imidazolium ILs to improve the biodegradability of this type of waste. Figure 5.1.9 shows the biodegradability of the initial and final effluent of ILs. Based on the results, BmimCl, $BmimNTf_2$, HmimCl and DmimCl are not readily biodegradable (Garcia et al., 2005; Quijano et al., 2011; Romero et al., 2008); in fact, no changes in

cation or TOC concentration, nor significant variations in SOUR, were detected in the biodegradability tests. However, the fact that endogenous respiration (ca. 3–4 mg O_2 g_{SV}^{-1} h^{-1}) was constant suggests that the poor biodegradability of the ILs was not associated to a high toxicity. Changes in SOUR and IL concentration exhibited a differential pattern for BmimAc; thus, SOUR increased and TOC proportionally decreased over the first few hours of reaction. The decrease in TOC was a result of degradation of acetate anion with no change in $Bmim^+$ concentration. As with the other ILs, SOUR and TOC levelled off after 5 h. The CWPO effluents for each IL treated were subjected to the same test. In all cases, SOUR increased by effect of the decomposition of easily degraded species formed in the CWPO reaction (e.g., acetate ion). A second increase in SOUR occurred between 20 and 40 h of reaction in the BmimCl and BmimAc effluents concomitantly with a decrease in TOC due to degradation of some reaction intermediates that required pre-acclimation to the activated sludge. Some authors have suggested that the short-chain acids oxalic and formic, which are typically involved in Fenton and CWPO reactions, can be degraded by conventional biological treatment (Mena et al., 2016; Monsalvo et al., 2015). In fact, both were easily removed from the effluents within 50 h. No second SOUR increase was observed with $BmimNTf_2$. However, a slightly decreased endogenous respiration was observed in the activated sludge between 30 and 70 h as a result of a decrease in microbial population. This result may have arisen from the formation of toxic intermediates in the CWPO reaction. As regards TOC degradation, the biodegradability assay revealed a decrease in TOC by 35 % in the BmimCl and $BmimNTf_2$ effluents, and one of 40 % in the BmimAc effluent. Combining CWPO and the biodegradability assay led to a total TOC

conversion level roughly 55–60 % higher than that achieved by CWPO at 90 ºC (ca. 40 %), which was the highest temperature studied. The high toxicity of HmimCl and DmimCl, required carrying out the CWPO reactions at the maximum possible temperature, which ensures a greater transformation of the starting compound. The effluents present a first SOUR increased in the first hours as the Bmim-ILs, and a second increased at 40 h wider than the Bmim-IL ones.

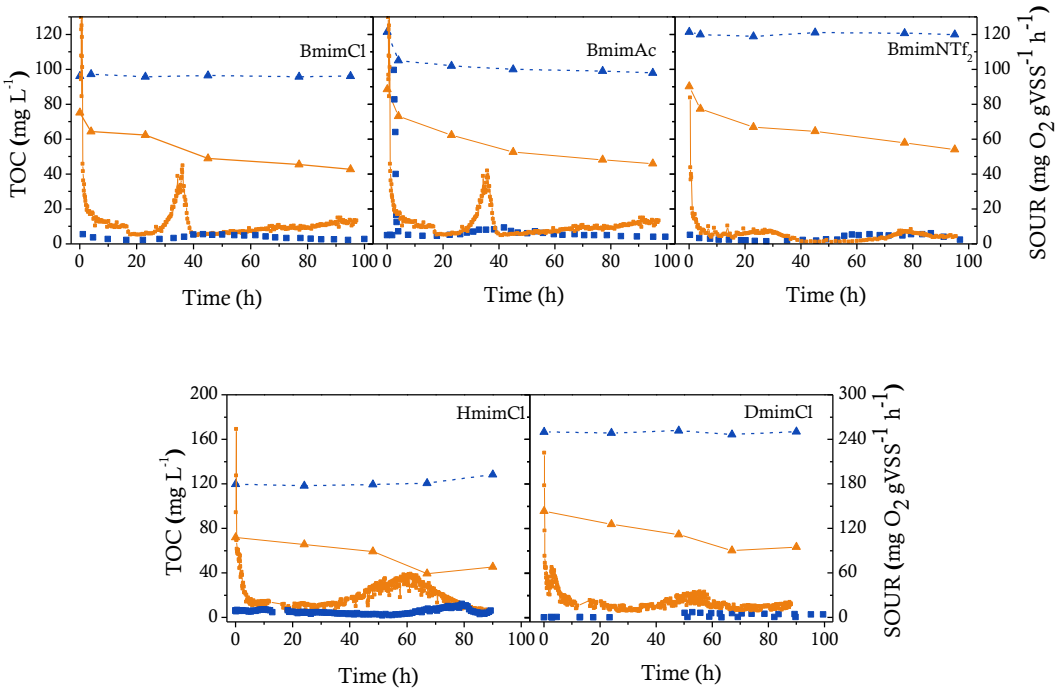

Figure 5.1.9. Time course of TOC (triangles) and SOUR (squares) of the initial (1 mM, open symbols) and final effluents (solid symbols) in the CWPO of BmimCl, BmimAc and $BmimNTf_2$ at T = 80 ºC, HmimCl and DmimCl at T = 90 ºC, $[H_2O_2]_0$ = stoichiometric dose, $[Fe_2O_3/Al_2O_3]_0$ = 1 g $L^{-1}$and pH_0 = 3. Operating conditions for the biodegradability assay: 350 mg L^{-1} VSS, T = 25 ºC, t = 100 h.

The *Daphnia* toxicity test was used to assess the effect of CWPO on the IL solutions. As can be seen in the Table 5.1.5 the EC_{50} values for BmimCl and BmimAc were similar but greater than that for $BmimNTf_2$. Also, toxicity increased with increasing length of the alkyl side chain (Diaz et al., 2018; Liu et al., 2015; Thuy Pham et al., 2010); thus, DmimCl toxicity was more than 300 times higher than BmimCl toxicity. Ecotoxicity values upon CWPO exhibited two different trends. The Bmim-based ILs became more toxic through the production of more toxic intermediates than the initial ILs, toxicity increasing in the sequence BmimCl < BmimAc < $BmimNTf_2$. Also, BmimCl toxicity decreased with increasing CWPO temperature as a result of the intermediates being converted into less toxic species. By contrast, the ILs with the longest alkyl side chains were much less toxic after CWPO, but their effluents were still more toxic than those of BmimCl.

Table 5.1.5. Results of the *Daphnia* assay for the initial and final CWPO effluents.

	Initial solution		**CWPO effluent, 80 °C**	**CWPO effluent, 90 °C**
IL	**Log EC_{50}**	**EC_{50} (mM)**	**log IC_{50}**	**log IC_{50}**
BmimCl	2.017 ± 0.041	104.1	1.637 ± 0.060	1.799 ± 0.068
BmimAc	2.000 ± 0.016	100.0	1.383 ± 0.050	–
$BmimNTf_2$	1.913 ± 0.077	81.9	1.291 ± 0.028	–
HmimCl	1.090 ± 0.056	12.8	–	1.679 ± 0.031
DmimCl	–0.530 ± 0.168	0.29	–	1.401 ± 0.029

Catalyst stability

A long-term experiment was carried out to assess the stability of the catalyst in the CWPO reaction with a view to removing ILs from wastewater. The experiment was performed with BmimAc because it had previously exhibited high mineralization in the combined process (CWPO + biodegradability assay). Figure 5.1.10 shows the variation of the $Bmim^+$ cation and also TOC and H_2O_2 conversion at 3.33 $kg_{Fe2O3/Al2O3}$ h mol_{IL}^{-1}. The $Bmim^+$ concentration rapidly decreased from 1.0 to 0.4 mM and then remained at that level for more than 75 h. The cation transformation resulted in an increase in the initial acetate concentration by 0.1 mM by effect of the formation of acetic acid. TOC and H_2O_2 conversion gradually increased while the system stabilized and eventually leveled off at 18 % and 30 %, respectively. In terms of short-chain acids, acetic and formic were detected at a concentration of 1.1 and 0.2 mM, respectively, and oxalic at a much lower level (0.02 mM). Based on the proposed reaction pathway for $Bmim^+$, the reaction medium contained heteroaromatic compounds with an equivalent carbon concentration of 4.5 mM of unidentified TOC.

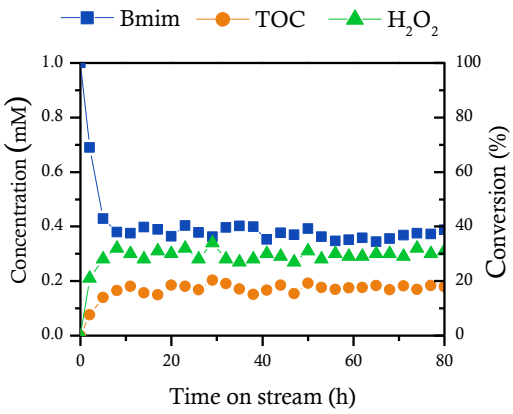

Figure 5.1.10. Evolution of $Bmim^+$ concentration and TOC and H_2O_2 conversion in long-term performance of the Fe_2O_3/Al_2O_3 catalyst upon CWPO of BmimAc at 80 °C. [BmimAc] = 1 mM, [H_2O_2] = stoichiometric dose, pH_0 = 3, τ = 3.33 $kg_{Fe2O3/Al2O3}$ h mol^{-1}_{IL}.

The properties of the used catalyst were compared with those of the fresh catalyst in Table 5.1.3. The used catalyst exhibited no significant difference in pore structure (A_{BET} = 120 m^2 g^{-1}; $V_{mesopores}$ = 0.110 cm^3 g^{-1}). As regards Fe leaching, which is the most plausible cause of catalyst deactivation in CWPO reactions (Bedia et al., 2017; Mena et al., 2016; Mohedano et al., 2014; Munoz et al., 2013), TXRF analysis revealed little loss of Fe during the reaction on stream, the total amount of Fe in the used catalyst (3.86 % w/w) being quite similar to that in the fresh catalyst. Fe_{XPS} was identical in the fresh and used catalyst, which can therefore be deemed stable in the CWPO of ILs. Elemental analyses revealed slight deposition of residual carbon (2.5 % w/w) on the catalyst surface which seemingly caused no blockage of active sites. The consistency of IL and TOC conversion in the process is correlated with the stability in the catalyst properties.

5.1.4. Conclusions

Catalytic wet peroxidation (CWPO) in the presence of a Fe_2O_3/Al_2O_3 catalyst proved an effective treatment for the removal of imidazolium ILs (BmimCl, BmimAc, $BmimNTf_2$, HmimCl and DmimCl) from wastewater. Thus, $Bmim^+$ cation was completely removed after 240 min at 80 ºC with similar efficiency (0.033 mg_{TOC} mg_{H2O2}^{-1}) irrespective of the H_2O_2 dose used. The highest mineralization rate was obtained by using the stoichiometric amount of H_2O_2 at 90 ºC (40%). In terms of anions, the acetate concentration increased along reaction time, due to its refractory behavior in CWPO reactions, whereas chloride and NTf_2^- concentration remained unalterable. Mineralization increased with increasing length of the alkyl side chain, but the extent of imidazolium cation removal was essentially the same. The Fe_2O_3/Al_2O_3 catalyst showed a fairly low Fe leaching, below 0.05 mg L^{-1} in all cases. A degradation pathway involving heteroaromatic and hydroxylated derivatives of $Bmim^+$ cation, short-chain acids and nitrate detected at the end of the reaction (240 min) is proposed. CWPO increased biodegradability in the final effluents relative to the initial ones and TOC conversion after CWPO-biodegradability process being 55–60 %. The Fe_2O_3/Al_2O_3 catalyst used exhibited long-term stability along CWPO of BmimAc (3.33 $kg_{Fe2O3/Al2O3}$ h mol_{IL}^{-1}); thus, it remained stable for 70 h in an on-stream experiment lasting 100 h. The used catalyst had essentially the same Fe content as the starting catalyst, which confirms the absence of Fe leaching.

5.1.5. References

- Abrusci, C., Palomar, J., Pablos, J.L., Rodriguez, F., Catalina, F., 2011. Efficient biodegradation of common ionic liquids by *Sphingomonas paucimobilis bacterium*. Green Chem. 13, 709–717.
- Amde, M., Liu, J., Pang, L., 2015. Environmental Application, Fate, Effects and Concerns of Ionic Liquids : A Review. Environ. Sci. Technol. 49, 12611–12627
- Bautista, P., Mohedano, A.F., Casas, J.A., Zazo, J.A., Rodriguez, J.J., 2011. Highly stable Fe/γ-Al_2O_3 catalyst for catalytic wet peroxide oxidation. J. Chem. Technol. Biotechnol. 86, 497–504.
- Bautista, P., Mohedano, A.F., Menéndez, N., Casas, J.A., Rodriguez, J.J., 2010. Catalytic wet peroxide oxidation of cosmetic wastewaters with Fe-bearing catalysts. Catal. Today 151, 148–152.
- Bedia, J., Monsalvo, V.M., Rodriguez, J.J., Mohedano, A.F., 2017. Iron catalysts by chemical activation of sewage sludge with $FeCl_3$ for CWPO. Chem. Eng. J. 318, 224–230.
- Biczak, R., Pawlowska, B., Balczewski, P., Rychter, P., 2014. The role of the anion in the toxicity of imidazolium ionic liquids. J. Hazard. Mater. 274, 181–190.
- Bocos, E., Pazos, M., Sanromán, M.Á., 2016. Electro-Fenton treatment of imidazolium-based ionic liquids: Kinetics and degradation pathways. RSC Adv. 6, 1958–1965.
- Centi, G., Perathoner, S., Torre, T., Verduna, M.G., 2000. Catalytic wet oxidation with H_2O_2 of carboxylic acids on homogeneous and heterogeneous Fenton-type catalysts. Catal. Today 55, 61–69.
- Chen, F., Xie, S., Huang, X., Qiu, X., 2017. Ionothermal synthesis of Fe_3O_4 magnetic nanoparticles as efficient heterogeneous Fenton-like catalysts for degradation of organic pollutants with H_2O_2. J. Hazard. Mater. 322, 152–162.
- Cheng, H., Chen, G., Qiu, Y., Li, B., Stenstrom, M.K., 2016. Factors that influence the degradation of 1-ethyl-3-methylimidazolium hexafluorophosphate by Fenton oxidation. R. Soc. Chem. 6, 59889–59895.
- Cho, C.-W., Jeon, Y.-C., Pham, T.P.T., Vijayaraghavan, K., Yun, Y.-S., 2008. The ecotoxicity of ionic liquids and traditional organic solvents on microalga *Selenastrum capricornutum*. Ecotoxicol. Environ. Saf. 71, 166–171.
- Costa, S.P.F., Pinto, P.C.A.G., Lapa, R.A.S., Saraiva, M.L.M.F.S., 2015a. Toxicity assessment of ionic liquids with *Vibrio fischeri*: An alternative fully automated methodology. J. Hazard. Mater. 284, 136–142.
- Costa, S.P.F., Pinto, P.C.A.G., Saraiva, M.L.M.F.S., Rocha, F.R.P., Santos, J.R.P., Monteiro, R.T.R., 2015b. The aquatic impact of ionic liquids on freshwater organisms. Chemosphere 139, 288–294.

- Czerwicka, M., Stolte, S., Müller, A., Siedlecka, E.M., Gołebiowski, M., Kumirska, J., Stepnowski, P., 2009. Identification of ionic liquid breakdown products in an advanced oxidation system. J. Hazard. Mater. 171, 478–483.
- Diaz, E., Monsalvo, V.M., Lopez, J., Mena, I.F., Palomar, J., Rodriguez, J.J., Mohedano, A.F., 2018. Assessment the ecotoxicity and inhibition of imidazolium ionic liquids by respiration inhibition assays. Ecotoxicol. Environ. Saf. 162, 29–34.
- Docherty, K.M., Dixon, J.K., Kulpa, C.F., 2007. Biodegradability of imidazolium and pyridinium ionic liquids by an activated sludge microbial community. Biodegradation 18, 481–493.
- Domínguez, C.M., Munoz, M., Quintanilla, A., de Pedro, Z.M., Casas, J.A., 2017. Kinetics of imidazolium-based ionic liquids degradation in aqueous solution by Fenton oxidation. Environ. Sci. Pollut. Res.
- Domínguez, C.M., Munoz, M., Quintanilla, A., Pedro, M. De, Ventura, S.P.M., Coutinho, J.A.P., Casas, A., Rodriguez, J.J., 2014. Degradation of imidazolium-based ionic liquids in aqueous solution by Fenton oxidation. J Chem Technol Biotechnol 89, 1197–1202.
- E.B. Sandell, 1959. Determination of Traces of Metals, third ed. ed. Interscience Pubs, New York, NY.
- Eisenberg, G., 1943. Colorimetric Determination of Hydrogen Peroxide. Eng. Chem. Anal. Ed. 15, 327–328.
- Fabiańska, A., Ossowski, T., Stepnowski, P., Stolte, S., Thöming, J., Siedlecka, E.M., 2012. Electrochemical oxidation of imidazolium-based ionic liquids: The influence of anions. Chem. Eng. J. 198-199, 338–345.
- Garcia, M.T., Gathergood, N., Scammells, P.J., 2005. Biodegradable ionic liquids - Part II. Effect of the anion and toxicology. Green Chem. 7, 9–14.
- Garcia-Segura, S., Lima, Á.S., Cavalcanti, E.B., Brillas, E., 2016. Anodic oxidation, electro-Fenton and photoelectro-Fenton degradations of pyridinium- and imidazolium-based ionic liquids in waters using a BDD/air-diffusion cell. Electrochim. Acta 198, 268–279.
- Gomez-Herrero, E., Tobajas, M., Polo, A., Rodriguez, J.J., Mohedano, A.F., 2018. Removal of imidazolium- and pyridinium-based ionic liquids by Fenton oxidation. Environ. Sci. Pollut. Res. 25, 34930–34937.
- Hernández-Fernández, F.J., Bayo, J., Pérez de los Ríos, A., Vicente, M.A., Bernal, F.J., Quesada-Medina, J., 2015. Discovering less toxic ionic liquids by using the Microtox® toxicity test. Ecotoxicol. Environ. Saf. 116, 29–33.
- Inchaurrondo, N., Cechini, J., Font, J., Haure, P., 2012. Strategies for enhanced CWPO of phenol solutions. Appl. Catal. B Environ. 111-112, 641–648.

- Jordan, A., Gathergood, N., 2015. Biodegradation of ionic liquids - a critical review. Chem. Soc. Rev. 44, 8200–8237.
- Khan, M.I., Zaini, D., Shariff, A.M., 2016. Framework for Ecotoxicological Risk Assessment of Ionic Liquids. Procedia Eng. 148, 1141–1148.
- Liu, H., Zhang, X., Chen, C., Du, S., Dong, Y., 2015. Effects of imidazolium chloride ionic liquids and their toxicity to *Scenedesmus obliquus*. Ecotoxicol. Environ. Saf. 122, 83–90.
- Markiewicz, M., Piszora, M., Caicedo, N., Jungnickel, C., Stolte, S., 2013. Toxicity of ionic liquid cations and anions towards activated sewage sludge organisms from different sources - Consequences for biodegradation testing and wastewater treatment plant operation. Water Res. 47, 2921–2928.
- Mena, I.F., Cotillas, S., Díaz, E., Sáez, C., Mohedano, Á.F., Rodrigo, M.A., 2018a. Influence of the supporting electrolyte on the removal of ionic liquids by electrolysis with diamond anodes. Catal. Today 313, 203–210.
- Mena, I.F., Cotillas, S., Díaz, E., Sáez, C., Mohedano, Á.F., Rodrigo, M.A., 2017. Sono- and photoelectrocatalytic processes for the removal of ionic liquids based on the 1-butyl-3-methylimidazolium cation. J. Hazard. Mater.
- Mena, I.F., Cotillas, S., Díaz, E., Sáez, C., Rodríguez, J.J., Cañizares, P., Mohedano, Á.F., Rodrigo, M.A., 201b. Electrolysis with diamond anodes: Eventually, there are refractory species! Chemosphere 195, 771–776.
- Mena, I.F., Diaz, E., Rodriguez, J.J., Mohedano, A.F., 2016. CWPO of bisphenol A with iron catalysts supported on microporous carbons from grape seeds activation. Chem. Eng. J. 318, 153–160.
- Mohedano, A.F., Monsalvo, V.M., Bedia, J., Lopez, J., Rodriguez, J.J., 2014. Highly stable iron catalysts from sewage sludge for CWPO. J. Environ. Chem. Eng. 2, 2359–2364.
- Monsalvo, V.M., Lopez, J., Munoz, M., de Pedro, Z.M., Casas, J.A., Mohedano, A.F., Rodriguez, J.J., 2015. Application of Fenton-like oxidation as pre-treatment for carbamazepine biodegradation. Chem. Eng. J. 264, 856–862.
- Munoz, M., de Pedro, Z.M., Menendez, N., Casas, J.A., Rodriguez, J.J., 2013. A ferromagnetic γ-alumina-supported iron catalyst for CWPO. Application to chlorophenols. Appl. Catal. B Environ. 136-137, 218–224.
- Munoz, M., Dominguez, C.M., De Pedro, Z.M., Quintanilla, A., Casas, J.A., Rodriguez, J.J., 2015a. Ionic liquids breakdown by Fenton oxidation. Catal. Today 240, 16–21.
- Munoz, M., Domínguez, C.M., de Pedro, Z.M., Quintanilla, A., Casas, J.A., Rodriguez, J.J., 2016. Degradation of imidazolium-based ionic

liquids by catalytic wet peroxide oxidation with carbon and magnetic iron catalysts. J. Chem. Technol. Biotechnol. 91, 2882–2887.

- Munoz, M., Domínguez, C.M., De Pedro, Z.M., Quintanilla, A., Casas, J.A., Ventura, S.P.M., Coutinho, J.A.P., 2015b. Role of the chemical structure of ionic liquids in their ecotoxicity and reactivity towards Fenton oxidation. Sep. Purif. Technol. 150, 252–256.
- Neodo, S., Rosestolato, D., Ferro, S., De Battisti, A., 2012. On the electrolysis of dilute chloride solutions: Influence of the electrode material on Faradaic efficiency for active chlorine, chlorate and perchlorate. Electrochim. Acta 80, 282–291.
- Neumann, J., Pawlik, M., Bryniok, D., Thöming, J., Stolte, S., 2014. Biodegradation potential of cyano-based ionic liquid anions in a culture of *Cupriavidus spp.* and their in vitro enzymatic hydrolysis by nitrile hydratase. Environ. Sci. Pollut. Res. 21, 9495–9505.
- Neyens, E., Baeyens, J., 2003. A review of classic Fenton's peroxidation as an advanced oxidation technique. J. Hazard. Mater. 98, 33–50.
- Pieczyńska, A., Ofiarska, A., Borzyszkowska, A.F., Białk-Bielińska, A., Stepnowski, P., Stolte, S., Siedlecka, E.M., 2015. A comparative study of electrochemical degradation of imidazolium and pyridinium ionic liquids: A reaction pathway and ecotoxicity evaluation. Sep. Purif. Technol. 156, 522–534.
- Pignatello, J.J., Oliveros, E., MacKay, A., 2006. Advanced oxidation processes for organic contaminant destruction based on the Fenton reaction and related chemistry. Crit. Rev. Environ. Sci. Technol. 36, 1–84.
- Polo, A.M., Tobajas, M., Sanchis, S., Mohedano, A.F., Rodriguez, J.J., 2011. Comparison of experimental methods for determination of toxicity and biodegradability of xenobiotic compounds. Biodegradation 22, 751–761.
- Poza-Nogueira, V., Arellano, M., Rosales, E., Pazos, M., González-Romero, E., Sanromán, M.A., 2018. Heterogeneous electro-Fenton as plausible technology for the degradation of imidazolinium-based ionic liquids. Chemosphere 199, 68–75.
- Quijano, G., Couvert, A., Amrane, A., Darracq, G., Couriol, C., Le Cloirec, P., Paquin, L., Carrié, D., 2011. Toxicity and biodegradability of ionic liquids: New perspectives towards whole-cell biotechnological applications. Chem. Eng. J. 174, 27–32.
- Ranke, J., Mölter, K., Stock, F., Bottin-Weber, U., Poczobutt, J., Hoffmann, J., Ondruschka, B., Filser, J., Jastorff, B., 2004. Biological effects of imidazolium ionic liquids with varying chain lengths in acute *Vibrio fischeri* and *WST-1* cell viability assays. Ecotoxicol. Environ. Saf. 58, 396–404.
- Rey, A., Hungria, A.B., Duran-valle, C.J., Faraldos, M., Bahamonde, A., Casas, J.A., Rodriguez, J.J., 2016. On the optimization of activated

carbon-supported iron catalysts in catalytic wet peroxide oxidation process. Appl. Catal. B, Environ. 181, 249–259.

- Romero, A., Santos, A., Tojo, J., Rodriguez, A., 2008. Toxicity and biodegradability of imidazolium ionic liquids. J. Hazard. Mater. 151, 268–273.
- Santiago, A., Castillo, R., Guihéneuf, S., Le, R., 2016. Synthesis and toxicity evaluation of hydrophobic ionic liquids for volatile organic compounds biodegradation in a two-phase partitioning bioreactor. J. Hazard. Mater. 307, 221–230.
- Siedlecka, E.M., Fabiańska, A., Stolte, S., Nienstedt, A., Ossowski, T., Stepnowski, P., Thöming, J., 2013. Electrocatalytic oxidation of 1-butyl-3-methylimidazolium chloride: Effect of the electrode material. Int. J. Electrochem. Sci. 8, 5560–5574.
- Siedlecka, E.M., Gołebiowski, M., Kaczyński, Z., Czupryniak, J., Ossowski, T., Stepnowski, P., 2009. Degradation of ionic liquids by Fenton reaction; the effect of anions as counter and background ions. Appl. Catal. B Environ. 91, 573–579.
- Siedlecka, E.M., Mrozik, W., Kaczyński, Z., Stepnowski, P., 2008. Degradation of 1-butyl-3-methylimidazolium chloride ionic liquid in a Fenton-like system. J. Hazard. Mater. 154, 893–900.
- Siedlecka, E.M., Stolte, S., Golebiowski, M., Nienstedt, A., Stepnowski, P., Thöming, J., 2012. Advanced oxidation process for the removal of ionic liquids from water: The influence of functionalized side chains on the electrochemical degradability of imidazolium cations. Sep. Purif. Technol. 101, 26–33.
- Spasiano, D., Siciliano, A., Race, M., Marotta, R., Guida, M., Andreozzi, R., Pirozzi, F., 2016. Biodegradation, ecotoxicity and UV_{254}/H_2O_2 treatment of imidazole, 1-methyl-imidazole and N,N'-alkyl-imidazolium chlorides in water. Water Res. 106, 450–460.
- Stepnowski, P., Zaleska, A., 2005. Comparison of different advanced oxidation processes for the degradation of room temperature ionic liquids. J. Photochem. Photobiol. A Chem. 170, 45–50.
- Stolte, S., Abdulkarim, S., Arning, J., Blomeyer-Nienstedt, A.K., Bottin-Weber, U., Matzke, M., Ranke, J., Jastorff, B., Thoming, J., 2008. Primary biodegradation of ionic liquid cations, identification of degradation products of 1-methyl-3-octylimidazolium chloride and electrochemical wastewater treatment of poorly biodegradable compounds. Green Chem. 10, 214–224.
- Stolte, S., Steudte, S., Areitioaurtena, O., Pagano, F., Thöming, J., Stepnowski, P., Igartua, A., 2012. Ionic liquids as lubricants or lubrication additives: An ecotoxicity and biodegradability assessment. Chemosphere 89, 1135–1141.

- Thuy Pham, T.P., Cho, C.W., Yun, Y.S., 2010. Environmental fate and toxicity of ionic liquids: A review. Water Res. 44, 352–372.
- Vekariya, R.L., 2017. A review of ionic liquids: Applications towards catalytic organic transformations. J. Mol. Liq. 227, 44–60.
- Ventura, S.P.M., e Silva, F.A., Gonçalves, A.M.M., Pereira, J.L., Gonçalves, F., Coutinho, J.A.P., 2014. Ecotoxicity analysis of cholinium-based ionic liquids to *Vibrio fischeri* marine bacteria. Ecotoxicol. Environ. Saf. 102, 48–54.
- Ventura, S.P.M., Marques, C.S., Rosatella, A.A., Afonso, C.A.M., Gonçalves, F., Coutinho, J.A.P., 2012. Toxicity assessment of various

5.2

Stability of carbon-supported iron catalysts for catalytic wet peroxide oxidation of ionic liquids

Mena, I.F., Diaz, E., Moreno-Andrade, I., Rodriguez, J.J., Mohedano, A.F. 2018. Stability of carbon-supported iron catalysts for catalytic wet peroxide oxidation of ionic liquids. J. Environ. Chem. Eng. 6, 6444-6450

Stability of carbon-supported iron catalysts for catalytic wet peroxide oxidation of ionic liquids

Abstract

The stability of two carbon-supported Fe catalysts in the catalytic wet peroxide oxidation (CWPO) of 1-Butyl-3-methylimidazolium acetate (BmimAc) was examined. One catalyst (Fe/AS) was obtained by chemical activation of dried sewage sludge with iron chloride at a $FeCl_3$:sewage sludge mass ratio of 3 and the other (Fe/HTCS) by hydrothermal carbonization of the sludge in the presence of $FeCl_3$ at a mass ratio of also 3. Fe/AS catalyst exhibited a well-developed porosity, whereas Fe/HTCS one did not show porosity. The carbon content was high in both catalysts, with a total Fe content of 5.2 and 6.6 % (w/w) for Fe/AS and Fe/HTCS catalysts, respectively. An additional Fe catalyst prepared by incipient wetness impregnation on a commercial active carbon support (Fe/AC) was used for comparison with the previous two. All catalysts were active in experiments of H_2O_2 decomposition and long-term CWPO runs (0.133 kg_{Fe} h mol_{BmimAc}^{-1} at 80 ºC). Whereas Fe/AC catalyst lost activity largely due to Fe leaching (90 % of Fe_{Bulk}), Fe/AS and Fe/HTCS catalysts exhibited virtually no Fe leaching and hence fairly good stability. Fe/AS catalyst, which afforded complete removal of $Bmim^+$ and TOC conversion values around 30 %, proved the most efficient catalyst.

5.2 Stability of carbon-supported iron catalysts for catalytic wet peroxide oxidation of ionic liquids

5.2.1. Introduction

Ionic liquids (ILs) are salts formed by an organic cation and an organic or inorganic anion that possess a low vapor pressure and a melting point below 100 ºC (Jordan and Gathergood, 2015; Stolte and Neumann, 2011). Because of their relative high solubility in water, ILs can be released to an aqueous medium during synthetic processes or used as solvents in many catalytic, biocatalytic, chemical and electrochemical processes (Santiago et al., 2016; Ventura et al., 2012). The consideration of ILs as "green solvents" remains a subject of debate. Thus, ionic liquids exhibit a wide range of environmental toxicity depending mainly on their structural features and on the particular target biological system (Diaz et al., 2016). The imidazolium family of compounds is the most widely studied among ILs, which is unsurprising if one considers their excellent properties as solvents for a number of chemical processes (Vekariya, 2017). Imidazolium-based ILs have a low ecotoxicity (Liu et al., 2015; Thuy Pham et al., 2010) which, however, increases with increasing length of the alkyl chain; also, they possess a low biodegradability (Quijano et al., 2011; Romero et al., 2008; Stolte et al., 2008) that can be improved by lengthening the alkyl chain to more than 6 C atoms (Docherty et al., 2007; Stolte et al., 2008). Advanced oxidation processes (AOPs) have emerged as the best choice for removing poorly biodegradable compounds from wastewater under mild operating conditions (Lal and Garg, 2015). For example, imidazolium-based ILs can be efficiently removed by electrochemical oxidation (Garcia-Segura et al., 2016; Mena et al., 2018; Siedlecka et al., 2013), ultraviolet photolysis (Czerwicka et al., 2009; Spasiano et al., 2016) and Fenton oxidation (Gomez-Herrero et al., 2018; Munoz et al., 2015; Siedlecka et al., 2008). Catalytic wet peroxide oxidation (CWPO), which involves decomposing H_2O_2 into $HO^{\cdot}$ radical in the

presence of a supported Fe catalyst at an acid pH, has been successfully used for IL degradation (Munoz et al., 2016). The main advantage of this process is that Fe is immobilized and retained on a support, which dispenses with the need to remove the metal from wastewater (Bautista et al., 2011). Although CWPO reactions are usually conducted under mild conditions, some authors have found that raising the temperature improves mineralization (Inchaurrondo et al., 2012; Mena et al., 2016; Zazo et al., 2012). However, conventional catalysts lose activity during the reaction, largely through Fe leaching (Bautista et al., 2011; Mena et al., 2016; Ribeiro et al., 2015; Zazo et al., 2012). The need thus remains to obtain active and stable catalysts for CWPO under operating conditions.

Carbon-based materials have been used as sorbents in wastewater treatments (Dabrowski et al., 2005; Moreno-Castilla, 2004; Radovic et al., 1997) and also as catalyst supports (Diaz et al., 2015; Rey et al., 2009). The best choices for this purpose have a high carbon content in addition to well-developed porosity, which leads to a high surface area and facilitates metal adsorption and dispersion as a result (Angin, 2014; Rodriguez-Reinoso, 1998). However, carbon-supported Fe catalysts for CWPO are prone to Fe leaching through poor fixation of the metal onto the carbon surface (Bautista et al., 2011; Diaz et al., 2015). Also, some carbon materials impair H_2O_2 decomposition into hydroxyl radicals (Quintanilla et al., 2012). A variety of carbonaceous residues such as agricultural waste including olive and grape bagasse (Encinar et al., 1996), pomegranate seeds (Uçar and Karagöz, 2009) or grape seeds (Jimenez-Cordero et al., 2013; Mena et al., 2016); tire waste (Heras et al., 2014; Li et al., 2015); polyethylene (Baeza et al., 2015) and medical waste (Li et al., 2017) have been the targets of increasing efforts at their valorization over the last decade. For example, sewage sludge is

produced in very large amounts in wastewater treatment plants —as large as 85 g dry solids per population per day according to the International Water Assotiation (IWA). Spain produces an estimated 1.2 millions tonnes each year (Government of Spain, 2017). At present, sewage sludge is managed by composting, landfilling or incineration (Fytili and Zabaniotou, 2008; Singh and Agrawal, 2008), which poses so serious a problem that efficiently handling of this waste has become a priority action in various strategic plans focusing on recycling (e.g., Council Directive 91/271/EEC of 21 May 1991 concerning urban waste water treatment) or its banning from agriculture (e.g., Council Directive 86/278/EEC of 12 June 1986 on the protection of the environment, and in particular of the soil, when sewage sludge is used in agriculture). There remains, however, the need to find sustainable ways of valorizing sewage sludge, which can be converted into effective catalytic supports by pyrolysis, activation or hydrothermal carbonization (HTC). In a previous work, carbon-supported Fe catalysts were obtained through pyrolysis of sewage sludge with $FeCl_3 \cdot 6H_2O$ as precursor of the active phase, showing good results in CWPO of phenol, bromophenol and dimethoate in terms of mineralization rates and Fe leaching (< 1 %) (Mohedano et al., 2014). Moreover, a new method for preparing supported Fe catalysts based on chemical activation of dried sludge with $FeCl_3$ at 750 ºC in an N_2 atmosphere was developed, exhibing the catalyst a high mineralization rate (ca. 80 %) and low Fe leaching (2.5 %) in antipirine CWPO (Bedia et al., 2017). Unlike pyrolysis, HTC efficiently converts wet sewage sludge into a carbonaceous material by using less energy and minimizing CO_2 emissions (Libra et al., 2011). The exothermic reactions involved take place in an aqueous environment at a moderate temperature (180–350 ºC) at autogenous pressure (2–10 MPa) (Lu et al.,

2015; Wood et al., 2013). On the other hand, the carbonaceous materials obtained by HTC are characterized by a poor porosity development against that the obtained by pyrolysis or chemical activation processes (Kambo and Dutta, 2015; Wang et al., 2018). HTC allows sewage sludge to be converted into char for use as an energy source (solid fuel) and/or an activated carbon precursor potentially useful as a sorbent (Van Wesenbeeck et al., 2014; Zhai et al., 2017) or catalytic support, for example.

The main aim of this work is to examine the stability of two different Fe carbon catalysts prepared by activation with $FeCl_3$ and HTC in the presence of $FeCl_3$ from sewage sludge in the CWPO of the ionic liquid 1-Butyl-3-methylimidazolium acetate (BmimAc). Stability was assessed mainly in terms of Fe fixation in the carbonaceous support.

5.2.2. Materials and methods

Catalyst preparation and characterization

Aerobic granular sludge was obtained from a membrane bioreactor (MBR) of industrial cosmetic water located at Madrid (Spain). Before using, the sludge was washed with distilled water, dried at 105 ºC for 24 h, ground and sieved to a particle size of 0.10-0.25 mm (Bedia et al., 2017; Mohedano et al., 2014). Fe/AS catalyst was prepared from mixing $FeCl_3{\cdot}6H_2O$ with dried biosolid in a mass ratio of 3 (mg $FeCl_3$/mg biosolid) and dried in an oven at 60 ºC for 20 h. Following, the activation process consisted of a heating at 750 ºC for 2 h, under an N_2 atmosphere (30 mL N min^{-1}), in a Nabertherm Series R tubular furnace (ramping up 10 ºC min^{-1}). Finally, the catalyst was washed with 3 M HCl at 80 ºC for 1 h and then to neutral pH with distilled water in order to remove excess activating reagent and dried at 60 ºC.

The second catalyst (Fe/HTCS) was obtained by HTC of a mixture of $FeCl_3 \cdot 6H_2O$ salt and wet granular sludge in a mass ratio of 3 (mg $FeCl_3$/ mg dried sludge; sludge moisture content, 85 %) in a 250 mL stainless steel batch reactor with an inner Teflon lining. The HTC process was performed at 208 °C for 1 h, with heating at 10 ºC min^{-1}. Then, the material was washed with a 3 M HCl solution at 80 ºC to remove excess Fe.

A Fe/AC catalyst was prepared by incipient wetness impregnation from a $FeCl_3 \cdot 6H_2O$ solution followed by drying at room temperature for 2 h and standing at 60 ºC overnight before calcining at 200 ºC for 3 h by heating at 10 ºC min^{-1}. The activated carbon was supplied by Merck (BET surface area ≈ 950 m^2 g^{-1}, bulk density ≈ 0.5 g cm^{-3}).

The pore structure of the catalysts was established from N_2 adsorption–desorption isotherms at −196 ºC obtained with a MicromeriticsTristar 3020 automated volumetric gas adsorption instrument. Prior to the adsorption measurements, a sample of 0.15 g of each catalyst was degassed to vacuum in a glass container at 150 ºC for 7 h by using a Micromeritics VacPrep 061 degassing apparatus. The iron content of the catalysts was determined by total reflection X-ray fluorescence (TXRF) spectroscopy on an Extra-II Rich & Seifert spectrometer equipped with a Si–Li detector. The C, H, N and S contents of the catalysts were determined with a LECO CHNS-932 analyzer. Ash was quantified according to ASTM D1506-99 and the oxygen content calculated by difference from 100 %. Available Fe in the outer catalyst surface was determined by X-ray photoelectron spectroscopy (XPS) on a Physical Electronics 5700C Multitechnique instrument using MgKa radiation (1253.6 eV) and energy dispersive X-ray spectroscopy (EDAX).

CWPO tests

The activity of the three catalysts in H_2O_2 decomposition was assessed in a stirred batch reactor (400 mL) equipped with a magnetic stirrer (500 rpm) and temperature control. Tests were conducted at pH 3 at 80 ºC, using a catalyst mass equivalent to a concentration of 40 mg_{Fe} L^{-1} based on the Fe_{Bulk} content of each catalyst. CWPO long-term experiments (80 h on stream) were performed in a continuous stirred tank reactor (CSTR, 400 mL) fitted with an autosampler (Gilson FC 203B) to collect aliquots of reaction medium. All CWPO runs were conducted at atmospheric pressure in duplicate. IL and H_2O_2 solutions were pumped to the reactor at a 1 mL min^{-1} flow rate in order to feed an IL concentration of 1 mM and the stoichiometric H_2O_2 dose, the resulting space–time being 0.133 kg_{Fe} h mol_{BmimAc}^{-1}. The imidazolium concentration was determined with Varian Prostar 325 high performance liquid chromatography (HPLC) using UV–Vis detection at 218 nm, a Phenomenex Synergy 4 mm Polar-RP 80 A column (15 cm long, 4.6 mm i.d.) as stationary phase and a mixture of phosphate buffer and acetonitrile (95:5 % v/v) at a flow rate of 0.75 mL min^{-1} as mobile phase. Acetate anion (Ac), short chain organic acids (formic, malonic and oxalic) and anionic species (nitrite and nitrate) were quantified on a Dionex ICS-900 ion chromatograph with chemical suppression and furnished with a Dionex IonPac AS22 4 × 250 mm column, using a stream of 1.4 mM $NaHCO_3$/4.5 mM Na_2CO_3 at 1 mL min^{-1} as mobile phase. Total organic carbon (TOC) and total nitrogen (TN) were determined with a Shimadzu TOC-VCSH analyzer. Finally, H_2O_2 was determined with a Cary 60 UV/Vis spectrophotometer from Agilent Technologies that was operated at 410 nm (Eisenberg, 1943) to monitor the colorimetric titration leading to the formation of Ti(IV)–H_2O_2 complex. Iron leached from the catalyst to the liquid phase being

measured by the same apparatus at 510 nm with the *o*-phenanthroline method (E.B. Sandell, 1959).

5.2.3. Results and discussion

Catalyst characterization

Table 5.2.1 shows the main characteristics of the sewage sludge and the catalysts. As can be seen, Fe/AC catalyst exhibited a well-developed micropore structure with a fair contribution of mesopores. Fe/AS catalyst was essentially microporous and had a BET area similar to that of the catalyst prepared from commercial activated carbon as a result of $FeCl_3$ being used as activating agent (Bedia et al., 2017; Theydan and Ahmed, 2012). Finally, the catalyst obtained by HTC and activation with $FeCl_3$ barely developed BET area. The N_2 adsorption-desorption isotherms plots are presented in Figure 5.2.1. The Fe/HTCS isotherm corresponds to a non-porous material, whereas Fe/AC and Fe/AS isotherms are typical of high porosity materials.

Table 5.2.1. Characteristics of sewage sludge and Fe-carbon catalysts.

Characteristic	Sludge	Fe/AS	Fe/HTCS	Fe/AC
BET area ($m^2\ g^{-1}$)	< 2	836	5	839
Outer surface area ($m^2\ g^{-1}$)	< 2	148	3	184
Micropore volume ($cm^3\ g^{-1}$)	< 0.010	0.331	< 0.010	0.316
Mesopore volume ($cm^3\ g^{-1}$)	< 0.010	< 0.010	< 0.010	0.016
Fe_{Bulk} (w/w %)	–	5.2	6.6	5.4
Fe_{XPS} (w/w %)	–	5.3	–	6.2
Fe_{Bulk}/Fe_{XPS}	–	0.98	–	0.87
C (w/w %)	48.7	54.8	71.7	64.6
H (w/w %)	7.5	1.8	7.6	1.4
N (w/w %)	9.4	4.3	1.6	0.6
S (w/w %)	0.6	0.8	0.3	0.9
O* (w/w %)	10.8	12.5	12	12.8
Ash (w/w %)	23.0	25.8	6.8	19.7

* Oxygen content calculated by difference from 100 %.

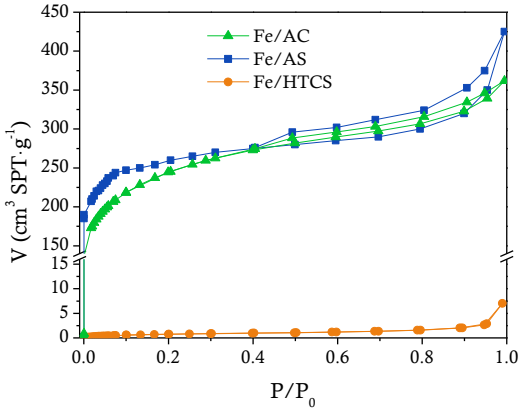

Figure 5.2.1. N_2 adsorption-desorption isotherms of the synthesized catalysts.

Table 5.2.1 also shows the bulk iron content of each catalyst determined by TXRF spectroscopy and its iron mass surface concentration as

obtained by XPS. The iron content ranged from 5.2 to 6.6 w/w % and was scarcely dependent on the preparation method used. It should be stressed that the Fe_{Bulk} values for Fe/AS and Fe/HTCS catalysts correspond to iron remaining in the catalysts after acid washing during preparation. The fact that the Fe_{XPS}/Fe_{Bulk} ratio was close to 1 in Fe/AS and Fe/AC catalysts is suggestive of uniform distribution of the metal phase. By exception, no Fe_{XPS} was detected in Fe/HTCS catalyst, possibly as a result of carboxyl groups formed by carbonization of the sludge being incorporated into the catalyst (Wood et al., 2013) and blocking access of Fe particles to the outer surface. Consequently, Fe particles in Fe/HTCS catalyst were less readily accessed and retained a greater total amount of Fe after the catalyst was washed with HCl. Fe/AC catalyst showed a moderate carbon content and contained around 20 % of ash. The carbon content of the catalyst prepared by $FeCl_3$ activation over dry biosolids was close to 55 % —and hence higher than that of the raw material as a result of the activation procedure— and ash content was also high (Al Bahri et al., 2012; Angin, 2014). Carbonizing dried sewage sludge by HTC in the presence of $FeCl_3$ provided a material with a high carbon content (> 70 %). As a result of the HTC treatment, considerably decreased the O/C ratio and its ash content was mainly associated with the incorporation of Fe.

Catalytic activity in H_2O_2 decomposition

The three catalysts were assessed for activity in H_2O_2 decomposition. This reaction is usually faster with Fe supported on carbon than on other materials. However, carbon-supported Fe catalysts are not necessarily more active in CWPO reactions. In fact, Fe particles can produce HO· radicals but a carbon surface facilitates consumption of active radicals to produce O_2 in parasitic reactions (Domínguez et al.,

2013; Munoz et al., 2016). As can be seen from Figure 5.2.2, H_2O_2 decomposition was faster with Fe/AS than with the other catalysts. Whereas Fe/AC catalyst allowed H_2O_2 to be completely removed within 20 min, more than 70 % of reactant remained in the medium after 30 min of reaction in the presence of Fe/HTCS catalyst.

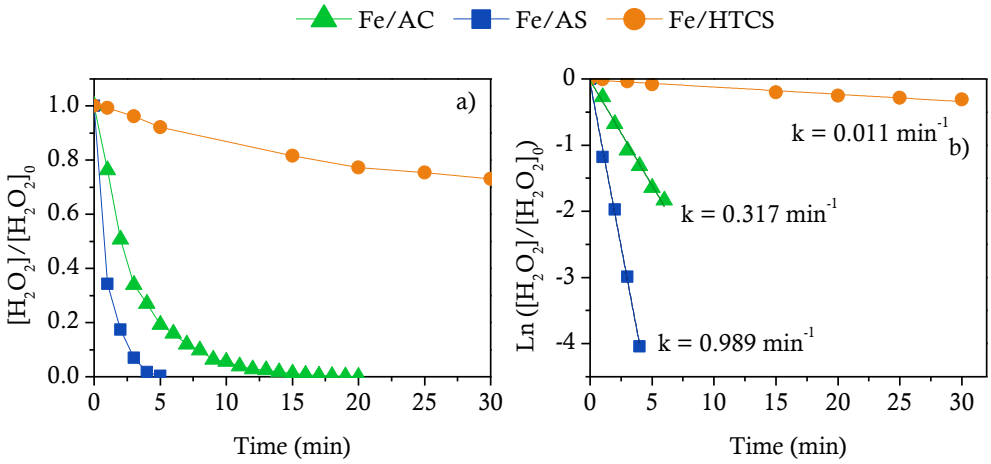

Figure 5.2.2. a) Time course of hydrogen peroxide decomposition with the Fe catalysts and b) pseudo first-order kinetics of the process ($[H_2O_2]_0$ = 27 mM, T = 80 ºC, pH_0 = 3).

Figure 5.2.2b illustrates the decomposition of H_2O_2 as fitted to a pseudo first-order rate equation describing the kinetics of the process with activated carbon (Mena et al., 2016; Rey et al., 2011) and the kinetic constants involved. Bedia et al. (Bedia et al., 2017) obtained a smaller kinetic constant (0.136 min^{-1}) with Fe/AS catalyst at 50 ºC and found raising the temperature to facilitate H_2O_2 decomposition. The differential performance of the catalysts may be related to their BET areas, which decreased in the same sequence as catalyst activity, namely: Fe/AS > Fe/CA >> Fe/HTCS. Also, the catalyst leading to the fastest H_2O_2 decomposition (Fe/AS) was that exhibiting the most

uniform Fe distribution (a near-unity Fe_{Bulk}/Fe_{XPS} ratio). Finally, Fe/HTCS was the least active catalyst, probably as a result of its outer surface containing no Fe.

Catalytic activity and stability

Figure 5.2.3 shows the time course of $Bmim^+$ and TOC conversion, H_2O_2 concentration and Fe leaching on stream with the three catalysts. As can be seen, all catalysts were active in the CWPO reaction but differed in activity and stability. Because of the characteristics of the support, in a first stage the pollutant may have been removed in part by effect of the adsorption capacity of the catalysts. Fe/AC catalyst exhibited high activity and ensured almost complete $Bmim^+$ removal within the first few hours of reaction; after 10 h, however, it gradually lost activity as reflected in its TOC conversion (mineralization ≈ 5 %). Also, H_2O_2 started to accumulate in the reactor after 20 h and reached a concentration of 5 mM (equivalent to 19 % of that fed) after 80 h, all with extensive leaching of metal phase (ca. 90 %) from the catalyst. Similar results were previously obtained with an Fe/AC catalyst prepared by incipient wetness impregnation in other CWPO reactions (Rey et al., 2009; Zazo et al., 2006), which suggests that Fe particles failed to strongly bind to the activated carbon surface.

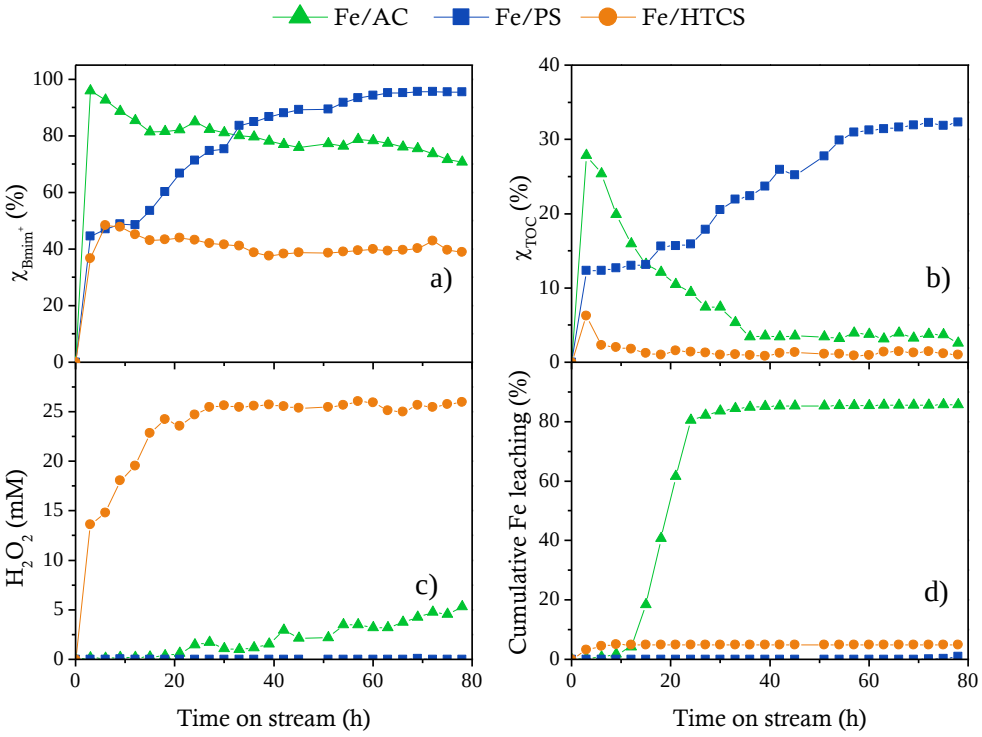

Figure 5.2.3. Long-term performance of the Fe catalysts: a) $Bmim^+$ conversion, b) TOC conversion, c) H_2O_2 concentration and d) cumulative Fe leaching in the CWPO of BmimAc ([BmimAc] = 1 mM, $[H_2O_2]$ = 27 mM, T = 80 °C, pH_0 = 3, τ = 0.133 kg_{Fe} h mol_{BmimAc}^{-1}).

$Bmim^+$ conversion with Fe/AS catalyst increased gradually during the first 50 h and then levelled off (Figure 5.2.3). The activity and stability of this catalyst also reflected in TOC conversion, which remained unchanged at a degree of mineralization of 30 % after 50 h time on stream. Total consumption of H_2O_2 and insubstantial Fe leaching (less than 1 %) to the space–time used helped increase stability. Finally, Fe/HTCS catalyst was highly stable —$Bmim^+$ conversion was constant over time— but markedly less active than the other two. With this Fe/HTCS catalyst, H_2O_2 was accumulated in the reactor from the

beginning, so, as reflected in a near-zero degree of mineralization, the oxidation reaction developed to a negligible extent. Although Fe leaching from the solid was less than 3 % —which could be a strong point for use as a catalyst— the Fe_{XPS} value suggests that Fe could not be readily accessed by the reactants.

Figure 5.2.4 shows the efficiency of the catalysts in terms of mg_{TOC} removed per mg_{H2O2} decomposed. As can be seen, Fe/AS catalyst exhibited the best performance, followed by Fe/HTCS one. The high Fe leaching from Fe/AC catalyst resulted in low pollutant mineralization and hence in also low efficiency (ca. 0.005 mg_{TOC} mg_{H2O2}^{-1}).

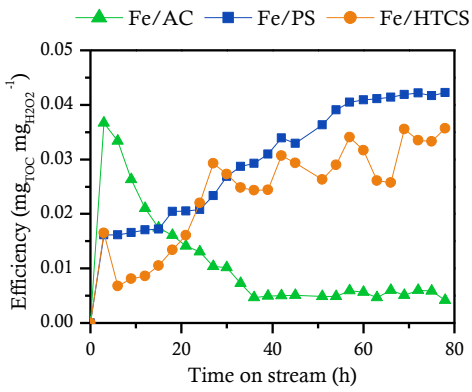

Figure 5.2.4. Long-term efficiency of the Fe catalysts in the CWPO of BmimAc ([BmimAc] = 1 mM, $[H_2O_2]$ = 27 mM, T = 80 ºC, pH_0 = 3, τ = 0.133 kg_{Fe} h mol_{BmimAc}^{-1}).

Some studies have focused on the degradation route of imidazolium-based ILs in AOPs. The hydroxyl radicals attack the imidazolium core or the alkyl side chain, giving place the formation of heteroaromatic and hydroxylated derivatives (Table 5.2.2, intermediates 1-6), some of them

with higher molecular weight than the initial $Bmim^+$ (Czerwicka et al., 2009; Garcia-Segura et al., 2016; Gomez-Herrero et al., 2018; Munoz et al., 2015; Siedlecka et al., 2013). After that, the radicals attack the imidazolium ring generating the open ring compounds (Table 5.2.2, intermediates 7 and 8). Finally, these compounds are degraded, given rise the generation of short-chain organic acids, nitrate, NO_x, H_2O and CO_2.

Table 5.2.2. Intermediates detected along the long-term CWPO of BmimAc.

Nº	Molecular structure	*m/z*
1	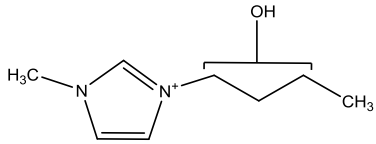	154
2	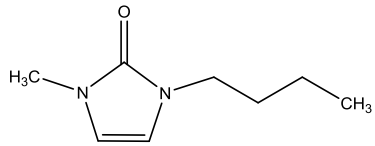	154
3	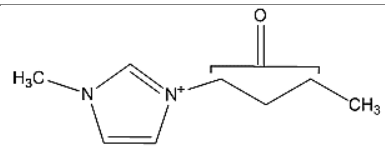	153
4	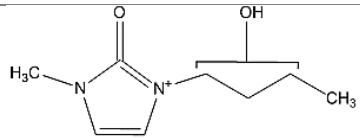	170
5	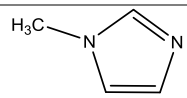	82
6	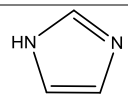	68
7	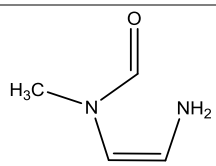	102
8	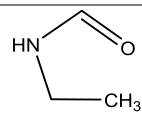	73

In order to learn more about the potential of each catalyst for oxidizing BmimAc, the formation of short-chain organic acids (Figure 5.2.5) has been studied, being acetic, formic and oxalic acids detected in all reaction media. These compounds were previously deemed refractory to oxidation (Monsalvo et al., 2015) and found to account for a fraction of residual TOC equivalent to 5–9 % of the initial TOC concentration. The high concentration of acetate in the reaction medium mainly corresponded to the initial acetate concentration (1 mM). Due to the refractory behavior of this compound in CWPO reactions and its formation as reaction product (Munoz et al., 2015), acetate concentration increased by 20 % for the reactions with Fe/AS and Fe/HTCS catalysts, whereas for Fe/AC catalyst the increment was around 9.6 %. The formic acid concentration remained unchanged during the CWPO reaction with Fe/AC and Fe/HTCS catalysts, but increased with time on stream with the Fe/AS one. Finally, the concentration of oxalic acid was always below 0.04 mM. In CWPO process, the presence of oxalic acid seems to play a significant role in the Fe leaching from carbon and silica catalysts prepared by impregnation methods (Xiang et al., 2009; Zazo et al., 2006). Previous studies revealed a relationship between Fe leaching and the concentration of oxalic acid in the reaction medium (Rey et al., 2009; Zazo et al., 2006). Therefore, Fe leaching can be related to the initial appearance of the oxalic acid in the presence of catalyst Fe/AC. On the other hand, the formation of a low oxalic acid concentration with Fe/AS and Fe/HTCS catalysts (< 0.015 mM) resulted in increased stability in both. No change in TN content or nitrate formation was observed in any case; therefore, the imidazolium ring was not completely degraded under the experimental conditions used.

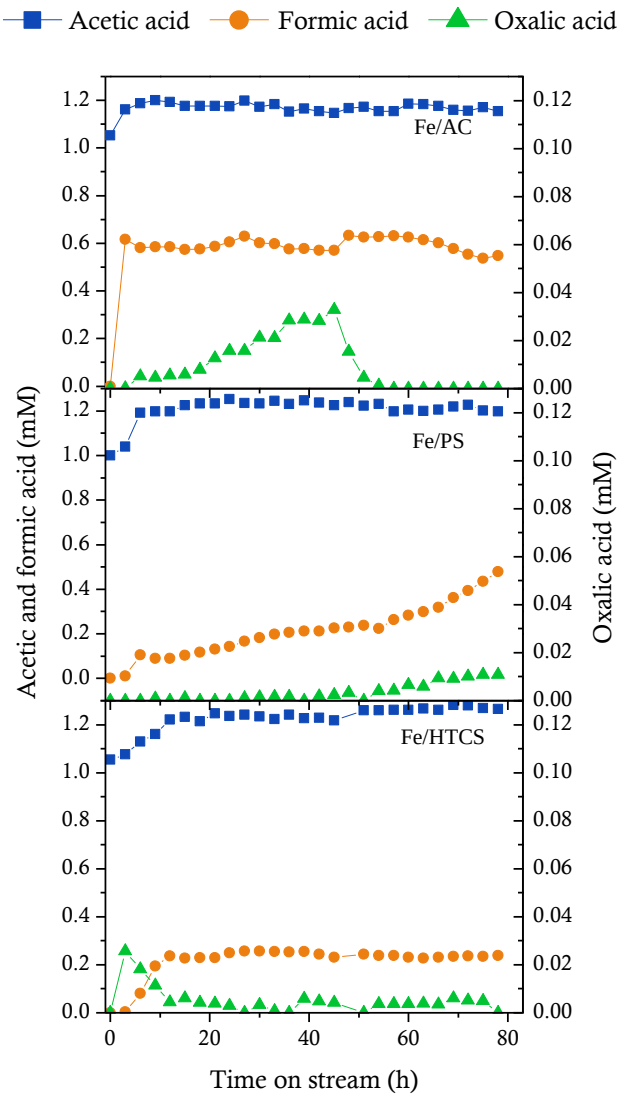

Figure 5.2.5. Long-term variation of the concentrations of short-chain organic acids in the CWPO of BmimAc with the different Fe catalysts ([BmimAc] = 1 mM, $[H_2O_2]$ = 27 mM, T = 80 ºC, pH_0 = 3, τ = 0.133 kg_{Fe} h mol_{BmimAc}^{-1}).

5.2.4. Conclusions

Highly active and stable iron on activated carbon catalysts, prepared by chemical activation of dried sewage sludge with $FeCl_3$ using a 1:3 mass ratio (Fe/AS), has been used for CWPO of BmimAc in long term experiments. Fe/AS catalyst developed high BET area and a homogeneous Fe distribution. Using a space-time of 0.133 kg_{Fe} h mol_{BmimAc}^{-1} at 80ºC, a $Bmim^+$ conversion up to 80 % was obtained, and a high stability along 30 h reaction time. Iron leaching was almost negligible because of the low concentration of oxalic acid in the reaction medium. The catalyst prepared by hydrothermal carbonization of sewage sludge with $FeCl_3$ showed high stability for more than 60 h, but very low activity (40 % of $Bmim^+$ removal), being the H_2O_2 accumulated in the medium. In conclusion, $FeCl_3$ chemical activation of dried sewage sludge can be used to prepare inexpensive and efficient catalysts for CWPO.

5.2.5. References

- Al Bahri, M., Calvo, L., Gilarranz, M.A., Rodriguez, J.J., 2012. Activated carbon from grape seeds upon chemical activation with phosphoric acid: Application to the adsorption of diuron from water. Chem. Eng. J. 203, 348–356.
- Angin, D., 2014. Production and characterization of activated carbon from sour cherry stones by zinc chloride. Fuel 115, 804–811.
- Baeza, J.A., Alonso-Morales, N., Calvo, L., Heras, F., Rodriguez, J.J., Gilarranz, M.A., 2015. Hydrodechlorination activity of catalysts based on nitrogen-doped carbons from low-density polyethylene. Carbon N. Y. 87, 444–452.
- Bautista, P., Mohedano, A.F., Casas, J.A., Zazo, J.A., Rodriguez, J.J., 2011. Highly stable Fe/γ-Al_2O_3 catalyst for catalytic wet peroxide oxidation. J. Chem. Technol. Biotechnol. 86, 497–504.
- Bedia, J., Monsalvo, V.M., Rodriguez, J.J., Mohedano, A.F., 2017. Iron catalysts by chemical activation of sewage sludge with $FeCl_3$ for CWPO. Chem. Eng. J. 318, 224–230.
- Czerwicka, M., Stolte, S., Müller, A., Siedlecka, E.M., Gołebiowski, M., Kumirska, J., Stepnowski, P., 2009. Identification of ionic liquid breakdown products in an advanced oxidation system. J. Hazard. Mater. 171, 478–483.
- Dabrowski, A., Podkoscielny, P., Hubicki, Z., Barczak, M., 2005. Adsorption of phenolic compounds by activated carbon - A critical review. Chemosphere 58, 1049–1070.
- Diaz, E., Mohedano, A.F., Casas, J.A., Calvo, L., Gilarranz, M.A., Rodriguez, J.J., 2015. Deactivation of a Pd/AC catalyst in the hydrodechlorination of chlorinated herbicides. Catal. Today 241, 86–91.
- Diaz, E., Monsalvo, V., Palomar, J., Mohedano, A.F., 2016. Ionic Liquids: Bacterial Degradation in Wastewater Treatment Plants, in: Encyclopedia of Inorganic and Bioinorganic Chemistry. John Wiley & Sons, Ltd.
- Docherty, K.M., Dixon, J.K., Kulpa, C.F., 2007. Biodegradability of imidazolium and pyridinium ionic liquids by an activated sludge microbial community. Biodegradation 18, 481–493.
- Domínguez, C.M., Ocón, P., Quintanilla, A., Casas, J.A., Rodriguez, J.J., 2013. Highly efficient application of activated carbon as catalyst for wet peroxide oxidation. "Applied Catal. B, Environ. 140-141, 663–670.
- E.B. Sandell, 1959. Determination of Traces of Metals, third ed. ed. Interscience Pubs, New York, NY.
- Eisenberg, G., 1943. Colorimetric Determination of Hydrogen Peroxide. nd. Eng. Chem. Anal. Ed. 15, 327–328.

- Encinar, J.M., Beltrán, F.J., Bernalte, A., Ramiro, A., González, J.F., 1996. Pyrolysis of two agricultural residues: Olive and grape bagasse. Influence of particle size and temperature. Biomass and Bioenergy 11, 397–409.
- Fytili, D., Zabaniotou, A., 2008. Utilization of sewage sludge in EU application of old and new methods-A review. Renew. Sustain. Energy Rev. 12, 116–140.
- Garcia-Segura, S., Lima, Á.S., Cavalcanti, E.B., Brillas, E., 2016. Anodic oxidation, electro-Fenton and photoelectro-Fenton degradations of pyridinium- and imidazolium-based ionic liquids in waters using a BDD/air-diffusion cell. Electrochim. Acta 198, 268–279.
- Gomez-Herrero, E., Tobajas, M., Polo, A., Rodriguez, J.J., Mohedano, A.F., 2018. Removal of imidazolium- and pyridinium-based ionic liquids by Fenton oxidation. Environ. Sci. Pollut. Res. 25, 34930–34937.
- Heras, F., Jimenez-Cordero, D., Gilarranz, M.A., Alonso-Morales, N., Rodriguez, J.J., 2014. Activation of waste tire char by cyclic liquid-phase oxidation. Fuel Process. Technol. 127, 157–162.
- Inchaurrondo, N., Cechini, J., Font, J., Haure, P., 2012. Strategies for enhanced CWPO of phenol solutions. Appl. Catal. B Environ. 111-112, 641–648.
- Jimenez-Cordero, D., Heras, F., Alonso-Morales, N., Gilarranz, M.A., Rodriguez, J.J., 2013. Porous structure and morphology of granular chars from flash and conventional pyrolysis of grape seeds. Biomass and Bioenergy 54, 123–132.
- Jordan, A., Gathergood, N., 2015. Biodegradation of ionic liquids - a critical review. Chem. Soc. Rev. 44, 8200–8237.
- Kambo, H.S., Dutta, A., 2015. A comparative review of biochar and hydrochar in terms of production, physico-chemical properties and applications. Renew. Sustain. Energy Rev. 45, 359–378.
- Lal, K., Garg, A., 2015. Catalytic wet oxidation of phenol under mild operating conditions: development of reaction pathway and sludge characterization. Clean Technol. Environ. Policy 17, 199–210.
- Li, G., Shen, B., Lu, F., 2015. The mechanism of sulfur component in pyrolyzed char from waste tire on the elemental mercury removal. Chem. Eng. J. 273, 446–454.
- Li, G., Wang, S., Wang, F., Wu, Q., Tang, Y., Shen, B., 2017. Role of inherent active constituents on mercury adsorption capacity of chars from four solid wastes. Chem. Eng. J. 307, 544–552.
- Libra, J.A., Ro, K.S., Kammann, C., Funke, A., Berge, N.D., Neubauer, Y., Titirici, M.-M., Fühner, C., Bens, O., Kern, J., Emmerich, K.-H., 2011. Hydrothermal carbonization of biomass residuals: a comparative review of

the chemistry, processes and applications of wet and dry pyrolysis. Biofuels 2, 71–106.

- Liu, H., Zhang, X., Chen, C., Du, S., Dong, Y., 2015. Effects of imidazolium chloride ionic liquids and their toxicity to *Scenedesmus obliquus*. Ecotoxicol. Environ. Saf. 122, 83–90.
- Lu, Y., Levine, R.B., Savage, P.E., 2015. Fatty acids for nutraceuticals and biofuels from hydrothermal carbonization of microalgae. Ind. Eng. Chem. Res. 54, 4066–4071.
- Mena, I.F., Cotillas, S., Díaz, E., Sáez, C., Rodríguez, J.J., Cañizares, P., Mohedano, Á.F., Rodrigo, M.A., 2018. Electrolysis with diamond anodes: Eventually, there are refractory species! Chemosphere 195, 771–776.
- Mena, I.F., Diaz, E., Rodriguez, J.J., Mohedano, A.F., 2016. CWPO of bisphenol A with iron catalysts supported on microporous carbons from grape seeds activation. Chem. Eng. J. 318, 153–160.
- Mohedano, A.F., Monsalvo, V.M., Bedia, J., Lopez, J., Rodriguez, J.J., 2014. Highly stable iron catalysts from sewage sludge for CWPO. J. Environ. Chem. Eng. 2, 2359–2364.
- Monsalvo, V.M., Lopez, J., Munoz, M., de Pedro, Z.M., Casas, J.A., Mohedano, A.F., Rodriguez, J.J., 2015. Application of Fenton-like oxidation as pre-treatment for carbamazepine biodegradation. Chem. Eng. J. 264, 856–862.
- Moreno-Castilla, C., 2004. Adsorption of organic molecules from aqueous solutions on carbon materials. Carbon N. Y. 42, 83–94.
- Munoz, M., Dominguez, C.M., De Pedro, Z.M., Quintanilla, A., Casas, J.A., Rodriguez, J.J., 2015. Ionic liquids breakdown by Fenton oxidation. Catal. Today 240, 16–21.
- Munoz, M., Domínguez, C.M., de Pedro, Z.M., Quintanilla, A., Casas, J.A., Rodriguez, J.J., 2016. Degradation of imidazolium-based ionic liquids by catalytic wet peroxide oxidation with carbon and magnetic iron catalysts. J. Chem. Technol. Biotechnol. 91, 2882–2887.
- Quijano, G., Couvert, A., Amrane, A., Darracq, G., Couriol, C., Le Cloirec, P., Paquin, L., Carrié, D., 2011. Toxicity and biodegradability of ionic liquids: New perspectives towards whole-cell biotechnological applications. Chem. Eng. J. 174, 27–32.
- Quintanilla, A., García-Rodríguez, S., Domínguez, C.M., Blasco, S., Casas, J.A., Rodriguez, J.J., 2012. Supported gold nanoparticle catalysts for wet peroxide oxidation. Appl. Catal. B Environ. 111-112, 81–89.
- Radovic, L.R., Silva, I.F., Ume, J.I., Menéndez, J.A., Leon y Leon, C.A., Scaroni, A.W., 1997. An experimental and theoretical study of the adsorption of aromatics possessing electron-withdrawing and electron-

donating functional groups by chemically modified activated carbons. Carbon N. Y. 35, 1339–1348.

- Rey, A., Faraldos, M., Casas, J.A., Zazo, J.A., Bahamonde, A., Rodriguez, J.J., 2009. Catalytic wet peroxide oxidation of phenol over Fe/AC catalysts : Influence of iron precursor and activated carbon surface. Appl. Catal. B Environ. 86, 69–77.
- Rey, A., Zazo, J.A., Casas, J.A., Bahamonde, A., Rodriguez, J.J., 2011. Influence of the structural and surface characteristics of activated carbon on the catalytic decomposition of hydrogen peroxide. Appl. Catal. A Gen. 402, 146–155.
- Ribeiro, R.S., Silva, A.M.T., Pastrana-Martinez, L.M., Figueiredo, J.L., Faria, J.L., Gomes, H.T., 2015. Graphene-based materials for the catalytic wet peroxide oxidation of highly concentrated 4-nitrophenol solutions. Catal. Today 249, 204–212.
- Rodriguez-Reinoso, F., 1998. The role of carbon materials in heterogeneous catalysis. Carbon N. Y. 36, 159–175.
- Romero, A., Santos, A., Tojo, J., Rodriguez, A., 2008. Toxicity and biodegradability of imidazolium ionic liquids. J. Hazard. Mater. 151, 268–273.
- Santiago, A., Castillo, R., Guihéneuf, S., Le, R., 2016. Synthesis and toxicity evaluation of hydrophobic ionic liquids for volatile organic compounds biodegradation in a two-phase partitioning bioreactor. J. Hazard. Mater. 307, 221–230.
- Siedlecka, E.M., Fabiańska, A., Stolte, S., Nienstedt, A., Ossowski, T., Stepnowski, P., Thöming, J., 2013. Electrocatalytic oxidation of 1-butyl-3-methylimidazolium chloride: Effect of the electrode material. Int. J. Electrochem. Sci. 8, 5560–5574.
- Siedlecka, E.M., Mrozik, W., Kaczyński, Z., Stepnowski, P., 2008. Degradation of 1-butyl-3-methylimidazolium chloride ionic liquid in a Fenton-like system. J. Hazard. Mater. 154, 893–900.
- Singh, R.P., Agrawal, M., 2008. Potential benefits and risks of land application of sewage sludge. Waste Manag. 28, 347–358.
- Spasiano, D., Siciliano, A., Race, M., Marotta, R., Guida, M., Andreozzi, R., Pirozzi, F., 2016. Biodegradation, ecotoxicity and UV_{254}/H_2O_2 treatment of imidazole, 1-methyl-imidazole and N,N'-alkyl-imidazolium chlorides in water. Water Res. 106, 450–460.
- Stolte, S., Abdulkarim, S., Arning, J., Blomeyer-Nienstedt, A.K., Bottin-Weber, U., Matzke, M., Ranke, J., Jastorff, B., Thoming, J., 2008. Primary biodegradation of ionic liquid cations, identification of degradation products of 1-methyl-3-octylimidazolium chloride and electrochemical

wastewater treatment of poorly biodegradable compounds. Green Chem. 10, 214–224.

- Stolte, S., Neumann, J., 2011. Ion chromatographic determination of structurally varied ionic liquid cations and anions - A reliable analytical methodology applicable to technical and natural matrices. Anal. methods 3, 919–926.
- Theydan, S.K., Ahmed, M.J., 2012. Adsorption of methylene blue onto biomass-based activated carbon by $FeCl_3$ activation: Equilibrium, kinetics, and thermodynamic studies. J. Anal. Appl. Pyrolysis 97, 116–122.
- Thuy Pham, T.P., Cho, C.W., Yun, Y.S., 2010. Environmental fate and toxicity of ionic liquids: A review. Water Res. 44, 352–372.
- Uçar, S., Karagöz, S., 2009. The slow pyrolysis of pomegranate seeds: The effect of temperature on the product yields and bio-oil properties. J. Anal. Appl. Pyrolysis 84, 151–156.
- Van Wesenbeeck, S., Prins, W., Ronsse, F., Antal, M.J., 2014. Sewage sludge carbonization for biochar applications. Fate of heavy metals. Energy and Fuels 28, 5318–5326.
- Vekariya, R.L., 2017. A review of ionic liquids: Applications towards catalytic organic transformations. J. Mol. Liq. 227, 44–60.
- Ventura, S.P.M., Marques, C.S., Rosatella, A.A., Afonso, C.A.M., Gonçalves, F., Coutinho, J.A.P., 2012. Toxicity assessment of various ionic liquid families towards *Vibrio fischeri* marine bacteria. Ecotoxicol. Environ. Saf. 76, 162–168.
- Wang, T., Zhai, Y., Zhu, Y., Li, C., Zeng, G., 2018. A review of the hydrothermal carbonization of biomass waste for hydrochar formation : Process conditions, fundamentals, and physicochemical properties. Renew. Sustain. Energy Rev. 90, 223–247.
- Wood, B.M., Jader, L.R., Schendel, F.J., Hahn, N.J., Valentas, K.J., Mcnamara, P.J., Novak, P.M., Heilmann, S.M., 2013. Industrial symbiosis: Corn ethanol fermentation, hydrothermal carbonization, and anaerobic digestion. Biotechnol. Bioeng. 110, 2624–2632.
- Xiang, L., Royer, S., Zhang, H., Tatibouët, J.M., Barrault, J., Valange, S., 2009. Properties of iron-based mesoporous silica for the CWPO of phenol: A comparison between impregnation and co-condensation routes. J. Hazard. Mater. 172, 1175–1184.
- Zazo, J.A., Bedia, J., Fierro, C.M., Pliego, G., Casas, J.A., Rodriguez, J.J., 2012. Highly stable Fe on activated carbon catalysts for CWPO upon $FeCl_3$ activation of lignin from black liquors. Catal. Today 187, 115–121.
- Zazo, J.A., Casas, J.A., Mohedano, A.F., Rodriguez, J.J., 2006. Catalytic wet peroxide oxidation of phenol with a Fe/active carbon catalyst. Appl. Catal. B Environ. 65, 261–268.

5.2 Stability of carbon-supported iron catalysts for catalytic wet peroxide oxidation of ionic liquids

- Zhai, Y., Peng, C., Xu, B., Wang, T., Li, C., Zeng, G., Zhu, Y., 2017. Hydrothermal carbonisation of sewage sludge for char production with different waste biomass: Effects of reaction temperature and energy recycling. Energy 127, 167–174.

6

Electrotreatments for the removal of imidazolium- based ionic liquids in aqueous phase

6.1

Influence of the supporting electrolyte on the removal of ionic liquids by electrolysis with diamond anodes

Mena, I.F., Cotillas, S., Diaz, E., Sáez, C., Mohedano, A.F, Rodrigo, M.A. 2018. Influence of the supporting electrolyte on the removal of ionic liquids by electrolysis with diamond anodes. Cat. Tod. 313, 203–210

Influence of the supporting electrolyte on the removal of ionic liquids by electrolysis with diamond anodes

Abstract

In this work, it is studied the electrolysis with diamond anodes of three different ionic liquids (ILs): 1-butyl-3-methylimidazolium chloride (BmimCl), 1-hexyl-3-methylimidazolium chloride (HmimCl) and 1-decyl-3-methylimidazolium chloride (DmimCl), which differ only in the length of the aliphatic carbon chain attached to the imidazolium group. In addition, the effect of the presence of sulfate in the electrolyte is also evaluated. Results confirmed that this type of ILs can be completely transformed into carbon dioxide, nitrates, ammonium (the imidazolium cation) and perchlorate and chloramines (the chloride anion) during the electrolysis of the synthetic waste containing sulfate. The electrolysis of wastes without sulfate anions leads to a much less efficient process, with the same final products in the case of the BmimCl and HmimCl ILs and with the formation of a polymer as the main final product in the case of the DmimCl. These results are of a paramount significance from a mechanistic point of view since, because of the high conductivity of the ILs, there is not a necessity of salt addition and they inform about the pure removal of these compounds by electrolysis with BDD, pointing out the important influence of peroxodisulfate on the electrolysis with diamond of organic wastes.

6.1 Influence of the supporting electrolyte on the removal of ionic liquids by electrolysis with diamond anodes

6.1.1. Introduction

Ionic liquids (ILs) are salts that exhibit high thermal stability and low melting point (Yue et al., 2011). They can be used as substitutes of conventional organic solvents (Welton, 1999) and they are more environmentally-friendly species. For this reason, they are commonly known as "green" solvents (Plechkova and Seddon, 2007). In the recent years, their use has been studied for many applications, such as the removal of carbon dioxide by absorption (Ziobrowski and Rotkegel, 2017), the extraction of dyes and emerging contaminants (Li et al., 2007; Yao et al., 2011), the separation of hydrocarbons (Meindersma et al., 2006), the removal of chromium (Goyal et al., 2011) or the photodegradation of organochlorine compounds (Subramanian et al., 2007).

Despite of the large number of potential applications, recently, ILs have been identified as persistent pollutants, because of their stability towards biological degradation (Liwarska-Bizukojc and Gendaszewska, 2013) typically associated to their complex structure (cations typically consists of derivatives of imidazolium, pyridinium or phosphonium rings). Furthermore, several authors have proved the toxicity of these compounds, as well as the environmental hazards that they may produce (Amde et al., 2015; Costa et al., 2015; Cvjetko Bubalo et al., 2014; Perales et al., 2016). For this reason, in order to promote their applications, it is necessary to develop efficient processes that allow the removal of ILs from wasted industrial effluents.

Advanced Oxidation Processes (AOPs) can be considered as suitable technologies for the treatment of wastewater polluted with ILs. AOPs are based on the production of large amounts of hydroxyl radicals by different technologies, which significantly contribute to the degradation

of the pollutants present in the effluents (Moreira et al., 2017; Pera Tituset al., 2004). Technologies based on ozone or Fenton reagent have been the most studied AOPs for many decades (Pignatello et al., 2006, Ternes et al., 2003; Esplugas et al., 2007). However, from the nineties of the last century, electrolytic technologies have emerged as very promising alternatives (Comninellis, 1994; Comninellis and Nerini 1995; Martinez-Huitle et al., 2015). These processes produce hydroxyl radicals from electrolysis of water on the anode surface (Eq. (1)) (Cañizares et al., 2007; Cañizares et al., 2009b; Sirés et al., 2014), being the choice of asuitable electrode material a key to obtain high efficiencies (Comninellis, 1994 ; Panizza and Cerisola, 2004; Siedlecka et al., 2013; Steter et al., 2016; Urtiaga et al. 2014).

$$H_2O \rightarrow HO^{\cdot} + H^{+} + e^{-} \quad (1)$$

One of the electrodes that has awakened great interest in the recent years is boron doped diamond (BDD) (Fryda et al., 1999; Kraft et al., 2003). This material has a large electrochemical window and, hence, it allows to generate large amounts of free hydroxyl radicals (Fierro, 2010; Alfaro et al., 2006). For this reason, it has been evaluated in the oxidation of hundreds of pollutants including ILs (Brillas and Martinez-Huitle, 2011; Brillas and Martinez-Huitle, 2015; Feng et al., 2013; Martinez-Huitle and Brillas, 2009; Martinez-Huitle et al., 2015; Rodrigo et al., 2014, Sirés et al., 2014;). In this context, Fabianska et al. (2012) reported the electrolysis of imidazolium-based ionic liquids with diamond electrodes, evaluating the influence of the ionic liquid anion in different media (sulfate, chloride and bromide) by cyclic voltammetries and galvanostatic electrolyses with and without membrane. They concluded that hydroxyl radical is the main oxidant for the removal of the different ionic liquids studied and, the nature of

the supporting electrolyte significantly influences the IL removal. However, the electrogenerated peroxodisulfate does not play a key role on the electrolysis process in this work. Later, Pieczynska et al. (2015) assessed the removal of imidazolium and pyridinium ionic liquids, studying the influence of the pH and temperature. Alkaline pHs showed a decrease in the process efficiency whereas higher temperatures slightly increase the degradation of ILs. Likewise, the removal of pyridinium salts was more efficient in comparison with the imidazolium ILs depletion. They informed that $HO^{\cdot}$ and $O_2^{\cdot -}$ were the main oxidants responsible for the removal of ILs. Finally, more recently, García-Segura et al. (2016) have described the degradation of pyridinium- and imidazolium-based ionic liquids in sulfate media by anodic oxidation, electro-Fenton and photoelectro-Fenton using BDD anodes. They concluded that photoelectro-Fenton was the most efficient technology for the removal of those ILs and proposed the potential formation of hydroxyl radicals as the main mechanism for the removal of pollutants. The production of ozone and peroxodisulfate was also described but they not seemed to be the primary responsible of the degradation.

Opposite to those results, other works focused on the degradation of species different of ILs indicate that peroxocompounds formed during the electrolysis with BDD may behave as the most important species to explain the mineralization processes (Cañizares et al., 2009a; Lanet al., 2017; Rubí-Juárez et al., 2016). Hence, there exists a real necessity to clarify the specific contribution of hydroxyl radicals and/or other electrogenerated oxidants on the removal of ILs. With this background, the main aim of this work is to shed light about the real mechanisms of electrolysis with diamond anodes for the removal of ILs. To do this, three different ILs were selected: they have the same anion (Cl^-) and

different cations with an imidazolium group derivative: $Bmim^+$ (1-Butyl-3-methlyimidazolium), $Hmim^+$ (1-Hexyl-3-methylimidazolium) and $Dmim^+$ (1-Decyl-3-methylimidazolium). Solutions polluted with these compounds were electrolyzed in electrolytes with absence and presence of sulfate anions, in order to evaluate the contribution of hydroxyl radicals and electrogenerated peroxodisulfate (and related derivative species, such as radical sulfate) during the degradation of the ILs.

6.1.2. Materials and methods

Chemicals

Analytical grade BmimCl (1-Buthyl-3-methlyimidazolium chloride), HmimCl (1-Hexyl-3-methylimidazolium chloride), DmimCl (1-Decyl-3- methylimidazolium chloride) and sulfuric acid were used as received. Double deionized water (Millipore Milli-Q system, resistivity: 18.2 MΩcm at 25 °C) was used to prepare all solutions.

Analytical techniques

The concentration of ILs was measured by chromatography using an Agilent 1100 series chromatograph equipped with a UV detector and a Synergy 4 mm Polar-RP 80 A column. For the determination of $Bmim^+$ and $Hmim^+$, the mobile phase consisted of 95:5 v/v phosphate buffer/acetonitrile (flow rate: 0.75 cm^3 min^{-1}). In the case of $Dmim^+$, the percentage of acetonitrile was increased to 40%. The DAD detection wavelength was 218 nm, the temperature was kept at 35 °C and the injection volume was 20 μL.

Total Organic Carbon (TOC) was monitored using a Multi N/C 3100 Analytik Jena analyzer. Inorganic ions were measured by ion

chromatography using a Metrohm 930 Compact IC Flex coupled to a conductivity detector. A Metrosep A Supp 7 column was used to determine the anions and a Metrosep A Supp 4 column was used to analyze the cations. The mobile phase consisted of 85:15 v/v 3.6 mM Na_2CO_3/acetone solution for the determination of anions (flow rate: 0.80 cm^3 min^{-1}) and 1.7 mM HNO_3 and 1.7 mM 2,6-pyridinedicarboxylic acid solution for the determination of cations (flowrate: 0.90 cm^3 min^{-1}). The temperature of the oven was 45 and 30 °C for the determination of anions and cations, respectively. The volume injection was 20 µL.

The molecular weight of the polymer formed was measured by Gel Permeation Chromatography (GPC) using a Viscotek chromatograph equipped with a Styragel HR2 column and a Styragel HR0.5 column. The system was operated at 35 °C with a flowrate of 1 cm^3 min^{-1}. THF was used as eluent and calibration curves were obtained with polyethylene glycol standards (Waters).

Electrochemical cell

Electrolyses were carried out in a single compartment electrochemical flow cell operating in recirculation mode (50 dm^3 h^{-1}). Boron doped diamond (BDD) (WaterDiam, Switzerland) was used as anode and cathode. The electrodes were circular with a geometric area of 78 cm^2, boron concentration of 500 mg dm^{-3}, a thickness of 2.72 µm, sp^3/sp^2 ratio of 220 and p-Si as support. The electrode gap between anode and cathode was 3 mm. The electric current was provided by a Delta Electronika ES030-10 power supply (0–30 V, 0–10 A). The temperature was maintained at 25 °C using a thermostatized bath.

Synthetic wastewater consisted of a solution (1.0 dm^3) containing 1 mM of ionic liquid. For the study of the influence of the supporting electrolyte, 3000 mg dm^{-3} of sulfuric acid were added to synthetic wastewater. The initial conductivity of wastewater without sulfuric acid was within the range 103–137 μS cm^{-1} whereas values around 8 mS cm^{-1} were obtained when sulfate ions were added to the solution.

6.1.3. Results and discussion

Figure 6.1.1 shows changes undergone by the concentration of the three ILs during the electrolysis at 30 mA cm^{-2} of synthetic wastes, with presence or absence of sulfate ions in the electrolyte.

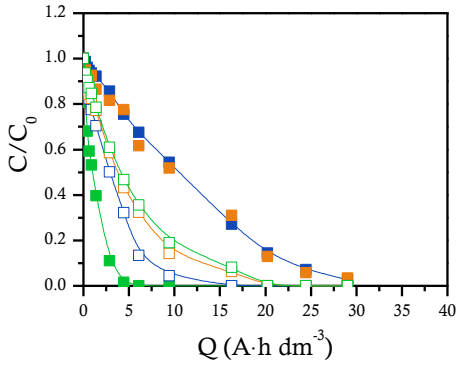

Figure 6.1.1. Removal of ionic liquids with the applied electric charge during the electrolysis of wastewater polluted with 1 mM of ionic liquid. j: 30 mA cm^{-2}; (blue) BmimCl; (orange) HmimCl; (green) DmimCl. Full symbols: electrolyte without SO_4^{2-}; empty symbols: 3000 mg L^{-3} H_2SO_4

In every case, the concentration of ILs decreases down to almost zero, indicating that total depletion of these imidazolium ILs can be attained from the synthetic wastes using this electrochemical technology,

regardless the molecular weight of the cation and the presence of sulfate anions in the electrolyte. Even so, degradation results are not overlapped but, just on the contrary, significant differences can be observed in the removal of the ILs, depending on the length of the carbon chain attached to the imidazolium ring and the electrolyte used. As indicated in the introductory section of this work, in the electrolysis of solutions without sulfate, only oxidation mediated by chlorine or by hydroxyl radicals (Eq. (1)) can supplement the direct anodic oxidation, whereas in the case of the electrolysis carried out to sulfate-containing solutions, peroxosulfates and sulfates radicals are also expected to play an important role (Panizza and Cerisola 2009). On the other hand, it is expected a slower degradation as the molecular weight of the ILs cation increases, since the degradation of linear alkane chains is known to be a low efficiency process for AOP, because of the nonexistence of functional groups to start the attack of the carbon chain.

A second important remark that should be pointed out is the higher efficiency observed in the degradation of the DmimCl polluted solution as compared to the results of the other two ILs. Thus, during the electrolysis tests of solutions without sulfate, the concentration of $Bmim^+$ and $Hmim^+$ cations decreases down to less than 3% of their initial value for electric current charges of 30 Ah dm^{-3}, whereas $Dmim^+$ is completely depleted at electric current charges even lower than 10 Ah dm^{-3}, indicating an improved efficiency in more than three times, because of the higher theoretical oxygen demand (ThOD) associated to these larger cations, in this later case. As pointed out before, this is an unexpected behavior, in particular taking into account that the molecule structure of $Dmim^+$ is much more complex than that of the other two ILs (larger carbon chain) and, hence, it was expected that its

electrochemical degradation was much more difficult. However, this fact can be explained in terms of the generation of a polymer during the electrolysis of $Dmim^+$ with BDD anodes. In this context, the occurrence of particles and even of a thin layer of polymer was observed on the surface of the pipes and tanks of the bench-scale plant during the electrolysis. This behavior was previously reported in literature for the electrolysis of nitrophenols polluted wastes with BDD anodes (Cañizares et al., 2004a; Cañizares et al., 2004b), being one of the rare cases in which polymerization reactions are found during electrolysis with the powerful BDD electrodes. Therefore, the efficient removal of $Dmim^+$ in comparison with $Bmim^+$ and $Hmim^+$ during electrolysis is mainly due to the polymerization of the ionic liquid and not to its mineralization, which was the expected treatment. In order to confirm this production of polymer and to know more about its formation, the electrolysis of $Dmim^+$ was repeated three times, under exactly the same conditions, being stopped the electrolysis in each of the three tests at different electric current charge passed. Then, the solids were carefully collected and their amount (by gravimetry) and molecular weight (using GPC) were measured. Results of these experiments are shown in Figure 6.1.2 and confirms the production of a polymer whose amount and molecular weight increase during the electrolysis reaching a molecular weight of 720 mg mol^{-1} at the end of the electrolysis. The trends observed show that the molecular weight linearly increases (Figure 6.1.2a) whereas the concentration of solids follows an exponential increase (Figure 6.1.2b) with the applied electric charge. These results suggest that the formation of the polymer could take place by an addition polymerization where monomers are coupled between them using their multiple bonds to form the polymer. For this reason, the concentration of solids abruptly increases at the beginning of the

experiment (formation of monomers and low molecular weight of the polymer) and starts to remain constant at the end of the process, corresponding to the higher molecular weight of the polymer and to a low concentration of monomers.

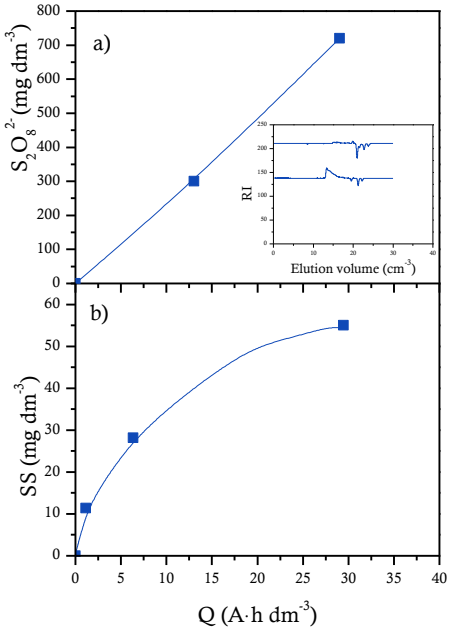

Figure 6.1.2. Mean molecular weight (a) and concentration (b) of the solids produced during the electrolysis of DmimCl, obtained from three different tests operated exactly under the same conditions.

Another important observation which can be drawn from Figure 6.1.1 is that the removal efficiency of $Bmim^+$ and $Hmim^+$ cations is higher when sulfate ions are contained in the electrolyte. As pointed out before, during electrolysis in sulfate media, significant amounts of peroxodisulfate are produced, either by direct (Eq. (2)) or by hydroxyl radicals mediated (Eq. (3)) mechanisms. In turn, peroxodisulfate can interact with other oxidants and produce sulfate radicals. All these

species are known to be powerful oxidants that favors the removal of organic matter in wastewater (Faousi et al., 2009; Kayan et al., 2010; Roshani et al., 2011).

$$2SO_4^{2-} \rightarrow S_2O_8^{2-} + 2e^- \quad (2)$$

$$2SO_4^{2-} + HO^{\cdot} \rightarrow S_2O_8^{2-} + HO^- + e^- \quad (3)$$

The trend observed in $Bmim^+$ and $Hmim^+$ concentration in presence of sulfate anions clearly points out the important contribution of peroxodisulfate in the electrolysis with BDD in the treatment of wastes containing sulfate, which is complementary to the contribution of the hydroxyl radicals and chlorine oxidation (if this oxidation may really occur in this system, as it will be pointed out afterwards). It is important to highlight that electrolysis of ILs is a very special case of study for the understanding of the oxidation of these organic compounds, because due to their very high ionic conductivity, it is not necessary to dope the synthetic waste with any salt in order to decrease the operation cell voltage. Hence, the oxidation of wastes in supporting electrolytes without sulfates only shows pure electrochemical mechanisms.

Effect observed on the degradation of DmimCl is the opposite of that observed for BmimCl and HmimCl in presence of sulfates. Thus, the concentration of $Dmim^+$ cation decreases with the applied electric charge until reaching its total depletion at current charge values around 17 Ah dm^{-3}. This value is much higher than that obtained during the electrolysis without sulfate and, therefore, it may initially suggest a lower efficiency. However, at this point, it is important to highlight that the presence of a polymer was not detected during the electrolysis carried out when sulfate ions are contained in the electrolyte. This means that the production of peroxodisulfate does not only contributes to the more efficient degradation of the ILs by electrolysis but also

prevents the formation of a polymer and, hence, the removal of $Dmim^+$ by an electropolymerization process.

To evaluate the significance of the formation of peroxodisulfate during the electrolysis of ILs with BDD anodes, its concentration was measured. Figure 6.1.3 shows the changes in the concentration of this oxidant with the applied electric charge in the three tests carried out to solutions containing sulfate anions.

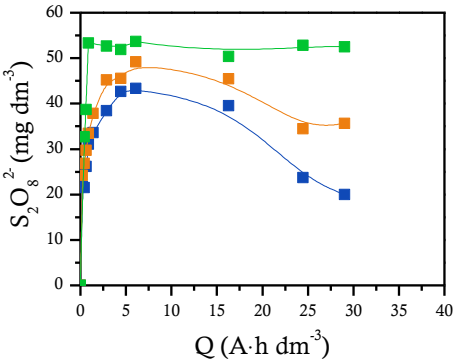

Figure 6.1.3. Evolution of peroxodisulfate with the applied electric charge during the electrolysis of wastewater polluted with 1 mM of ILs. j: 30 mA cm^{-2}; supporting electrolyte: 3000 mg dm^{-3} H_2SO_4; (blue) BmimCl; (orange) HmimCl; (green) DmimCl.

It is important to note that, the concentration of peroxodisulfate measured corresponds to that which has not reacted with the ILs or reaction intermediates and, hence, that higher concentrations may be produced, because the observed concentration is the balance between the production and the consumption of this oxidant. As it can be observed, peroxodisulfate increases with the applied electric charge for all the tests carried out. However, different behaviors can be seen

depending on the particular ionic liquid treated. In the case of $Bmim^+$ cation, the concentration of peroxodisulfate increases until reaching a maximum value (for around 10 Ah dm^{-3}) from which it starts to decrease. This means that a higher consumption of this species takes place at intermediate stages during the treatment process. This result agrees the removal of BmimCl previously observed (Figure 6.1.1) where this compound is completely removed at lower applied electric charges. A similar trend can be seen during the treatment of HmimCl: an initial increase followed by a decrease. Nonetheless, in this case, the maximum concentration measured is higher and, the decrease observed is less marked. Finally, the peroxodisulfate concentration remains constant (at about 53 mg dm^{-3}) during the electrolysis of DmimCl, which suggests that the generation and consumption rates of this species are balanced from the very early stages of the electrolysis. The important decreases observed after the initial stages in the case of the $Bmim^+$ and $Hmim^+$ cations may suggest a high affinity of the peroxosulfate for the intermediates formed from the oxidation of these two ILs.

For comparison purposes, the ILs decay was fitted to a first order kinetics and the removal rate constants are presented in Figure 6.1.4.

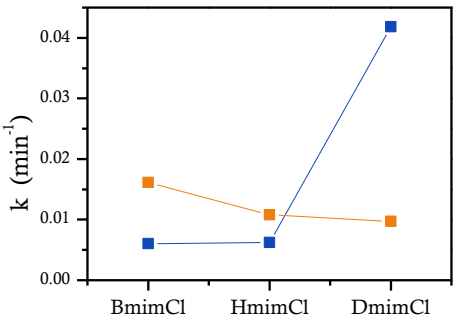

Figure 6.1.4. Kinetic constants calculated for the removal of ionic liquids by electrolysis with BDD anodes. Blue symbols: without sulfate; orange symbols: 3000 mg dm^{-3} H_2SO_4.

As it can be observed, the kinetic constants for $Bmim^+$ and $Hmim^+$ cations are similar during the electrolyses in absence of sulfate in the electrolyte. However, the value obtained for $Dmim^+$ is much higher, which is due to the polymerization of ionic liquid, previously described. Likewise, the use of sulfate as supporting electrolyte significantly increases the kinetic constants for BmimCl and HmimCl, being higher in the first case. In the case of DmimCl, the kinetic constant for the oxidation was expected to be higher than that obtained during the electrolysis in absence of sulfate. Unfortunately, it is not possible to compare, in terms of oxidation, both processes (with and without sulfate) because of the polymerization produced in absence of sulfate. This is not the case in the electrolysis of the ILs in solutions containing sulfates, for which the kinetic constants are observed to decrease with the molecular weight of the ionic liquid ($Bmim^+ > Hmim^+ > Dmim^+$). This means that there is a clear influence of the molecule structure on

the removal of ILs by electrolysis with BDD anodes and that it is promoted the oxidation of the ILs containing the shorter carbon chains.

As for many other pollutants, the electrolysis of ionic liquids may lead to the formation of other intermediate organic compounds and/or to a complete mineralization of the organic matter to carbon dioxide. Intermediates can be more harmful than the initial pollutants and, hence, they should be removed from wastewater. In this context, to provide information about the evolution of the organic matter, the concentration of TOC was monitored during the treatment. It is important to take in mind that this parameter informs only about the complete mineralization of the organic matter (conversion of organic carbon into carbon dioxide) and not about the progress of the oxidation. Results obtained are shown in Figure 6.1.5.

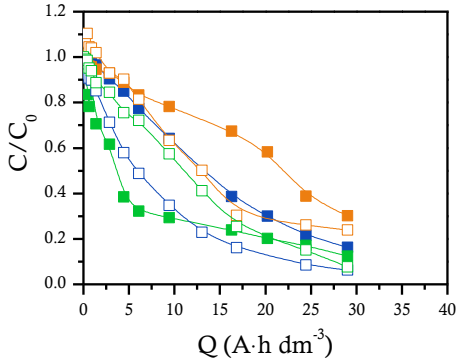

Figure 6.1.5. TOC decay as function of the applied electric charge during the electrolysis of wastewater polluted with 1 mM of ionic liquid. j: 30 mA cm^{-2}; (blue) BmimCl; (orange) HmimCl; (green) DmimCl. Full symbols: without sulfate; empty symbols: 3000 mg dm^{-3} H_2SO_4.

As it can be seen, TOC concentration decreases very importantly with the applied electric charge for all the tests carried out. However, it is not possible to attain a complete mineralization of the organic matter within the current charges applied (30 Ah dm^{-3}), regardless the IL studied and the supporting electrolyte. Anyhow, trends produced clearly points out that total depletion of the ILs can be obtained for larger applied charges.

The presence of sulfate leads to a more efficient TOC removal. In this context, a final percentage removal of 93.8 and 76.2% were obtained for BmimCl and HmimCl, respectively, whereas only 83.7 and 69.8% were achieved for both ionic liquids in absence of sulfate anions at the same electric current charges applied. This agrees with the results previously obtained for the removal of the ILs molecules (Figure 6.1.1), and indicates again the positive effect of the electrogenerated peroxodisulfate, not only in the oxidation of ILs, but also in the total removal of the intermediates formed.

On the other hand, the case of the DmimCl is different because of the polymerization observed in electrolysis of electrolytes without sulfate. Thus, the formation of polymer leads to an initial higher efficiency in the absence of sulfate, but this situation reverses at higher charges passed and the final percentage removal of TOC was 87.6% in wastes without sulfate and 92.5% when using sulfate as supporting electrolyte (polymer formation was not observed). The intermediates detected by HPLC–MS are reported in Table 6.1.1.

Table 6.1.1. Intermediates detected during the electrolysis of synthetic wastewater polluted with 1 mM of ILs using diamond anodes.

Nº	Molecular structure	Retention time (min)	*m/z*	Presence in $Bmim^+$ 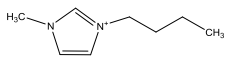	Presence in $Hmim^+$ 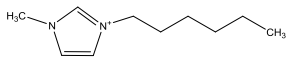	Presence in $Dmim^+$ 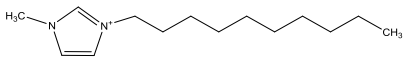
1	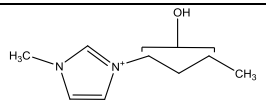	4.5	154	Yes	Yes	No
2	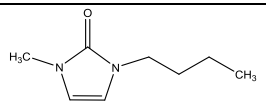	4.5	154	Yes	Yes	No
3	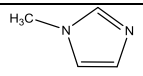	4.5	82	Yes	Yes	Yes
4	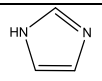	2.5	68	Yes	Yes	Yes
5	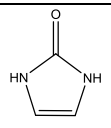	2.5	84	Yes	Yes	Yes

Table 6.1.1. Continued

Nº	Molecular structure	Retention time (min)	*m/z*	Presence in $Bmim^+$ 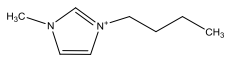	Presence in $Hmim^+$ 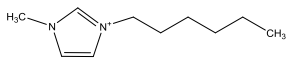	Presence in $Dmim^+$ 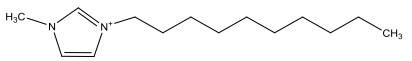
6	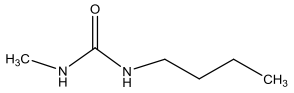	4.8	130	Yes	No	Yes
7	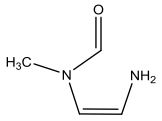	2.5	102	Yes	Yes	Yes
8	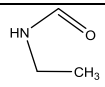	4.5	73	Yes	Yes	Yes
9	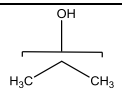	3.2	60	Yes	Yes	Yes
10	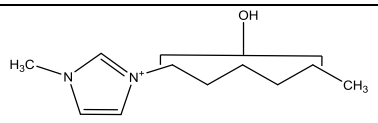	10.5	183	No	Yes	No
11	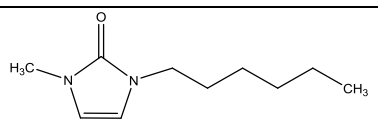	10.5	183	No	Yes	No

Table 6.1.1. Continued

Nº	Molecular structure	Retention time (min)	*m/z*	Presence in Bmim$^+$ 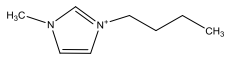	Presence in Hmim$^+$ 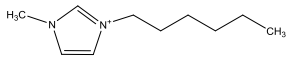	Presence in Dmim$^+$ 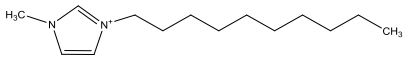
12	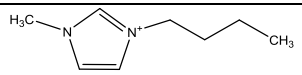	10	139	No	Yes	No
13	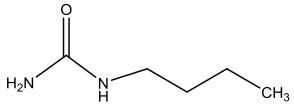	20	117	No	Yes	Yes
14	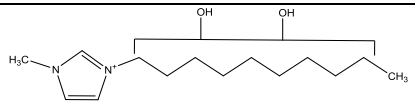	18.8	255	No	No	Yes
15	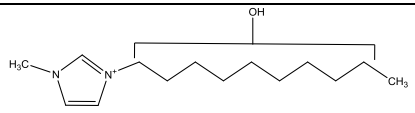	15.6	239	No	No	Yes
16	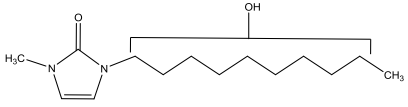	18.8	255	No	No	Yes
17	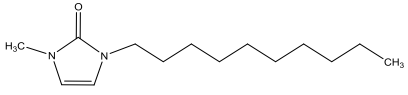	15.6	239	No	No	Yes

Table 6.1.1. Continued

Nº	Molecular structure	Retention time (min)	*m/z*	Presence in Bmim$^+$ 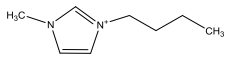	Presence in Hmim$^+$ 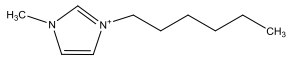	Presence in Dmim$^+$ 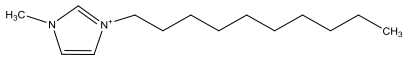
18	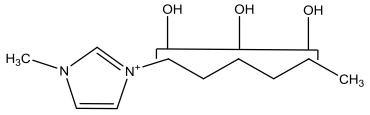	18.8	215	No	No	Yes
19	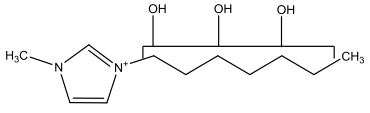	16.5	229	No	No	Yes
20	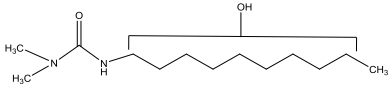	16.5	231	No	No	Yes
21	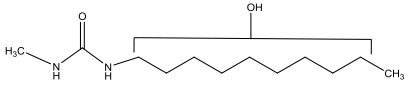	16.6	245	No	No	Yes

As can be observed, the electrolysis of $Dmim^+$ cation leads to the higher production of organic intermediate compounds. Specifically, 16 compounds were detected whereas 12 and 9 were found during the electrolysis of HmimCl and BmimCl, respectively. This is an expected behavior, taking into account that the carbon chain is the highest for Dmim+ cation. Likewise, it is important to point out that the electrolysis of the three ILs studied with diamond electrodes favors the formation of similar intermediates compounds at the end of the experiments. This fact suggests that the ILs are attacked on the carbon chain by electrogenerated oxidants at the beginning of the experiment followed by the ring opening.

The three ILs salts studied in this work contained a chloride anion. This anion is known to be oxidized during the electrolysis with BDD anodes, favoring the production of other chlorine compounds in higher oxidation state (Sánchez-Carretero et al., 2011). Specifically, chloride can be oxidized to chlorine gas in a first step (Eq. (5)) and, depending on the pH, chlorine gas can favor the production of hypochlorous acid/hypochlorite (Eqs. (5)–(6)). Next, these species can disproportionate to chlorate and chloride or undergo electrochemical oxidation to chlorate.

$$2Cl^- \rightarrow Cl_2 + 2\ e^- \quad (4)$$

$$Cl_2 + H_2O \rightarrow HClO + Cl^- + H^+ \quad (5)$$

$$HClO \rightarrow ClO^- + H^+ \quad (6)$$

$$2ClO^- \rightarrow ClO_2^- + Cl^- \quad (7)$$

$$ClO^- + ClO_2^- \rightarrow ClO_3^- + Cl^- \quad (8)$$

In addition, chloride can also react with hydroxyl radicals, favoring the production of chlorine compounds in higher oxidation state including perchlorate (Eqs. (9)–(12)).

$$Cl^- + HO^\cdot \rightarrow ClO^- + H^+ + e^- \quad (9)$$

$$ClO^- + HO^\cdot \rightarrow ClO_2^- + H^+ + e^- \quad (10)$$

$$ClO_2^- + HO^\cdot \rightarrow ClO_3^- + H^+ + e^- \quad (11)$$

$$ClO_3^- + HO^\cdot \rightarrow ClO_4^- + H^+ + e^- \quad (12)$$

Several of these chlorinated species can contribute to the degradation of the ILs (chlorine, hypochlorite and hypochlorous acid) due to their high oxidant capacity, whereas other such as chlorate and perchlorate do not contribute, because the oxidation carried out by them is not favored kinetically at room temperature. Figure 6.1.6 shows the changes in the concentration of these two non-active ions (chlorate and perchlorate) with the applied electric charge during the electrolysis of different ionic liquids in absence of sulfate. Unfortunately, the presence of high concentrations of sulfate makes not possible the analysis of different ions in the effluent and, therefore, these data cannot be shown.

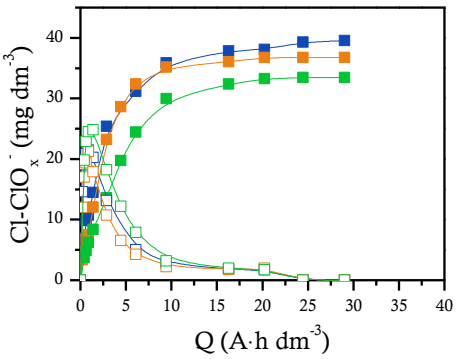

Figure 6.1.6. Chlorine speciation as function of the applied electric charge during the electrolysis of different ionic liquids in absence of sulfuric acid. j: 30 mA cm^{-2}; (blue) BmimCl; (orange) HmimCl; (green) DmimCl. Empty symbols: chlorate; full symbols: perchlorate.

As it can be observed, large amounts of chlorates and perchlorates are produced during the treatment, resulting in almost total conversion of the initial chloride contained in the solutions. Chlorate shows the typical behavior of an intermediate: there is an initial increase associated to the disproportionation of hypochlorite (or its electro-oxidation) followed by a later decrease until reaching zero values. The decrease observed corresponds to the increase in the concentration of perchlorate. This species, which behaves as final product, reaches a maximum value, from which it remains constant. The three ILs studied follow the same behavior during chlorine speciation. However, the total production of perchlorate decreases in the sequence BmimCl>HmimCl>DmimCl, suggesting that other final products are formed in the case of the Hmim$^+$ and the Dmim$^+$ electrolysis (Souza et al., 2017). From the mechanistic point of view looked for in this study, the formation of perchlorate is very positive, because it minimizes the

mediated oxidation of the ILs by chlorinated species and, hence, results of the oxidation in the absence of sulfate can only be caused by hydroxyl radicals mediated oxidation or, alternatively, by direct oxidation.

A last important piece of information regarding the degradation of the ILs can be obtained from the nitrogen contained in the three imidazolium cations degraded. This species can be degraded during the electrolysis with BDD anodes, favoring the formation of inorganic nitrogen compounds (Martin De Vidales et al., 2016; Rubí-Juárez et al., 2016). In this context, organic nitrogen oxidation start with the formation of nitrites (Eq. (13)). These species are quickly oxidized into nitrates by different mechanisms (Eqs. (14)-(15)) and, in turn, nitrates can be cathodically reduced to ammonium cations (Eqs. (16)-(17)), which is the most important final product in the electrolysis of organic nitrogen species (Lacassa et al. 2012).

$$N_2 + 2O_2 + 2\,e^- \rightarrow 2NO_2^- \quad (13)$$

$$3NO_2^- + 2H^+ \leftrightarrow 2NO + NO_3^- + H_2O \quad (14)$$

$$NO_2^- + \tfrac{1}{2}O_2 \rightarrow NO_3^- \quad (15)$$

$$NO_3^- + 6H_2O + 8e^- \leftrightarrow NH_3 + 9\,HO^- \quad (16)$$

$$NH_3 + H_2O \leftrightarrow NH_4^+ + HO^- \quad (17)$$

Figure 6.1.7 shows the maximum nitrogen formation of each species during the electrolysis of each ionic liquid at 30 mA cm^{-2} in absence of sulfuric acid. Once again, inorganic nitrogen measurements were not possible during the process in sulfate media and, unfortunately, data cannot be shown.

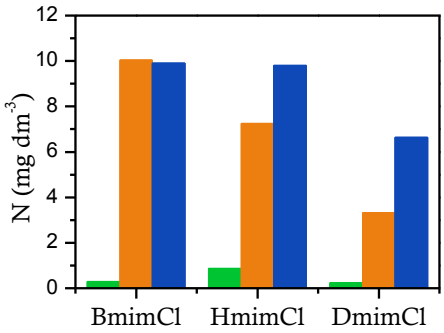

Figure 6.1.7. Maximum concentration of inorganic nitrogen release during the electrolysis of different ionic liquids in absence of sulfuric acid. j: 30 mA cm^{-2}; green bars: NO_2^-; orange bars: NO_3^-; blue bars: NH_4^+.

As it can be observed, nitrite presents the lower concentration in comparison with nitrate and ammonium for all the ionic liquids studied. This reveals the potential oxidation of nitrite to nitrate during the electrolysis with BDD anodes. The higher nitrite concentration was obtained for HmimCl. Regarding the evolution of nitrate, its maximum concentration is reached during the treatment of BmimCl whereas the minimum is obtained for DmimCl (in which the oxidation of the imidazolium group competes with the polymerization). Likewise, the maximum concentration of ammonium is also lower for this ionic liquid. This means that ammonium may be consumed by other way. At this point, it is important to highlight that the presence of chlorine compounds in high oxidation state can promote its reaction with ammonium. Specifically, hypochlorite can react with ammonium, favoring the production of inorganic chloramines (Eqs. (18)–(20)) and finally nitrogen gas and chloride.

$$NH_4^+ + ClO^- \rightarrow NH_2Cl + H_2O \quad (18)$$

$$NH_2Cl + ClO^- \rightarrow NHCl_2 + H_2O \quad (19)$$

$$NHCl_2 + ClO^- \rightarrow NCl_3 + HO^- \quad (20)$$

This is consistent with the previous chlorine speciation observed in Figure 6.1.6, where the generation rate of perchlorate (the final product of chloride oxidation) is lower during the treatment of DmimCl, followed by HmimCl and finally, BmimCl. This suggests that there were higher concentrations of hypochlorite in the solution which reacted with ammonium to form chloramines in a first stage and, eventually, gaseous nitrogen and chloride. This reactivity of the hypochlorite with the ammonium ion prevents reactivity with the organic carbon and make the electrolysis of the ILs in the absence of sulfate a very clean case of study.

6.1.4. Conclusions

From this work, the following conclusions can be drawn:

- Ionic liquids based on imidazolium group can be completely removed by electrolysis with diamond anodes.
- Despite an applied electric charge of 30 Ah dm^{-3} is not enough to mineralize completely 1 mM of ILs, results obtained confirm that the electrolytic technology can attain the total transformation of the imidazolium ring into carbon dioxide and nitrates, being this anion later transformed into ammonium.
- Presence of sulfate in the waste electrolyzed improve the efficiency of the oxidation process, clearly pointing out that the contribution of peroxosulfate and sulfate radicals in the electrolysis with diamond anodes of ILs is very important.

6.1 Influence of the supporting electrolyte on the removal of ionic liquids by electrolysis with diamond anodes

- The electrolysis of solutions containing 1 mM of DmimCl leads to the formation of a polymer, whose molecular weight increases during the treatment. Presence of sulfate prevents the formation of this polymer and favor the mineralization of the ILs.
- Chloride is mainly oxidized to chlorate and perchlorate during the electrolysis of the three ILs. Chloramines are also formed by the combination of the ammonium released from the imidazolium group with hypochlorite.

6.1.5. References

- Alfaro, M.A.Q., Ferro, S., Martínez-Huitle, C.A., Vong, Y.M., 2006. Boron doped diamond electrode for the wastewater treatment. J. Braz. Chem. Soc. 17, 227–236.
- Amde, M., Liu, J.F., Pang, L., 2015. Environmental application, fate, effects, and concerns of ionic liquids: A review. Environ. Sci. Technol. 49, 12611–12627.
- Brillas, E., Martínez-Huitle, C.A., 2011. Synthetic Diamond Films: Preparation, Electrochemistry, Characterization and Applications. Wiley.
- Brillas, E., Martínez-Huitle, C.A., 2015. Decontamination of wastewaters containing synthetic organic dyes by electrochemical methods. An updated review. Appl. Catal. B: Environ. 166–167, 603–643.
- Cañizares, P., Sáez, C., Lobato, J., Rodrigo, M.A., 2004a. Electrochemical treatment of 2,4-dinitrophenol aqueous wastes using boron-doped diamond anodes. Electrochim. Acta 49, 4641–4650.
- Cañizares, P., Sáez, C., Lobato, J., Rodrigo, M.A., 2004b. Electrochemical treatment of 4-nitrophenol-containing aqueous wastes using boron-doped diamond anodes. Ind. Eng. Chem. Res. 43, 1944–1951.
- Cañizares, P., Paz, R., Sáez, C., Rodrigo, M.A., 2007. Electrochemical oxidation of wastewaters polluted with aromatics and heterocyclic compounds. J. Electrochem. Soc. 154, E165–E171.
- Cañizares, P., Hernández, M., Rodrigo, M.A., Saez, C., Barrera, C.E., Roa, G., 2009a. Electrooxidation of brown-colored molasses wastewater. Effect of the electrolyte salt on the process efficiency, Ind. Eng. Chem. Res. 48, 1298–1301.
- Cañizares, P., Hernández-Ortega, M., Rodrigo, M.A., Barrera-Díaz, C.E., Roa-Morales, G., Sáez, C., 2009b. A comparison between Conductive-Diamond Electrochemical Oxidation and other Advanced Oxidation Processes for the treatment of synthetic melanoidins. J. Hazard. Mater. 164, 120–125.
- Comninellis, C., 1994. Electrocatalysis in the electrochemical conversion/combustion of organic pollutants for waste water treatment. Electrochim. Acta 39, 1857–1862.
- Comninellis, C., Nerini, A., 1995. Anodic oxidation of phenol in the presence of NaCl for wastewater treatment. J. Appl. Electrochem. 25, 23–28.
- Costa, S.P.F., Pinto, P.C.A.G., Saraiva, M.L.M.F.S., Rocha, F.R.P., Santos, J.R.P., Monteiro, R.T.R., 2015. The aquatic impact of ionic liquids on freshwater organisms. Chemosphere 139, 288–294.
- Cvjetko Bubalo, M., Radošević, K., Radojčić Redovniković, I., Halambek, J., Gaurina Srček, V., 2014. A brief overview of the potential environmental hazards of ionic liquids. Ecotoxicol. Environ. Saf. 99, 1–12.

- Esplugas, S., Bila, D.M., Krause, L.G.T., Dezotti, M., 2007. Ozonation and advanced oxidation technologies to remove endocrine disrupting chemicals (EDCs) and pharmaceuticals and personal care products (PPCPs) in water effluents. J. Hazard. Mater. 149, 631–642.
- Fabiańska, A., Ossowski, T., Stepnowski, P., Stolte, S., Thöming, J., Siedlecka, E.M., 2012. Electrochemical oxidation of imidazolium-based ionic liquids: the influence of anions. Chem. Eng. J. 198, 338–345.
- Faouzi Elahmadi, M., Bensalah, N., Gadri, A., 2009. Treatment of aqueous wastes contaminated with Congo Red dye by electrochemical oxidation and ozonation processes. J. Hazard. Mater. 168, 1163–1169.
- Feng, L., van Hullebusch, E.D., Rodrigo, M.A., Esposito, G., Oturan, M.A., 2013. Removal of residual anti-inflammatory and analgesic pharmaceuticals from aqueous systems by electrochemical advanced oxidation processes. A review. Chem. Eng. J. 228, 944–964.
- Fierro, S., 2010. Electrochemical oxidation of organic compounds in aqueous acidic media on ‘active' and ‘non-active' type electrodes, electrolysis: theory, types and applications. Nova Science Publishers, Inc., 135–209.
- Fryda, M., Herrmann, D., Schäfer, L., Klages, C.P., Perret, A., Haenni, W., Comninellis, C., Gandini, D., 1999. Properties of diamond electrodes for wastewater treatment. New Diamond Front. Carbon Technol. 9, 229–240.
- Garcia-Segura, S., Lima, Á.S., Cavalcanti, E.B., Brillas, E., 2016. Anodic oxidation, electro-Fenton and photoelectro-Fenton degradations of pyridinium- and imidazoliumbased ionic liquids in waters using a BDD/air-diffusion cell. Electrochim. Acta 198, 268–279.
- Goyal, R.K., Jayakumar, N.S., Hashim, M.A., 2011. Chromium removal by emulsion liquid membrane using [BMIM] + $[NTf_2]^-$ as stabilizer and TOMAC as extractant. Desalination 278, 50–56.
- Kayan, B., Gözmen, B., Demirel, M., Gizir, A.M., 2010. Degradation of acid red 97 dye in aqueous medium using wet oxidation and electro-Fenton techniques. J. Hazard. Mater. 177, 95–102.
- Kraft, A., Stadelmann, M., Blaschke, M., 2003. Anodic oxidation with doped diamond electrodes: a new advanced oxidation process, J. Hazard. Mater. 103, 247–261.
- Lacasa, E., Cañizares, P., Llanos, J., Rodrigo, M.A., 2012. Effect of the cathode material on the removal of nitrates by electrolysis in non-chloride media. J. Hazard. Mater. 213–214, 478–484.
- Lan, Y., Coetsier, C., Causserand, C., Groenen Serrano, K., 2017. On the role of salts for the treatment of wastewaters containing pharmaceuticals by electrochemical oxidation using a boron doped diamond anode. Electrochim. Acta 231, 309–318.

- Li, C., Xin, B., Xu, W., Zhang, Q., 2007. Study on the extraction of dyes into a room-temperature ionic liquid and their mechanisms. J. Chem. Technol. Biotechnol. 82, 196–204.
- Liwarska-Bizukojc, E., Gendaszewska, D., 2013. Removal of imidazolium ionic liquids by microbial associations: study of the biodegradability and kinetics. J. Biosci. Bioeng. 115, 71–75.
- Martin De Vidales, M.J., Millán, M., Sáez, C., Cañizares, P., Rodrigo, M.A., 2016. What happens to inorganic nitrogen species during conductive diamond electrochemical oxidation of real wastewater? Electrochem. Commun. 67, 65–68.
- Martínez-Huitle, C.A., Brillas, E., 2009. Decontamination of wastewaters containing synthetic organic dyes by electrochemical methods: a general review. Appl. Catal. B: Environ. 87, 105–145.
- Martínez-Huitle, C.A., Rodrigo, M.A., Sirés, I., Scialdone, O., 2015. Single and coupled electrochemical processes and reactors for the abatement of organic water pollutants: A critical review. Chemical Reviews.
- Meindersma, G.W., Podt, A., Klaren, M.B., de Haan, A.B., 2006. Separation of aromatic and aliphatic hydrocarbons with ionic liquids. Chem. Eng. Commun. 193, 1384–1396.
- Moreira, F.C., Boaventura, R.A.R., Brillas, E., Vilar, V.J.P., 2017. Electrochemical advanced oxidation processes: a review on their application to synthetic and real wastewaters. Appl. Catal. B: Environ. 202, 217–261.
- Panizza, M., Cerisola, G., 2004. Influence of anode material on the electrochemical oxidation of 2-naphthol: part 2. Bulk electrolysis experiments. Electrochim. Acta 49, 3221–3226.
- Panizza, M., Cerisola, G., 2009. Direct and mediated anodic oxidation of organic pollutants. Chem. Rev. 109, 6541–6569.
- Pera-Titus, M., García-Molina, V., Baños, M.A., Giménez, J., Esplugas, S., 2004. Degradation of chlorophenols by means of advanced oxidation processes: a general review. Appl. Catal. B: Environ. 47, 219–256.
- Perales, E., García, C.B., Lomba, L., Aldea, L., García, J.I., Giner, B.,2016. Comparative ecotoxicology study of two neoteric solvents: imidazolium ionic liquid vs. glycerol derivative. Ecotoxicol. Environ. Saf. 132, 429–434.
- Pieczyńska, A., Ofiarska, A., Borzyszkowska, A.F., Białk-Bielińska, A., Stepnowski, P., Stolte, S., Siedlecka, E.M., 2015. A comparative study of electrochemical degradation of imidazolium and pyridinium ionic liquids: a reaction pathway and ecotoxicity evaluation. Sep. Purif. Technol. 156 (Part 2), 522–534.
- Pignatello, J.J., Oliveros, E., MacKay, A., 2006. Advanced oxidation processes for organic contaminant destruction based on the fenton reaction and related chemistry. Crit. Rev. Environ. Sci. Technol. 36, 1–84.

- Plechkova, N.V., Seddon, K.R., 2007. Ionic liquids designer solvents for green chemistry, methods and reagents for green chemistry: An introduction. John Wiley & Sons, Inc., 103–130.
- Rodrigo, M.A., Oturan, N., Oturan, M.A., 2014. Electrochemically assisted remediation of pesticides in soils and water: a review. Chem. Rev. 114, 8720–8745.
- Roshani, B., Karpel Vel Leitner, N., 2011. Effect of persulfate on the oxidation of benzotriazole and humic acid by e-beam irradiation. J. Hazard. Mater. 190, 403–408.
- Rubí-Juárez, H., Cotillas, S., Sáez, C., Cañizares, P., Barrera-Díaz, C., Rodrigo, M.A., 2016. Removal of herbicide glyphosate by conductive-diamond electrochemical oxidation. Appl. Catal. B: Environ. 188, 305–312.
- Sánchez-Carretero, A., Sáez, C., Cañizares, P., Rodrigo, M.A., 2011. Electrochemical production of perchlorates using conductive diamond electrolyses. Chem. Eng. J. 166, 710–714.
- Siedlecka, E.M., Fabiańska, A., Stolte, S., Nienstedt, A., Ossowski, T., Stepnowski, P., Thöming, J., 2013. Electrocatalytic oxidation of 1-butyl-3-methylimidazolium chloride: effect of the electrode material. Int. J. Electrochem. Sci. 8, 5560–5574.
- Sirés, I., Brillas, E., Oturan, M.A., Rodrigo, M.A., Panizza, M., 2014. Electrochemical advanced oxidation processes: today and tomorrow. A review. Environ. Sci. Pollut. Res. 21, 8336–8367.
- Souza, F., Quijorna, S., Lanza, M.R.V., Sáez, C., Cañizares, P., Rodrigo, M.A., 2017. Applicability of electrochemical oxidation using diamond anodes to the treatment of a sulfonylurea herbicide. Catal. Today 280, 192–198.
- Steter, J.R., Brillas, E., Sirés, I., 2016. On the selection of the anode material for the electrochemical removal of methylparaben from different aqueous media. Electrochim. Acta 222, 1464–1474.
- Subramanian, B., Yang, Q., Yang, Q., Khodadoust, A.P., Dionysiou, D.D., 2007. Photodegradation of pentachlorophenol in room temperature ionic liquids. J. Photochem. Photobiol. A: Chem. 192, 114–121.
- Ternes, T.A., Stüber, J., Herrmann, N., McDowell, D., Ried, A., Kampmann, M., Teiser, B., 2003. Ozonation A tool for removal of pharmaceuticals, contrast media and musk fragrances from wastewater? Water Res. 37, 1976–1982.
- Urtiaga, A., Gómez, P., Arruti, A., Ortiz, I., 2014. Electrochemical removal of tetrahydrofuran from industrial wastewaters: anode selection and process scale-up. J. Chem. Technol. Biotechnol. 89, 1243–1250.
- Yao, C., Li, T., Twu, P., Pitner, W.R., Anderson, J.L., 2011. Selective extraction of emerging contaminants from water samples by dispersive

liquid–liquid microextraction using functionalized ionic liquids. J. Chromatogr. A 1218, 1556–1566.

- Yue, C., Fang, D., Liu, L., Yi, T.F., 2011. Synthesis and application of task-specific ionic liquids used as catalysts and/or solvents in organic unit reactions. J. Mol. Liq. 163, 99–121.
- Welton, T., 1999. Room-temperature ionic liquids. Solvents for synthesis and catalysis. Chem. Rev. 99, 2071–2083.
- Ziobrowski, Z., Rotkegel, A., 2017. The influence of water content in imidazolium based ILs on carbon dioxide removal efficiency. Sep. Purif. Technol. 179, 412–419.

6.2

Sono- and photoelectrocatalytic processes for the removal of ionic liquids based on the 1-butyl-3-methylimidazolium cation

Mena, I.F., Cotillas, S., Diaz, E., Sáez, C., Mohedano, A.F, Rodrigo, M.A. 2017. Sono- and photoelectrocatalytic processes for the removal of ionic liquids based on the 1-butyl-3-methylimidazolium cation. J. Hazard. Mat. (In press)

Sono- and photoelectrocatalytic processes for the removal of ionic liquids based on the 1-butyl-3-methylimidazolium cation

Abstract

In this work, sono- and photoelectrolysis of synthetic wastewaters polluted with the ionic liquids 1-Butyl-3-methylimidazolium acetate (BmimAc) and chloride (BmimCl) were investigated with diamond anodes. The results were compared to those attained by enhancing bare electrolysis with irradiation by UV light or with the application of high-frequency ultrasound (US). Despite its complex heterocyclic structure, the $Bmim^+$ cation was successfully depleted with the three technologies that were tested and was mainly transformed into four different organic intermediates, an inorganic nitrogen species and carbon dioxide. Regardless of the technology that was evaluated, removal of the heterocyclic ring is much less efficient (and much slower) than oxidation of the counter ion. In turn, the counter ion influences the rate of removal of the ionic liquid cation. Thus, the electrolysis and photoelectrolysis of BmimAc are much less efficient than sonoelectrolysis, but their differences become much less important in the case of BmimCl. In this later case, the most efficient technology is photoelectrolysis. This result is directly related to the generation of free radicals in the solution by irradiation of the electrochemical system with UV light, which contributes significantly to the removal of $Bmim^+$.

6.2.1. Introduction

Electrolysis is known to be an effective wastewater treatment method and is highly recommended for the depletion of pollutants that become refractory in other treatment technologies (Martinez-Huitle et al., 2015; Rodrigo et al., 2014; Sires et al., 2014). In the last two decades, the development of conductive-diamond coatings and their application as electrodes has definitively contributed to this success, and there are currently hundreds of papers that have reported the attainment of outstanding efficiencies and mineralization in the treatment of a great variety of species, ranging from very simple carboxylic acids to very complex organic dyes (Brillas and Martinez-Huitle et al., 2015; Sires et al., 2014). For this reason, it is important for this technology to be used for new challenges to better understand the mechanisms that are involved in the removal of organics.

In recent years, the high performance of electrolysis with diamonds has been improved by combining it with irradiation by UV light and ultrasound (Bebelis et al., 2013). In the first case, the main mechanism that is promoted is the activation of oxidants that form on the anode (peroxosulfates, peroxophosphates, peroxocarbonates, chlorine, etc.) and cathode (hydrogen peroxide) surfaces through the formation of corresponding radicals (Araújo et al., 2015; Bebelis et al., 2013; Cañizares et al., 2009). In the second case, improvement in the mass transport (for low frequency US) or promotion of the formation of radicals (not only by activation of electro-generated oxidant but also by the sonochemical oxidation of water) are the expected mechanisms to explain the changes that are caused by irradiation (Yaqub and Ajab, 2013).

6.2 Sono- and photoelectrocatalytic processes for the removal of ionic liquids based on the 1-butyl-3-methylimidazolium cation

The treatment of ionic liquids (ILs) is one of the most important challenges that still needs to be studied, not only because of the very complex structure of these molecules (often containing heterocycles) but also because of their conductivity, which is high enough to allow for the electrolysis of wastes that are polluted with these molecules at suitable cell voltages without the addition of further supporting electrolyte salts. This point is very important because it is well-known that oxidants form from the anions that are contained in supporting electrolyte salts (chloride, sulfates, phosphates, etc.) that are added in high concentrations during the electrochemical treatment, which definitively affects the process performance and efficiency (Cotillas et al., 2016; Martín de Vidales et al., 2016a).

Ionic liquids (ILs) commonly consist of a cation such as pyridinium, imidazolium, sulfonium, or phosphonium (among others) and an anion such as acetate, a halide, NTf_2 (bis(trifluoromethanesulfonimide)) or PF_6 (hexafluorophosphate) (Gore and Gatherhood, 2013; Reichardt and Welton, 2010; Yang and Pam 2005). One of the most representative ionic liquids is 1-Butyl-3-methylimidazolium ($Bmim^+$), which can be purchased as different salts, e.g., the chloride (BmimCl) and acetate (BmimAc) salts, which only differ in their counter ions. The common heterocyclic imidazolium ring, usually classified as diazole, presents non-adjacent nitrogen atoms in its structure where carbon chains join to formthe $Bmim^+$ cation (Huddleston et al., 2001; Mun and Sim, 2012). However, it is important to highlight that these ILs that are based on $Bmim^+$ are used for different industrial applications (Plechkova and Seddon, 2008) including enzymatic reactions (Frade and Afonso, 2010), solvents (Sheldon, 2005; Swatlovski et al., 2001), catalysis (Welton, 2004; Wasserscheid and Keim, 2000), extraction and purification (Hanet al., 2011), Li-ion batteries (Goodenough and Park,

2013), capacitors (McEwen et al.; 1999), fuel cells (Armand et al., 2009) and others. Likewise, these industries produce large volumes of wastewater that contain these compounds in low concentrations, which are not biologically degraded (Costa et al., 2015; Perales et al., 2016). Likewise, these compounds have high toxicity and can produce environmental hazards (Amde et al., 2015; Cvjetko Bubalo et al., 2014; Costa et al., 2015; Perales et al., 2016). For this reason, it is necessary to develop clean and efficient technologies that allow for the removal of these compounds from wastewater, such as electrochemical techniques (Fabiańska et al., 2012; García-Segura et al., 2015).

Considering these points, this work reports results that were obtained during electrolysis of synthetic wastewater that was polluted with two different ionic liquids with the same cation ($Bmim^+$) and two different anions (acetate and chloride). This study was initially planned to elucidate the mechanisms of electrochemical oxidation with diamond anodes. In the specific case of the ionic liquids that were used, because of their high conductivity (BmimAc and BmimCl), the addition of different salts is not necessary to perform electrolysis at a reasonable cell voltage. Thus, only peroxoacetate was expected to form in addition to hydroxyl radicals and oxidants that formed from them (hydrogen peroxide and ozone) through the oxidation of the acetate anion within the IL molecule during the electrolysis of BmimAc (Eq. (1)) (Cotillas et al., 2011).

$$CH_3COO^- + 2\ HO^{\cdot} \rightarrow CH_3COOO^- + H_2O \qquad (1)$$

Because peroxoacetate is not efficient in the oxidation of organics, the electrolysis of BmimAc will provide information about the most fundamental mechanisms for the oxidation of organics by electrolysis with diamonds. In contrast, in the case of the chloride salt, other active

chlorine species could be present in addition to hydroxyl radicals, ozone and hydrogen peroxide through the electrochemical oxidation of chloride anion (Eqs. (2)–(4)) (Sánchez-Carretero et al., 2011).

$$2\ Cl^- \rightarrow Cl_2 + 2e^- \quad (2)$$

$$Cl_2 + H_2O \rightarrow HClO + Cl^- + H^+ \quad (3)$$

$$HClO \leftrightarrow H^+ + ClO^- \quad (4)$$

6.2.2. Materials and methods

Chemicals

Bmim (1-butyl-3-methylimidazolium) acetate and chloride were of analytical grade and were used as received. HPLC-grade acetonitrile (Sigma-Aldrich, Spain) was used for the mobile phase. Sodium carbonate and acetone (Sigma-Aldrich, Spain) were used as mobile phases for the determination of ions. Double deionized water (Millipore Milli-Q system, resistivity: 18.2 MΩ cm at 25◦C) was used to prepare all solutions.

Anaytical methods

Samples were filtered with 0.22 μm nylon Scharlau filters provided by Scharlab. Determining the concentration of the $Bmim^+$ cation was followed by reversed-phase chromatography. The chromatography system was an Agilent 1100 series coupled with a UV detector. A Synergy 4 mm Polar-RP 80 A analytical column was used. The mobile phase consisted of 95:5 phosphate buffer:acetonitrile (flow rate: 0.75 $cm^3\ min^{-1}$). The UV detection wavelength was 218 nm, the temperature was maintained at 35 ^{O}C, and the injection volume was 20 μL. The TOC concentration was monitored using a Multi N/C 3100 Analytik Jena

analyzer. In this case, samples were directly measured without filtration to quantify all of the organic carbon that was present in the system. Ion concentrations were measured by ion chromatography using a Metrohm 930 Compact IC Flex coupled to a conductivity detector. A Metrosep A Supp 7 column was used for the determination.The mobile phase consisted of 85:15 v/v 3.6 mM Na_2CO_3:acetone with a flow rate of 0.8 mL min^{-1}. The temperature of the oven was 45 ^{o}C, and the volume injection was 20 µL. Likewise, a Metrosep ASupp 4 column was used to analyze the cations, mainly ammonium (NH_4^+). The mobile phase consisted of 1.7 mM HNO_3 and 1.7 mM 2,6-pyridinedicarboxylic acid with a flow rate of 0.9 ml min^{-1}. The temperature of the oven was 30 ^{o}C. Intermediates found during the degradation of the ionic liquids were followed by HPLC-MS.

Electrochemical cell

Electrolysis experiments were performed in a single-compartment electrochemical flow cell. Boron-doped diamond (BDD) with a geometric area of 78 cm^2 (WaterDiam, Switzerland) was used as the anode and cathode. However, to allow for irradiation with UV light inside the electrochemical cell, the cathode material consisted of a stainless steel grid, and one of the cell covers was made of quartz. The inter-electrode gap between both electrodes was 9 mm. A low-pressure Hg vapor UV lampVL-215MC (Vilber Lourmat), λ= 254 nm, intensity of 930 µW cm^{-2} and energy 4.89 eV irradiated the quartz cover directly at 4 W. High-frequency ultrasound (Epoch 650 ultrasound horn, Olympus) was used to introduce waves into the system at 10 MHz. The power of the ultrasound was 200 W. A Delta Electronika ES030-10 power supply (0–30 V, 0–10 A) provided the electric current. Wastewater was stored in a glass tank (0.6 dm^3). The BDD anode

presents a boron concentration of 500 mg dm^{-3}, a thickness of 2.72 μm and an sp3/sp2 ratio of 220, and it is supported on p-Si. Experiments were performed under galvanostatic conditions (30 mA cm^{-2}) and a discontinuous mode.

6.2.3. Results and discussion

Figure 6.2.1 shows the decay observed in the concentration of the $Bmim^+$ cation during the electrolysis of the BmimCl and BmimAc aqueous solutions (1 mM). No other chemicals were added to the synthetic wastewater. Hence, opposite to what has occurred in other electrolysis experiments in which it was found that electro-generated oxidants that are produced from the oxidationof the supporting electrolyte salts have a key role (Aquino et al., 2012). Here, the decay can only be associated with three mechanisms that are directly related to the degradation of the pollutant: direct electrolysis, hydroxyl-radical-mediated oxidation (including ozone and hydrogen peroxide), or chemical oxidation promoted by oxidants electro-generated from the anions of the ionic liquid salt (i.e.,chlorine/hypochlorite and peroxoacetic acid).

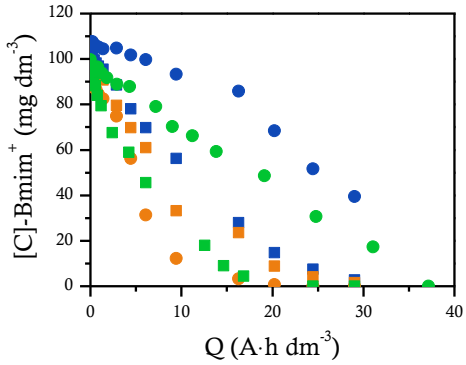

Figure 6.2.1. Changes observed in the concentration of the $Bmim^+$ cation during the electrolysis of BmimCl (squares) and BmimAc (circles). (Blue) electrolysis; (orange) sonoelectrolysis; (green) photoelectrolysis. $[IL]_0$: 1 mM; pH_0: 6.18; j: 30 mA cm^{-2}.

As shown in Figure 6.2.1, the concentration of $Bmim^+$ cation decreases to complete depletion in every case, but the differences in the efficiency associated with the applied technology and the counter ion are very remarkable. Thus, except for sonoelectrolysis, the removal of the $Bmim^+$ cation is much more efficient in the presence of the chloride ion compared to electrolysis with acetate. This result can be attributed to competitive oxidation between $Bmim^+$ and Cl^- during the treatment of BmimCl, whereas the oxidation of the cation seems to be the main process that occurs during the removal of BmimAc. Irradiation by UV light or high-frequency US always shows a positive effect on the removal efficiency, which is interesting because this is not always the expected out come, as was reported in previous studies (Cotillas et al., 2016; Souza et al., 2013). In the electrolysis of BmimCl, differences among the three technologies are smaller than in the case of BmimAc, where the results of the sonoelectrolysis differ significantly. This can

only be explained by taking into account that high-frequency sonolysis is sufficiently energetic to produce very high concentrations of hydroxyl radicals from bulk water (Thompson and Doraiswamy, 1999; Yaqub and Ajad, 2013), whereas photolysis is much less efficient in this process. The enhanced supply of hydroxyl radicals (electrolysis and sonolysis) may help to explain the remarkable increase in the oxidation rate of $Bmim^+$.

An additional observation that can be made regards the shape of the concentration versus Q plots. During the electrolysis of BmimCl, it follows a typical exponential decay, whereas during the electrolysis of BmimAc, the decay is linear, and the rate increases significantly from any given moment, which is a totally unexpected result. Exponential decay is typically associated with the electrolytic treatment of wastewater, and it is typically understood using a first-order kinetic model. This behavior is associated with either mass transport limitations in direct electrolysis or the proportionality of the rate to concentration in the case of kinetic control by mediated oxidation processes (Panizza and Cerisola, 2009).

Once the oxidation of $Bmim^+$ is discussed, it is important to consider that it is not only the cation that is oxidized by electrolytic technologies but also the counterions. Figure 6.2.2 shows the oxidation of chloride and acetate, two well-known anions in terms of their electrochemical reactivity.

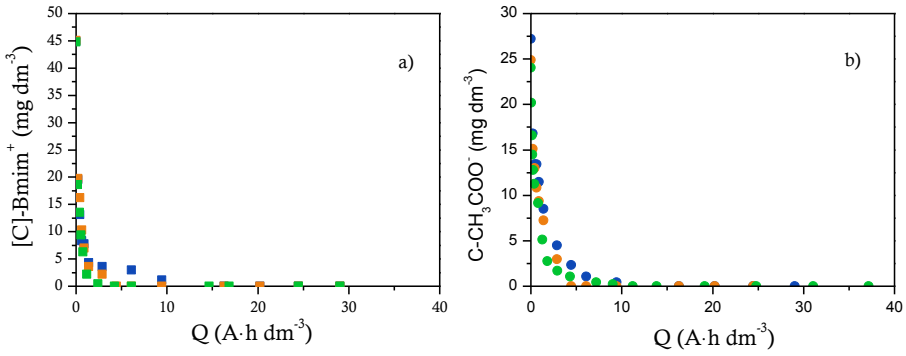

Figure 6.2.2. Changes in the concentration of chloride (a) and acetate (b) found during the electrolysis (blue), sonoelectrolysis (orange) and photoelectrolysis (green) of BmimCl and BmimAc, respectively. $[IL]_0$: 1 mM; pH_0: 6.18; j: 30 mA cm^{-2}.

The first important observation that should be made from the plot is that oxidation of the counter ions is much faster than the oxidation of $Bmim^+$. Here, electrostatic effects on the pollutants (discussed previously) should clearly be claimed. The negative charge of the anions allows for a better interaction with the positively charged surface of the anode. This fact, together with the much lesser number of electrons that must be exchanged, explains the faster removal. In comparing the technologies, it can be stated that both US and UV irradiation have very positive effects on the removal rate, with photoelectrolysis being slightly more efficient than sonoelectrolysis. Oxidation of the anion leads to the formation of reaction intermediates and final products (Figure 6.2.3).

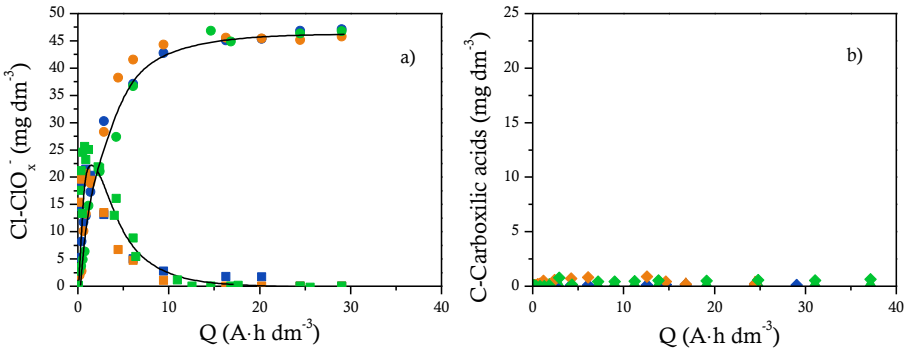

Figure 6.2.3. Concentrations of a) chlorate (square) and perchlorate (circle) and b) oxalic acid (triangle) and formic acid (diamond) found during the electrolysis (blue), sonoelectrolysis (orange) and photoelectrolysis (green) of BmimCl and BmimAc, respectively. $[IL]_0$: 1 mM; pH_0: 6.18; j: 30 mA cm^{-2}.

In the case of chloride, hypochlorite is the first species that formed during electrolysis with BDD anodes (Eqs. (2)–(4)). This compound can react with organic matter that is present in wastewater, favoring its degradation. However, hypochlorite can be rapidly oxidized by hydroxyl radicals to other chlorine compounds in a high oxidation state, such as chlorate and perchlorate (Eqs. (5)–(7)).

$$ClO^- + HO^\cdot \rightarrow ClO_2^- + H^+ + e^- \quad (5)$$

$$ClO_2^- + HO^\cdot \rightarrow ClO_3^- + H^+ + e^- \quad (6)$$

$$ClO_3^- + HO^\cdot \rightarrow ClO_4^- + H^+ + e^- \quad (7)$$

Perchlorate is the final oxidation product, and there is quantitative conversion of the chloride that was initially contained in the solution. Perchlorate is a toxic and harmful compound for humans and the

environment. For this reason, perchlorate production should be avoided, and future investigations should focus not only on the removal of organics but also the minimization of this type of inorganic pollutant. Chlorate is the main intermediate, and the only important difference that was observed when comparing the technologies was slightly faster oxidation with sonoelectrolysis, which can be explained by the higher $HO^{\cdot}$ production rate in the sonoelectrochemical process. In contrast to what it was observed for chloride, the role of intermediates during the oxidation of acetate is almost negligible, as is expected according to previous works (Cañizares et al., 2003), which suggest that there is nearly direct cold combustion for these species, and the concentrations of oxalic and formic acid that form are always below 1 ppm. Although carboxylic acids are typically difficult to oxidize by AOPS, the mineralization of carboxylic acids through electrolysis with diamond is not a difficult process. However, it is usually much slower, and thus less efficient, than oxidation of the aromatic species. The effective mineralization that is observed in this work is very valuable information because of the absence of other oxidants that are typically found in the electrolysis of organics, such as peroxosulfates or chlorine/hypochlorite. Thus, because carboxylic acids are refractory to hydroxyl radicals, and direct electrolysis is the only different mechanism that can develop in the system (in comparison to another raw AOP), this observation indicates that direct electrolysis plays a key role in the depletion of carboxylic acids, as was proposed by Savalland coworkers and Brillas' group in previous studies (Garcia-Segura and Brillas, 2011; Weiss et al., 2007).

Regarding the oxidation of the $Bmim^{+}$ cation, this species consists of a heterocyclic ring that contains nitrogen. Figure 6.2.4 shows the

concentrations of nitrites, nitrates and ammonium that were released to the solution during the treatment. It is important to consider that the electrochemistry of inorganic nitrogen species in solution is not simple from a mechanistic point of view. According to previous work, the main product in the oxidation of C–N bond is not ammonium but oxidized nitrogen (Martín de Vidales et al. 2016b). This result explains the concentrations of nitrites and nitrates that were observed. Both species behave as intermediates because nitrites are oxidized, either electrochemically or chemically by dissolved oxygen, into nitrates that are, in turn, reduced cathodically to ammonium ions over BDD and stainless steel electrodes, explaining their large observed concentrations (Lacassa et al., 2011; Lacassa et al., 2012b). The oxidation of ammonium to nitrates is not favored because of significant electrostatic repulsion forces that prevent the good interaction of this cation with the anodic surface. However, the oxidation of the C–N bond can also lead to the formation of other volatile NO_x species during electrochemical treatment with BDD anodes (Garcia-Segura et al., 2017). Nonetheless, its concentration is much lower than those of nitrite, nitrate and ammonium.

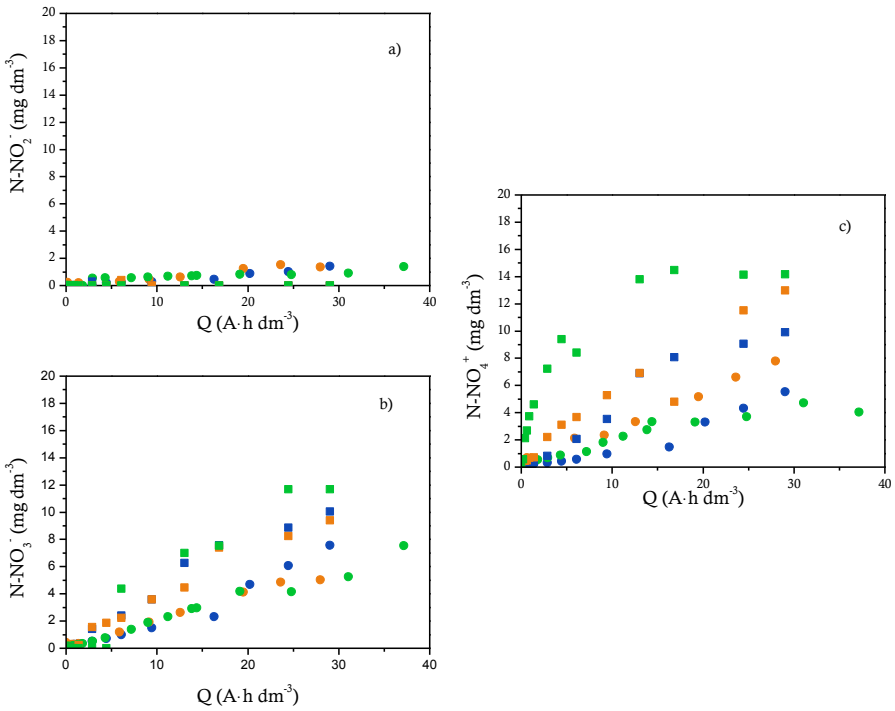

Figure 6.2.4. Inorganic nitrogen species observed during electrolysis (blue), sonoelectrolysis (orange) and photoelectrolysis (green) of BmimCl (square) and BmimAc (circle).(a) NO_2^-; (b) NO_3^-; (c) NH_4^+. $[IL]_0$: 1 mM; pH_0: 6.18; j: 30 mA cm^{-2}.

The total concentration of ammonium is much lower during electrolysis of the chloride salt. This observation can be explained by the interaction of hypochlorite with ammonium to sequentially form mono-, dichloramine, and nitrogen trichloride, as well as to regenerate chloride and produce nitrogen gas (Lacassa et al. 2012a).

Using HPLC, four organic intermediates were found. They were identified by mass spectrometry as: i1 (which was not clearly identified, but it may correspond to an intermediate with MW 102 g mol^{-1}),

isopropanol (i2), n,n-dimethylformamide (i3) and chlorosulfonic acid (i4). Figure 6.2.5 shows the chromatographic areas of the different intermediates as a function of the applied electric charge during the electrolytic and electro-irradiated treatment of the ionic liquids.

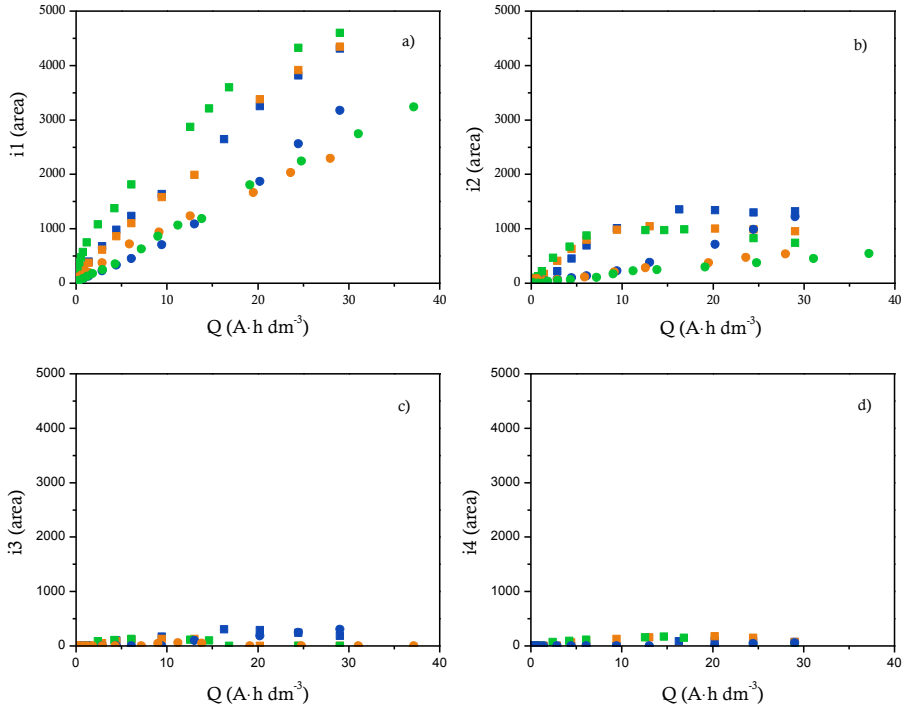

Figure 6.2.5. Intermediates observed during electrolysis (blue), sonoelectrolysis (orange) and photoelectrolysis (green) of BmimCl (square) and BmimAc (circle). $[IL]_0$: 1 mM; pH_0: 6.18; j: 30 mA cm^{-2}.

It is apparent that there is only one intermediate (i1) that has asignificant area during the process, following an increase trend for all tests that were performed. Likewise, the i2 profile, identified as isopropanol, initially increases and is followed by a decrease. Finally, i3 and i4 (n,n-dimethylformamide and chlorosulfonic acid, respectively)

show the lowest signals during the process. At this point, it is important to note that all concentrations are very low according to the TOC mass balance, regardless of the area that was registered in the HPLC analysis.

Considering these results, the mechanism that is described in Figure 6.2.6 is proposed for the degradation of the $Bmim^+$ cation by electrolysis with diamond electrodes.

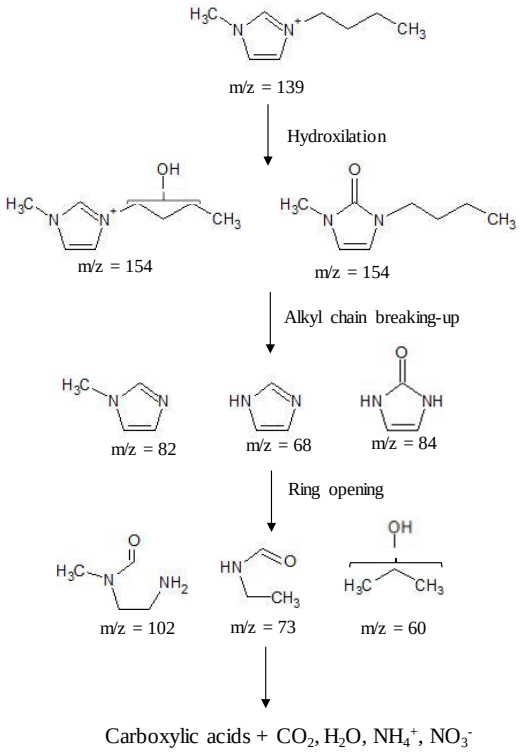

Figure 6.2.6. Pathway proposed for the degradation of the $Bmim^+$ cation by electrolysis

Figure 6.2.7 shows the changes in mineralization and summarizes the oxidation rates that were discussed above. The $Bmim^+$ cation is fully depleted, but the waste is not fully mineralized at the 40 Ah dm^{-3} of charge applied. The oxidation of the acetate salt is less efficient, except

for sonoelectrolysis, and the differences that were observed during the oxidation of chloride salts must be explained by chlorine mediated oxidation. During electrolysis of the chloride salt, irradiation with light has a clear positive effect. This result can be explained by the formation of $Cl^{\cdot}$ radicals, which contribute to faster oxidation of the $Bmim^{+}$ cation, in addition to delaying the formation of chlorate. This is not the case in the electrolysis of acetate salts, in which the irradiation by light does not show a similar clear improvement.

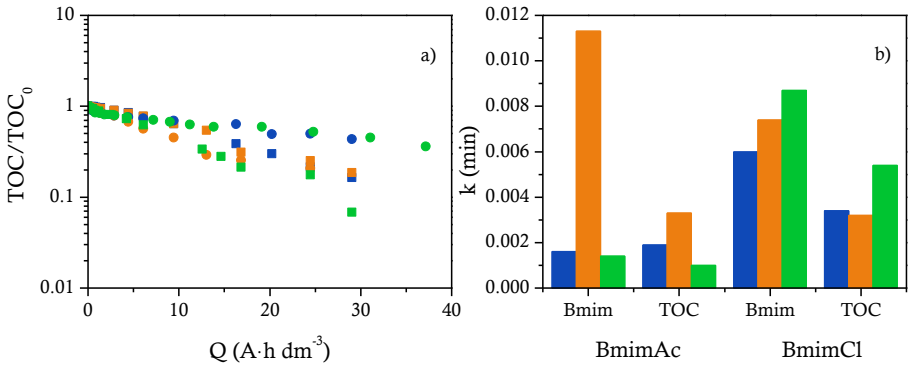

Figure 6.2.7. a) Mineralization of the ILs evaluated in this work: (square) BmimCl; (circle) BmimAc. b) First-order kinetic constants for the depletion of the $Bmim^{+}$ cation and for the mineralization of the ILs. (blue) electrolysis; (orange) sonoelectrolysis; (green) photoelectrolysis. $[IL]_0$: 1 mM; pH_0: 6.18; j: 30 mA cm^{-2}.

In contrast, the effect of high-frequency US clearly improves the oxidation of the TOC and the $Bmim^{+}$ cation during the electrolysis of acetate salts, becoming the more efficient process. The massive formation of hydroxyl radicals, not only at the anode surface but also in the bulk, and the increase in mass transport can help to explain this observation.

6.2.4. Conclusions

From this work, the following conclusions can be drawn:

- The 1-Butyl-3-methylimidazolium cation can be fully oxidized by electrolysis with diamond electrodes, leading to the formation of carbon dioxide, ammonium, nitrite and nitrate ions. The efficiency of the depletion depends on the counter ion and on irradiation by high-frequency US and UV light.
- The depletion of the counter ion is much more efficient than the oxidation of the $Bmim^+$ cation. In the case of BmimCl, the final product in the oxidation of the anion is perchlorate, and the main intermediate is chlorate. There are no differences among the technologies except for a faster reaction time in the case of sonoelectrolysis. In the case of BmimAc, oxalic acid and formic acid are the key intermediates, and carbon dioxide is the final product. The reluctance of hydroxyl radicals in the oxidation of carboxylic acids and the impossibility of other alternative oxidation mechanisms illustrate the importance of direct electrolysis in the oxidation of carboxylic acids.
- The oxidation of $Bmim^+$ leads to the formation of hydroxylated Bmim molecules as the main organic intermediate species and to nitrates and ammonium as the final nitrogen products. Because of the non-favored electrochemical oxidation of the ammonium cation to a nitrate anion, this speciation confirms that nitrate is the product obtained in the oxidation of C–N bonds.

6.2.5. References

- Amde, M., Liu, J.F., Pang, L., 2015. Environmental application, fate, effects, and concerns of ionic liquids: a review. Environ. Sci. Technol. 49, 12611–12627.
- Aquino, J.M., Rodrigo, M.A., Rocha-Filho, R.C., Sáez, C., Cañizares, P., 2012. Influence of the supporting electrolyte on the electrolyses of dyes with conductive-diamond anodes. Chem. Eng. J. 184, 221–227.
- Araújo, D.M.D., Cotillas, S., Sáez, C., Cañizares, P., Martínez-Huitle, C.A., Rodrigo, M.A., 2015. Activation by light irradiation of oxidants electrochemically generated during Rhodamine B elimination. J. Electroanal. Chem. 757, 144–149.
- Armand, M., Endres, F., MacFarlane, D.R., Ohno, H., Scrosati, B., 2009. Ionic-liquid materials for the electrochemical challenges of the future. Nat. Mater. 8, 621–629.
- Bebelis, S., Bouzek, K., Cornell, A., Ferreira, M.G.S., Kelsall, G.H., Lapicque, F., Ponce de León, C., Rodrigo, M.A., Walsh, F.C., 2013. Highlights during the developmentof electrochemical engineering. Chem. Eng. Res. Des. 91, 1998–2020.
- Brillas, E., Martínez-Huitle, C.A., 2015. Decontamination of wastewaters containing synthetic organic dyes by electrochemical methods. An updated review. Appl. Catal. B: Environ. 166–167, 603–643.
- Cañizares, P., García-Gómez, J., Lobato, J., Rodrigo, M.A., 2003. Electrochemical oxidation of aqueous carboxylic acid wastes using diamond thin-film electrodes. Ind. Eng. Chem. Res. 42, 956–962.
- Canizares, P., Saez, C., Sanchez-Carretero, A., Rodrigo, M.A., 2009. Synthesis of novel oxidants by electrochemical technology, J. Appl. Electrochem. 39, 2143–2149.
- Costa, S.P.F., Pinto, P.C.A.G., Saraiva, M.L.M.F.S., Rocha, F.R.P., Santos, J.R.P., Monteiro, R.T.R., 2015. The aquatic impact of ionic liquids on freshwater organisms. Chemosphere 139, 288–294.
- Cotillas, S., Sánchez-Carretero, A., Cañizares, P., Sáez, C., Rodrigo, M.A., 2011. Electrochemical synthesis of peroxyacetic acid using conductive diamond electrodes. Ind. Eng. Chem. Res. 50, 10889–10893.
- Cotillas, S., de Vidales, M.J.M., Llanos, J., Saez, C., Canizares, P., Rodrigo, M.A., 2016. Electrolytic and electro-irradiated processes with diamond anodes for the oxidation of persistent pollutants and disinfection of urban treated wastewater, J. Hazard. Mater. 319, 93–101.
- Cvjetko Bubalo, M., Radošević, K., Radojčić Redovniković, I., Halambek, J., Gaurina Srček, V., 2014. A brief overview of the potential environmental hazards ofionic liquids. Ecotoxicol. Environ. Safe 99, 1–12.

- Fabiańska, A., Ossowski, T., Stepnowski, P., Stolte, S., Thöming, J., Siedlecka, E.M., 2012. Electrochemical oxidation of imidazolium-based ionic liquids: the influence of anions. Chem. Eng. J. 198, 338–345.
- Frade, R.F.M., Afonso, C.A.M., 2010. Impact of ionic liquids in environment and humans: an overview. Hum. Exp. Toxicol. 29, 1038–1054.
- Garcia-Segura, S., Brillas, E., 2011. Mineralization of the recalcitrant oxalic and oxamic acids by electrochemical advanced oxidation processes using a boron-doped diamond anode. Water Res. 45, 2975–2984.
- Garcia-Segura, S., Lima, Á.S., Cavalcanti, E.B., Brillas, E., 2016. Anodic oxidation, electro-Fenton and photoelectro-Fenton degradations of pyridinium- and imidazolium-based ionic liquids in waters using a BDD/air-diffusion cell. Electrochim. Acta 198, 268–279.
- Garcia-Segura, S., Mostafa, E., Baltruschat, H., 2017. Could NO_x be released during mineralization of pollutants containing nitrogen by hydroxyl radical? As certaining the release of N-volatile species. Appl. Catal. B: Environ. 207, 376–384.
- Goodenough, J.B., Park, K.S., 2013. The Li-ion rechargeable battery: a perspective. J. Am. Chem. Soc. 135, 1167–1176.
- Gore, R.G., Gathergood, N., 2013. Safer and greener catalysts – design of high performance, biodegradable and low toxicity ionic liquids. INTECH OpenAccess Publisher.
- Han, J., Wang, Y., Yu, C., Li, C., Yan, Y., Liu, Y., Wang, L., 2011. Separation, concentration and determination of chloramphenicol in environment and food using anionic liquid/salt aqueous two-phase flotation system coupled with high-performance liquid chromatography. Anal. Chim. Acta 685, 138–145.
- Huddleston, J.G., Visser, A.E., Reichert, W.M., Willauer, H.D., Broker, G.A., Rogers, R.D., 2001. Characterization and comparison of hydrophilic and hydrophobicroom temperature ionic liquids incorporating the imidazolium cation, Green Chem. 3, 156–164.
- Lacasa, E., Cañizares, P., Llanos, J., Rodrigo, M.A., 2011. Removal of nitrates by electrolysis in non-chloride media: effect of the anode material. Sep. Purif. Technol. 80, 592–599.
- Lacasa, E., Cañizares, P., Llanos, J., Rodrigo, M.A., 2012a. Effect of the cathode material on the removal of nitrates by electrolysis in non-chloride media. J. Hazard. Mater. 213–214, 478–484.
- Lacasa, E., Llanos, J., Cañizares, P., Rodrigo, M.A., 2012b. Electrochemical denitrificacion with chlorides using DSA and BDD anodes. Chem. Eng. J. 184, 66–71.

- Martín de Vidales, M.J., Cotillas, S., Perez-Serrano, J.F., Llanos, J., Saez, C., Canizares, P., Rodrigo, M.A., 2016a. Scale-up of electrolytic and photoelectrolytic processes for water reclaiming: a preliminary study. Environ. Sci. Pollut. Res.23, 19713–19722.
- Martín De Vidales, M.J., Millán, M., Sáez, C., Cañizares, P., Rodrigo, M.A., 2016b. Whath appens to inorganic nitrogen species during conductive diamond electrochemical oxidation of real wastewater? Electrochem. Commun. 67, 65–68.
- Martinez-Huitle, C.A., Rodrigo, M.A., Sires, I., Scialdone, O., 2015. Single and coupled electrochemical processes and reactors for the abatement of organic water pollutants: a critical review. Chem. Rev. 115, 13362–13407.
- McEwen, A.B., Ngo, H.L., LeCompte, K., Goldman, J.L., 1999. Electrochemical properties of imidazolium salt electrolytes for electrochemical capacitor applications. J. Electrochem. Soc. 146, 1687–1695.
- Mun, J., Sim, H., 2012. Handbook of ionic liquids: properties, applications, and hazards. Nova Science Publishers.
- Panizza, M., Cerisola, G., 2009. Direct and mediated anodic oxidation of organic pollutants. Chem. Rev. 109, 6541–6569.
- Perales, E., García, C.B., Lomba, L., Aldea, L., García, J.I., Giner, B., 2016. Comparative ecotoxicology study of two neoteric solvents: imidazolium ionic liquid vs. glycerol derivative. Ecotoxicol. Environ. Safe 132, 429–434.
- Plechkova, N.V., Seddon, K.R., 2008. Applications of ionic liquids in the chemical industry. Chem. Soc. Rev. 37, 123–150.
- Reichardt, C., Welton, T., 2010. Solvents and solvent effects in organic chemistry. Fourth edition, Wiley-VCH.
- Rodrigo, M.A., Oturan, N., Oturan, M.A., 2014. Electrochemically assisted remediation of pesticides in soils and water: a review. Chem. Rev. 114, 8720–8745.
- Sánchez-Carretero, A., Sáez, C., Cañizares, P., Rodrigo, M.A., 2011. Electrochemical production of perchlorates using conductive diamond electrolyses. Chem.Eng. J. 166, 710–714.
- Sheldon, R.A., 2005. Green solvents for sustainable organic synthesis: state of the art. Green Chem. 7, 267–278.
- Sires, I., Brillas, E., Oturan, M.A., Rodrigo, M.A., Panizza, M., 2014. Electrochemical advanced oxidation processes: today and tomorrow. A review. Environ. Sci. Pollut. Res. 21, 8336–8367.
- Souza, F.L., Sáez, C., Cañizares, P., Motheo, A.J., Rodrigo, M.A., 2013. Sonoelectrolysis of wastewaters polluted with dimethyl phthalate. Ind. Eng. Chem. Res. 52, 9674–9682.

- Swatloski, R.P., Spear, S.K., Holbrey, J.D., Rogers, R.D., 2002. Dissolution of cellose with ionic liquids. J. Am. Chem. Soc. 124, 4974–4975.
- Thompson, L.H., Doraiswamy, L.K., 1999. Sonochemistry: science and engineering. Ind. Eng. Chem. Res. 38, 1215–1249.
- Wasserscheid, P., Keim, W., 2000. Ionic liquids—new 'solutions' for transition metal catalysis. Angew. Chem. Int. Ed. 39, 3773–3789.
- Weiss, E., Groenen-Serrano, K., Savall, A., Comninellis, C., 2007. A kinetic study of the electrochemical oxidation of maleic acid on boron doped diamond. J. Appl. Electrochem. 37, 41–47.
- Welton, T., 2004. Ionic liquids in catalysis. Coord. Chem. Rev. 248, 2459–2477.
- Yang, Z., Pan, W., 2005. Ionic liquids: green solvents for nonaqueous biocatalysis. Enzyme Microb. Technol. 37, 19–28.
- Yaqub, A., Ajab, H., 2013. Applications of sonoelectrochemistry in wastewater treatment system. Rev. Chem. Eng. 29, 123–130.

6.3

Electrolysis with diamond anodes: Eventually, there are refractory species!

Mena, I.F., Cotillas, S., Diaz, E., Sáez, C., Rodríguez, J.J., Cañizares, P., Mohedano, A.F, Rodrigo, M.A. 2018. Electrolysis with diamond anodes: Eventually, there are refractory species!
Chemosphere 195, 771–776

Electrolysis with diamond anodes: Eventually, there are refractory species!

Abstract

In this work, synthetic wastewater polluted with ionic liquid 1-butyl-3-methylimidazolium ($Bmim^+$) bis(trifluoromethanesulfonyl)imide (NTf_2^-) undergoes four electrolytic treatments with diamond anodes (bare electrolysis, electrolysis enhanced with peroxosulfate promoters, irradiated with UV light and with US) and results obtained were compared with those obtained with the application of Catalytic Wet Peroxide Oxidation (CWPO). Despite its complex heterocyclic structure, $Bmim^+$ cation is successfully depleted with the five technologies tested, being transformed into intermediates that eventually can be mineralized. Photoelectrolysis attained the lowest concentration of intermediates, while CWPO is the technology less efficient in their degradation. However, the most surprising result is that concentration of NTf_2^- anion does not change during the five advanced oxidation processes tested, pointing out its strong refractory character, being the first species that exhibits this character in wastewater undergoing electrolysis with diamond. This means that the hydroxyl and sulfate radicals mediated oxidation and the direct electrolysis are inefficient for breaking the C-S, C-F and S-N bounds of the NTf_2^- anion, which is a very interesting mechanistic information to understand the complex processes undergone in electrolysis with diamond.

6.3 Electrolysis with diamond anodes: Eventually, there are refractory species!

6.3.1. Introduction

Over the last two decades, hundreds of papers have demonstrated the outstanding performance of the electrolysis of different types of wastewater with diamond anodes. Very high current efficiencies, exceptional robustness and lack of refractory species can be considered as the three most important labels for this technology (Rodrigo et al., 2010) and, all together, they explain why, even after having passed by more than 20 years from the beginning of the massive study of applications, currently electrolysis with diamond is still a hot scientific topic (Sires et al., 2014; Martinez-Huitle et al., 2015).

To attain these conclusions, thousands of products have been tested, ranging from very high-molecular weight dyes (Martinez-Huitle and Brillas, 2009; Brillas and Martinez-Huitle, 2015) to small carboxylic acid molecules (Gandini et al., 2000), from linear aliphatic (Cañizares et al., 2003, 2008) to highly heterocyclic molecular structures (Cañizares et al., 2007a) and from natural (Raut et al., 2013) to anthropogenic molecules (Oturan et al., 2012). Likewise, different matrixes have been studied, ranging from real wastewater (Cabeza et al., 2007) to synthetic solutions enriched in salts (Cañizares et al., 2009a), passing through other different types of matrixes such as soil washing & soil flushing wastes (dos Santos et al., 2015) or pollutant-intensified matrixes. Results have been always the same: rate could be higher or lower but eventually, all organic molecules are fully degraded and, for non-heterocyclic compounds (or in the absence of chloride), mineralization, that is, conversion of organic carbon into carbon dioxide, is complete. To explain the impressive performance of this process, the combined action of many different oxidations mechanisms is proposed (Sires et al., 2014; Martinez-Huitle et al., 2015). Thus, in

addition to the formation of hydroxyl radical, first demonstrated at the turn of the century (Marselli et al., 2003), formation of many other oxidants is known to occur via direct and hydroxyl mediated processes, giving chance to the formation of a very important oxidants' cocktail (Cañizares et al., 2009b). Thus, presence of sulfates, carbonates and/or phosphates in the wastewater leads to the production of peroxosulfates, peroxocarbonates and/or peroxophosphates, respectively. Occurrence of chloride leads to the formation of hypochlorite/chlorine for low electric charge passed and, unfortunately, to chlorates and perchlorates for higher charges. Ozone and hydrogen peroxide are also known to be formed by interaction of hydroxyl radicals with water or oxygen. In addition, all these compounds can be transformed into more powerful oxidants by activation with UV light, high frequency US and even, with the simple interactions among them.

Taking into account these points, this work reports the results obtained during the electrolysis of an ionic liquid, the salt 1-butyl-3-methylimidazolium ($Bmim^+$) bis(trifluoromethanesulfonyl)imide (NTf_2^-). This compound presents a melting point about 2 ºC and a density of 1.44 g mL^{-1}. As most of the ionic liquids, it exhibits high thermal stability and it is very difficult to remove by biological degradation (Liwarska-Bizukojc and Gendaszewska, 2013). For this reason, this compound is considered as persistent pollutant and, hence, its presence in water should be avoided. The study was initially planned for understanding better the mechanisms of the electrochemical oxidation with diamond anodes, as because of the high conductivity of the pollutant used ($BmimNTf_2$), it is not necessary to add different salts in order to perform electrolysis at a reasonable cell voltage. However, in the results obtained, we found that bis(trifluoromethanesulfonyl)imide anion is refractory to the

electrolysis with diamond, which is a very interesting result which, in turn, gives very valuable mechanistic information about this very important environmental electrochemical technology.

6.3.2. Materials and methods

Chemicals

Analytical grade BminNTf$_2$ ($C_{10}H_{15}F_6N_3O_4S_2$) and sulfuric acid were used as received. Double deionized water (Millipore Milli-Q system, resistivity: 18.2MΩ cm at 25 ºC) was used to prepare all solutions.

Anaytical techniques

Bmin$^+$ cation was quantified by reverse-phase chromatography using an Agilent 1100 system coupled a UV detector. A Synergy 4mm Polar-RP 80 A column was used and the mobile phase consisted of 95:5 phosphate buffer/acetonitrile (flow rate: 0.75 mL min_1; λ: 218 nm; T: 35 ºC; $V_{injection}$: 20 µL, retention time: 9 min). NTf_2^- anion was identified by liquid chromatography coupled with mass spectrometry (Agilent Technologies 6120 Quadrupole LC/MS). An ACE Excel 3 C18-Amide column at 40 ºC as stationary phase. The mobile phase consisted of 10:90 formic acid (0.1% v)/acetonitrile (flow rate: 0.2 mL min^{-1}; $V_{injection}$: 1µL, retention time: 4.7 min). Inorganic nitrogen species were measured by ion chromatography using a Metrohm 930 Compact IC Flex coupled to a conductivity detector (Rubí-Juarez et al., 2016a). The mobile phase consisted of 85:15 v/v 3.6 mM Na_2CO_3/acetone solution for the determination of anions (flowrate: 0.80 mL min^{-1}) and 1.7 mM HNO_3 and 1.7 mM 2,6-pyridinedicarboxylic acid solution for the determination of cations (flowrate: 0.90 mL min^{-1}). The temperature of the oven was 45 and 30 ºC for the determination of anions and cations,

respectively. The volume injection was 20 µL. TOC concentration was monitored using a Multi N/C 3100 Analytik Jena analyzer.

Electrochemical cell

Electrolyses were carried out using the experimental setup and methodology described elsewhere (Cotillas et al., 2016). Boron doped diamond (BDD) with a geometric area of 78 cm^2 (Water-Diam, Switzerland) was used as anode and cathode. However, to allow the irradiation of UV light inside the electrochemical cell, the cathode material consisted of a stainless steel grid and one of the cell covers was made of quartz. The inter-electrode gap between both electrodes was 9 mm. A low pressure Hg vapor UV lamp VL-215MC (Vilber Lourmat), λ = 254 nm, intensity of 930 mW cm^{-2} and energy 4.89 eV irradiated 4W directly to the quartz cover. A high-frequency ultrasound (Epoch 650 ultrasound horn, Olympus) was used to provide waves into the system at 10 MHz. The power of ultrasound was 200 W. A Delta Electronika ES030-10 power supply (0-30 V, 0-10 A) provided the electric current. Wastewater was stored in a glass tank (0.6 L). BDD anode presents a boron concentration of 500 mg L^{-1}, a thickness of 2.72 mm, sp^3/sp^2 ratio of 220 and p-Si as support. Experiments were carried out under galvanostatic conditions and discontinuous mode. The current density employed was 30 mA cm^{-2}. This value was selected to guarantee the potential production of hydroxyl radicals during the process (Marselli et al., 2003).

Synthetic wastewater was prepared by dissolving 419 mg L^{-1} (1 mM) of $BmimNTf_2$ in double deionized water. For the study of the influence of the supporting electrolyte, 3000 mg L^{-1} of sulfuric acid were added to synthetic wastewater.

Catalytic Wet Peroxide Oxidation experiments

Catalytic Wet Peroxide Oxidation (CWPO) experiments were performed with a Fe/γ-Al_2O_3 catalyst prepared by incipient wetness impregnation of γ-Al_2O_3 (supplied by Merck) with an aqueous solution of $Fe(NO_3)_3 \cdot 9H_2O$ (Bautista et al., 2010a, Bautista et al., 2010b). The Fe load was adjusted to a nominal 4% (w/w). After impregnation, the catalyst was left at room temperature for 2 h, dried at 60 ºC for 18 h and calcined at 300 ºC for 4 h.

Oxidation experiments were carried out in batch in 400 mL glass batch reactor with temperature control and a magnetic stirring velocity of 500 rpm. The catalysts were used in powdered form (dp < 100 mm) and at 1 g L^{-1}. The operating conditions were: $[IL]_0$ = 419 mg L^{-1} (correspond to a concentration of 1 mM), pH = 3, T = 80 ºC and H_2O_2 starting concentration corresponding to the theoretical stoichiometric dose to achieve the complete mineralization (1377 mg L^{-1}).

6.3.3. Results and discussion

Figure 6.3.1 compares the time-course of normalized TOC after the application of electrolysis with diamond anodes for 8 h to 1.0 L of a solution containing 419 mg L^{-1} of the ionic liquid $BmimNTf_2$. Data of the raw electrolysis are marked with a continuous line. The other series show results of improved electrolysis technologies attained by the combination of this technique with UV light or US irradiation or by adding H_2SO_4 to the solution, a precursor for the formation of peroxosulfate. The trends of these results are not marked with lines in order to avoid a messy plot. These three technologies are known to yield synergistic effects according to the literature (Martinez-Huitle et al., 2015), and hence to improve the performance of the process as

compared to the raw electrolytic process. In addition, for comparison purposes, despite the very different type of technology, results obtained during the CWPO of the same synthetic wastewater are also plotted and marked with a discontinuous line (mass ratio oxidant/pollutant 3.3:1; 80 ºC, 8 h). This technology allows removing organic pollutants by hydroxyl radical-mediated oxidation (Mena et al., 2017) while electrolysis with diamond anodes not only favors the production of these species (HO·), but also other oxidants such as ozone or hydrogen peroxide. Therefore, a comparison of both technologies can serve to learn on the real contribution of hydroxyl radicals in the removal of $BmimNTf_2$.

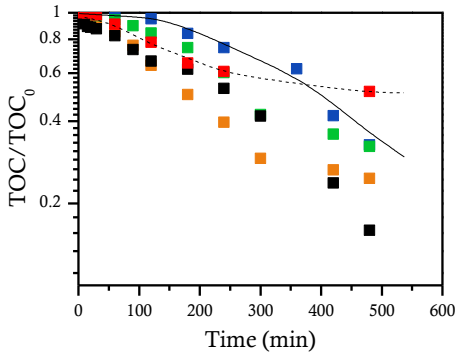

Figure 6.3.1. Mineralization of $BmimNTf_2$ with (blue) Electrolysis; (red) CWPO; (orange) Sonoelectrolysis; (green) Photoelectrolysis; (black) Electrolysis with addition of H_2SO_4.

As it can be observed, the complete mineralization of the synthetic wastes is not attained by any of the technologies tested. Nonetheless, the trends observed suggest that it would be possible to achieve a complete TOC removal by increasing the operation time during the

electrochemical treatments. In addition, great differences can be found among the different electrolytic treatments, indicating the great significance of mediated oxidation processes promoted in each of them. At this point, the most efficient result is obtained with the addition of sulfates to the synthetic waste and this clearly points out the significant role of persulfate and sulfate radicals formed by its activation in the electrolysis with diamond anodes (Eqs. (1)–(6)) (Almazán-Sánchez et al., 2017; Cotillas et al., 2018).

$$2\ SO_4^{2-} \rightarrow S_2O_8^{2-} + 2e^- \quad (1)$$

$$H_2O \rightarrow H^+ + HO^{\cdot} + e^- \quad (2)$$

$$SO_4^{2-} + HO^{\cdot} \rightarrow (SO_4^{-})^{\cdot} + HO^- \quad (3)$$

$$(SO_4^{-})^{\cdot} + (SO_4^{-})^{\cdot} \rightarrow S_2O_8^{2-} \quad (4)$$

$$S_2O_8^{2-} +))) \rightarrow 2\ (SO_4^{-})^{\cdot} \quad (5)$$

$$S_2O_8^{2-} + h\nu \rightarrow 2\ (SO_4^{-})^{\cdot} \quad (6)$$

This better performance is especially relevant at very low TOC concentrations, where it clearly overcomes the results obtained by sonoelectrolysis, which behaves as the most efficient technology for higher TOC concentrations. This behavior is directly related to the nature of the organics present in wastewater (Cañizares et al., 2007a). In this context, heterocyclic compounds are the predominant species at the beginning of the experiment, which are easily attacked by electrogenerated hydroxyl radicals, promoting the formation of aliphatics. However, those compounds are known not to be largely affected by these radicals and, hence, sonoelectrolysis is more efficient at higher TOC concentrations (high concentration of heterocyclic compounds) because of the generation of large amounts of hydroxyl

radicals during this process. On the other hand, the presence of persulfate in wastewater (from the oxidation of sulfate) contributes to the potential degradation of aliphatic compounds, which are formed at higher operation times (low TOC concentration). Therefore, electrolysis in sulfate-containing medium shows the highest efficiency at the end of the experiment. Performance of photoelectrolysis is worse than those exhibited by these other two combined technologies, although the mineralization attained is faster and more important than the observed with the raw electrolysis. Finally, in comparing electrolysis and CWPO, it can be clearly seen that the electrolytic technology lead to higher mineralization within the same experimental period, although this comparison is not relevant because of great difference between the technologies and the operation conditions.

Hence, $BmimNTf_2$ is a complex pollutant and the application of the different technologies reached very different mineralization and efficiencies, clearly indicating that the oxidants produced in each of them affects the organic in different ways. For this reason, it is important to compare the evolution of the different species involved. Figure 6.3.2a shows the TOC time-course associated to $Bmim^+$ and NTf_2^- concentration. As it can be seen, $Bmim^+$ concentration decreases for all the technologies tested and there are great differences in the rates of the processes, which, as pointed out before, indicates the occurrence of different oxidation mechanisms.

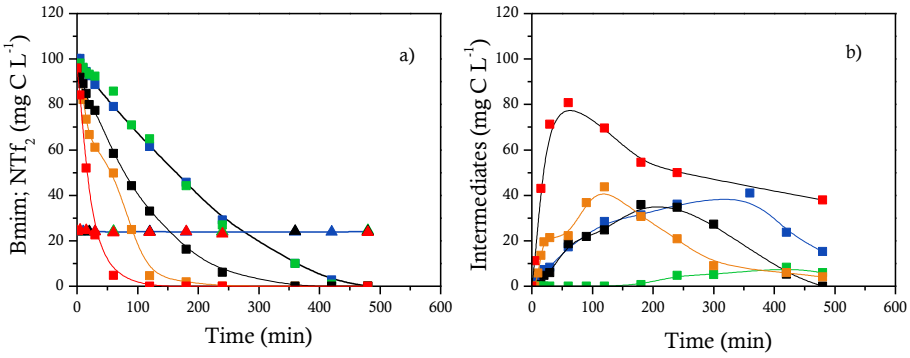

Figure 6.3.2. Time-course of $Bmim^+$ (square) and NTf_2^- (triangle) (a) and intermediates (b) according to C mass balance measured during the (blue) Electrolysis; (red) CWPO; (orange) Sonoelectrolysis; (green) Photoelectrolysis; (black) Electrolysis with addition of H_2SO_4 of synthetic wastewater polluted with 120 mg L^{-1} of $BmimNTf_2$.

In comparing the removal of $Bmim^+$, results are not surprising. As expected, the CWPO is the fastest process for the removal of the raw ionic liquid. In this case, only the oxidation by hydroxyl radicals is expected, which is known to be very efficient for molecular structures like the heterocycle $Bmim^+$ (Cañizares et al., 2007a). As the CWPO was run in discontinuous mode, by mixing the total concentration of hydrogen peroxide and wastewater at the beginning, the rate is expected to be higher than in the electrolytic processes, where current is progressively applied during the 8 h tests. This means that the production of large amounts of hydroxyl radicals takes place at the beginning of the experiment during CWPO whereas electrolysis favors the generation of these radicals along the treatment. Hence, CWPO leads to higher efficiencies on $Bmim^+$ removal. Anyhow, there are outstanding differences among the four electrolytic technologies tested,

which are particularly relevant in the case of the chemically enhanced electrolysis and in the sonoelectrolysis. In the first case, the role of the peroxosulfate and radicals sulfate can help to explain the better performance. On the other hand, high-frequency sonoelectrolysis promotes the formation of hydroxyl radicals from the oxidation of water (Thompson and Doraiswamy, 1999) and the higher supply rate of these radicals (the addition of the electrochemically and sonochemically produced) can help to explain the much better performance. In addition, direct electrolysis in sonoelectrochemical processes is also expected to be enhanced because of the increase in the turbulence produced by ultrasounds, which significantly affects to the mass transport of pollutant towards the anode surface (Souza et al., 2013; de Vidales et al., 2015). This is not the case for the photoelectrolysis, for which almost no differences are found in the destruction of the ionic liquid as compared with the bare electrolysis, although UV light irradiation is also known to promote the formation of hydroxyl radicals.

However, the most interesting result is the refractory behavior of the NTf_2^- anion for all the technologies tested, including CWPO. The concentration of this anion is kept constant during the five oxidation tests carried out. Despite the occurrence of refractory species is not excluded in most of the advanced oxidation technologies, it is the first time that it is reported such refractory behavior with diamond anodes and previous research demonstrated that very different types of molecules ranging from heterocyclic or dyes to carboxylic acids or alcohols are satisfactorily degraded with this technology (Panizza and Cerisola, 2009). At this point, it is worth to take into account that NTf_2^- anion cannot be considered a real organic compound, despite having two carbon atoms per molecule, because of the rather inorganic

structure of the molecule. It also points out that hydroxyl radicals, direct electrolysis and radical sulfate/persulfate oxidation are not able to break the C-F (ΔH = 513.8 kJ mol^{-1}), C-S (ΔH = 713.3 kJ mol^{-1}) or S-N ((ΔH = 467 kJ mol^{-1}) bounds of the NTf_2^- molecule. This is a very relevant mechanistic information because to the authors' knowledge, it has not been reported before and it is clearly observed in this work (Cañizares et al., 2007b; Martinez-Huitle and Andrade, 2011).

Figure 6.3.2b shows the concentration of total intermediates according to the TOC mass balance calculated taking into account the theoretical TOC values from $Bmim^+$ and NTf_2^- and the measured TOC ($TOC_{intermediates} = TOC_{measured} - TOC_{Bmim+} - TOC_{NTf2-}$). From the HPLC analysis, two peaks were observed corresponding to oxalic and formic acids. However, it was considered to be most suitable for this work the quantification of intermediate by TOC mass balance. As expected, CWPO is less efficient than the electrolytic technologies in the oxidation of already oxidized intermediate molecules. Thus, it has been reported (Cañizares et al., 2008) that carboxylic acids are oxidized much faster by electrolysis with diamond than by Fenton oxidation or ozonation. This was explained in terms of the contribution of oxidation mechanisms different of those directly associated to the hydroxyl radical, such as the direct electrolysis. In comparing the electrolytic technologies, it has to be pointed out that no great differences in terms of concentration of intermediates are found by comparing bare electrolysis with the sulfate-enhanced electrolysis and the sonoelectrolysis. Just the maximum is obtained at lower times and it can be explained in terms of the more efficient oxidation in these two technologies, which showed higher rate of removal of the $Bmim^+$. Opposite, the behavior of photoelectrolysis becomes a real surprise in terms of efficiency, as the concentrations detected is much lower and in

fact negligible during most of the oxidation tests. This informs about an almost direct mineralization of the $Bmim^+$ cation under those conditions where the production of large amounts of free radicals can take place by the photoactivation of the electrogenerated oxidants. Hence, direct mineralization process is favored versus the formation of intermediates.

A last important observation is related to the nitrogen speciation, which is illustrated in Figure 6.3.3. $Bmim^+$ concentration decreases, as can be previously observed for electrolytic technologies tested (Figure 6.3.3a). Nitrates and ammonium ions (nitrogen intermediate species) were the final degradation products in the electrolysis of $Bmim^+$. The time-course of these nitrogen species is shown in Figure 6.3.3b. According to literature, the degradation of the C-N bond lead to the formation of nitrates (Rubí-Juárez et al., 2016a, b), which can be cathodically reduced to ammonium ions, being the direct anodic oxidation of these latter species not promoted because of the electrostatic repulsion between the anode surface and the cation charge. This repulsion is also expected in the case of the $Bmim^+$ cation, although the larger size of this species can help to explain the lower impact detected in the performance of the process. Anyhow, it also helps to explain the lowest efficiency of the raw electrolysis, as compared to the other three electrochemically assisted processes. Finally, it is important to highlight that the oxidation of organics containing nitrogen atoms can lead to the release of oxidized nitrogen species such as NO and NO_2 (Garcia-Segura et al., 2017). In this context, the results obtained in Figure 6.3.3 suggest that these species are formed during the process since the mass balance of nitrogen is not closed only with the organic and inorganic compounds analyzed.

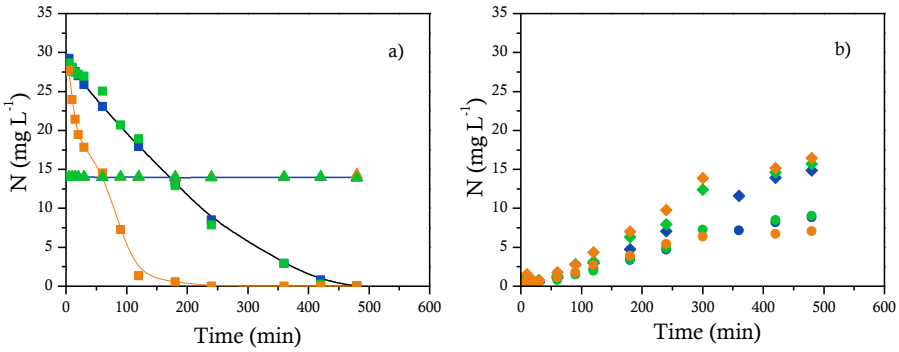

Figure 6.3.3. Time-course of $Bmim^+$ (square), NTf_2 (triangle) (a) and intermediates (nitrate (circle) and ammonium (diamond)) (b) according to N mass balance measured during the electrolysis (blue); sonoelectrolysis (orange) and photoelectrolysis (green).

6.3.4. Conclusions

From this work, the following conclusions can be drawn:

- The concentration of the anion bis(trifluoromethanesulfonyl)imide is kept constant during the five oxidation tests carried out, being the first time that it is reported a refractory behavior in electrolysis with diamond anodes. Hydroxyl radicals, direct electrolysis and radical sulfate/persulfate oxidation are not able to break the C-F, C-S or S-N bounds of the NTf_2 molecule.
- Cation 1-butyl-3-methylimidazolium can be fully oxidized by electrolysis with diamond electrodes, leading to the complete mineralization and to the formation of ammonium and nitrates ions. Concentrations of intermediates formed depends on the particular technology used being photoelectrolysis the technology

which shows the lowest concentration, that is, the almost direct transformation of the $Bmim^+$ into the final products

- The efficiency in the treatment of ionic liquid $BmimNTf_2$ decreases in the sequence sonoelectrolysis, electrolysis enhanced with peroxosulfate promoters, photoelectrolysis and bare electrolysis.

6.3.5. References

- Almazán-Sánchez, P.T., Cotillas, S., Sáez, C., Solache-Ríos, M.J., Martínez-Miranda, V., Cañizares, P., Linares-Hernández, I., Rodrigo, M.A., 2017. Removal of pendimethalin from soil washing effluents using electrolytic and electro-irradiated technologies based on diamond anodes. Appl. Catal. B 213, 190–197.
- Bautista, P., Mohedano, A.F., Casas, J.A., Zazo, J.A., Rodriguez, J.J., 2010a. Oxidation of cosmetic wastewaters with H_2O_2 using a Fe/γ-Al_2O_3 catalyst. Water Sci. Technol. 61, 1631–1636.
- Bautista, P., Mohedano, A.F., Menéndez, N., Casas, J.A., Rodriguez, J.J., 2010b. Catalytic wet peroxide oxidation of cosmetic wastewaters with Fe-bearing catalysts. Catal. Today 151, 148–152.
- Brillas, E., Martínez-Huitle, C.A., 2015. Decontamination of wastewaters containing synthetic organic dyes by electrochemical methods. An updated review. Appl. Catal. B 166–167, 603–643.
- Cabeza, A., Urtiaga, A.M., Ortiz, I., 2007. Electrochemical treatment of landfill leachates using a boron-doped diamond anode. Ind. Eng. Chem. Res. 46, 1439–1446.
- Cañizares, P., Garcia-Gomez, J., Lobato, J., Rodrigo, M., 2003. Electrochemical oxidation of aqueous carboxylic acid wastes using diamond thin-film electrodes. Ind. Eng. Chem. Res. 42, 956–962.
- Cañizares, P., Hernandez, M., Rodrigo, M.A., Saez, C., Barrera, C.E., Roa, G., 2009a. Electrooxidation of brown-colored molasses wastewater. Effect of the electrolyte salt on the process efficiency. Ind. Eng. Chem. Res. 48, 1298–1301.
- Cañizares, P., Paz, R., Saez, C., Rodrigo, M.A., 2008. Electrochemical oxidation of alcohols and carboxylic acids with diamond anodes - a comparison with other advanced oxidation processes. Electrochim. Acta 53, 2144–2153.
- Cañizares, P., Paz, R., Sáez, C., Rodrigo, M.A., 2007a. Electrochemical oxidation of wastewaters polluted with aromatics and heterocyclic compounds. J. Electrochem. Soc. 154, E165–E171.
- Canizares, P., Saez, C., Lobato, J., Paz, R., Rodrigo, M.A., 2007b. Effect of the operating conditions on the oxidation mechanisms in conductive-diamond electrolyses. J. Electrochem. Soc. 154, E37–E44.
- Cañizares, P., Saez, C., Sanchez-Carretero, A., Rodrigo, M.A., 2009b. Synthesis of novel oxidants by electrochemical technology. J. Appl. Electrochem. 39, 2143–2149.
- Cotillas, S., de Vidales, M.J.M., Llanos, J., Saez, C., Canizares, P., Rodrigo, M.A., 2016. Electrolytic and electro-irradiated processes with

diamond anodes for the oxidation of persistent pollutants and disinfection of urban treated wastewater. J. Hazard Mater. 319, 93–101.

- Cotillas, S., Lacasa, E., Sáez, C., Cañizares, P., Rodrigo, M.A., 2018. Electrolytic and electro-irradiated technologies for the removal of chloramphenicol in synthetic urine with diamond anodes. Water Res. 128, 383–392.
- de Vidales, M.J.M., Sáez, C., Pérez, J.F., Cotillas, S., Llanos, J., Cañizares, P., Rodrigo, M.A., 2015. Irradiation-assisted electrochemical processes for the removal of persistent organic pollutants from wastewater. J. Appl. Electrochem. 45, 799–808.
- dos Santos, E.V., Saez, C., Martinez-Huitle, C.A., Canizares, P., Rodrigo, M.A., 2015. Combined soil washing and CDEO for the removal of atrazine from soils. J. Hazard Mater. 300, 129–134.
- Gandini, D., Mahe, E., Michaud, P.A., Haenni, W., Perret, A., Comninellis, C., 2000. Oxidation of carboxylic acids at boron-doped diamond electrodes for wastewater treatment. J. Appl. Electrochem. 30, 1345–1350.
- Garcia-Segura, S., Mostafa, E., Baltruschat, H., 2017. Could NO_x be released during mineralization of pollutants containing nitrogen by hydroxyl radical? Ascertaining the release of N-volatile species. Appl. Catal. B 207, 376–384.
- Liwarska-Bizukojc, E., Gendaszewska, D., 2013. Removal of imidazolium ionicliquids by microbial associations: study of the biodegradability and kinetics. J. Biosci. Bioeng. 115, 71–75.
- Marselli, B., Garcia-Gomez, J., Michaud, P.A., Rodrigo, M.A., Comninellis, C., 2003. Electrogeneration of hydroxyl radicals on boron-doped diamond electrodes. J. Electrochem. Soc. 150, D79–D83.
- Martinez-Huitle, C.A., Andrade, L.S., 2011. Electrocatalysis in wastewater treatment: recent mechanism advances. Quím. Nova 34, 850–858.
- Martinez-Huitle, C.A., Brillas, E., 2009. Decontamination of wastewaters containing synthetic organic dyes by electrochemical methods: a general review. Appl. Catal. B 87, 105–145.
- Martinez-Huitle, C.A., Rodrigo, M.A., Sires, I., Scialdone, O., 2015. Single and coupled electrochemical processes and reactors for the abatement of organic water pollutants: a critical review. Chem. Rev. 115, 13362–13407.
- Mena, I.F., Diaz, E., Rodriguez, J.J., Mohedano, A.F., 2017. CWPO of bisphenol A with iron catalysts supported on microporous carbons from grape seeds activation. Chem. Eng. J. 318, 153–160.
- Oturan, N., Brillas, E., Oturan, M.A., 2012. Unprecedented total mineralization of atrazine and cyanuric acid by anodic oxidation and

electro-Fenton with a boron-doped diamond anode. Environ. Chem. Lett. 10, 165–170.

- Panizza, M., Cerisola, G., 2009. Direct and mediated anodic oxidation of organic pollutants. Chem. Rev. 109, 6541–6569.
- Raut, A.S., Cunningham, G.B., Parker, C.B., Klem, E.J.D., Stoner, B.R., Deshusses, M.A., Glass, J.T., 2013. Electrochemical disinfection of human urine for water-free and additive-free toilets using boron-doped diamond electrodes. ECS Trans. 1–11.
- Rodrigo, M.A., Canizares, P., Sanchez-Carretero, A., Saez, C., 2010. Use of conductive diamond electrochemical oxidation for wastewater treatment. Catal. Today 151, 173–177.
- Rubí-Juárez, H., Cotillas, S., Sáez, C., Cañizares, P., Barrera-Díaz, C., Rodrigo, M.A., 2016a. Removal of herbicide glyphosate by conductive-diamond electrochemical oxidation. Appl. Catal. B 188, 305–312.
- Rubí-Juárez, H., Cotillas, S., Sáez, C., Cañizares, P., Barrera-Díaz, C., Rodrigo, M.A., 2016b. Use of conductive diamond photo-electrochemical oxidation for the removal of pesticide glyphosate. Separ. Purif. Technol. 167, 127–135.
- Sires, I., Brillas, E., Oturan, M.A., Rodrigo, M.A., Panizza, M., 2014. Electrochemical advanced oxidation processes: today and tomorrow. A review. Environ. Sci. Pollut. Res. 21, 8336–8367.
- Souza, F.L., Sáez, C., Cañizares, P., Motheo, A.J., Rodrigo, M.A., 2013. Sonoelectrolysis of wastewaters polluted with dimethyl phthalate. Ind. Eng. Chem. Res. 52, 9674–9682.
- Thompson, L.H., Doraiswamy, L.K., 1999. Sonochemistry: science and engineering. Ind. Eng. Chem. Res. 38, 1215–1249.

Conclusiones
Conclusions

Conclusiones

Los resultados presentados en esta memoria permiten establecer las siguientes conclusiones:

Evaluación de la ecotoxicidad y la biodegradabilidad de los líquidos iónicos de las familias imidazolio y colina

1. La ecotoxicidad de los LIs de la familia imidazolio aumentó con la longitud de la cadena alquílica, lo que puede explicarse por el carácter lipofílico o la pérdida de polaridad de estos compuestos. En general, esta familia de LIs mostró una toxicidad superior, en términos de EC_{50} (Microtox®, *Vibrio fischeri*), a los LIs de la familia colina. La presencia de NTf_2^- aumentó considerablemente la toxicidad de los LIs respecto a otros aniones como Cl^-, Ac^- o BF_4^-, por lo que su toxicidad está asociada a la que presentan tanto el catión como el anión. Los ensayos de inhibición con fangos activos mostraron tendencias similares, aunque los valores de EC_{50} resultaron inferiores a los obtenidos en los ensayos con *Vibrio fischeri*.
2. Los ensayos de biodegradabilidad inherente y rápida evidenciaron la alta biodegradabilidad mostrada por $Choline^+$ y Ac^-, siendo $Bmim^+$ y NTf_2^- recalcitrantes al tratamiento biológico. Además, se observó una parcial inhibición del fango activo en el ensayo de biodegradabilidad rápida realizado con una concentración de 50 mg L^{-1} de $CholineNTf_2$, valor próximo a la EC_{50} obtenida en el ensayo de inhibición respirométrica para este compuesto. Por tanto, conviene destacar el impacto negativo que puede suponer en el medio ambiente la presencia de residuos acuosos que contengan NTf_2^-.

Oxidación biológica de líquidos iónicos de la familia colina en reactores biológicos secuenciales.

3. La degradación de LIs de la familia colina (0.5 a 15 mM) en reactores secuenciales discontinuos, empleando glucosa como cosubstrato, alcanzó valores de conversión de COT y reducción de DQO de 80-90 % y 75-85 %, respectivamente, para CholineCl y CholineAc. Como intermedios de degradación de $Choline^+$ se detectaron etanol y tri-, di- y metilamina, obteniéndose como productos finales CO_2, H_2O, nitrito y nitrato.
4. Se observó una inhibición parcial del fango activo durante la degradación biológica de $CholineNTf_2$ y la acumulación de NTf_2^- en el reactor debido a la ecotoxicidad intrínseca del anión y su carácter recalcitrante a la oxidación biológica. Sin embargo, el sistema de fangos activos degradó $Choline^+$ incluso para concentraciones de $CholineNTf_2$ de 15 mM en el alimento.

Oxidación húmeda catalítica con peróxido de hidrógeno para la eliminación de líquidos iónicos de la familia imidazolio.

5. La oxidación húmeda catalítica con peróxido de hidrogeno de LIs de la familia imidazolio empleando un catalizador de Fe_2O_3/Al_2O_3 permitió alcanzar una aceptable mineralización (40 % en el caso de $Bmim^+$), utilizando la cantidad estequiométrica de H_2O_2 a 90 ºC, siendo independiente del contraion usado (Cl^-, Ac^- o NTf_2^-). En términos del anión, la concentración de Ac^- aumentó a lo largo de la reacción, debido a su carácter refractario a la oxidación por radicales hidroxilo, mientras que las concentraciones de Cl^- y NTf_2^- no variaron. Además, la mineralización del catión aumentó con la longitud

de la cadena alquílica, siendo la velocidad de degradación de los cationes estudiados ($Bmim^+$, $Hmim^+$ and $Dmim^+$) similar en todos los casos.

6. Los efluentes de la oxidación catalítica con peróxido de hidrógeno mostraron una elevada biodegradabilidad, debido a la degradación del catión en compuestos hidroxilados, ácidos de cadena corta (ácidos fórmico, acético, malónico y oxálico), CO_2, H_2O y nitrato. Además, se apreció una signigicativa disminución de la ecotoxicidad en los efluentes obtenidos en el caso HmimCl y DmimCl. La combinación del tratamiento CWPO y la oxidación biológica consigue conversiones de COT del 55-60 %.
7. Los catalizadores de Fe soportados sobre alúmina y materiales carbonos mostraron diferentes comportamientos a lo largo la reacción CWPO de BmimAc durante 100 h (80 ºC, 0.133 kg_{Fe} h mol_{BmimAc}^{-1}). El catalizador de Fe_2O_3/Al_2O_3 exhibió una alta actividad (60 % de eliminación de $Bmim^+$ y 20 % de conversión de COT) y estabilidad, permaneciendo inalterable después de las primeras 10 h en una reacción de 80 h de duración. Los catalizadores de Fe soportados sobre carbón mostraron diferentes comportamientos en la reacción CWPO de BmimAc en función del procedimiento de síntesis empleado. El catalizador obtenido por impregnación a húmedad incipiente de un carbón activo comercial mostró una alta lixiviación de Fe (90 %), mientras que en el catalizador preparado por carbonización hidrotermal de fango activo con $FeCl_3$ se observó una relativamente alta estabilidad, junto con una baja actividad, debido al reducido contenido en Fe en la superficie del catalizador. Por último, el catalizador preparado mediante activación química con $FeCl_3$ de biosolidos de depuradora

exhibió alta estabilidad y alta degradación de BmimAc (eliminación completa del $Bmim^+$ y conversión de COT del 30 %)

Tratamientos electroquímicos para la eliminación de líquidos iónicos basados en imidazolio en fase acuosa

8. La electrólisis de LIs (sin adición de electrolito) con ánodos de diamante dopado con Boro mostró una elevada degradación y mineralización de LIs de la familia imidazolio (BmimCl, BmimAc, $BmimNTf_2$, HmimCl and DmimCl). La velocidad de oxidación de $Bmim^+$ resultó inferior en el caso de BmimAc, debido a la competencia de las especies oxidantes para la degradación de $Bmim^+$ y Ac^-. La adición de sulfato como electrolito originó una mejora en la mineralización de los LIs, asociada a la contribución de los radicales peroxosulfato y sulfato en el proceso de electrolisis. La electrolisis de DmimCl conllevó a la formación de un polímero, que fue evitada por la presencia de sulfato.
9. La electrólisis asistida con ultrasonidos de alta frecuencia (US) o luz UV aumentó la degradación de los LIs estudiados. La eficacia de eliminación de cada LIs dependió del contraion empleado y/o de la radiación de US o UV. En el caso de BmimAc y $BmimNTf_2$, la aplicación de US originó una reducción de la carga aplicada necesaria para conseguir la eliminación completa del catión respecto a la electrolisis (de 40 a 20 y de 30 a 6 A h dm^{-3}, respectivamente).
10. Como principales productos de reacción de la electrólisis de $Bmim^+$ se detectaron compuestos hidroxilados, ácidos de cadena corta (ácido acético y oxálico), nitrito, nitrato y amonio. También aparecieron clorato y perclorato como compuestos de

oxidación de cloruro. En el caso del $BmimNTf_2$, la concentración de NTf_2^- permaneció constante en todos los ensayos de electroxidación (electrólisis, sonoelectrólisis y fotoelectrólisis), por lo que puede considerarse refractario a los tratamientos empleados.

Conclusions

The results presented in this work support the following conclusions:

Assessment the ecotoxicity and biodegradability of imidazolium- and choline-based ionic liquids

1. The imidazolium-based ILs increased their toxicity with the alkyl side chain length, which can be related to the loss of IL polarity or their lipophilic character, and, in general, showed higher ecotoxicity than choline-based ones in terms of EC_{50} values by Microtox® test (*Vibrio fischeri*). The presence of the NTf_2^- increased considerably the toxicity with respect to other anions such as Cl^-, BF_4^- or Ac^-. Consequently, toxic effects of these ILs are directly related to both ILs constituents. The respiration inhibition test using activated sludge showed similar trends, although EC_{50} values tended to be lower in the case of Microtox® Test.
2. Inherent and fast biodegradability tests evidenced the higher biodegradability exhibited by $Choline^+$ and Ac^-, being $Bmim^+$ and NTf_2^- recalcitrant to biological treatment. Furthermore, a partial inhibition of the microbial activity was observed in the fast biodegradability test performed with 50 mg L^{-1} of $CholineNTf_2$, concentration close to the EC_{50} value obtained in the respiration inhibition test. Consequently, the negative environmental impact of NTf_2-containing ILs should take into account for their use in chemical processes, which can generate aqueous wastes.

Biological oxidation of choline-based ionic liquids in sequencing batch reactors

3. Choline-based ILs were efficiently degraded in SBRs (from 0.25 to 15 mM) using glucose as cosubstrate, achieving TOC conversions and COD reductions in the range of 80-90 % and 75-85 % for CholineCl and CholineAc, respectively. The $Choline^+$ was degraded to ethanol and tri-, di- and methylamine, being the end-products CO_2, H_2O, nitrite and nitrate.
4. The biodegradation of $CholineNTf_2$ led to a partial inhibition of the activated sludge and NTf_2^- accumulation due to the intrinsic ecotoxicity of the anion and its recalcitrant character to biodegradation. However, the activated sludge was able to biodegrade the $choline^+$ even for IL concentration of 15 mM in the feed.

Catalytic wet peroxide oxidation for the removal of imidazolium-based ionic liquids in aqueous phase

5. The degradation of imidazolium-based ILs was effectively carried out using a Fe_2O_3/Al_2O_3 catalyst in batch CWPO reactions. The highest mineralization yields of Bmim-based ILs (around 40 %) were obtained by using the stoichiometric H_2O_2 amount at 90 ºC, being regardless of the counter-anion (Cl^-, Ac^- or NTf_2^-) used. With respect to the anions, acetate concentration increased along reaction time, due to its refractory behavior in CWPO reactions, whereas chloride and NTf_2^- concentration remained unalterable. Moreover, the mineralization increased with the alkyl side chain length, although the cation depletion was very similar in all the cases ($Bmim^+$, $Hmim^+$ and $Dmim^+$).

6. An enhancement in the biodegradability of the ILs effluents was observed after the CWPO treatment, due to the degradation of the imidazolium cation into hydroxylated compounds, short-chain organic acids (formic, acetic, malonic and oxalic acids), CO_2, H_2O and nitrate. Besides, a substantial reduction in the ecotoxicity was obtained for the HmimCl and DmimCl effluents. The combination of CWPO and biodegradability test achieved 55-60 % TOC conversion.
7. The Fe catalysts supported on alumina and carbon materials showed different behaviors along CWPO of BmimAc for 100 h (80 ºC, 0.133 kg_{Fe} h mol_{BmimAc}^{-1}). The Fe_2O_3/Al_2O_3 catalyst exhibited high activity (60 % $Bmim^+$ removal and 20 % of TOC conversion) and stability, remaining inalterable for 70 h in an on-stream experiment lasting 80 h. The Fe carbon-supported catalysts behaved in a different way in the CWPO of BmimAc related to their synthesis procedures. The catalyst obtained by incipient wetness impregnation of a commercial active carbon led to a high Fe leaching (90 %), whereas the catalyst prepared by hydrothermal carbonization of sewage sludge with $FeCl_3$ showed relative high stability but a slight activity, due to the low Fe content in the external surface of the catalyst. Finally, the Fe catalyst based on chemical activation with $FeCl_3$ of dried sewage sludge exhibited high stability and high BmimAc degradation (almost complete $Bmim^+$ removal and 30 % TOC conversion).

Electrotreatments for the removal of imidazolium- based ionic liquids in aqueous phase

8. The bare electrolysis of the ILs (without electrolyte addition) with BDD anode caused high degradation and mineralization

rates of the imidazolium ILs (BmimCl, BmimAc, $BmimNTf_2$, HmimCl and DmimCl). In the BmimAc electrolysis, $Bmim^+$ oxidation rate resulted inferior to the other cases, due to both, $Bmim^+$ and Ac^-, compete to be oxidized. The addition of sulfate as electrolyte in the reaction medium produced an improvement in the mineralization of the ILs, associated with the contribution of peroxosulfate and sulfate radicals in the electrolysis process. The electrolysis of DmimCl led to the formation of a polymer, which was prevented by the presence of sulfate.

9. Enhancing the bare electrolysis with high-frequency ultrasound (US) or UV light improved the degradation of the ILs in aqueous phase. Cation removal efficiency depended on the counter ion and on irradiation by high-frequency US and UV light. In the case of the BmimAc and $BmimNTf_2$, the application of US led to a reduction in the charge need to be applied for complete cation degradation with respect to bare electrolysis (from 40 to 20 and from 30 to 6 A h dm^{-3}, respectively).
10. The main by-products obtained by ILs electrolysis were hydroxylated compounds, short-chain organic acids (acetic and oxalic acids), CO_2, H_2O, nitrite, nitrate and ammonium. Chloride was mainly oxidized to chlorate and perchlorate. In the case of $BmimNTf_2$, NTf_2^- concentration remained constant in all the electroxidation tests (bare electrolysis, sonoelectrolysis, photoelectrolysis and electrolysis adding sulfate anions), showing a refractory character to these treatments.

Abbreviations

Ac^-: acetate anion

AC: Activated carbon

AOP: Advanced Oxidation Process

BDD: Boron doped diamond

BET: Brunauer–Emmett–Teller

BF_4^-: tetrafluoroborate anion

$Bmim^+$: 1-Butyl-3-methylimidazolium cation

BmimAc: 1-Butyl-3-methylimidazolium acetate

$BmimBF_4$: 1-Butyl-3-methylimidazolium tetrafluoroborate

BmimCl: 1-Butyl-3-methylimidazolium chloride

$BmimNTf_2$: 1-Butyl-3-methylimidazolium bis(trifluoromethanesulfonyl)imide

$C(CN)_3^-$: tricyanomethanide

$CF_3SO_3^-$: trifluoromethanesulfonate

$Choline^+$: N,N,N-trimethylethanolammonium cation

CholineAc: Choline acetate

CholineCl: Choline chloride

$CholineNTf_2$: Choline bis(trifluoromethanesulfonyl)imide

COD: Chemical oxygen demand

CSTR: continuous stirred batch reactor

CWPO: Catalytic Wet Peroxide Oxidation

$Dmim^+$: 1-Decyl-3-methylimidazolium cation

$DmimBF_4$: 1-Decyl-3-methylimidazolium tetrafluoroborate

DmimCl: 1-Decyl-3-methylimidazolium chloride

$DmimNTf_2$: 1-Decyl-3-methylimidazolium bis(trifluoromethylsulfonyl) imide

EC_{50}: Half maximal effective concentration

Fe/AC: Fe catalyst supported on commertial activated carbon

Fe/AS: Fe catalyst supported on carbon obtained by chemical activation of sludge

Fe/HTCS: Fe catalyst supported on carbon obtained by hydrothermal carbonization of sludge

Fe_2O_3/Al_2O_3: Fe catalyst supported on alumina

$Hmim^+$: 1-Hexyl-3-methylimidazolium cation

$HmimBF_4$: 1-Hexyl-3-methylimidazolium tetrafluoroborate

HmimCl: 1-Hexyl-3-methylimidazolium chloride

$HmimNTf_2$: 1-Hexyl-3-methylimidazolium bis(trifluoromethylsulfonyl) imide

HTC: Hydrothermal carbonization

IC: Inorganic carbon

IL: Ionic liquid

j: current density

K_{ow}: octanol-water partition coefficient

NTf_2^-: bis(trifluoromethanesulfonyl)imide anion

$Omim^+$: 1-Methyl-3-octylimidazolium cation

$OmimBF_4$: 1-Methyl-3-octylimidazolium tetrafluoroborate

OmimCl: 1-Methyl-3-octylimidazolium chloride

$OmimNTf_2$: 1-Methyl-3-octylimidazolium bis(trifluoromethylsulfonyl) imide

PF_6^-: Hexafluorophosphate anion

Q: charge (A h L^{-1})

SBR: Sequencing batch reactor

SEM-EDX: Scanning Electron Microscopy - Energy Dispersive X-ray spectroscopy

SOUR: specific oxygen uptake rate

SS: Simulated sunlight

TC: Total carbon

TOC: Total organic carbon

TSS: Total suspend solids

TXRF: Total reflection X-Ray Fluorescence

UV: ultraviolet light

VSS: Volatile suspend solids

XPS-EDAX: X-ray photoelectron spectroscopy – Energy dispersive X-ray spectroscopy analysis

XRD: X-ray Diffraction

γ: inhibition

λ: wavelenght

τ: space-time